Testing the hyperfunction theory of ageing in *Caenorhabditis elegans*

Yila de la Guardia

University College London

PhD Thesis

Declaration

I, Yila de la Guardia, confirm that the work presented in this thesis is my own. Where information has been derived from other sources, I confirm that this has been indicated in the thesis.

………………………………………………………………………

Yila de la Guardia

Abstract

Ageing research in model organisms has accomplished great strides in finding genes and pathways that modulate the ageing process. However, the mechanism through which organisms age still remains a mystery. An influential ageing theory views ageing as the result of damage accumulation throughout an organism's lifespan, which eventually accumulates to noxious levels causing death. In this thesis we will explore an alternative theory proposed by M. Blagosklonny. The hyperfunction theory postulates that ageing is the result of the non-adaptive continuation of developmental and reproductive programmes in late adulthood. Thus, programmes that promote growth and reproductive fitness become quasi-programmes in later life that result in age-related pathologies, some of which cause death. In this thesis we examined two reproductive pathologies, yolk accumulation and gonad degeneration, to try to understand their causes and to test their role in age-related mortality.

A clear example of a quasi-programme in ageing worms is the run-on of yolk production in post-reproductive worms. During reproduction yolk is synthesized in the intestine to be transported to oocytes and provision embryogenesis. After reproduction ceases yolk protein accumulates in the body cavity of the worm. We found that yolk proteins accumulate to high levels during ageing. However, RNAi abrogation of vitellogenesis did not increase lifespan, implying that yolk protein accumulation does not cause mortality.

Gonad disintegration provides an intriguing example of how quasi-programmes can cause pathology via atrophy. We found that gonad disintegration, which occurs in post-reproductive hermaphrodite worms, is apoptosis dependant. At least half of all germ cells undergo "physiological" programmed cell death. Our results imply that the apoptotic program that ensures reproductive fitness to support oocyte growth continues in older worms giving rise to pathology.

I lovingly dedicate this thesis to:

My parents, Gonzalo and Valli de la Guardia

My siblings, Gonzalo, Vicky, Pati, Viola and Valli

And my soon to be husband Alvaro Mendez.

Without your encouragement, support and patience it would not have been

possible.

Aknowledgements

I would like to express my gratitude to the following people without whom the work presented here would not have been possible:

Past and present members of the Gems lab: Dan Ackerman, Sara Valentini, Caroline Araiz, Catherine Au, Alex Benedetto, Filipe Cabreiro, Jennifer Tullet, Michele Riesen, Marina Ezcurra, Ann Gilliat and Cassandra Coburn each of whom provided invaluable assistance at one time or another. I thank members of Institute of Healthy Ageing for useful discussions and help during my PhD. Sahar Emran and Jorge Castillo-Quan with whom I shared an office, heated discussions and a great deal of laughs. I must also thank my secondary supervisor Mathew Piper and tertiary supervisor Eugene Schuster who provided advice and insightful questions along the way.

Warm thanks to Eleanor Tyler, Ann Gilliat, and Josephine Hellberg who collaborated closely with me on this project. It's been a pleasure working with you.

I would like to thank IFARHU/SENACYT for funding this project.

To my family and friends in Panama who via long distance phone calls cheered me on every step of the way. Particularly Alvaro Mendez who provided the London based support. Your good humour always put a smile on my face especially on the stressful days.

And finally a special mention to my supervisor, David Gems. His help, encouragement, and support throughout my PhD were invaluable. Thanks for always being available for discussions and providing advice whenever it was needed.

Abbreviations

apoB-100	Apolipoprotein B-100
C. elegans	*Caenorhabditis elegans*
Daf	Abnormal dauer formation
DG	Distal gonad
DIC	Differential interference contrast
DR	Dietary restriction
FAC	ferric ammonium citrate
FUdR	5-fluoro-2'-deoxyuridine
GD	Gonad degeneration
IIS	Insulin/IGF-1 signalling
LDL	Low-density lipoproteins
PA	Physiological apoptosis
PG	Proximal gonad
RNAi	RNA interference reactive
Rol	Rollers
ROS	Reactive oxygen species
SEM	Standard error of the mean
SIA	Stress-induced apoptosis
Sp	Spermatheca
TOR	Target of rapamycin
WT	wildtype
Yol-d	Yolk accumulation deficient
Yol-o	Yolk over-accumulation
YP	Yolk protein

Table of Contents

Figures and tables

Chapter 1: Introduction

Chapter 3: Quasi-programmed yolk overproduction in ageing *C. elegans*

Chapter 4: Ageing in the *C. elegans* germline

Chapter 5: Gonad disintegration is driven by germ cell apoptosis in *C. elegans*

Appendices

Chapter 1:   Introduction

1.1   Ageing

To date there is no single widely accepted definition of ageing. It can be defined as the functional decline of an organism which increases with age resulting in reduced survival and death. Ageing has also been defined by the following series of postulates proposed by Bernard Strehler (Viña et al., 2007): 1) ageing is *universal* in that processes recognized as ageing occur in all individuals of a species to varying degrees. 2) Ageing is *intrinsic* in that it occurs due to endogenous factors and can be influenced by, but does not depend on, external factors. 3) Ageing is *progressive* and changes associated with ageing will occur throughout the organism's lifetime. 4) Ageing is *deleterious* and its associated phenomena will have a negative effect on the organism.

Ageing is an affliction shared by most living organisms. However, ageing does not appear to be a necessary characteristic of metazoans and some organisms, such as *Hydra vulgaris*, appear to be non-ageing (Martínez, 1998). This raises an important question: if ageing is not inevitable why then do most organisms age? Is there a benefit to ageing?

A very old notion is that ageing is the result of inevitable wear and tear of the body over time. This comes from the simple observation that structurally complex inanimate objects such as machines wear out and deteriorate with time. However, this reasoning misses the point that living organisms have endogenous repair mechanisms whereas machines do not. Darwin's theory of evolution postulates that random heritable variations that bestow an advantage to fitness of the individual will accumulate in populations over time (Darwin, 1859). As Darwin's evolutionary theory gained acceptance biologists began to ponder why natural selection was so adept at creating organisms that could survive and reproduce efficiently until adulthood and, yet was unable to prevent them from deteriorating and dying afterwards (Ljubuncic and Reznick, 2009). This led to the development of evolutionary theories of ageing to explain how a process that causes disease and death could be so widespread.

1.1.1 Evolutionary theories of ageing

A common question among biologists was how this maladaptive trait could be so widely conserved and why it evolved in the first place. One might think that natural selection should have resulted in the elimination of this apparently deleterious trait (Flatt and Schmidt, 2009). An early idea proposed by the Roman philosopher Lucretius speculated that ageing is necessary to make room for younger generations (Fabian and Flatt, 2011). Similarly, August Weismann proposed the idea of programmed death arguing that nature could produce a killing mechanism to remove old members of a population if this were to increase the success of the young population by freeing up resources, bestowing advantage to the population at the expense of the individual (Weismann, 1889). However, a long-lived variant individual could reproduce for longer thereby increasing reproductive fitness, arguing against Weismann's model. Why then does ageing exist?

In the 1940s and 1950s Haldane, Medawar, and Williams came to the conclusion that selective pressure is reduced in older adults. They argued that genes with early-acting deleterious effects are removed from the population by strong selection because they decrease fitness. On the other hand, genes that have deleterious effects in later life undergo weaker selection because reproduction has already taken place and genes have been passed to the next generation (Flatt and Schmidt, 2009). In the wild, most animals do not experience ageing because most of them die as a result of extrinsic hazards such as infectious disease, starvation and predation (Flatt and Schmidt, 2009). Thus, extrinsic hazards results in selection favouring genes conferring an early beneficial advantage assuring successful reproduction, more than favouring longevity (Kirkwood and Holliday, 1979; Medawar, 1952). If an organism has a mutation that confers a beneficial or harmful effect which is only expressed post-reproduction it will be out of the grasp of selection to favour or counteract and as such it is under the "selection shadow" because it will have already been passed on to the offspring (Fabian and Flatt, 2011) (Figure 1.1). This could explain the prevalence of some late life genetically dominant diseases such as Huntington's disease (Haldane, 1941).
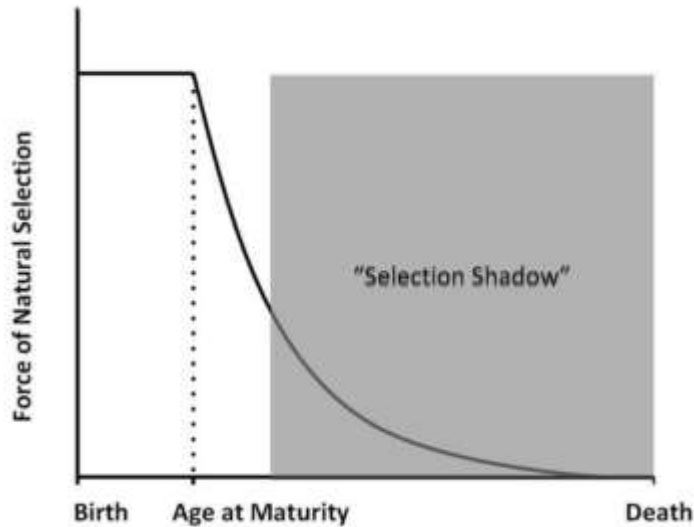
Figure 1.1 The force of natural selection decreases with age. Image reproduced from Fabian and Flatt 2011.

The mutation accumulation theory, proposes that weak selective pressures at older ages allow late-acting deleterious mutations to accumulate in individuals and that over time these accumulate in the population (Medawar, 1952). The theory of antagonistic pleiotropy elaborates upon this, arguing that alleles which are detrimental in old age can be favoured by natural selection if they bestow a significant fitness advantage in early life (Williams, 1957). Thus, the selective value of a gene is measured by how it affects reproductive success far more than longevity. A new allele that increases reproductive output earlier in life but has deleterious late life effects and can be selected for because it can increase overall reproductive fitness (Williams, 1957). Together these theories form the core modern evolutionary theory of ageing.

1.1.2 Disposable soma theory

The antagonistic pleiotropy theory proposes that ageing evolved as a by-product of selection of genes that benefit the organism at an early age but has negative effects on the organism post-reproduction (Williams, 1957). This theory also predicts trade-offs between reproduction and longevity, i.e. costs of from strong selection for genes that increase reproductive output at the expense of long term organismal health (Ljubuncic and Reznick, 2009). In the 1970s Thomas Kirkwood proposed a biological mechanism for antagonistic pleiotropy in his disposable soma theory.

The disposable soma theory proposes that in nature organisms typically have a limited supply of energy and other resources and must choose to allocate resources to

reproduction or cellular maintenance. A trade-off exists as evolution favours alleles that use energy to allow increased reproductive output at the expense of the long term organismal survival (Kirkwood 1977). Somatic maintenance is costly in energetic terms. for example, energy expenditure is necessary to monitor errors in DNA and protein translation. One idea is that, during development resources are allocated to the soma before reproduction, but this energy is later diverted to the germline resulting in poor maintenance of the soma, which result in ageing (Kirkwood and Holliday, 1979). This theory predicts a clear bias in energetic allocation that favours the reproductive cell lineage, which must be maintained to avoid damage that could affect subsequent generations, at the expense of somatic tissue maintenance which would only favour the individual (Ljubuncic and Reznick, 2009).

1.2 *C. elegans* in ageing research

Model organisms are species used to study conserved biological processes, including ageing. They are useful to researchers because they have been extensively studied, are inexpensive to breed and maintain in laboratory conditions, and have a relatively short generation time. Researchers can use model organisms to help elucidate ageing mechanisms, including the genes that control ageing, whilst maintaining them in a controlled environment. Model organisms can also be used to test the validity of mechanistic theories of ageing, which will be discussed later. Commonly used organisms in ageing research include the yeast *Saccharomyces cerevisiae*, the nematode *Caenorhabditis elegans*, the fruit fly *Drosophila melanogaster*, and the mouse *Mus musculus.* We used *C. elegans* for our studies testing the hyperfunction theory of ageing, and my thesis will focus on this organism.

1.2.1 Use of *C. elegans* as a model organism

The use of *C. elegans* as a model organism was first proposed by Sydney Brenner due to its convenience for genetic analysis (Brenner, 1974a). *C. elegans* is a small, soil-dwelling nematode of that can reach about 1.2mm in length. It exists as both hermaphrodites, with 5 pairs of autosomal chromosomes and a pair of sex chromosomes (XX), and males which have 5 autosomal chromosomes but only one sex chromosome

(XO). Hermaphrodites are predominant in populations, with males arising by X-chromosomal nondisjunction at a rate of ~ 0.02%. Males can be maintained by mating with hermaphrodites and can be used to carry out crosses to study multiple mutants. The self-fertilization of hermaphrodites leads to a population of genetically identical organisms (Brenner, 1974a).

C. elegans are easy and inexpensive to maintain in laboratory conditions. Their small size and rapid breeding allows them to be stored in large quantities on Petri plates containing agar seeded with OP50, a uracil-requiring *Escherichia coli* strain. In addition they recover from freezing which makes it easy to store strains of interest indefinitely (Riddle et al., 1997). The adult has less than 1000 somatic cells and all cell lineages are know (Sulston and Horvitz, 1977), which is ideal for performing microsurgery on specific cells to study their function. *C. elegans* are transparent, which makes them ideal system for examining age-related changes in the body in response to genetic manipulation using differential interference contrast (DIC) microscopy (also known as Nomarski microscopy) (Riddle *et al*., 1997). Their development and ageing rate is temperature sensitive, and at 20°C *C. elegans* worms live two 2-3 weeks (Klass, 1977). This short lifespan makes it a very advantageous organism for longevity studies.

C. elegans was the first animal to have its whole genome was sequenced in 1998 and a wealth of information on the organism is readily available on open source Internet sites such as WormBase, WormAtlas and WormBook.

1.2.2 *C. elegans* **anatomy**

C. elegans have a simple body plan made up of an outer tube with a fluid-filled body cavity known as the pseudocoelum, and two inner tubes. The cuticle, hypodermis, musculature, nervous system and excretory system compose the outer tube. The two inner tubes comprise: 1) the alimentary canal, made up of the pharynx and the intestine; 2) the gonad (Riddle *et al*., 1997) (Figure 1.2).
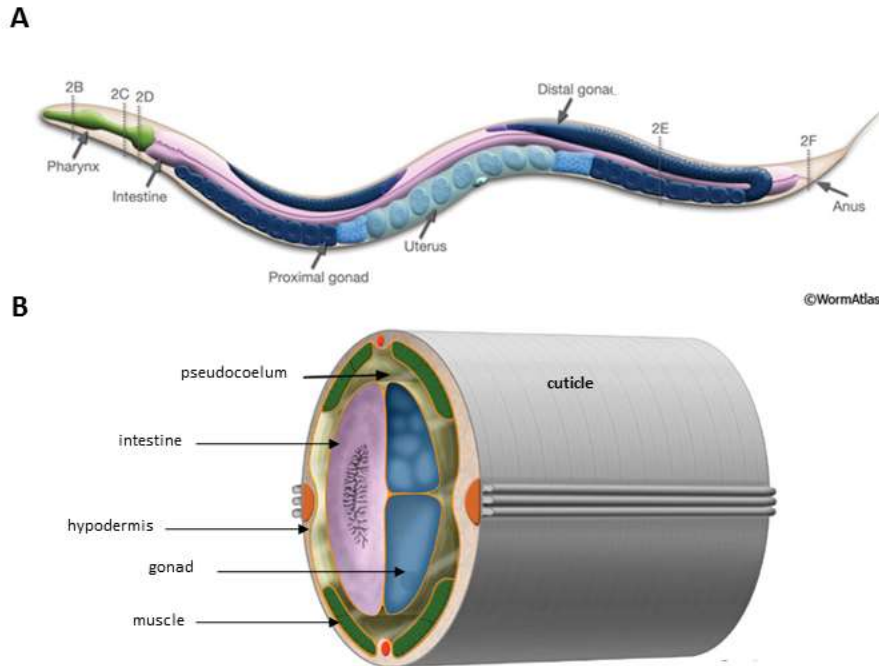
Figure 1.2 *C. elegans* anatomy. A) Schematic representation of *C. elegans* anatomy with labelled structures. B) Schematic cross-section with labelled tissues. Image modified and reproduced from Altun and Hall, 2009.

The body wall is made up of tough but flexible collagenous cuticle, which is secreted by the underlying hypodermis. Somatic musculature is striated and attached to the hypodermis forming long strips. Relaxation and contraction of these longitudinal strips cause the sinusoidal movement observed in *C. elegans* (Riddle *et al*., 1997). Muscles in the pharynx, vulva and excretory system are non-striated and contain only one sarcomere, in contrast to body wall muscle which may contain several (Altun and Hall, 2009). Food is ingested through the mouth where it is ground up in the pharynx. The pharynx is separated from the outer body wall and has its own basal lamina, muscles and nerves. Food passes through the intestinal pharyngeal valve into the intestine, which is essentially a tube composed of 20 cells with a central lumen at the end of which is the rectal valve (Altun and Hall, 2009). The adult *C. elegans* nervous system is divided into the somatic nervous system made up of 282 neurons and the pharyngeal nervous system containing 20 neurons (Altun and Hall, 2009).

1.2.3 Sexual dimorphism

C. elegans exist in nature as XX hermaphrodites or XO males. Hermaphrodites produce sperm and oocytes and can self-fetilize. If males are present they will mate with hermaphrodites and their sperm will outcompete hermaphrodite sperm (Ward and Carrel, 1979). Males are rare and arise from non-disjunction in hermaphrodite mothers at a frequency of 0.02% (Brenner, 1974a). The two sexes differ from each other in anatomy and behaviour and can be distinguished from early larval development. Many *C. elegans* tissues exhibit sexual specialization, which occurs in response to the global sex determination pathway (Zarkower, 2006). Differences can be observed in the musculature and neurons in response to reproductive needs, such as male mating and egg-laying behaviour (Riddle *et al.*, 1997; Zarkower, 2006).

Hermaphrodites and males can be distinguished from each other under a dissecting microscope by using gross morphological differences. Males are thinner and shorter than hermaphrodites. Their gonads consist of a single J- shaped arm, which appear be clear and their tails contain the copulatory apparatus (Lints and Hall, 2009a). The main distinguishing factor is the copulatory apparatus in the tail, which arises from an extension of the cuticle to create the fan made up of 9 pairs of sensory rays. The proctodeum is located after the intestine, it contains the cloaca and protruding spicules which probe and latch on to the vulva (Lints and Hall, 2009b) (Figure 1.3 A). Males are very active in their search to mate, whereas hermaphrodites are sexually passive. When the male tail comes in contact with a hermaphrodite it begins to move backwards while pressing its ventral side against the hermaphrodites body to locate the vulva. Once the vulva has been located they use their spicules to transfer sperm (Riddle *et al.*, 1997).

Hermaphrodites have a U-shaped bilaterally symmetrical gonad consisting of two arms that produces both sperm and oocytes Compared to age-matched males they are longer and wider, which could be a result of their larger gonads and presence of embryos. They can be distinguished under a dissecting microscope by their simple, pointed tail, and the presence of a vulva and eggs (Figure 1.3 B).
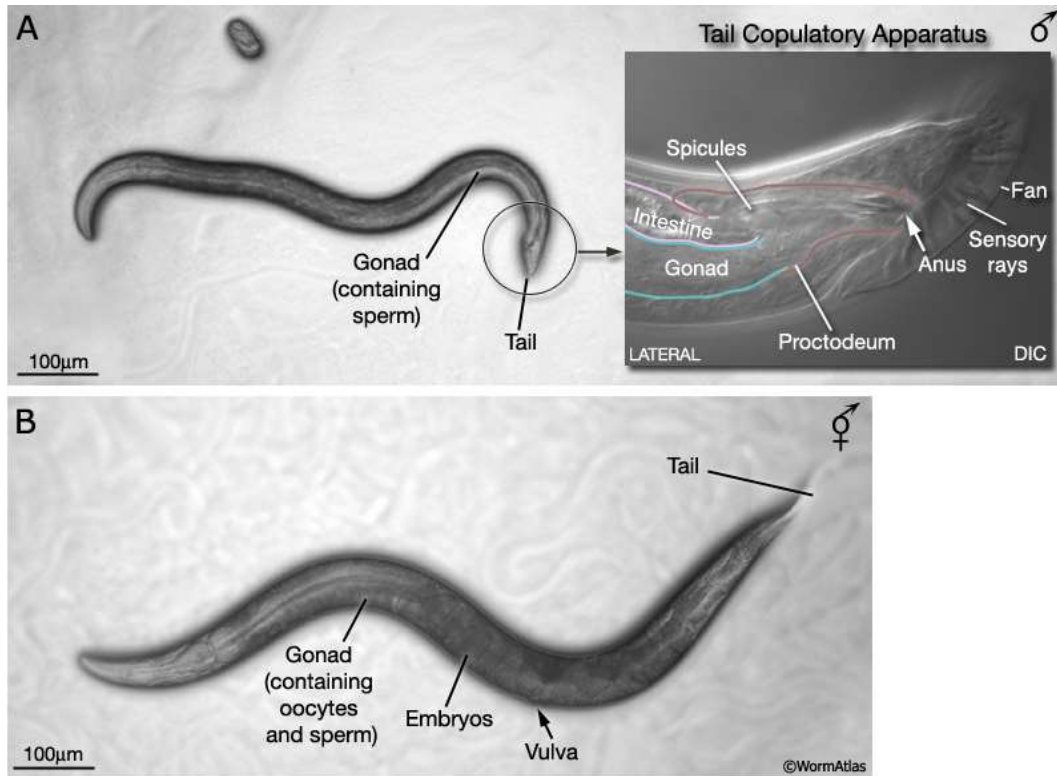
Figure 1.3 Hermaphrodite versus male anatomy. A) Male worms are long and thin compared to age-matched hermaphrodites and can be identified by presence of the tail (copulatory apparatus). B) By comparison hermaphrodites are larger and have a pointed tail. Hermaphrodite worms have a visible vulva and embryos. Image reproduced from Lints and Hall, 2009.

1.2.4 *C. elegans* life cycle

The *C. elegans* life cycle is similar to that of other nematodes in that it comprises a series of larval stages which progress by moults where the cuticle is shed and a new stage-specific cuticle is synthesized by the hypodermis. The *C. elegans* life cycle comprises the embryonic stage followed by 4 larval stages (L1, L2, L3 and L4) culminating in adulthood. The progression from egg to adult takes approximately three days at 20°C, but varies with temperature. Post-embryonic development begins with food intake, in the absence of food worms arrest at the L1 stage until supplied with food where they will proceed through development normally. If environmental conditions are not favourable such as low food, overcrowding and high temperature *C. elegans* can enter an alternative larval stage known as dauer. The decision to enter this alternative dauer stage

occurs during late L1 and thus worms progress through an alternative L2 stage knows as pre-dauer or L2d. If conditions improve L2d worms progress to L3, otherwise they progress to form dauer (Altun and Hall, 2009). Dauer larvae are morphologically and behaviourally distinct from other larval states. Dauer larvae are very thin, long and have a thicker cuticle. They have no pharyngeal pumping and reduced locomotion, increased lipid, and are resistant to desiccation (Cassada and Russell, 1975). These traits help confer dauer larvae with exceptional resistance to noxious conditions, e.g. by sheltering their internal environment from toxins. Dauer larvae can survive up to 4 months without food and appear to be non-ageing, since the length of time spent in dauer does not affect post-dauer life span or fertility (Klass and Hirsh, 1976).
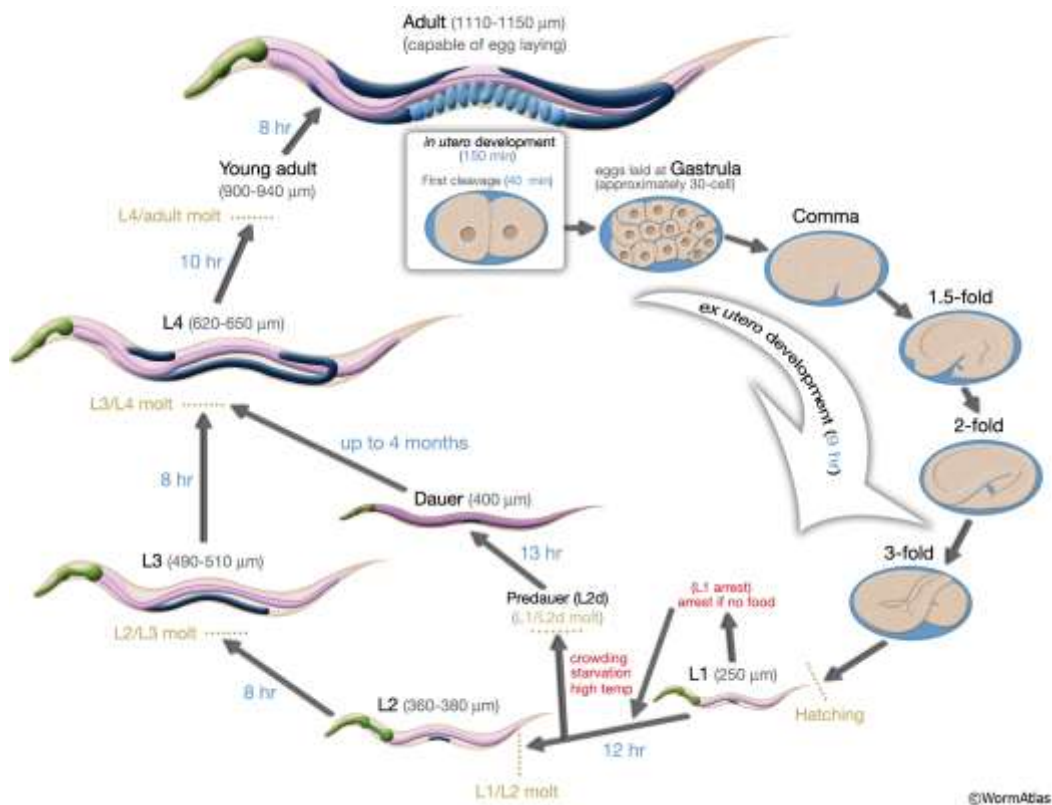
Figure 1.4 *C. elegans* **life cycle at 22˚C.** This diagram shows the development of *C. elegans* from egg to adulthood. Arrows indicate the time spent at each stage. Image reproduced from Altun and Hall, 2009.

1.2.5 Genetics and nomenclature

A simple, uniform genetic nomenclature for *C. elegans* was proposed in 1979 that was introduced by Brenner (Brenner, 1974a; Horvitz et al., 1979; Riddle et al., 1997). Most *C. elegans* mutants are derived from the Bristol N2 strain (Brenner, 1974a) which is referred to as the genetic wildtype. *C. elegans* nomenclature is as follows.

Genes names consist of three or four italicized letters, which usually refer to an observed phenotype discovered by mutational analysis. Genes with broadly similar phenotypic characteristics are differentiated from each other by a hyphen (-) followed by an Arabic number that corresponds to the order in which genes were discovered. For example, *egl-1* and *egl-2* are different genes that result in an egg-laying defect phenotype. Usually genes are followed by a roman numeral corresponding to its linkage group. Protein products of genes are denoted by using block capital letters of the relevant gene, for example DAF-2 for the protein encoded by the *daf-2* gene.

Mutations (alleles) are denoted using 1 to 3 italicized letters followed by an italicized Arabic number, e.g. *e1370* or *wu250*. The 1 to 3 letter code specifies the laboratory of origin and is registered with CGC, e.g. the Gems lab code is *wu*. If a mutant allele has been specified in an account of the work, it can be sufficient to use the gene name to refer to the allele; e.g. *ced-3(n717)* may be subsequently refereed to as *ced-3*. Special characteristics of a mutation may be annotated as a non-italicized suffix after the allele; e.g. *e1370*ts, where ts refer to temperature sensitive. Wildtype alleles can be indicated by a plus sign (+), e.g. *daf-2* (+). Animals carrying more than one mutation have genes listed by linkage group separated by semicolons, e.g. *daf-2(e1370) III*; *daf-13(m66) X*. To specify differences between homologous chromosomes in heterozygote animals genes are separated by a forward slash (/). If both chromosomes contain a mutation this can be annotated as *unc-32/dpy-18*, if the mutation is only present on one chromosome it would be *unc-32*/+. Transformations of *C. elegans* by introducing DNA may lead to transmissible extra-chromosomal arrays or chromosomally integrated arrays. Transgenes are annotated in a similar manner to gene mutations. First there is the 1-2 letter lab code followed by whether the array is extra chromosomal (*Ex*) or integrated (*Is*) and a description of the transgene in brackets, e.g. *wuEx166[rol-6(su1006)]*.

A strain corresponds to a group of animals of a specific genotype with the capability of producing progeny with the same genotype. Strain numbers are given by using 2 or 3 uppercase letters followed by an Arabic number. The letters in a strain name correspond to a laboratory, e.g. GA is the Gems lab letter code.

1.2.6 RNA interference mechanism

Forward genetics is an approach through which worms are treated with a mutagen and animals with a desired phenotype are selected to identify the mutation affecting the trait of interest. In reverse genetics, a gene sequence is already known and can be used to disrupt gene function and study its effects on phenotype. Reverse genetics can de performed in *C. elegans* by perturbing gene function by gene deletion or RNA-mediated interference (RNAi) (Ahringer, 2006). Gene inactivation using RNAi is inexpensive and less labour intensive than gene deletion and as such is a particularly powerful tool to study gene function.

RNAi is a non-permanent technique that reduces gene expression by introducing double stranded RNA (dsRNA) which causes the degradation of its target mRNA (Timmons and Fire, 1998). This RNAi mechanism was first discovered in *C. elegans* in 1998 and has since become an invaluable tool in cell biology (Fire *et al*., 1998). The RNAi mechanism of action involves the detection of exogenous dsRNA by the endonuclease Dicer which cleaves dsRNA to form small interfering RNAs (siRNA). The siRNAs are unwound and associate with the RNA-induced silencing complex (RISC) acting as a guide to target the protein complex to the appropriate mRNA sequence for degradation (Figure 1.5) (Azorsa et al., 2006).

RNAi can be performed in *C. elegans* by injection of dsRNA, soaking in a solution containing dsRNA or feeding worms *E. coli* which produces the dsRNA for the gene of interest (Fire et al., 1998; Tabara et al., 1998; Timmons and Fire, 1998). Gene silencing by RNAi in *C. elegans* is both systemic and heritable (Fire *et al*., 1998). RNAi allows rapid and effective gene inactivation, which can be performed at different developmental stages. This allows scientists to study when a specific genes activity is necessary. It also allows inactivation of genes that are essential during early development, for which

mutations would be lethal, in later life. In this thesis we use the feeding protocol due to its simplicity and the availability of a feeding clone library (Kamath and Ahringer, 2003) kindly provided by S. Nurrish.
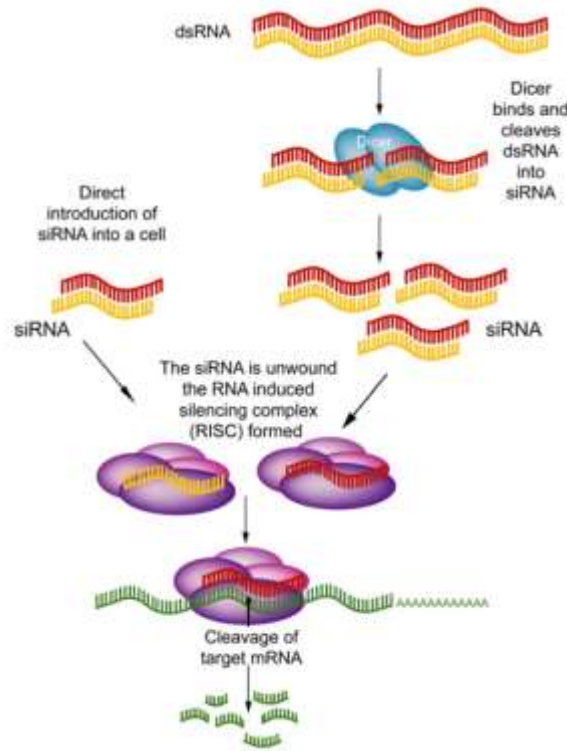
Figure 1.5 RNAi mechanism. Schematic representation of RNAi in *C. elegans.* Double stranded RNA (dsRNA) is digested into small interfering RNAs (siRNA) by the enzyme Dicer. Unwound siRNA form the RNA induced silencing complex (RISC) complex, which targets complimentary mRNA for degradation. Figure reproduced from Azorsa *et al* 2006.

1.3   Longevity pathways

1.3.1 Discovery of long lived mutants

Ageing is not an adaptive trait and is deleterious to the survival of the individual. This implies that it is not programmed in the sense that development is. This led to the assumption that there are no genes for ageing. It was not until the last few decades that the genetics of ageing was properly studied, and interest was sparked by a study published by Michael Klass in 1983. Klass conducted a genetic screen using ethyl methanesulphonate (EMS) and surprisingly was able to isolate long lived mutants (Klass, 1983). However, amongst the long lived mutants he discovered several had decreased pharyngeal pumping so he concluded that their longevity was due to dietary restriction effects and that longevity genes must be extremely rare, if they exist at all (Klass, 1983). Tom Johnson continued to experiment on these mutants and found that by backcrossing

them with wildtype males the feeding defect could be separated from the longevity (Age) phenotype (Johnson, 1986). The Age phenotype was found to be caused by the recessive mutation *age-1(hx546)* which results in a lifespan extension of 40-65% and also reduced fertility (Friedman and Johnson, 1988). However, the possibility remained that the Age phenotype could be caused by the 75% reduction in fertility and not by reducing programmed ageing functions (Friedman and Johnson, 1988; Kenyon, 2011).

A study from the lab of Cynthia Kenyon examined temperature sensitive mutations which induce dauer formation and found that mutations in *daf-2* result in active, fertile hermaphrodites that live twice as long as wildtype even in the absence of a gonad (Kenyon et al., 1993). This proved that despite the low fecundity observed in *daf-2(e1370)* mutants its longevity is not dependent on it. A later study examined many *daf-2* alleles and found that they can be separated into two classes based on behavioural defects and that reduced feeding and fertility can be uncoupled from the Age phenotype (Gems *et al*., 1998). The study by Kenyon *et al* also found that the longevity bestowed by *daf-2(e1370)* was dependent on DAF-16 (Kenyon et al., 1993) which is also required for dauer formation (Riddle et al., 1981). Lifespan extension in *age-1(hx546)* was also found to require DAF-16, suggesting they were part of the same pathway (Dorman et al., 1995). It has since been discovered that DAF-2, AGE-1 and DAF-16 are components of the insulin/IGF-1 signalling (IIS) pathway in *C. elegans*.

1.3.2 Insulin/IGF-1 signalling in *C. elegans*

The first gene in this pathway to be indentified was *age-1*, which encodes the *C. elegans* homologue of the catalytic subunit of the phosphatidylinositol-3-OH kinase (PI(3)K), which generates phosphatidylinositol (3,4,5)-triphosphate (PIP3) (Morris et al.1996). *daf-2* was found to encode the *C. elegans* homolog of the insulin and IGF-1 receptors (Kimura, 1997). This was an important finding because it meant that conserved hormonal cues involved in nutrient sensing were also part of the ageing process (Kenyon, 2011). Cloning of *daf-16* revealed it to be a member of the FOXO family of forkhead transcription factors (Kenyon et al., 1993; Lin et al., 1997; Ogg et al., 1997). When DAF-2 is ligand bound it activates AGE-1 initiating a phosphorylation cascade involving AKT-1, AKT-2 and SGK-1 protein kinases resulting in the phosphorylation of DAF-16 (Hertweck *et al*, 2004; Paradis and Ruvkun, 1998). SGK-1 is crucial in mediating stress

responses, development and lifespan regulation, while AKT is necessary for regulating dauer formation (Hertweck *et al*, 2004).When DAF-16 is phosphorylated it cannot translocate to the nucleus and regulate its target genes (Lin et al., 2001). Disruption in the IIS pathway by mutations in *daf-2* or *age-1* allows DAF-16 to enter the nucleus and regulate its target genes resulting in increased lifespan (Figure 1.6).

The discovery that DAF-16 is a transcription factor that could regulate lifespan in *C. elegans* provoked a search for the DAF-16 gene targets that cause lifespan extension (Kenyon, 2011). Microarray data implies that DAF-16 regulates expression of as many as 10% of *C. elegans* genes and RNAi knockdown of regulated genes, can cause small changes in lifespan (McElwee et al., 2004; Murphy et al., 2003; Partridge and Gems, 2006). Evolutionary theory predicts that single genes will not evolve to cause ageing; however, a single mutation can have large effect on lifespan by regulating many genes at once each of which contributes small effects (Partridge and Gems, 2006).
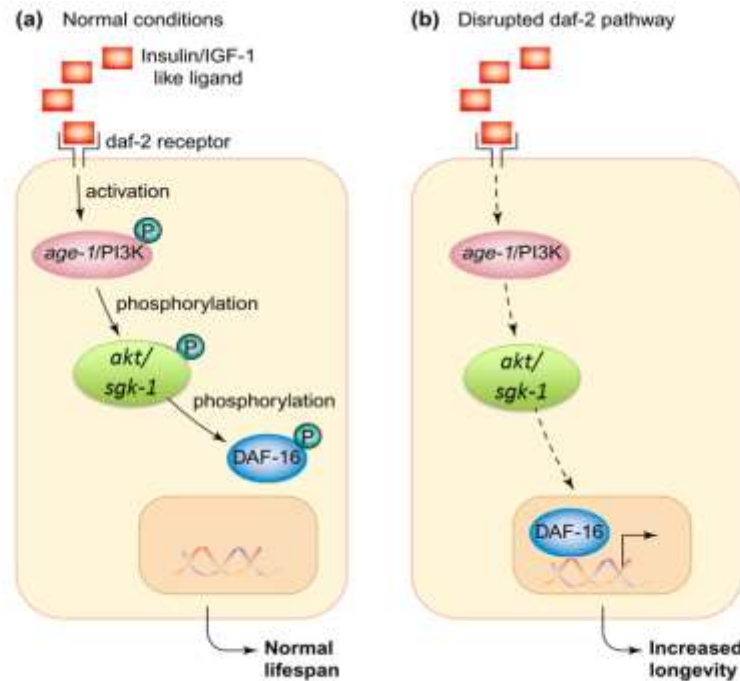
Figure 1.6 IIS pathway in *C. elegans*. a) Insulin-like ligands bind to the DAF-2 receptor activating a signalling cascade resulting in the phosphorylation of DAF-16 and its nuclear exclusion. b) When no ligands are bound, or there is a disruption in binding to DAF-2, DAF-16 is dephosphorylated and may translocate to the nucleus where it can regulate its target genes, increasing longevity. Figure reproduced and modified from Carter *et al*, 2002.

1.3.3 TOR signalling pathway

A soil sample collected from Easter Island in the 1970s contained the bacterium *Streptomyces hygroscopicus* that produces a strong anti-fungal metabolite. This metabolite, now called rapamycin, was found to inhibit cell division of mammalian cells and this intriguing effect prompted further studies on this compound (Wullschleger et al., 2006). The genes TOR1 and TOR2 (Target of Rapamycin) which regulate the toxic effects of rapamycin were first discovered in yeast (Heitman et al., 1991). All eukaryotic cells, from slime molds to mammals, have since been shown to have at least one TOR complex (Wullschleger *et al*., 2006) and mutations in the TOR pathway increase lifespan in model organisms (Evans et al., 2011). The TOR kinase promotes cell growth in response to nutrient cues whilst blocking cell maintenance processes such as autophagy (Kenyon, 2010).

TOR belongs to a family of kinases known as phosphatidylinositol kinase-related kinases (PIKK) (Wullschleger *et al*., 2006). The TOR protein is located in the centre of the signal transducing pathway and receives imputs from several other pathways which are relayed through TOR to regulate apoptosis, stress resistance, autophagy and protein translation (Evans *et al*., 2011). Thus, the TOR pathway is interconnected with other signalling pathways such as IIS forming a network (Gems and Partridge, 2013). Akt which is a kinase in the IIS pathway phosphorylates TOR/LET-363 antagonist proteins to allow Raptor/DAF-15 to form a complex with TOR (Jia et al., 2004; Kapahi et al., 2010). Once the TOR complex 1 (TORC1) is formed it activates its downstream target ribosomal p70 S6 protein kinase (S6K) which regulates protein translation (Kapahi *et al*., 2010). Inhibition of the *C. elegans* S6K homologue RSKS-1 can extend lifespan, reduce fecundity, inhibit growth and reduce protein translation (Hansen et al., 2007; Pan et al., 2007). TOR activation inhibits the activity of 4E-BP which antagonizes the translation initiation factor eIF4E, thus promoting protein translation and growth under nutrient rich conditions (Hay and Sonenberg, 2004; Sonenberg and Gingras, 1998) (Figure 1.7). However, to date no homologue of 4E-BP has been found in *C. elegans* (Syntichaki et al., 2007).
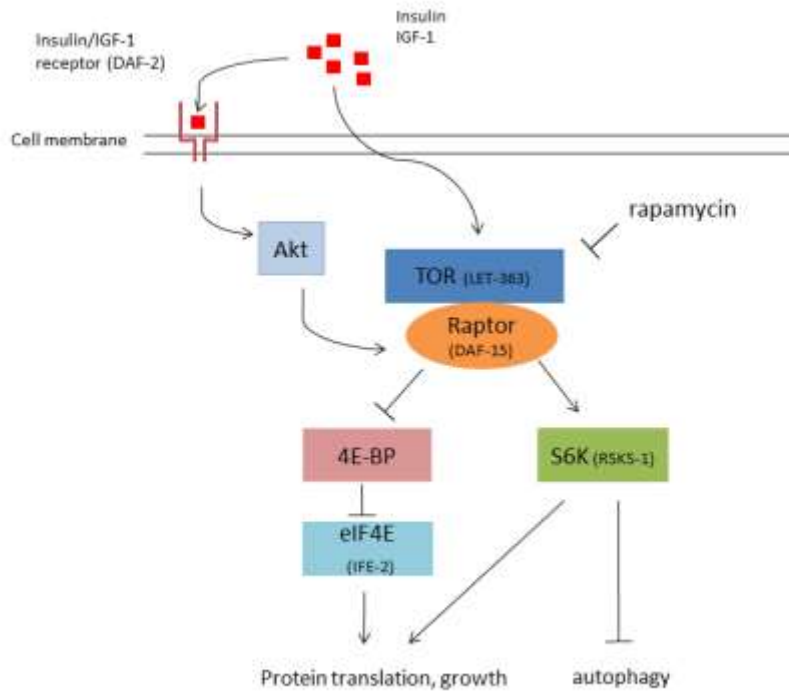
Figure 1.7 TOR signalling pathway. Simplified representation of the TOR pathway with *C. elegans* protein homologues labelled in parenthesis. Under conditions of nutrient availability TOR1 is activated forming a complex with Raptor (TORC1). TORC1 activates S6K by phosphorylation. TORC1 results in e1F4E being released from inhibition to initiate protein translation. If food is available the TOR pathway promotes protein translation and growth and blocks autophagy.

1.4   Lifespan regulation by nutritional and reproductive cues

The evolutionary theory proposes that trade-offs exist between reproduction and longevity (Ljubuncic and Reznick, 2009). In this section we discuss the effect of reproduction and nutrition on longevity.

1.4.1 Ageing and reproduction

The disposable soma theory sees ageing as the result of a trade-off between reproduction and somatic maintenance (Kirkwood and Holliday, 1979). Support for this notion comes from observations in animals that die shortly after reproduction (e.g. Pacific salmon) and a common thread among longevity mutants (IIS and TOR), which often have

lower fertility. However, there are examples in nature that seem to contradict the notion that reproduction will necessarily cause an organism to age. For instance, guppies in an environment where predation is removed as the main extrinsic hazard have higher fecundity and a longer lifespan, suggesting a short lifespan is not a necessarily the result of a trade-off with increased fecundity (Kenyon, 2005; Reznick et al., 2004). Furthermore, *C. elegans* longevity and low fecundity can also be uncoupled in some *daf-2(-)* mutant strains, which can also extend the reproductive period (Gems et al., 1998; Kenyon, 2010). Thus, it is possible to attain a long life without lowering reproductive capacity.

In *C. elegans* removal of the entire gonad does not affect lifespan in wildtype worms (Kenyon et al., 1993), but laser ablation of germ cell progenitor cells does (Hsin and Kenyon, 1999). Thus, an empty gonad appears to emit a pro-longevity signal which can extend lifespan by up to 60% (Hsin and Kenyon, 1999). The extended lifespan in these germline-less worms is DAF-16 dependant, the loss of which completely abrogates the longevity effect (Hsin and Kenyon, 1999). The loss of germ cells results in an increase in nuclear localization of DAF-16 in the intestine (Lin *et al*., 2001). Intestinal rescue of DAF-16 in *daf-16(-)* germline-less mutants is enough to rescue around half of the longevity phenotype, indicating that DAF-16 activity in the intestine is the main site promoting lifespan extension in germline-less worms (Libina et al., 2003). A similar up regulation in FOXO activity was observed in *Drosophila melanogaster* following elimination of germ cells (Flatt *et al*., 2008). The somatic gonad, sensing a lack of germ cells, may send signals that increase longevity by modulating the IIS pathway to make the organism 'wait' until reproduction can begin (i.e. to promote reproductive diapause) (Yamawaki et al., 2008).

Germline-less worms are also resistant to oxidative stress, implying that longevity in these worms could be the result of increased detoxification processes (Arantes-Oliveira et al., 2002). However, removal of both the somatic gonad and the germline also confers stress resistance without the benefit on a longer life, implying that stress resistance does not account for the longevity induced by germline removal (Yamawaki *et al*., 2008).

31

1.4.2 Dietary restriction and longevity

During the great depression there was a concern that prolonged food shortages could have long term detrimental effects on human lifespan (Kenyon, 2010). The potential effect of DR on human lifespan was attempted to be addressed by experiments in rats. Surprisingly, studies using rats found the opposite to be true. Mice that were fed a diet of restricted calories where all other essential vitamins and minerals were supplied, had retarded growth but lived approximately 30% longer than mice fed ad libitum (McCay et al., 1935; Weindruch and Walford, 1988). While chronic malnutrition shortens lifespan, a moderate dietary restriction (DR) can provide health benefits and increased longevity. The effects of DR have been tested in other organisms ranging from yeast to primates and extension in lifespan was seen in most cases, perhaps reflecting evolutionary conservation (Houthoofd et al., 2007; Piper et al., 2011). If an organism can modulate its lifespan in response to nutritional cues this could tie in nicely with the lifespan extension observed in mutations in the IIS and TOR pathways, which are also nutrient sensitive.

The mechanisms that lead to the lifespan benefits observed under dietary restriction are still unknown. A possible mechanism is that during times of scarcity resources are allocated to preserve the soma in lieu of reproduction, this would provide a useful strategy allowing the organism to survive now and reproduce later (Holliday, 1989) Consistent with this, rodents under dietary restriction have reduced fecundity (Weindruch and Walford, 1988). Rodents under DR exhibit less incidence of cancer and autoimmune disease, in addition to an increase in heat shock factor suggesting the possibility that stress response is activated under DR (Heydari et al., 1993; Weindruch et al., 1986). Another hypothesis links DR with the free radical theory by proposing that animals subjected to DR have lower production of reactive oxygen species (ROS), which might occur due to decreased mitochondrial respiration accompanying a DR-induced decrease in metabolic rate (Sohal and Weindruch, 1996).

1.5 Mechanisms of ageing

The ultimate causes of ageing, as explained by the evolutionary theory, provide a plausible account for the emergence of ageing; but its proximate cause, or mechanism of

action, remain unknown (Gems and Partridge, 2013). In the following section we will present a widely accepted mechanistic theory and discuss its shortcomings. We will then discuss a new theory that integrates the proximate and ultimate causes of ageing.

1.5.1 The oxidative damage theory of ageing

The free radical theory of ageing is a prominent mechanistic theory of ageing that was originally proposed by Denham Harman. He proposed that free radicals produced during normal metabolic processes within cells cause damage which accumulates with time and causes ageing (Harman, 1956). As the organism progresses in age, its innate antioxidant defences fail to counteract the increase in oxidative damage (Viña *et al*., 2007). This theory has since developed into the oxidative damage theory of ageing; reactive oxygen species (ROS) such as superoxide (O_2^-) and hydrogen peroxide (H_2O_2) are by-products of mitochondrial respiration and other metabolic processes, which cause damage to cellular constituents. This molecular damage accumulates over time, causing ageing (Sohal and Weindruch 1996; Beckman and Ames 1998).

The oxidative damage theory makes a number of predictions: 1) Molecular damage caused by ROS accumulates with time. 2) Antioxidant mechanisms should increase lifespan by reducing ROS and thus, molecular damage. 3) Long-lived animals have extended lifespan due to decrease of molecular damage (Sohal and Weindruch, 1996). Many experimental results support the theory. For example, protein oxidation levels do increase with age (Adachi et al., 1998). Furthermore, levels of ROS generation the mitochondria is doubled in ageing flies (Sohal and Sohal, 1991). Long-lived insulin/IGF-1 signalling (IIS) mutants are resistant to oxidative stress and have increased antioxidant activity, lending further support for the theory (Honda and Honda, 1999; Vanfleteren, 1993). The increase in lifespan in these animals has long been thought to be a direct result of increased ROS detoxification.

The oxidative stress theory of ageing is an attractive model because it is consistent with common sense (all things decay), supported by experimental data, and suggests the possibility of simple interventions in the form of antioxidant supplementation (Viña *et al*., 2007). However, problems arise when the role of antioxidant defence in ageing is put to the test. This can be done experimentally by examining effects of manipulation of antioxidant defence on damage and ageing. If the

presence of ROS and its induced damage are the limiting factor for longevity one would expect that reducing antioxidant defence would lead to increased molecular damage and thus a shortened lifespan (Gems and Doonan, 2009). Some studies have found this to be the case. For example, increasing oxygen concentrations should cause an increase in ROS production. Worms treated under 60% oxygen, as expected, show reduced lifespan (Adachi et al., 1998; Honda et al., 1993). However, reduction of lifespan by hyperoxia may be reflecting a toxic effect in worms, and may not be indicative of normal ageing, consistent with this, worms under 40% oxygen were not short lived (Adachi et al., 1998; Honda et al., 1993).

On the other hand, decreasing ROS should cause a decrease in molecular damage, resulting in a longer-lived organism. The discovery of antioxidant enzymes allowed this prediction to be put to the test. To examine the role of endogenous antioxidant enzymes a number of studies used superoxide dismutase (SOD). For example, in *C. elegans* deletion of antioxidant gene *sod-2* while increasing susceptibility to superoxide and increasing molecular damage has no effect on lifespan (Doonan *et al*., 2008) or may even increase it (Van Raamsdonk and Hekimi, 2010). Additionally, effects of chemical treatments that increase ROS levels have been studied. Exposure to low levels of ROS-generators such as 40 μM juglone (Heidler et al., 2010) and 0.1 mM paraquat (Yang and Hekimi, 2010a) can actually extend lifespan in *C. elegans*.

Tests on antioxidant supplementation in worms have garnered mixed results. For example, vitamin E supplementation increased *C. elegans* lifespan in two out of three studies (Harrington and Harley, 1987; Ishii et al., 2004; Schulz et al., 2007). The antioxidant vitamin C did not have any effect on *C. elegans* lifespan in two studies (Schulz et al., 2007; Yang and Hekimi, 2010a). Administration of synthetic catalytic antioxidants, EUK-8 and EUK-134 (SOD mimetics), increased SOD activity in vivo and increased resistance to paraquat in *C. elegans* (Keaney et al., 2004; Sampayo et al., 2003). One group reported that EUK-8 and EUK-134 increased lifespan in wildtype worms by up to 54% (Melov *et al*., 2000); however four other studied saw no increase in lifespan (Keaney and Gems, 2003; Keaney et al., 2004; Kim et al., 2008; Uchiyama et al., 2005). In fact, at higher concentrations SOD mimetics shortened lifespan in a dose dependent manner (Keaney and Gems, 2003; Keaney et al., 2004; Kim et al., 2008).

The many studies that fail to support the oxidative damage theory suggest that ageing occurs by a mechanism other that ROS-induced damage. This opens the door to explore new possible theories to explain ageing in *C. elegans*.

1.5.2 New theory: Ageing as hyperfunction

An interesting theory by Mikhail Blagosklonny that provides an alternative to the oxidative damage theory was presented in a series of review papers (Blagosklonny, 2006, 2007, 2008). In them he proposes that whilst oxidative damage does occur, it is largely a consequence of ageing and not its cause. He also proposes that unregulated biosynthesis or "hyperfunction" is driven by growth promoting pathways such as the insulin/IGF-1 signalling (IIS) and target of rapamycin (TOR) pathways which promote early life fitness (Blagosklonny 2008). The idea of hyperfunction being the cause of ageing can be integrated conceptually with the antagonistic pleiotropy theory. The same processes that promote early life fitness in an individual also lead to its demise with increasing age, in this case, because evolution fails to switch-off these processes.

Blagosklonny takes a stab at answering a long-standing conundrum in the ageing field: Is ageing, a deleterious process, programmed? He proposes that ageing is not programmed but 'quasi-programmed' in that it is genetically programmed, but is not programmed in the sense of being an adaptation (Figure 1.8 B). He illustrates the idea of quasi-programme with an analogy: "if you left water running after taking a bath, then a 'program' for filling the bathtub would become a 'quasi-program' to flood your apartment" (Blagosklonny 2007). These developmental and reproductive programmes become quasi-programmes, which promote excess biosynthesis, or continuation of other needless processes, leading to hypertrophic pathologies associated with ageing. No programme has emerged to cause ageing because in the wild, most animals do not live long enough to age due to death from extrinsic hazards. Thus, ageing is the result of failure to optimally modulate fitness promoting programs in later life. Quasi-programmed ageing can be reconciled with the evolutionary theory because these are late-life side-effects of early fitness promoting programmes that have been selected for and therefore have no intended purpose (Blagosklonny 2007).

Blagosklonny also provides an explanation for the effect of dietary restriction on lifespan. Longevity observed in animals subjected to DR has been previously explained

in terms of the disposable soma theory as the result of diversion of energy away from reproduction towards somatic maintenance, in order to survive now for the possibility to reproduce later (Shanley and Kirkwood, 2000). Blagosklonny argues that reducing resource availability for somatic maintenance by DR should, according to the disposable soma theory, shorten lifespan (Blagosklonny, 2007, 2008). Moreover, trials in *Drosophila* manipulating amino acid composition during dietary restriction have been able to restore fecundity to levels similar to control fully fed animals without reducing longevity (Grandison et al., 2009). Mutations that inhibit the IIS and TOR pathways cause lifespan extension across different species (Kapahi et al., 2010; Kenyon, 2010). TOR has also been implied to have a role in mediating the dietary restriction response (Bishop and Guarente, 2007; Mair and Dillin, 2008). An alternative to the disposable soma theory interpretation is that the extended lifespan observed under dietary restriction is caused by reduced activity of these pathways (particularly TOR), resulting a decreased hyperfunction (Blagosklonny, 2007, 2008).

Inhibition of TOR leads to reduced protein translation and increased autophagy. Several studies in *C. elegans* have shown that decreased mRNA translation can increase lifespan (Hansen et al., 2007; Pan et al., 2007). Moreover, lifespan extension by dietary restriction, IIS and TOR pathway mutants requires autophagy in *C. elegans* (Hansen *et al*., 2008). The oxidative stress theory suggested that autophagy could promote longevity by increasing somatic maintenance by removing damaged proteins, but it provides no simple explanation for why inhibition of protein synthesis extends lifespan (Gems and de la Guardia, 2013). The hyperfunction theory proposes that TOR, which increases protein synthesis and decreases autophagy, promotes biomass production thereby promoting hypertrophy and hyperplasia (Blagosklonny, 2008). When food is scarce TOR signalling is reduced which causes an increase in autophagy and decreased protein translation both of which increase lifespan (Hansen et al., 2007, 2008). Autophagy promotes longevity by removing excess biomass preventing hyperfunction rather than removing damaged molecules, as previously supposed (Blagosklonny, 2008). Reduced protein synthesis slows the emergence of diseases of hyperfunction by reducing biomass (Blagosklonny 2008) (Figure 1.8 A).
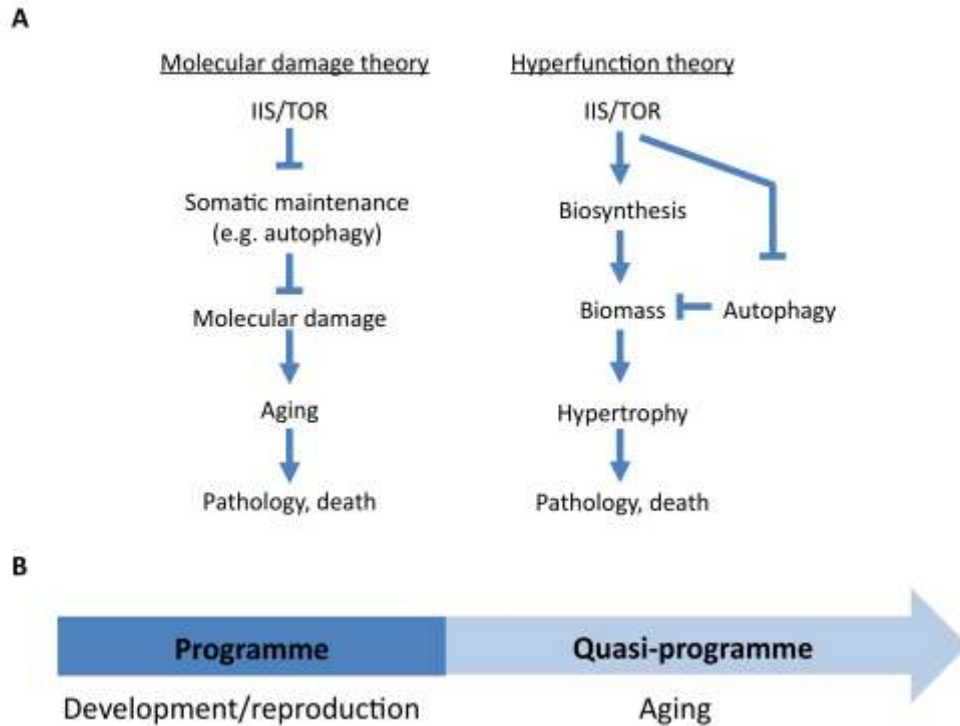
Figure 1.8 Representation of the hyperfunction theory. A) Simplified diagram of how IIS and TOR promote ageing as explained by the molecular damage and hyperfunction theories of ageing. B) The hyperfunction theory proposes that the same developmental and reproductive programs promoting early life fitness become quasi-programs during ageing due to failure to "switch-off" these mechanisms. A) Figure reproduced and modified from Gems and de la Guardia 2013.

1.5.2.1   Evidence of hyperfunction in *C. elegans*

Despite being vastly studied, the mechanism by which *C. elegans* age is not known. During ageing many anatomical changes can be observed in old worms, some of which are clearly pathological (Figure 1.9). Is it possible that the cause of death in this organism can be traced back to hyperfunction? We reviewed the *C. elegans* literature and found the following age-related changes which are consistent with hyperfunction-driven pathology (Gems and de la Guardia, 2013) (Figure 1.9, Appendix 2).

The reproductive system undergoes notable changes after reproduction stops. At about day 5 of adulthood hermaphrodite worms run out of sperm, causing reproduction to cease (Ward and Carrel, 1979). However, oocyte production is not tightly regulated with sperm availability and oocytes continue to be produced and are laid unfertilized (Ward

and Carrel, 1979). This continuation of oocyte production results in a two-fold increase in oocytes in the gonad and these excess oocyte become stacked (i.e. increase in number and density) inside the proximal gonad (Jud et al., 2007). Additionally, post-reproductive worms develop large uterine tumours (McGee *et al*., 2011). These tumours have increased DNA content and are thought to be a result of endoreduplication in unfertilized oocytes (Golden *et al*., 2007). Changes observed in the gonad of post-reproductive hermaphrodite adults are consistent with the idea of quasi-programmed hyperfunction.

The nervous system of *C. elegans* was thought to maintain its integrity throughout old age (Garigan *et al*., 2002). However, it was recently discovered that neurons develop new branches in older worms (Pan et al., 2011; Tank et al., 2011). These additional extensions or branches correlate with age and decreased motility (Tank *et al*., 2011). These neuronal outgrowths are another potential example of hyperfunction in ageing worms.

The cuticle in older worms has been observed to increase in thickness up to ten-fold in certain areas with respect to young worms (Herndon *et al*., 2002). One possibility is that this increase in cuticle thickness is due to continued synthesis of collagen by the hypodermis (Herndon *et al*., 2002). Such cuticular hypertrophy is yet another potential example of hyperfunction.

Yolk and lipid distribution changes in old worms. Vitellogenins are yolk proteins encoded by genes *vit-1* through *vit-6* (Spieth et al., 1985). Vitellogenins are synthesized in the intestine and transported to the gonad where they are taken up by oocytes (Kimble and Sharrock, 1983). In early adulthood yolk is observed in the intestine and oocytes, however after sperm depletes yolk is observed throughout the body cavity (Garigan *et al*., 2002; Herndon *et al*., 2002). This increase in yolk observed in old worms suggests that yolk production is not regulated post-reproduction (Herndon *et al*., 2002). Lipid inclusions have been observed in muscle, intestine, and hypodermal tissue in ageing worms (Herndon *et al*., 2002). Inclusion of lipid in these tissues may reflect the redistribution of yolk to the body cavity. Vitellogenins in *C. elegans* have domains homologous to human low-density lipoprotein (LDL) apoB-100 (Baker, 1988a), which contribute to atherosclerosis. Accumulation of lipid in non-adipose tissue in mammals is thought to be responsible for metabolic syndrome observed in obese individuals (Unger

and Scherer, 2010; Virtue and Vidal-Puig, 2008). Thus, hyperfunction of yolk could possibly contribute to age-related mortality by causing lipotoxicity in the worm (Ackerman and Gems, 2012).
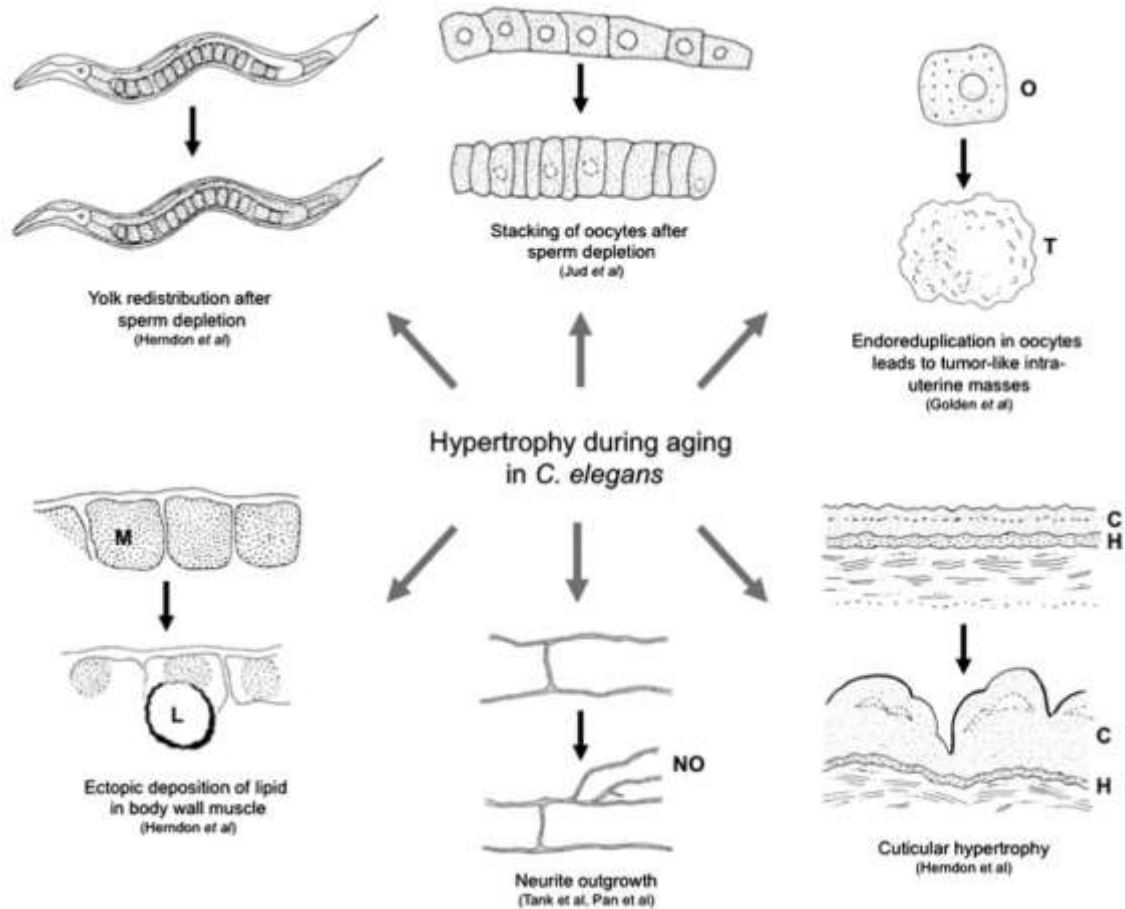
Figure 1.9 Examples of age-related hypertrophy in ageing *C. elegans.* Representations of previously published data (referenced under each figure) on age-related phenomena in ageing hermaphrodites (clockwise): yolk redistribution pattern after sperm depletion (shading represents VIT-2: GFP); Oocyte stacking in post-reproductive worms, Tumour-like growth in the uterus (O, oocyte; T, tumour); Hypertrophy in the cuticle (C, cuticle; H, hypodermis); Neurite branching (NO, neurite outgrowth); Lipid deposition in muscle (M, muscle; L, lipid). Image reproduced from Gems and de la Guardia 2013.

The hyperfunction theory provides a plausible explanation for the aforementioned anatomical changes in older worms. It is possible that molecular damage has a bigger role in ageing pathologies in mammals where cancer, which emerges at least in part through

DNA damage, is a big killer amongst the elderly (Gems and de la Guardia, 2013). However, in short-lived *C. elegans* where somatic tissues are post-reproductive DNA damage is not likely to be a major contributor to diseases of ageing. In support of this, adult *C. elegans* are highly resistant to UV radiation and ionizing radiation and lifespan was only shortened by very high doses (Johnson and Hartman, 1988; Klass, 1977). Thus, the hyperfunction theory might better explain *C. elegans* ageing pathologies. However, as this is a novel theory there should be more rigorous testing to establish its validity in both *C. elegans* and other model organisms.

1.6   Aims

The main goal of this thesis is to test ageing theories. To do this, I used the model organism *C. elegans* to conduct experiments due to its extensive use in biogerontology field and the wealth of available information on its biology and genetics. We took advantage of its transparency to examine age-related anatomical changes by observing ageing worms using differential interference contrast microscopy. This allowed us to study *C. elegans* age-related pathology and test possible mechanisms for their emergence.

One of the most widely accepted mechanistic ageing theories is the oxidative damage theory. However as previously discussed rigorous testing of this theory argues against it (see section 1.5.1). Problems with the oxidative damage theory sparked our interest in testing the novel hyperfunction theory of ageing to explain age-related changes in *C. elegans*. We focused on the following potential reproductive quasi-programmes: yolk protein accumulation and germline hypertrophy and atrophy. In chapter 3 we examine post-reproductive yolk synthesis and its accumulation in the body cavity of ageing *C. elegans* hermaphrodites. This has previously shown to not occur in IIS pathway mutants (DePina *et al*., 2011), which led us to test whether there is a link between yolk production and a pro-ageing phenotype. Chapters 4 and 5 focus on age-related changes that occur with ageing in the hermaphrodite germline. In chapter 4 we provide a detailed description of changes observed in the germline of ageing hermaphrodite *C. elegans*. Amongst these changes are the degradation of the reproductive organ – the gonad, the development of uterine tumour-like masses and the appearance of hypertrophic oocytes. In this chapter we propose a mechanism for gonad degradation, quasi-programmed

germline apoptosis. In Chapter 5 we examine gonad degeneration in greater detail and test its proposed causal mechanism.

During my PhD I supervised and worked in close collaboration three students: Ann Gilliat, Eleanor Tyler and Josephine Hellberg. Therefore, the data generated from these collaborations has been included in this thesis in order to give a clear account of the entire story. Results that were obtained by these students or came from collaboration with students has been clearly attributed to them throughout this thesis. With their help we were able to gain a greater understanding of the ageing phenomena studied here.

Chapter 2:   Materials and Methods

2.1   *C. elegans* maintenance and methods

2.1.1 Culture conditions

Worms were grown and maintained on 60mm Petri dishes containing nematode growth medium (NGM) seeded with (~100µl) OP50 *E. coli* as a food source (Brenner, 1974a). OP50 is an uracil auxotroph with limited growth on NGM agar, which allows for better visualisation of the worms. To avoid starvation individual worms were regularly transferred to fresh seeded plates using a thin platinum wire (worm pick), which is flame sterilized. Picking individual worms allows for the precise selection of worms based on their larval stage or other relevant quality desired.

The previous method is not ideal for quickly transferring a large amount of worms. An alternative technique is chunking, in which a small piece of agar is cut using a flame sterilized scalpel and transferred to a new plate.

2.1.2 Male stock maintenance

Male *C. elegans* occur at low frequency in wildtype populations (~0.02%). Picking L4 worms and mating with hermaphrodites at a 3 males: 1 hermaphrodite ratio maintained male populations. Males were also generated by heat shock in which L4 hermaphrodite worms are incubated at 30°C for 6 hours. For experiments performed using male worms, matings were set up on multiple NGM plates to get a high yield of males. After picking L4 males they were maintained in cohorts of 5 worms per plate to reduce life-shortening effects of homosexual mating behaviour (Gems and Riddle, 2000).

2.1.3 *C. elegans* brief mating protocol

Worms were mated as previously described (Gems and Riddle, 1996). Mating was performed by maintaining male stock plates and separating hermaphrodite and males at L4 onto separate plates and allowing them to reach adulthood overnight. Worms were

then placed in a ratio of 3 males: 1 hermaphrodite on NGM plates seeded with a small OP50 lawn (~2 cm width) to improve mating efficiency. Worms were allowed to mate for 3 hours before removing males from the plate. Mated hermaphrodites were transferred to fresh plates daily throughout their reproductive period.

2.1.4 Freezing and thawing stocks

C. elegans strains can be maintained as frozen stocks indefinitely. To freeze strains, animals were allowed to grow on 100mm diameter plates until they run out of food. Recently starved plates contain a large amount of worms at the L1 larval stage, which survive freezing successfully. Worms were washed off plates with M9 buffer and transferred to a Falcon tube and allowed to settle at the bottom by gravity. Supernatant was removed, leaving worm in 2ml of M9 buffer. An equal amount (2ml) of freezing medium (see section 2.6.2) was added to the Falcon tubes. The worms were aliquoted into microcentrifuge Eppendorf tubes (1.5ml) and placed at -80°C in metal freezing racks within a styrofoam box to slowly lower the temperature.

To recover frozen strains the desired vial was removed from the -80°C freezer and allowed to thaw at room temperature. The contents of the vial were placed on a seeded NGM plate and worms were allowed to recover and grow.

2.1.5 Removing sources of contamination

The nutritious richness of NGM agar permits the growth of unwanted microorganisms such as non-*E. coli* bacteria, yeast, and mold. To remove fungal contamination a small chunk of agar or individual worms were transferred to a seeded plate, allowed to move around the OP50 lawn and retransferred to a new plate. To remove bacterial and yeast contamination worms were treated with alkaline hypochlorite, known as an egg prep.

Egg prep

Alkaline hypochlorite treatment was used to remove all types of contamination. This treatment kills the worms, but not the eggs which are protected by their eggshell. Plates with many gravid hermaphrodite adults were used to obtain a high yield of eggs. Worms were washed off plates using 2ml of M9 buffer and transferred to a microcentrifuge Eppendorf tube using a pipette. Worms were allowed to settle at the

bottom of the Eppendorf by gravity and supernatant was removed, leaving worms in ~200 µl of M9. 125µl of 7:8 alkaline hypochlorite (700µl sodium hypochlorite: 800µl 4M NaOH) was added to the Eppendorf and incubated at room temperature for 4 minutes inverting the Eppendorf at frequent intervals. Treatment was ended by adding 1ml of M9 buffer, vortexing, and centrifuging at 3000 rpm for 30 seconds. Supernatant was removed and washing was repeated 2 more times. After the last wash, the supernatant was removed leaving ~100µl, eggs were re-suspended and pipetted onto OP50 seeded plates.

If high egg yields were not necessary a small-scale egg drop prep was performed. A small drop ~10µl of a 1:1 bleach solution (100µl sodium hypochlorite: 100µl 1M NaOH) was placed on the agar away from the bacterial lawn and gravid adults were picked directly onto the drop. The following day larvae were picked from the *E. coli* lawn and transferred to a fresh plate.

2.1.6 Population synchronization

Egg prep or egg drop procedures were used to obtain large numbers of worms synchronized to the same larval stage. An alternative method is the egg lay in which 20-30 gravid adults were placed on a fresh seeded plate and allowed to lay eggs for 3-4 hours. Gravid adults were then removed leaving only eggs on the plates.

2.1.7 Lifespan measurements

Animals were synchronised by one of the two methods previously described or by picking L4s from mixed stage cultures. Lifespans using RNAi to reduce gene expression were conducted on NGM plates supplemented with 1mM IPTG and 20mg/L carbenicillin and *E. coli* HT115 as a food source. For experiments conducted on RNAi worms were grown on OP50 plates and egg prepped onto IPTG plates seeded with HT115 to remove OP50. To prevent progeny contamination 5-fluoro-2′-deoxyuridine (FUdR) was added topically to the bacteria to make a 15µM concentration 1 day before worms were placed on agar plates. Lifespan measurement trials were set up by picking 100 hermaphrodite worms per strain and placing 25 worms per 60mm Petri Plate. L4 larval stage was taken as t=0 and worms were scored every two days. Animals were transferred to fresh plates at least once a week. If an animal failed to respond to gentle prodding it was considered dead. Worms that were on contaminated plates, or suffered a non-ageing related death

such as internal hatching (bagging), severely extruding uterus (the rupture phenotype) or desiccation were censored.

2.1.8 Whole animal staining methods

DAPI staining

Worms were stained as previously described (Angelo and Van Gilst, 2009). Adult worms were picked into a microcentrifuge Eppendorf tube with 1ml of M9 buffer and centrifuged a 6000 rpm for 3 minutes to pellet worms, as much of the M9 as possible was removed. Worms were then fixed by adding 200µl of ice cold 100% methanol and placed on ice for 5 minutes. Worms were washed with M9 buffer once, centrifuged, and M9 was removed. Fixed animals were incubated at room temperature for 40 minutes in 100µl of 4', 6'-diamino-2-phenylidole hydrochloride (DAPI) at a concentration of 500ng/ml protected from light. Worms were once again washed in M9 and pelleted by centrifugation. Glass pipettes were used to transfer worms to an unseeded NGM plate to lessen the amount of worms lost by sticking to plastic pipette tips. NGM plates were left to dry protected from light. Worms were then mounted on slides and imaged under the DAPI filter set (excitation: 350/50nm; emission 460/50nm) at 20X to obtain an image of the gonad arm.

SYTO 12 staining

SYTO 12 is a vital dye that permeates cells with reduced membrane integrity and stains nucleic acid allowing visualization of apoptotic corpses. To stain worms we modified a previously described protocol (Gumienny et al., 1999). A small piece of parafilm was placed on an agar slide and small round indentations were made using the back of a ballpoint pen. A drop (~10µl) of 33µM SYTO 12 was added to each indentation.15-20 worms along with some OP50 were placed onto each drop using a worm pick. Worms were incubated for 3-4 hours in a dark, humid chamber at room temperature. The humid chamber was constructed by using an empty pipette tip box wrapped in tin foil to reduce light exposure. Water was poured in the bottom of the box and the slide was put on top of the pipette tip holder. This was done to keep the SYTO 12 drops from drying out and causing the worms to dissicate. After the 30-40 minute incubation time worms were transferred to a fresh seeded plate for an hour for the stain to

be expelled from the gut. We then imaged the worms under the GFP filter (excitation: 470/40nm; emission 525/50nm) to count apoptotic corpses.

2.2   Microscopy

2.2.1 Hardware and software

C. elegans strain maintenance and lifespan measurements were conducted using a Nikon SMZ645 dissecting microscope attached to a Nikon super high-pressure mercury lamp. Differential interference contrast microscopy (DIC) and fluorescent microscopy images were obtained using one of the following systems: Leica DMRXA2 microscope connected to a Hamamatsu C10600 – Orca R2 camera or a Zeiss Axioskop2plus microscope connected to a Hamamatsu C10600 – Orca ER camera. Both microscopes are connected to iMac computers. The software used to acquire and analyse images is Volocity 5.2 for Macs (Improvision, Perkin Elmer).

2.2.2 Slide preparation

A 2% agar solution was prepared and aliquoted into several microcentrifuge Eppendorf tubes. To melt agar aliquots were placed in a heating block at 100°C until melted. A 50µl drop of the 2% agar solution was placed on a clean slide and pressed down using another clean slide to form a thin, circular agar pad. A 2µl drop of 0.2% anaesthetic (levamisole) was pipetted onto the pad and worms were picked onto the drop. A cover slip was placed carefully on top of the agar pad using tweezers.

2.2.3 Fluorescence quantitation

Quantification of GFP in strains containing *vit-2*::GFP reporter was accomplished by taking images on a Leica DMRXA2 microscope. Images were taken at 10x magnification with bright field and epifluorescence using the GFP filter cube (excitation: 470/40nm; emission: 525/50nm) and overlaid using Volocity acquisition. Exposure times were maintained constant between trials (500ms). After image acquisition GFP levels were obtained by tracing around the worm using Intuos 4 graphics tablet (Wacom) to get an intensity reading.   The worm outline was then dragged to the side to subtract

background reading for overall intensity. The mean pixel intensity readouts were exported to Microsoft Excel for further analysis.

2.3 RNAi interference

In *C. elegans* RNAi can be induced by cloning a gene of interest into the L4440 vector in *E. coli* HT115 and feeding it to the worms. All experiments performed on RNAi used HT115 containing the empty vector L4440 as a control.

RNAi feeding clones were obtained from the Ahringer or Vidal libraries (Kamath and Ahringer, 2003; Rual et al., 2004) and were kindly provided by Dr. Stephen Nurrish (UCL). Clones obtained from frozen stocks were streaked on LB-ampicillin agar plates and incubated at 37°C overnight. A single colony was selected and grown in LB media + ampicillin + tetracycline shaking at 37°C overnight. The stock solution is 20ml LB, 20µl ampicillin (from a stock 50mg/ml), and 10µl tetracycline (from a stock of 10mg/ml). The working solution in which colonies are grown is 5ml. The following day the culture was centrifuged at 4000rpm for 15 minutes to pellet bacteria and the supernatant was removed. The pellet was re-suspended in 10ml of LB + 20µl ampicillin. Agar plates containing IPTG are seeded with 200µl of culture and the bacteria lawn was allowed to grow for 2 days at room temperature. Plates were then stored at 4°C until use.

2.4 Stress Assay

2.4.1 Iron supplementation treatment

Increasing levels of free iron (III) via iron supplementation increases protein carbonylation in *C. elegans* (Valentini *et al*., 2012).

Worms were synchronized by egg prep and grown at 20°C on seeded NGM plates until they reached L4 larval stage. At this point, worms were washed off plates with M9 buffer and transferred to 9mM ferric ammonium [iron (III)] citrate (FAC) NGM plates for the remainder of the experiment. NGM FAC plates were kept away from light to avoid reduction of iron (III) to iron (II).

2.5   Biochemistry

2.5.1 Electrophoresis of *C. elegans* protein

2.5.1.1   Sample collection

Unless otherwise stated, worms were synchronized by performing an egg prep and allowing worms to grow at 15°C until they reach the L4 stage. For experiments using strains that develop at different rates, mutant and wildtype egg preps were staggered to ensure worms reached L4 on the same day. L4 worms were then transferred to fresh seeded plates and switched to 25°C for the remainder of the experiment. For samples of n=100 worms were washed off plates using M9 and transferred to microcentrifuge Eppendorf tubes using glass pipettes. If n=25-50 worms were used per sample worms were picked individually into microcentrifuge Eppendorf tubes containing M9 buffer. Worms washed 3 times using M9 and centrifuged for 1 minute at 6000 rpm. The supernatant was removed leaving worms in 25µl of M9 and samples were stored at -80°C.

2.5.1.2   Sample preparation

Samples were thawed and 25µl of 2x Laemmli sample buffer (Sigma) was added. Samples were incubated at 70°C and vortexed continuously for 15 minutes, they were then incubated at 95°C for 5 minutes. Samples were centrifuged for 15 minutes at 6000 rpm.

2.5.1.3   Protein gels

We loaded 40µl of sample into Criterion XT Precast Gel 4-12% Bis-Tris (Bio-rad) placed in and SDS-PAGE chamber. We added the running buffer which was prepared by mixing 25ml XT MOPS (Bio-rad) with 475ml distilled H_2O. We used Precision Plus Protein Western Standard (Bio-rad) as a size marker ladder and loaded 5µl to the left and 10µl to the right of the gel to maintain orientation of gels after staining. The gels were run at 200V for 45 minutes.

2.5.1.4   Coomassie staining

Gels were removed from plastic cassette and soaked in fixing solution for 30 minutes in a plastic container. Fixing solution was poured out and gels were soaked 40 minutes in Coomassie staining solution. Coomassie solution was replaced with destaining solution and gels were soaked for 20 minutes. Destaining solution was poured out and replaced before allowing gels to destain overnight.

Densitometry

Gels were scanned and saved as 16 bit grayscale TIFF files. Scanned images of gels were analysed using 1D analysis option in ImageQuant TL software (GE Healthcare Europe). Lanes and/or bands of interest (e.g. myosin, actin, YP170, YP115, YP88) were detected manually and rubber band background removal was used. Lane and/or band densities were exported to Microsoft Excel for further analysis.

2.5.2 Western blot/Oxyblot

2.5.2.1   Sample collection

Synchronized day 1 adults were washed off 100mm plates with M9 and transferred to a 1.5ml Eppendorf tube. Worms were allowed to pellet by gravity and washed 3 times with M9. Supernatant was removed leaving worms in ~50µl of M9. Samples were stored at -80°C.

Protein extraction

Samples were thawed, centrifuged and supernatant was removed. 100µl of protein buffer was added to samples and they were sonicated 3 times for 10 seconds using a Bioruptor (Cosmo Bio). Samples were checked visually to ensure complete fragmentation of the pellet. Between sonication steps samples were kept in an ice box. Samples were centrifuged for 30 minutes at 13000 rpm at 4°C and the supernatant was transferred to a new Eppendorf tube. The protein concentration of each sample was determined by the Bradford assay; a typical concentration of 15-20 µg/µl was obtained.

2.5.2.2   Oxyblot and western blot sample preparation

After the protein concentration was determined for each sample, the required volumes were transferred to new Eppendorf tubes. The volume for each sample was adjusted to 5µl by adding distilled H_2O. 5µl of 12% SDS was added to samples for

protein denaturation. 10µl of a 1:10 dilution of dinitrophenylhydrazine (DNPH) was added and samples were incubated at room temperature for 15 minutes. After incubation, 7.5µl of neutral solution was added to stop the reaction. At this point samples can be processed or stored at 4ºC for 1 week.

2.5.2.3   Western blot

Hybond nitrocellulose membrane (Amersham Biosciences) was measured and cut roughly slightly bigger than the size of the gel. The membrane was soaked for 5 minutes in transfer solution. Two pieces of blotting paper were cut slightly larger than the membrane and were soaked in transfer solution for 5 minutes. For the transfer one piece of blotting paper was placed on the anode plate of a Trans-Blot Semi-dry electrophoretic transfer cell (Bio-Rad). The nitrocellulose membrane was placed above the blotting paper taking care to remove any air bubbles. The gel was placed on top of the membrane and the remaining piece of blotting paper was set on top. The cathode plate and safety cover were put on top and the cell was run for 45 minutes at 100V.

After the transfer, the membrane was incubated in PBS-Tween-milk solution in a tray on a shaker for 1 hour. After incubation the membrane was soaked in fresh PBS-Tween-milk solution containing primary antibody and left on a shaker at 4°C overnight. The following day, three 20 minute washes were performed on the membrane using PBS-Tween buffer. The membrane was incubated in PBS-Tween-milk solution containing secondary antibody shaking for 1 hour at room temperature. Again, three 20 minute washes were performed using PBS-Tween buffer. ECL Plus Western Blotting Detection System (Amersham Biosciences) was used to detect binding of the antibody as recommended by the manufacturer. Detection of actin, which was our internal control, was performed by washing the membrane with Restore Plus Western Blot Stripping Buffer as recommended by the manufacturer (Thermo Scientific).

ECL-treated membranes were placed in a developing cassette and taken to a dark room. A sheet of Hyperfilm (Amersham Biosciences) was placed on the membrane inside the developing cassette and exposed for 1 minute. The sheet was developed using a Kodak X-Omat developer and exposed for longer or shorter amounts of time depending on the outcome of the first exposure

2.6   Reagents

2.6.1 *C. elegans* strains used

N2 worms, obtained from the Caenorhabditis Genetics Center (CGC) are used as the wildtype (WT) control thoughout this thesis.

Strain	Genotype
AV106	*spo-11(ok79) IV/nT1[unc-?(n754) let-?] (IV;V).*
BE13	*sqt-1(sc13)* II.
CB4037	*glp-1(e2141)* III.
CF1442	*daf-16(mu86)* I; *daf-2(e1370)* III; *muEx169[unc-119p::GFP::daf-16 + rol-6(su1006)].*
CF1449	*daf-16(mu86)* I; *daf-2(e1370)* III; *muEx176 [daf-16p::GFP::daf-16 + rol-6].*
CF1514	*daf-16(mu86)* I; *daf-2(e1370)* III; *muEx211[pNL213(ges-1p::GFP::daf-16) + rol-6(su1006)].*
CF1515	*daf-16(mu86)* I; *daf-2(e1370)* III; *muEx212[pNL212(myo-3p::GFP::daf-16) + rol-6(su1006)].*
CF1595	*daf-16(mu86)* I; *daf-2(e1370)* III; *muEx227[pNL213(ges-1p::GFP::daf-16) + rol-6(su1006)].*
CY401	*sqt-1(sc13) age-1(mg109)/mnC1 dpy-10(e128) unc-52(e444)* II.
DR1563	*daf-2(e1370)* III.
DR1567	*daf-2(m577)* III.
GA14	*fog-2(q71)* V.
GA66	*eat-2(ad1116)* II.
GA91	*daf-16(mgDf50)* I*; daf-2(m577)* III.
GA184	*sod-2(gk257)* I
GA507	*daf-16(mgDf50)* I; *glp-4(bn2)* I.
GA1500	*sqt-1(sc103)* II; *bIs1[vit-2::GFP + rol-6(su1006)]* X.
GA1501	*sqt-1(sc103)* II; *daf-2(e1370)* III; *bIs1[vit-2::GFP + rol-6(su1006)]* X.
MD701	*bcIs39 [(lim-7)ced-1p::GFP + lin-15(+)]* V.
MT1522	*ced-3(n717)* IV.

MT2547   *ced-4(n1162)* III.

MT3002   *ced-3(n1286)* IV.

MT4770   *ced-9(n1950)* III.

MT8313   *ced-3(n2885)* IV.

MT8354   *ced-3(n2454)* IV.

MQ887   *isp-1(qm150)* IV.

MQ1333   *nuo-6(qm200)* I.

N2   wildtype

RB1206   *rsks-1(ok1255)* III.

SS104   *glp-4(bn2)* I.

TG34   *gld-1(op236)* I.

TJ1   *cep-1(gk138)* I.

TJ1052   *age-1(hx546)* II.

XR1   *abl-1(ok171)* X.

2.6.2 Media

Nematode growth media (NGM)

Add 3g NaCl, 2.5g peptone, 20g agar to a clean glass bottle and make solution up to 1L with distilled H_2O. Autoclave, allow to cool and add the following sterile solutions: 1ml 1M $MgSO_4$, 1ml 1M $CaCl_2$, 1ml 5g/ml cholesterol and 25ml 1M KH_2PO_4.

NGM IPTG agar

Add 3g NaCl, 2.5g peptone, 20g agar to a clean glass bottle and make solution up to 1L with distilled H_2O. Autoclave, allow to cool and add the following sterile solutions: 1ml 1M $MgSO_4$, 1ml 1M $CaCl_2$, 1ml 5g/ml cholesterol, 25ml 1M KH_2PO_4, 1ml 1M IPTG and 400µl 50mg/ml carbenicillin.

M9 solution

Add 7g $Na_2HPO_4.2H_2O$, 5g NaCl, 3g KH_2PO_4, 0.25g $MgSO_4.7H_2O$ to a clean glass bottle, make solution up to 1L with distilled H_2O and autoclave.

OP50 growth medium

Add 5g tryptone and 2.5g yeast extract to a clean glass bottle, make solution up to 1L with distilled H_2O and autoclave.

Luria-Bertani (LB) medium

Add 5g yeast extract, 10g NaCl and 10g tryptone to a clean glass bottle, make solution up to 1L with distilled H_2O, adjust pH to 7.5 with 5M NaOH and autoclave.

LB-ampicillin agar plates

Add 10g bactotryptone, 5g bacto yeast extract, 10g NaCl and 17g agar to a clean glass bottle, make solution up to 1L with distilled H_2O, adjust pH to 7.5 with 5M NaOH. Autoclave, allow to cool and add sterile 1ml 50mg/ml ampicillin.

Freezing medium

Add 20ml 1M NaCl, 10ml 1M KH_2PO_4 and 60ml 100% glycerol to a clean glass bottle and make solution up to 200ml with distilled H_2O. Autoclave, allow to cool and add 0.6ml sterile 0.1M $MgSO_4$.

9mM Ferric ammoniun citrate (FAC) agar

Add 3g NaCl, 2.5 g peptone, 20g agar to a clean glass bottle and make solution up to 500ml with distilled H_2O. Autoclave, allow to cool and add the following sterile solutions: 1ml 1M $MgSO_4$, 1ml 1M $CaCl_2$, 1ml 5g/ml cholesterol, 25ml 1M KH_2PO_4, 4.5ml 1M FAC.

Fixing solution

Mix 500ml methanol, 100ml acetic acid and 400ml distilled H_2O in a clean glass bottle by inverting 3 times.

Coomassie staining solution

To make stock solution add 12g brilliant blue R-250, 300ml methanol and 60ml acetic acid to a clean glass bottle and mix by inverting 3 times. For working solution mix

500ml methanol, 30ml Coomassie stock solution, 400ml distilled H_2O and 100ml acetic acid and mix by inverting 3 times.

Destaining solution

Mix 450ml methanol, 100ml ascetic acid and 450ml distilled H_2O in a clean glass bottle by inverting 3 times.

PBS-Tween buffer (1X)

Mix 100ml 10X PBS, 1ml Tween-20 and 900ml distilled H_2O in a clean glass bottle and mix by inverting 3 times.

Running buffer (10X)

Add 30.3g Tris-base, 144g glycine and 10g SDS to a clean glass bottle and make solution up to 200ml with distilled H_2O. To make working solution (1X) mix 100ml running buffer and make up to 1L with distilled H_2O.

PBS-Tween-milk solution

Add 100ml 1X PBS, 0.5ml Tween and 2.5g milk powder to a clean bottle and mix by inverting 3 times.

Western transfer buffer (10X)

Add 144g glycine and 30.2g Tris-base to a clean glass bottle, make solution up to 1L with distilled H_2O. To make working solution (1X) mix 200ml transfer solution and 200ml ethanol make solution up to 1L with distilled H_2O. Keep refrigerated.

2.7   Statistics

Survival analysis

Statistical comparison of mean lifespan were performed using JMP 9 (SAS Institute Inc.) the non-parametric Log-rank test was executed to obtain p-values.

Students t-test

Experiments in which several treatments were compared to a single control were analysed for statistical significance by performing pair wise Student's t-tests (Excel) to obtain p-values.

ANOVA-Tukey Kramer

Turkey's HSD (honestly significance difference) test is a statistical analysis that allows for multiple comparisons. First a one-way ANOVA was performed on the data to determine if there were differences among means. The Tukey HSD test was then performed to obtain comparisons between the means of all treatments. ANOVA and Tukey HSD tests were performed using JMP 9 (SAS Institute Inc.) to obtain p-values.

Wilcoxon-Mann Whitney test

The non-parametric Wilcoxon-Mann Whitney test was used in experiments measuring ageing tissues to determine if there were statistical differences in population mean ranks between samples. The Wilcoxon-Mann Whitney test was performed using JMP 9 (SAS Institute Inc.) to obtain p-values.

Chapter 3: Quasi-programmed yolk overproduction in ageing *C. elegans*

3.1 Introduction to yolk protein

Yolk is a lipoprotein produced by most egg-laying organisms to provide nutrients necessary for developing embryos. The main protein component of yolk is known as 'vitellogenin', a term that was first used in insects (Pan et al., 1969). Sequencing of vitellogenin (Vtg) genes have revealed striking similarities in morphologically distinct oviparous animal groups such as chickens, frogs and nematodes (Nardelli *et al*., 1987; Spieth *et al*., 1985) implying evolutionary conservation.

An additional study found that vitellogenin of chickens, *Xenopus laevis*, *Drosophila melanogaster* and *C. elegans* contain domains homologous to human genes for the apoprotein of low density lipoprotein (LDL), apoB-100, and to Von Willebrand factor (Baker, 1988a, 1988b). In *C. elegans*, yolk proteins bind and transport lipids such as triglycerides and cholesterol to oocytes, thereby showing a similar function to LDL in mammals (Matyash *et al*., 2001). The similarity in function between apoB-100 and vitellogenin suggests that vitellogenin may be an ancestral relative of apoB-100. Von Willebrand factor has adhesive properties allowing it to bind platelets, collagen and proteins, suggesting a similarity with vitellogenin adhesion to oocyte receptors for uptake (Baker, 1988b). The similarity between *C. elegans* vitellogenin and vertebrate blood clotting factor Von Willebrand may also reflect an unknown role apart from nourishment of developing embryos (Baker, 1988b).

3.1.1 *C. elegans* yolk protein

In response to hormonal cues, yolk proteins are synthesized in different tissues (such as the intestine, ovary and liver) across oviparous species (Byrne et al., 1989). Yolk proteins are synthesized in the fat body and ovary of *Drosophila* (Bownes et al., 1983) and in the liver of frogs (Wiley and Wallace, 1981) and chickens (Jost et al., 1978). A common feature among all egg-laying organisms is that yolk is synthesized in tissues outside of its intended final destination, the egg (Byrne *et al*., 1989).

In *C. elegans* yolk proteins are synthesized outside of the gonad (Kimble and Sharrock, 1983). Worms in which gonad precursor cells have been ablated and thus are gonad-less still accumulate yolk proteins, ruling out the gonad as the tissue of yolk origin (Kimble and Sharrock, 1983). The production of yolk proteins is a sex-specific trait, as male worms do not produce yolk proteins, regardless of whether they possess a gonad or not (Kimble and Sharrock, 1983). Male *C. elegans* live ~19% longer than hermaphrodite worms (Gems and Riddle, 2000). This poses the interesting question whether differences in mortality reflect detrimental effects of yolk in hermaphrodites. Yolk production in hermaphrodite worms begins at L4, to ensure an abundant supply before egg production begins (Kimble and Sharrock, 1983). Tissue examination by dissection of the body wall, gonad, intestine and embryos revealed the intestine as the site of yolk synthesis by a process of elimination (Kimble and Sharrock, 1983). Vitellogenin precursors are synthesized in the intestine and then secreted into the pseudocoelum, from which yolk is taken up by developing oocytes by endocytosis via the LDL-like receptor RME-2 (Grant and Hirsh, 1999).

Vitellogenin can be synthesized by a single gene as in echinoderms (Shyu et al., 1986) or from multiple genes as in *Drosophila* and chickens, both of which have 3 vitellogenin genes (Terpstra and Ab, 1988). Curiously, *C. elegans* has more vitellogenin genes than more complex oviparous species. *C. elegans* vitellogenins are divided into two distinct subclasses named according to their molecular weight: the large yolk proteins YP170A and YP170B and the smaller proteins YP115 and YP88. Of these YP170, YP115 and YP88 are electrophoretically distinct (Kimble and Sharrock, 1983; Spieth and Blumenthal, 1985).

Yolk proteins are coded for by six genes *vit-1* through *vit-6*, *vit-1* is thought to be pseudogene with a stop codon in the protein-coding region of the gene (Spieth *et al*., 1985). However, a more recent study suggests that the sequence encoded by *vit-1* is translated into protein, arguing against it being a pseudogene (Depuydt *et al*., 2013). There is a high degree of homology between *C. elegans vit* genes. Genes *vit-3, vit-4* and *vit-5* have 96% sequence similarity, and these three genes are 68% homologous to *vit-2* (Spieth *et al*., 1985). The sequence of *vit-6* is 50% similar to the other 5 *vit* genes (Spieth *et al*., 1985). Genes *vit-3*, *vit-4* and *vit-5* contribute to make YP170A, while *vit-2*

produces YP170B (Spieth and Blumenthal, 1985). Both YP170A and YP170B are taken up by oocytes intact. The two smaller yolk proteins are encoded for by *vit-6*, which produces the precursor protein YP180 (Spieth and Blumenthal, 1985). After leaving the intestine and before being taken up by oocytes YP180 is cleaved to produce YP115 and YP88 (**Figure 3.1**) (Spieth and Blumenthal, 1985).

The four yolk proteins associate into two lipoprotein particles. These lipoproteins are composed of vitellogenin, 8% phospholipids, 3% triglycerides and 3% other lipids (Sharrock et al., 1990). The 'A complex' contains YP170A, YP115 and YP88 and the 'B Dimer' contains YP170B (Sharrock *et al*., 1990).
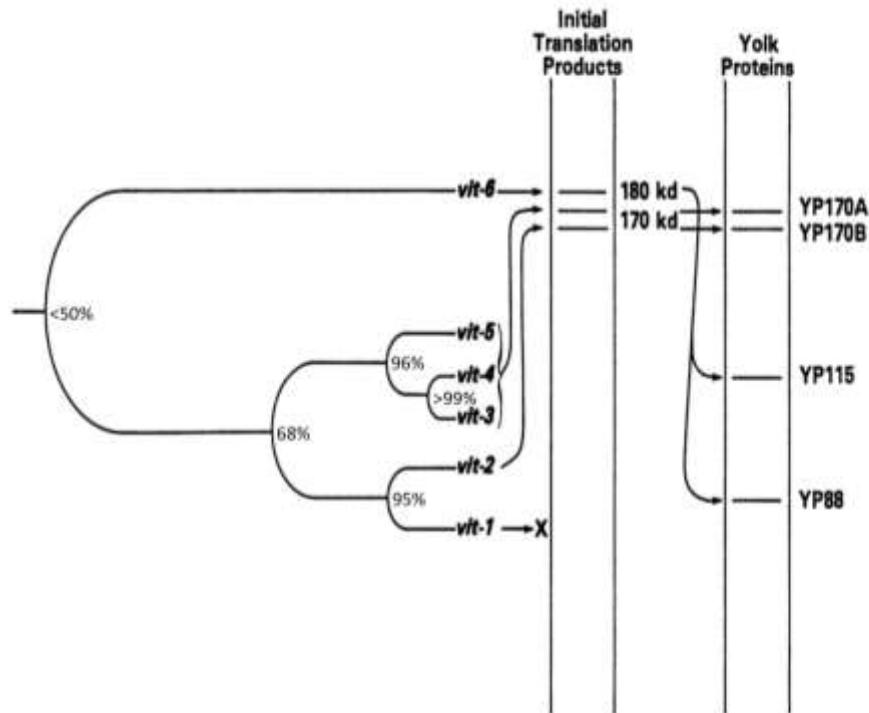
Figure 3.1 *C. elegans* **vitellogenin genes and their encoded yolk proteins.** Reproduced and modified from Spieth and Blumenthal, 1995; Spieth *et al*, 1985.

3.1.2 Yolk proteins in ageing *C. elegans*

Using a VIT-2::GFP reporter allows visualisation of YP170 yolk protein. Prior to sperm depletion yolk protein is observed within the intestine and oocytes of young hermaphrodite worms. After sperm runs out, oocyte production ceases and yolk protein

accumulates throughout the body cavity (Brandt et al., 2005; Herndon et al., 2002) (Figure 3.2). Consistent with the redistribution of yolk protein, lipid inclusions have been observed in the muscle and hypodermis of old worms (Herndon *et al*., 2002). Late life yolk accumulation implies that it continues to be synthesized in post-reproductive worms in a "tap left on" (or open faucet) type mechanism (Herndon *et al*., 2002). *C. elegans* vitellogenin has been found to be similar in structure and function to mammalian LDL protein apoB-100 which is a risk factor in the development of arteriosclerosis (Contois et al., 2011). This poses the question whether yolk accumulation may also have a lipotoxic effect in *C. elegans* (Ackerman and Gems, 2012). The continuous production of yolk in post-reproductive worms is consistent with the notion of a quasi-programme.
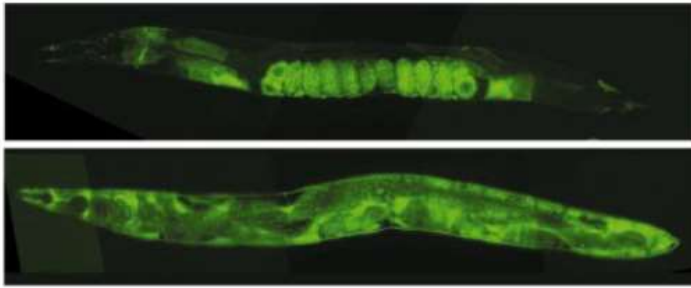
Figure 3.2 Accumulation of yolk protein in the body cavity of post-reproductive worms. Using VIT-2::GFP to visualize yolk protein revealed that at 20°C day 4 worms have yolk protein in the intestine and oocytes (top panel). On day 12 yolk protein is redistributed accumulating throughout the body cavity (lower panel). Figure reproduced from Herndon *et al* 2002.

Increased yolk production in ageing worms could have a toxic effect and thus limit their lifespan. In support of this, microarray data found an apparent reduction in *vit-2* and *vit-5* mRNA in day 1 of adulthood long-lived *daf-2(-)* worms compared to wildtype (Murphy *et al*., 2003). Furthermore, RNAi of *vit-2* or *vit-5* have been reported to modestly extend lifespan (Murphy *et al*., 2003). When worm lysates were run on Coomassie-stained gels a large increase in yolk protein was observed in wildtype worms between day 1 and 4, but this increase was absent in long lived *daf-2(e1370)* mutants (DePina *et al*., 2011). In contrast, *vit-2, vit-5* and *vit-6* mRNA have been shown to decline with age in wildtype (Fabian and Johnson, 1995). Another study found mRNA levels of *vit-2* and *vit-5* to decline progressively from day 1 to day 6 and a similar pattern was observed in *daf-2(e1368)*, and *daf-2(e1370)* showed similar mRNA levels to wildtype on day 1 to 4 but a stronger reduction on day 6 (DePina *et al*., 2011). The disparity between

the general trend of reduction in *vit* mRNA in both wildtype and *daf-2(-)* and the observation that yolk protein is reduced in *daf-2(-)* with respect to wildtype, in which a large increase is observed between day 1 and 4, argues against a simple model in which DAF-16 represses *vit* gene transcription. More plausibly, *vit* genes are transcribed at high levels during early adulthood and DAF-16 can block translation of these transcripts (DePina *et al*., 2011).

Accumulation of yolk protein in wildtype worms is a potential example of post-reproductive unregulated biosynthesis and is consistent with Blagosklonny's hyperfunction theory. In this chapter we test the possibility that lifespan in *C. elegans* is limited by yolk accumulation. We examine genetic interventions that increase lifespan to assess their effect on yolk protein levels and tested whether manipulating yolk protein levels has an effect on lifespan.

The data in this chapter was collected by myself and Eleanor Tyler. Eleanor was a masters student who worked closely with me and whom I directly supervised. Data that was collected by Eleanor is ascribed to her as follows: Figure 3.4, 3.5 (B-D), 3.7, 3.8, 3.9, 3.10, 3.11, 3.14, 3.15, 3.16, 3.17, 3.18, 3.19, 3.20. Her contributions are also noted in the corresponding figure legends.

3.2   Results

3.2.1 Measuring yolk protein levels in ageing worms

We asked whether yolk production acts as "tap left on", continuing its synthesis in an unregulated fashion throughout adulthood. In this study we used the following methods to measure yolk protein (YP) levels.

3.2.1.1   VIT-2::GFP fluorescence measurements

To examine changes in yolk protein levels and where yolk is located in the worm a VIT-2::GFP reporter strains were used. The VIT-2::GFP reporter strains used for these experiments are GA1500 *bIs1*[*vit-2*::GFP + *rol-6(su1006)*] and GA1501 *daf-2(e1370)*, *bIs1*[*vit-2*::GFP + *rol-6(su1006)*]. GA1500 derived from DH1033 *sqt-1(sc103)* II, *bIs1*[*vit-2*::GFP + *rol-6(su1006)*] mated with N2 males to remove *sqt-1(sc103)* from the background by segregating away the *sqt-1(sc103)* mutation. We then used GA1500 and crossed it with *daf-2(e1370)* males and selected for plates in which all worms formed dauer at 25°C and are rollers. Unless otherwise stated, worms were raised at 15ºC and transferred to 25ºC at L4 larval stage (see section 2.2.3). The exposure time used for microfluorimety was maintained at 500ms throughout the experiments. This exposure was selected because it is long enough to detect fluorescence in young adults without leading to image saturation in micrographs of older worms.

3.2.1.2   Coomassie stained SDS-PAGE gels

Yolk levels were also quantified by running worm protein extracts on Coomassie-stained gels (see section 2.4.1). Myosin, YP170, YP88 and YP115 bands were recognized using published data (DePina et al., 2011; Kimble and Sharrock, 1983). The actin band was identified by western blotting (see section 2.5.2). Bands of interest were analysed using densitometry to obtain abundance measurements. Levels of yolk proteins YP170, YP115 and YP88 were normalized to myosin as an internal standard. Actin is a housekeeping gene and its expression should be constant, and the ratio of actin to myosin was used to give an indication of the reliability of myosin as a standard (DePina *et al.*, 2011). Protein   abundance   (YP170/myosin,   YP115/myosin,   YP88/myosin   and

actin/myosin) on days 4, 8 and 12 are shown as a ratio to their respective day 1 wildtype control levels.

Unless otherwise stated, worms were grown at 15°C to L4 larval stage and then transferred to 25°C for the duration of the experiment. Worms were collected in microcentrifuge Eppendorf tubes and immediately stored at -80°C until samples were processed.

3.2.1.3   New yolk terminology

For convenience in this study we propose a new terminology to describe yolk accumulation (Yol) phenotype observed. In accordance with *C. elegans* nomenclature we propose the use of Yol-o for yolk over-accumulation and Yol-d for yolk accumulation-deficient using wildtype yolk protein levels as a baseline.

3.2.2 Yolk synthesis continues throughout adulthood

A previous study observed an increase in yolk protein levels in ageing *C. elegans* from day 1 to day 4 of adulthood (DePina *et al*., 2011). The hyperfunction theory would suggest that after reproduction ceases, yolk synthesis is not regulated and continues being produced, resulting in its accumulation in a tap left on type mechanism. To examine if this is the case, and how long the tap is left on, GA1500 worms were observed on slides and levels of GFP were measured on day 1, 4 and 8 of adulthood. On day 1 GFP was observed mainly in the oocytes. By day 4 a large increase in GFP is observed throughout the body cavity, indicating a major increase in yolk levels and change in distribution, consistent with earlier observations (DePina *et al*., 2011). However, on day 8 GFP was observed mainly in the intestine and there is a significant decrease in fluorescence levels between day 4 and day 8 (Figure 3.3 A,B). This suggests that VIT-2::GFP accumulates in the body cavity at high levels during reproduction and from then on declines post-reproduction but remains at levels twice as high as those observed on day 1.
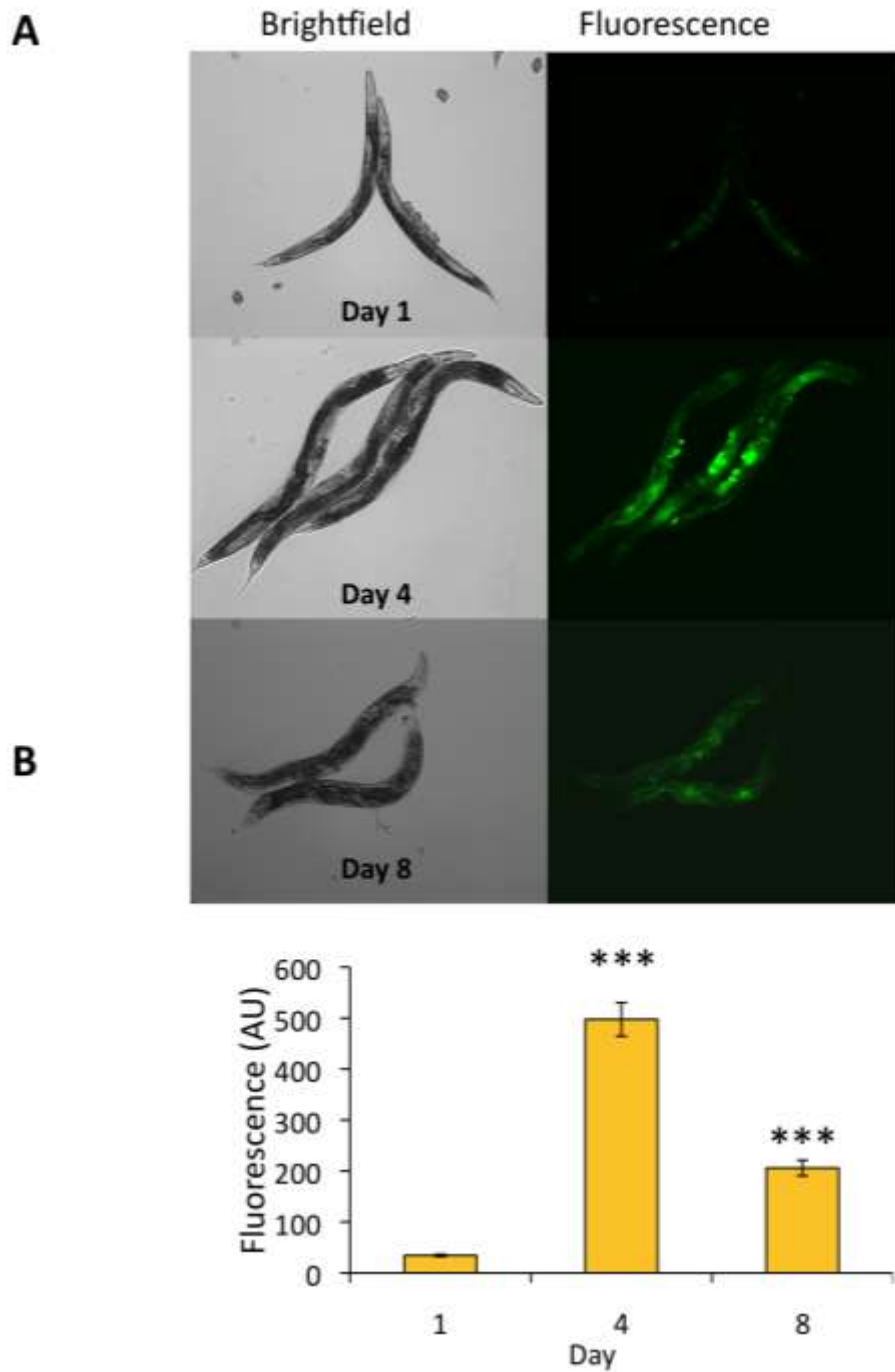
Figure 3.3 Yolk levels increase in ageing worms. A) An increase in level and change in distribution of yolk was observed using the VIT-2::GFP reporter strain GA1500. B) A significant increase in VIT-2::GFP fluorescence was observed between day 1 and 4, after which there was a reduction. Data is the mean of 35-45 worms; error bars, SEM; ANOVA ($p<0.0001$) and post-hoc Tukey's (HSD) test on consecutive days *** $p<0.001$.

As a more direct measure of yolk accumulation, wildtype worms were collected on days 1, 4, 8, and 12 and relative YP170, YP115 and YP88 levels were measured by running whole worm lysates on SDS-PAGE gels (Figure 3.4 A). We found a constant increase in YP170 levels from day 4 to day 8, but no further significant increase on day 12 (Figure 3.4 B). A similar trend was observed for YP115 and YP88, however it is not statistically significant, probably reflecting variability between trials (Figure 3.4 C,D). The magnitude of the increase in YP170 between day 1 and 4 was double in this experiment; results by DePina *et al* showed a 4-fold increase (DePina *et al*., 2011). The difference in the magnitude of the effect of age on YP170 abundance may reflect saturation due to overloading of the gels in our trials.
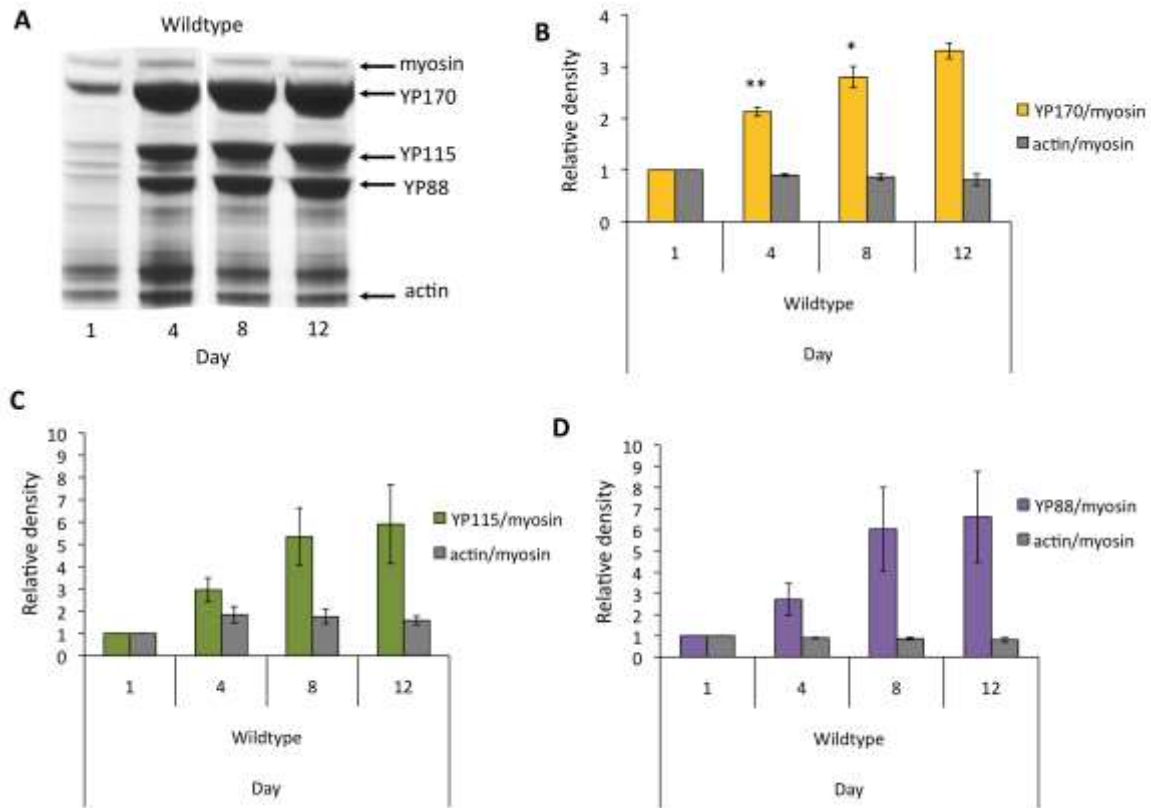
Figure 3.4 Yolk proteins remain constantly high after day 4 of adulthood. A) Coomassie stained SDS-PAGE gels showing yolk protein abundance. B) YP170 levels continue to increase up to at least day 8. C,D) YP115 and YP88 follow the same trend. Data is the mean of three biological replicates (100 worms per replicate); error bars, SEM; ANOVA ($p < 0.0001$), Tukey's (HSD) test on consecutive days, ** $p < 0.01$, * $p < 0.05$.

Thus, using protein lysates to measure yolk levels showed a gradual increase in YP170 with age, which is similar to what was observed using VIT-2::GFP, where levels increased approximately 10-fold between day 1 and 4. However, VIT-2::GFP data suggests a decrease in YP170 on day 8. Worm lysates provide a more reliable method than VIT-2::GFP because GFP may give a less reliable indication of protein accumulation, e.g. due to GFP degradation with age. Additionally, VIT-2::GFP only reflects YP170B, whereas measuring YP170 bands on gels gives a readout of levels of YP170A and YP170B. In conclusion, yolk accumulation continues until at least day 8. The reduced accumulation after that could reflect effects of senescence on yolk biosynthetic capacity.

3.2.3 No age increase in yolk levels in *daf-2(-)* worms

It has been previously reported that *daf-2(e1370)* mutation suppresses the increase in yolk protein levels that otherwise occurs in wildtype worms between day 1 and day 4 of adulthood (DePina *et al*., 2011). Mutations in *daf-2* extend lifespan in worms (Kenyon et al., 1993). Could the absence of yolk accumulation contribute to this? We wanted to investigate how DAF-2 controls yolk levels. First, we set out to verify the results of DePina *et al*. We first tested the effect of *daf-2(e1370)* on the age increase in yolk by looking at VIT-2::GFP levels on days 1, 4 and 6. On day 1 VIT-2::GFP levels were the same in *daf-2(+)* and *daf-2(e1370)*. However, *daf-2(e1370)* worms showed no age increase in GFP levels, implying that IIS promotes yolk accumulation (Figure 3.5 A). This confirms the finding by DePina *et al* that *daf-2(e1370)* blocks yolk accumulation on day 4 and extends the finding to day 6.

We then sought to verify the reduced yolk phenotype of *daf-2(e1370)* worms by studying protein gels. In addition *daf-2(m577)* was also tested to rule out the feeding defect and reduced fertility present in *daf-2(e1370)* as the cause of yolk reduction. *daf-2(m577)* is a class 1, less pleiotropic allele, which does not exhibit fertility or feeding defects (Gems *et al*., 1998). Both *daf-2(-)* alleles show a marked reduction in YP levels on day 4 relative to wildtype (Figure 3.5 B,C,D ; Appendix 1, Figure A-1.1).
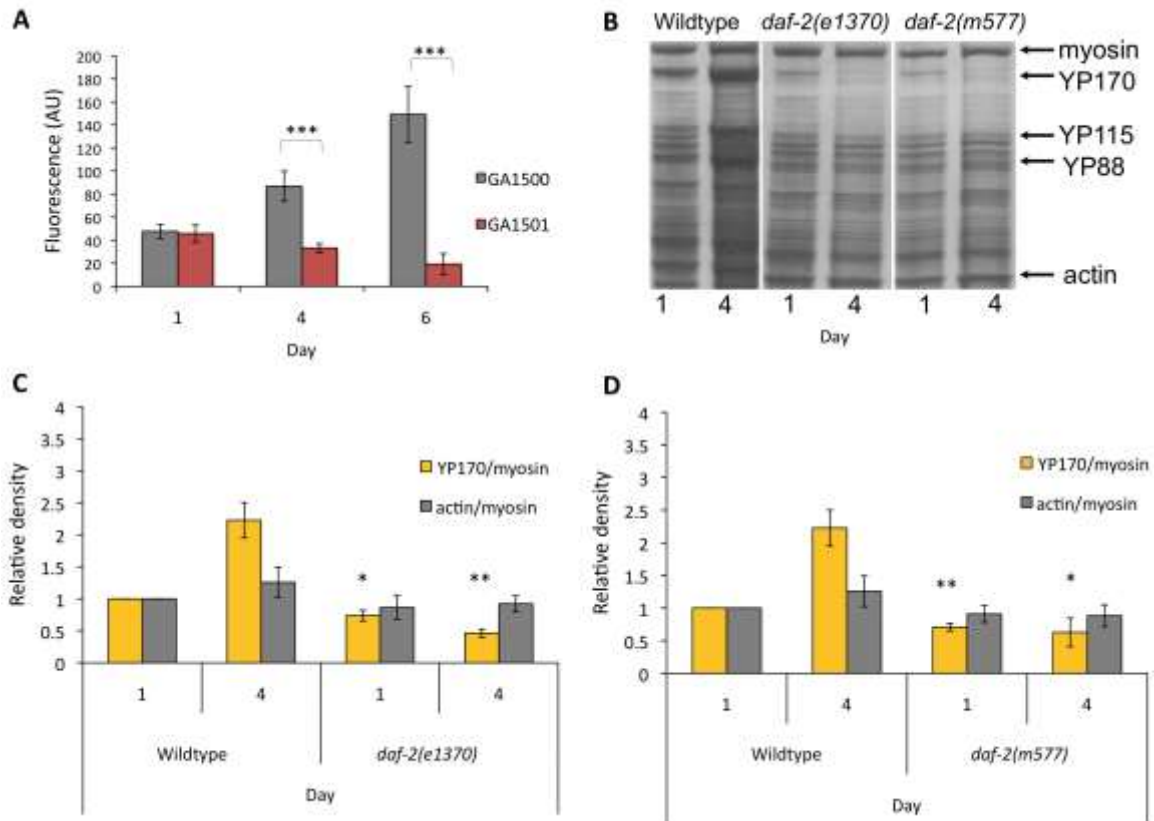
Figure 3.5 No age increase in yolk levels in day 4 *daf-2(-)* worms (25°). A) VIT-2::GFP levels are reduced in *daf-2(e1370)* worms. B) Coomassie stained SDS-PAGE gels showing YP abundance. C,D) *daf-2(e1370)* and *daf-2(m577)* both have reduced levels of YP on day 1 and 4 compared to wildtype. Data is the mean of (A) one replicate (10 worms), (C-D) three biological replicates (100 worms per replicate); error bars, SEM; Student's t-test ***p<0.001, **p<0.01, *p<0.05 (versus age-matched control). B-D) Data collected by E. Tyler.

Having found that yolk accumulates throughout adulthood we wanted to observe whether *daf-2(m577)* suppresses yolk accumulation throughout life, or whether yolk accumulates after day 4. To this end we compared yolk levels at day 1, 4, 8 and 12 of adulthood in wildtype and *daf-2(m577)* worms at 25˚C.

In this trial we saw a significant increase in YP170 between day 1 and 4 in wildtype worms, but no further significant increase was observed on days 8 and 12, probably due to high variability between gels (Figure 3.6 A,B). A similar trend was observed for YP115 and YP88 but, again, increases did not reach statistical significance.

Additionally it should be noted that the actin to myosin ratio fluctuated on day 12 (Figure 3.6 C).

Yolk did not accumulate in *daf-2(m577)* worms from day 1 to day 12. YP170 levels remained similar to those of day 1 wildtype worms. YP115 and YP88 mostly followed a similar trend than YP170 (Figure 3.6 A,B). With the exception that YP115 was lower than wildtype on day 1 and YP88 was lower than wildtype levels in day 4 worms (Figure 3.6 C). These results imply that YP does not accumulate at all in ageing *daf-2(-)* worms, though the possibility remains that YP accumulates at a later age.
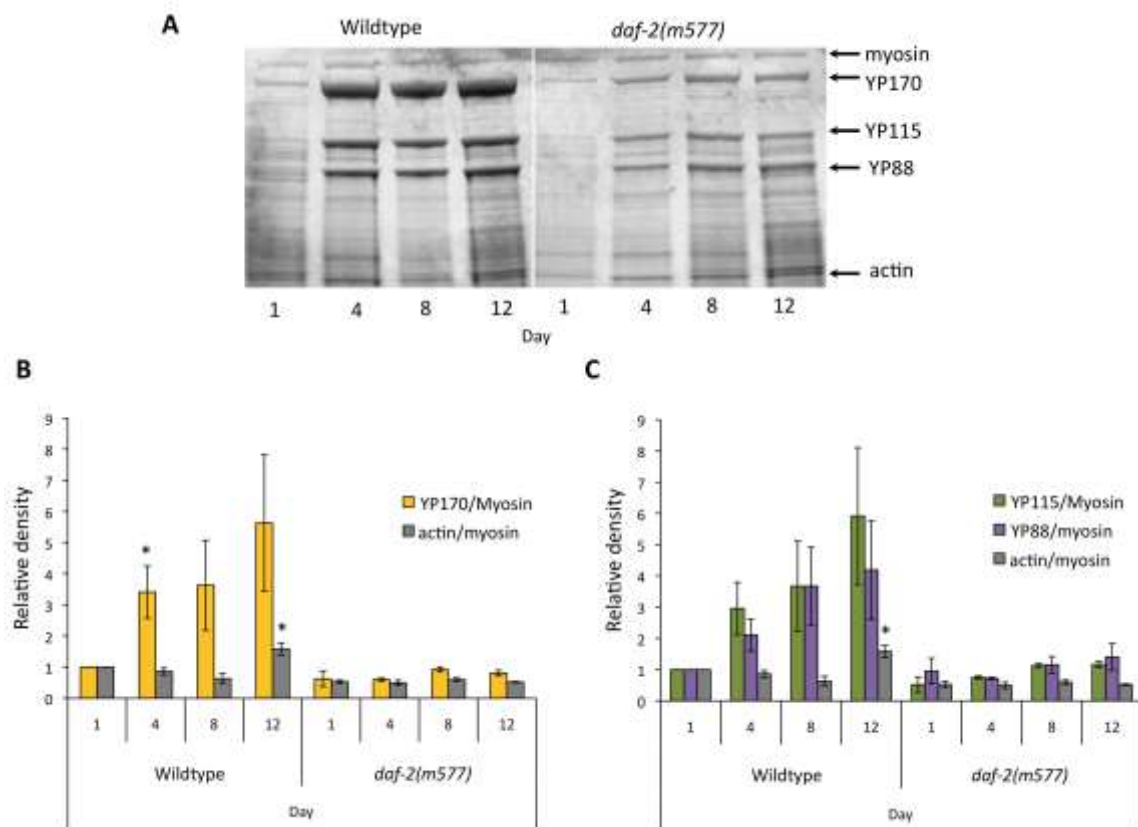
Figure 3.6 Yolk does not accumulate in *daf-2(-)* worms between day 1 and 12. A) Coomassie stained SDS-PAGE gels showing yolk protein abundance. Panels on same gel were rearranged for clarity. B) Age increase in YP170 levels in wildtype worms, but not *daf-2(m577)* mutants. C) YP115 and YP88 do not accumulate in *daf-2(m577)* mutants. Data is the mean of three biological replicates (25 worms per replicate); error bars, SEM; ANOVA ($p<0.0001$), Tukey's (HSD) test compared to day 1 control *$p<0.05$.

3.2.4 Other IIS mutants also prevent yolk accumulation

AGE-1 is the *C. elegans* ortholog of phosphatidylinositol-3-kinase catalytic subunit (PI3K) which acts downstream of the DAF-2 receptor (Morris *et al*., 1996). To further test the role of IIS in yolk regulation we examined *age-1(hx546)* mutants which are ~40% longer lived than wildtype and exhibit a 75% decrease in fecundity at 20°C (Friedman and Johnson, 1988). A previous study reported that *age-1(hx546)* mutants show a wildtype yolk distribution pattern (Herndon *et al*., 2002). However, effects of *age-1(hx546)* on overall YP levels have not been reported. Yolk protein levels were measured for this mutant and were found to be lower than wildtype on day 1 but not day 4 for YP170 (Figure 3.7 A,B). A similar trend was observed for YP115 and YP88 (Appendix 1, Figure A-1.2).

The *age-1(hx546)* is a weak reduction of function allele containing a missense mutation (Ayyadevara et al., 2008), which could explain why YP levels are only weakly reduced in this strain. We performed tests on stronger allele *age-1(mg109)* which is a missense mutation resulting in a non-functional protein (Morris *et al*., 1996). In the absence of maternal rescue, *age-1(mg109)* homozygotes form dauers at all temperatures (Gottlieb and Ruvkun, 1994), so the balancer strain GY401 [*sqt-1(sc13) age-1(mg109)/mnC1 dpy-10(e128) unc-52(e444)*] was used. *sqt-1(sc13)* homozygotes are rollers (Rol). Rol segregants were found among progeny of heterozygous mothers. These worms were homozygous for *age-1(mg109)* but did not form dauers due to maternal rescue thanks to the presence of wildtype AGE-1. A *sqt-1(sc13)* control was used to check that this marker mutation did not affect yolk protein levels. Consistent with the results seen in *daf-2(-)*, *age-1(mg109)* shows a reduction in YP170 levels on day 4 (Figure 3.7 C,D). Levels of YP115 and YP88 follow a similar trend but did not attain statistical significance (Appendix 1, Figure A-1.2).
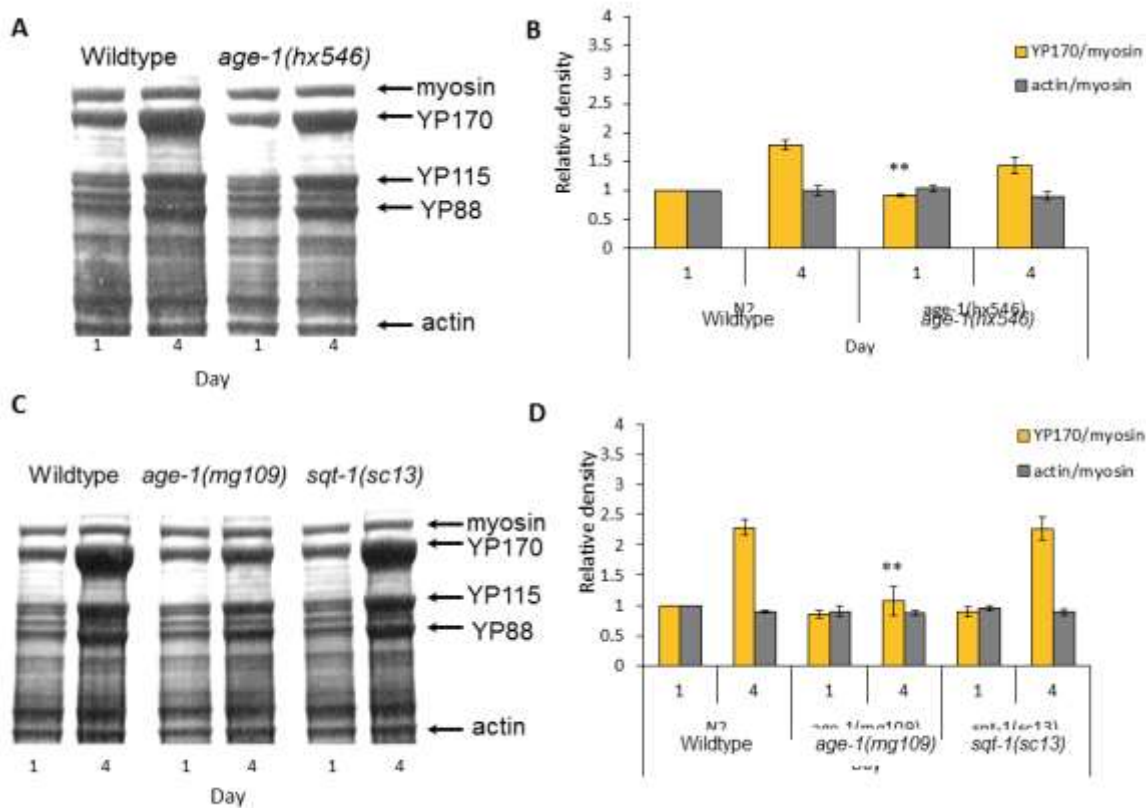
Figure 3.7 Yolk protein levels in *age-1* mutants. A,B) Lysates of *age-1(hx546)* mutants show reduced levels of YP on day 1 worms compared to wildtype, but not on day 4. C,D) Lysates of *age-1(mg109)* mutants show a reduction in YP levels on day 4 compared to wildtype. Data is the mean of three biological replicates (100 worms per replicate); error bars, SEM; Student's t-test **p<0.01, *p<0.05 (versus age-matched wildtype). Data collected by E. Tyler.

3.2.5 Suppression of yolk protein accumulation in *daf-2(-)* is DAF-16 dependent

DAF-16 is required for the lifespan extension observed in *daf-2(-)* mutants (Kenyon et al., 1993). A previous study showed that the reduced YP levels observed in *daf-2(e1370)* mutants is dependent on DAF-16 (DePina *et al.*, 2011). We previously showed a decrease in yolk protein levels in *daf-2(m577)* mutants. We sought to replicate the results obtained by DePina *et al* by using *daf-16(mgDf50); daf-2(m577)* and found similar results. *daf-16(mgDf50), daf-2(m577)* mutants have wildtype YP levels on day 1 and 4 (Figure 3.8; Appendix 1, Figure A1.3). These findings verify that IIS stimulates yolk accumulation, perhaps by inactivating DAF-16.
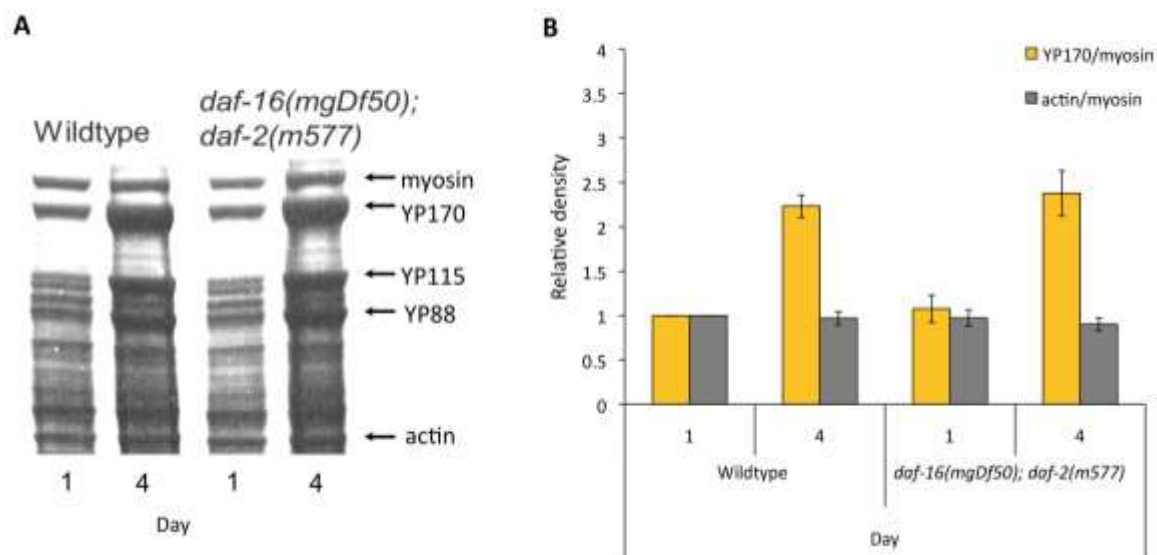
Figure 3.8 Yolk protein levels in *daf-16(mgDf50); daf-2(m577).* A) Coomassie stained SDS-PAGE gels showing yolk protein abundance. B) YP levels in *daf-16(mgDf50); daf-2(m577)* worms are similar to wildtype on day 1 and 4. Data is the mean of three biological replicates (100 worms per replicate); error bars, SEM; Student's t-test (versus age-matched wildtype). Data collected by E. Tyler.

3.2.6 Effects of tissue-specific expression of DAF-16 in the intestine, muscle and neurons on yolk protein levels

Our data so far suggests that IIS promotes yolk protein synthesis. Longevity of germline ablated and *daf-2(-)* worms is dependent on DAF-16 activity (Hsin and Kenyon, 1999; Kenyon et al., 1993). A previous study constructed strains in which *daf-16* expression in *daf-16(mu86); daf-2(e1370)* mutants was rescued either in the intestine, musculature or nervous system using transgene arrays (Libina *et al*., 2003). To further examine how and where yolk synthesis is regulated we these used strains with tissue-specific rescue of *daf-16* expression.

The strain CF1449 in which *daf-16* expression is driven ubiquitously by its own promoter has been shown to rescue lifespan of *daf-16(mu86); daf-2(e1370)* mutants to nearly *daf-2(e1370)* levels (Libina *et al*., 2003). We first tested this strain to see if it had

the Yol-d phenotype previously observed in *daf-2(e1370)* worms, and found that it did; YP levels were reduced on day 1 and 4 compared to wildtype. However, actin levels were slightly higher relative to myosin on day 1 (Figure 3.9; Appendix 1, Figure A-1.4). Only two replicates were obtained due to high frequency of bagging (maternal hatching of larvae) in this strain. A comparison with effects of *daf-2(e1370)* on YP levels (Figure 3.5 C) suggests greater suppression of yolk synthesis in CF1449, perhaps reflecting higher *daf-16* copy number resulting in further activation of DAF-16.
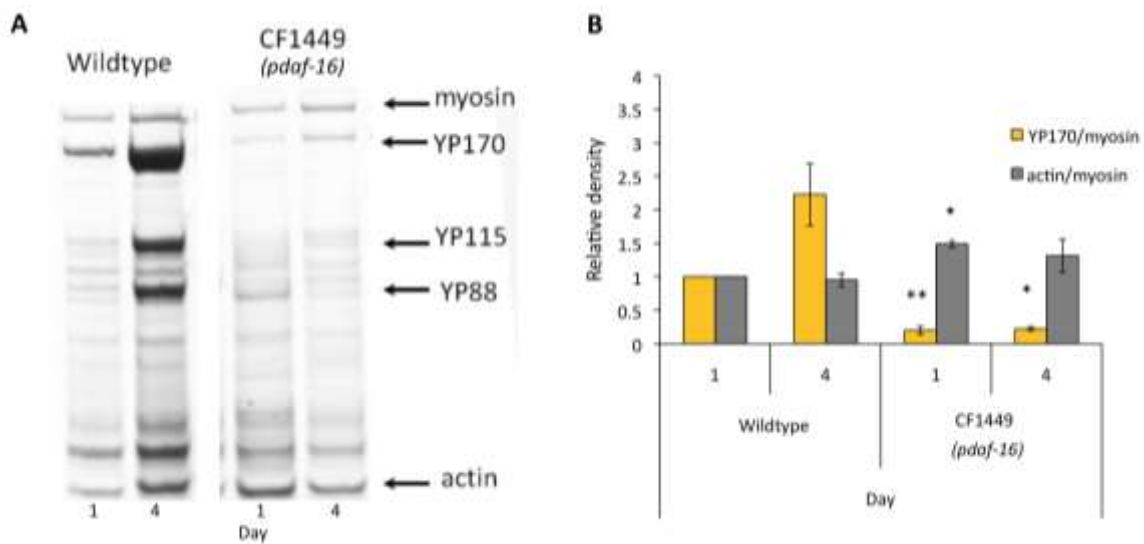
Figure 3.9 *daf-16* expression by its own promoter causes Yol-d in *daf-16(mu86); daf-2(e1370)*. A) Coomassie stained SDS-PAGE gels showing yolk protein abundance. B) DAF-16 driven by its own promoter causes a reduction in YP levels on day 1 and 4 compared to wildtype. Data is the mean of two biological replicates (100 worms per replicate); error bars, SEM; Student's t-test **p<0.01, *p<0.05 (versus age-matched wildtype). Data collected by E. Tyler.

Yolk is synthesized in the intestine in *C. elegans* hermaphrodites (Kimble and Sharrock, 1983). Transgenic strains CF1595 and CF1515 that have DAF-16 rescued in the intestine of *daf-16(mu86); daf-2(e1370)* worms restore lifespan extension to approximately 50-60% that of *daf-2(e1370)* worms (Libina *et al*., 2003). We examined both transgenic strains by running worm lysates on Coomassie stained gels. In CF1595 YP levels were reduced on day 1. In both strains there was an apparent reduction (~30%)

71

of YP on day 4, however in neither case did this reach statistical significance (Figure 3.10; Appendix 1, Figure A-1.5). That both *pges-1::daf-16* strains show an apparent reduction in yolk levels suggests that these trials may have failed to detect an existing effect on YP levels due to high inter-trial variance. Further trials would be required to establish whether this is the case.
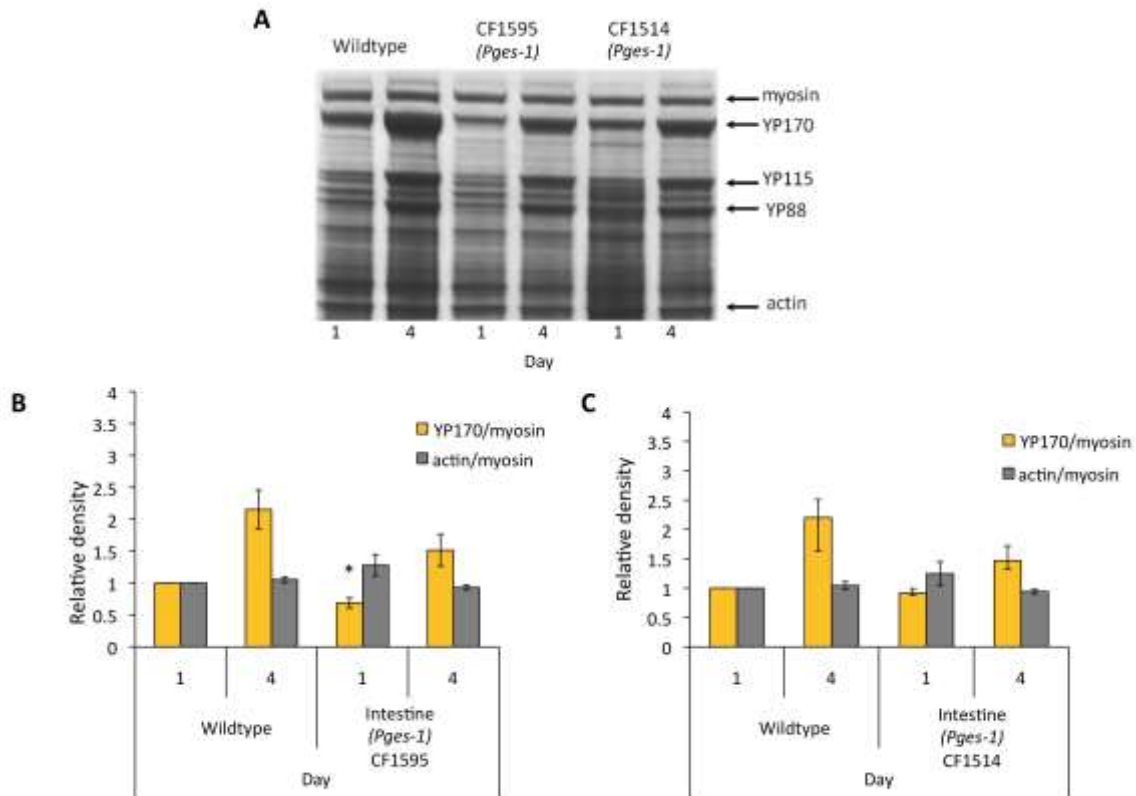
Figure 3.10 Intestinal *daf-16* expression does not rescue Yol-d phenotype in day 4 *daf-16(mu86); daf-2(e1370)* worms. A) Coomassie stained SDS-PAGE gels showing yolk protein abundance. B) DAF-16 activity in the intestine restored Yol-d phenotype on day 1 but not day 4 compared to wildtype. C) DAF-16 activity in the intestine does not reduce yolk to statistically significant levels in CF1514. Data is the mean of three (B) or two (C) biological replicates (100 worms per replicate); error bars, SEM; Student's t-test *p<0.05 (versus age-matched wildtype). Data collected by E. Tyler.

We also looked at YP levels in CF1515 and CF1442 *daf-16(mu86); daf-2(e1370)* with DAF-16 rescued in muscle and neurons, respectively. Of these strains DAF-16 rescue in the muscle has no effect on lifespan, and neuronal DAF-16 has a mild beneficial effect (Libina *et al*., 2003). DAF-16 rescue in the muscle caused a decrease in YP170

levels on day 1 but not day 4 compared to wildtype (Figure 3.11 A,B). Levels of YP similar to wildtype were observed for YP115 and YP88 (Appendix 1, Figure A-1.6). For worms with DAF-16 rescued in the neurons only one replicate was performed due to problems with bagging, thus no statistics can be conducted but the trend suggests no difference in YP levels compared to wildtype (Figure 3. B, C ; Appendix 1, Figure A-1.6).
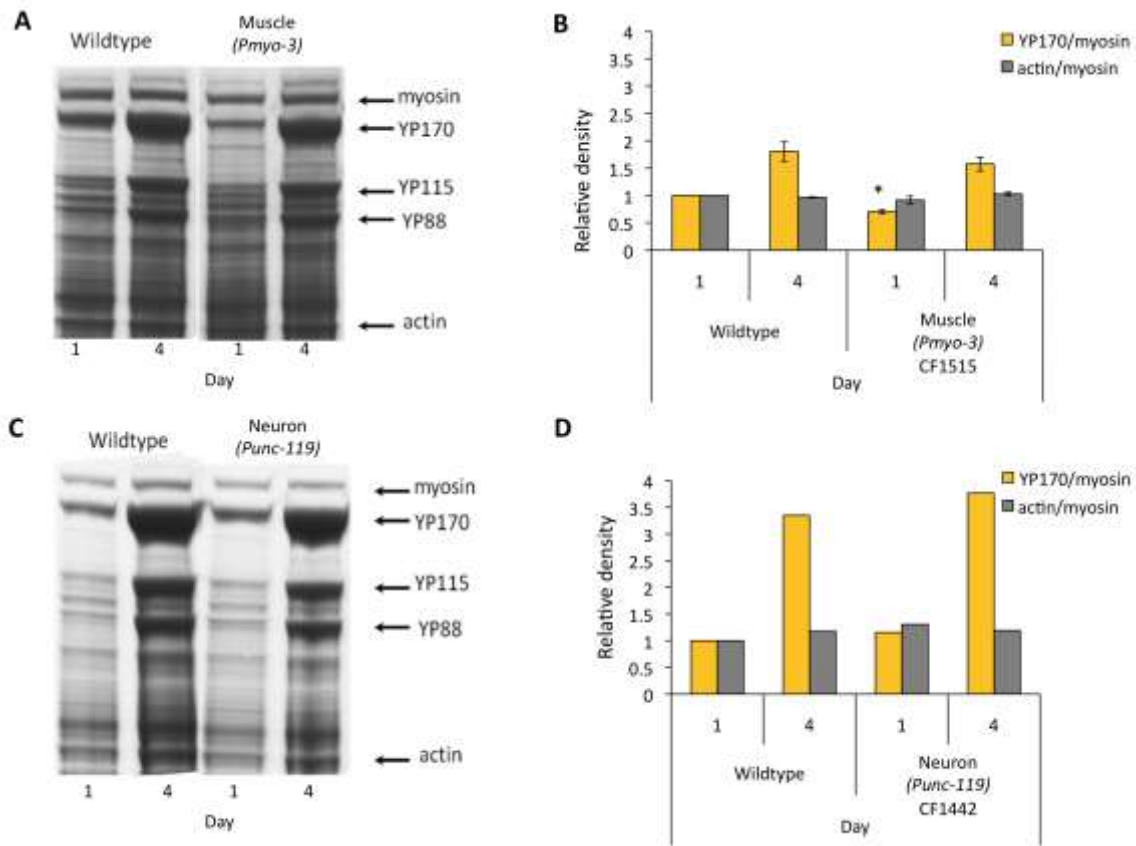
Figure 3.11 Muscle and neuronal DAF-16 do not rescue Yol-d phenotype in day 4 *daf-16(mu86); daf-2(e1370)* worms. A,C) Coomassie stained SDS-PAGE gels showing yolk protein abundance. B) DAF-16 activity in the muscle reduced yolk protein levels on day 1 but not day 4 compared to wildtype. Data mean of two biological replicates (100 worms per replicate). D) DAF-16 activity in the neurons does not reduce yolk levels in *daf-16(mu86); daf-2(e1370)*. Data is the mean of one (D) or two (B) biological replicates (100 worms per replicate); error bars, SEM; Student's t-test *p<0.05 (versus age-matched wildtype). Data collected by E. Tyler.

3.2.7 RNAi screening for genes mediating effects of *daf-2* on yolk synthesis

Understanding IIS and how DAF-16 affects yolk accumulation might provide insight into how this pathway controls ageing. We therefore tried to identify additional downstream mediators of the effect of DAF-2 on yolk synthesis. To do this we used RNAi and VIT-2::GFP reporter strains. We tested whether *daf-2(-)* Yol-d could be reversed by RNAi knockdown of selected genes involved in longevity (Figure 3.12). Worms were grown at 15°C on control RNAi (L4440) and transferred at L4 larval stage to 25°C onto plates seeded with the RNAi clone of interest and 10µM FUdR.

daf-16 RNAi was used as a positive control because it was previously shown to be necessary for yolk reduction observed in *daf-2(-)* worms (DePina *et al*., 2011). In *daf-2* mutants autophagy is increased, and *daf-2(-)* longevity is autophagy dependant (Hansen *et al*., 2008; Meléndez *et al*., 2003). To probe whether yolk reduction in *daf-2(-)* worms involves enhanced yolk removal by autophagy we used *bec-1* (BECLIN) RNAi (Meléndez *et al*., 2003). *daf-18* (PTEN) RNAi was expected to increase yolk levels in *daf-2(-)* worms because wildtype DAF-18 negatively regulates IIS by reducing PIP3 levels (Ogg and Ruvkun, 1998). RNAi clones for additional downstream regulators were also tested: *aak-2* the α-subunit of AMP kinase, which is a downstream effector of *daf-2* (Apfeld et al., 2004), *skn-1*, which is a Nrf-2 type transcription factor involved in stress response (Tullet et al., 2008) and *daf-12*, a nuclear receptor for dafachronic acid involved in dauer formation (Antebi et al., 1998).

Out of the RNAi treatments tested, only *daf-16* RNAi caused an increase in VIT-2::GFP levels in day 4 GA1501 worms (Figure 3.12). This suggests that suppression of yolk protein in *daf-2(-)* worms requires DAF-16 but not *bec-1*, *aak-2*, *skn-1*, *daf-12*, or *daf-18*. GFP levels were normalized to GA1500 on day 1 and treatments were compared to GA1500 day 1 to determine if statistically different from wildtype. The result of *daf-18* RNAi is unexpected, as it should suppress reduction of yolk levels by GA1501. It remains a possibility that RNAi treatments did not rescue wildtype yolk levels due to maternal rescue effect. Tests could be repeated by placing worms on RNAi for two generations to reduce the possibility of maternal rescue. Another possibility is that RNAi is being hindered by the feeding defect (Eat) of *daf-2(e1370)*. Additionally, *daf-2(m577)* is more susceptible to suppression than *daf-2(e1370)* (Gems *et al*., 1998). This

experiment could be repeated using *daf-2(m577)* to exclude this possibility. These questions could also be better addressed by running worm lysates on Coomassie stained gels, and by using double mutants containing *daf-2(-)* and the suppressor of interest.
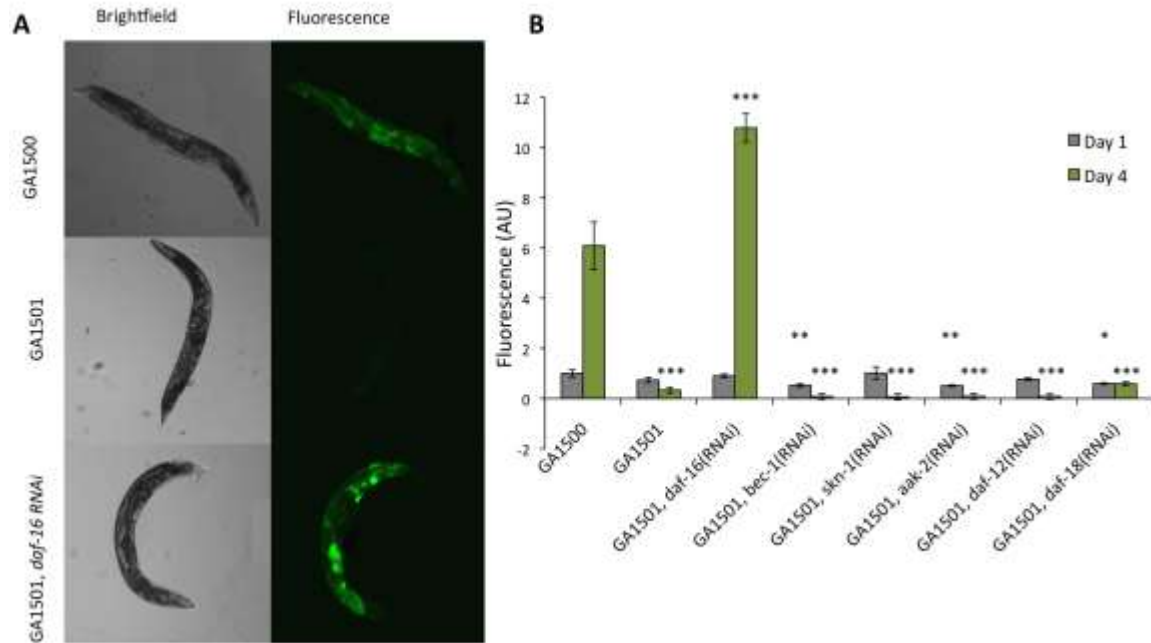
Figure 3.12 Effect of RNAi on VIT-2::GFP on day 4 of adulthood. A) Images of worms showing localization of YP170 using VIT-2::GFP. On day 4 GA1500 worms show yolk throughout the body cavity. This accumulation is absent in GA1501, this suppression is dependent on *daf-16*. B) An RNAi screen was conducted to examine if knockdown of genes involved in longevity restored wildtype yolk levels in GA1501. RNAi of *aak-2*, *daf-12*, *daf-18*, *skn-1* and *bec-1* did not increase yolk levels. RNAi of *daf-16* did cause an increase in YP, above those of wildtype. One trial was perfomed (10 worms); error bars, SEM; Student's t-test ***p<0.001, **p<0.01, *p<0.05 (versus age-matched control).

3.2.8 Effect of the germline on yolk protein

3.2.8.1 Effect of FUdR on yolk protein

5-fluoro-2′-deoxyuridine (FUdR) is a drug commonly used to treat cancer (e.g. colon cancer). It is also widely used by *C. elegans* researchers in lifespan assays as it inhibits DNA synthesis, inducing sterility in hermaphrodite worms (Mitchell et al., 1979). We were interested in the effect sterility has on YP levels. We wanted to test if reduction of the main yolk sink (oocytes) would cause an increase in yolk protein levels. To avoid

blocking development worms were raised without FUdR to the L4 larval stage, and they were then transferred to plates containing 10μM FUdR for the remainder of the experiment. GFP levels in GA1500 worms were observed on day 1 and 4. Because of the use of some temperature sensitive mutations, e.g. *glp-4(bn2)*, worms were raised at 15˚C and switched to 25˚C at the L4 stage. As predicted, FUdR treatment caused a significant increase of VIT-2::GFP on day 1 and 4 compared to worms on control plates (Figure 3.13 A).
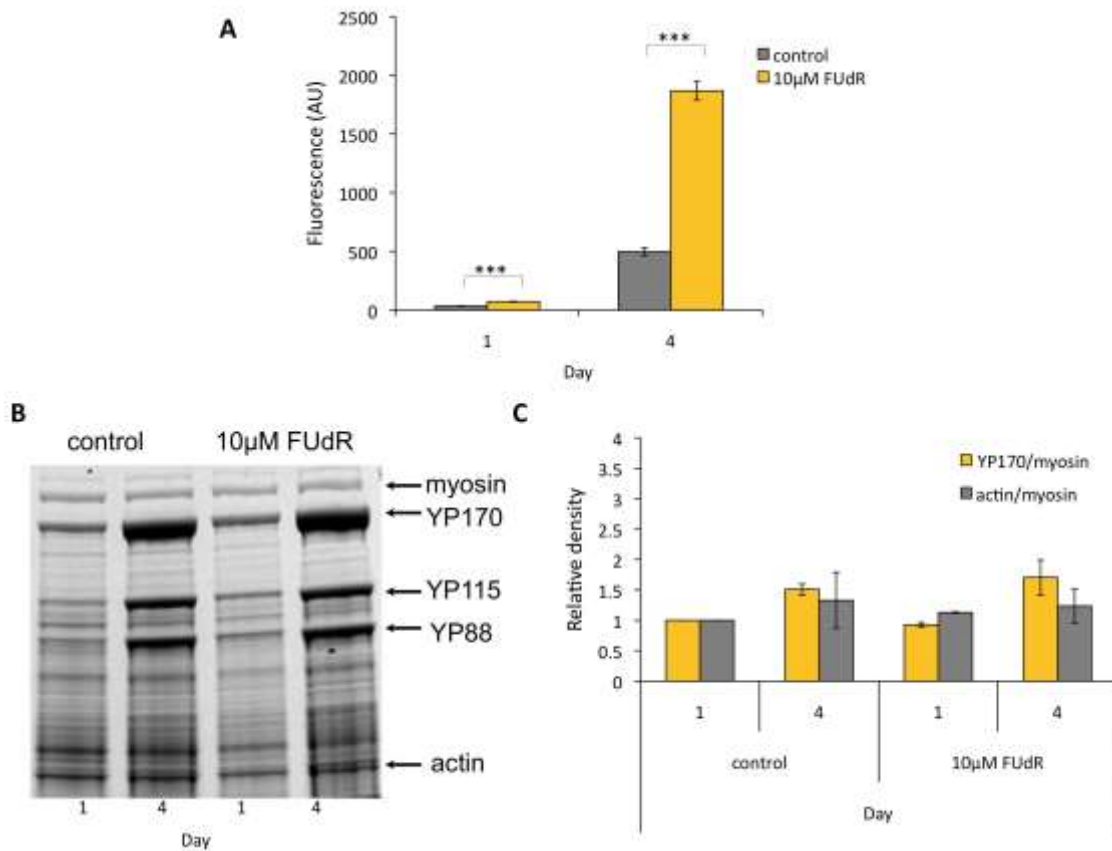
Figure 3.13 Effect of 10μM FUdR on yolk protein levels. A) Worms on 10μM FUdR have higher VIT-2::GFP levels on both day 1 and 4 compared to worms on control plates. B,C) Protein gels show no increase in yolk protein in day 4 worms on FUdR compared to control. Data is the mean of (A) one trial (40 worms) (B,C) two biological replicates (25 worms per replicate); error bars, SEM; Student's t-test ***p<0.001 (versus age-matched control).

The effects of FUdR on yolk were also examined by running worm lysates on Coomassie stained gels. Surprisingly, no increase in YP levels was observed with FUdR treatment as of day 4 (Figure 3.13 B,C; Appendix 1; Figure A-1.7). Protein lysate analysis should provide a more accurate depiction of changes in YP170 levels because VIT-2::GFP only shows abundance of YP170B, whereas on YP170 bands on gels reflect total amount of YP170A and YP170B. Taken together these results could imply that FUdR increases abundance of the less abundant YP170B, but not the more abundant YP170A. However, it is unknown how FUdR could do this.

3.2.8.2 Signals from the germline stimulate yolk protein production

Removal of gonad and germline precursor cells by laser ablation results in loss of the entire gonad structure and these worms have a wildtype lifespan (Hsin and Kenyon, 1999; Kimble and Hirsh, 1979). Worms without a somatic gonad or a germline have been previously shown to produce large amounts yolk protein (Kimble and Sharrock, 1983). We were interested in observing the effect of the germline on yolk protein levels by using temperature sensitive germline proliferation *glp-4(bn2)* mutants. When raised and maintained at 15°C *glp-4* mutants have a complete germline, wildtype lifespan and reduced fertility (Beanan and Strome, 1992; Qiao et al., 1995). If raised at 25°C from hatching *glp-4* mutants have an extended lifespan and few to no germ cells (Arantes-Oliveira *et al*., 2002). However, if *glp-4* mutants are raised at 15°C to L4 and then transferred to 25°C they will develop a germline but proliferation will be arrested after sperm production (no oocytes), these worms exhibit a wildtype lifespan (Arantes-Oliveira *et al*., 2002; McElwee *et al*., 2004).

To account for changes in developmental rate at different temperatures worms which were maintained at 15°C were collected on day 1 and 8 of adulthood. We calculated that given the slower development of worms at 15°C day 8 would be an equivalent to a day 4 worm cultured at 25°C and worms should be at the end of their reproductive period (Byerly et al., 1976). We found that at 15°C, day 1 *glp-4* mutants have higher levels of yolk than wildtype (Figure 3.14). This is likely due to the reduced fecundity of this strain as there are less oocytes to take up the yolk produced. By day 8 there is no difference in YP levels between *glp-4* mutants and wildtype worms (Figure

3.14; Appendix 1, A-1.8 A,B). Worms shifted from 15°C to 25°C at L4 have increased levels of YP170 on day 1 and 4 compared to wildtype (Figure 3.15). However, this increase was not observed in YP115 and YP88 (Appendix 1, Figure A-1.8 C,D). Worms raised at 25°C had increased YP170 levels on day 1 but wildtype levels of YP115 and YP88 (Figure 3.16; Appendix 1, Figure A-1.9 A,B).

The difference between *glp-4* worms raised at 15°C versus 25°C is the presence of a germline. The increase in YP170 observed in *glp-4* mutants shifted from 15°C to 25°C on day 4 suggest that germ cells signal to increase YP170 production. This should result in less YP being produced in worms at 25°C, however loss of the main yolk sink (oocytes), results in day 1 YP170 accumulation.
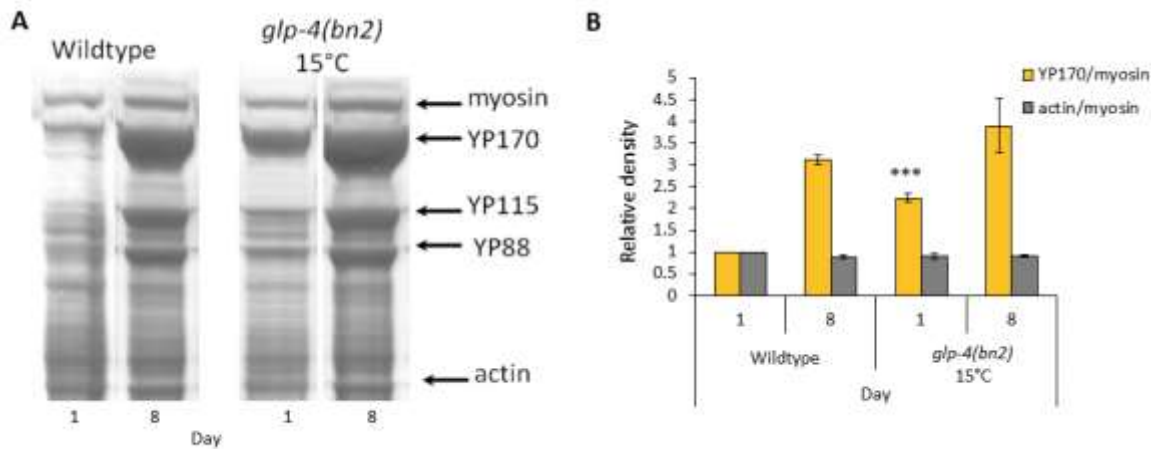
Figure 3.14 Increased levels of YP on day 1 *glp-4(bn2)* at 15°C. A) Coomassie stained SDS-PAGE gels showing yolk protein abundance. B) *glp-4(bn2)* with a complete germline, but reduced fertility, has higher levels of yolk protein on day 1 compared to wildtype. Data is the mean of three biological replicates (100 worms per replicate); error bars, SEM; Student's t-test ***p<0.001 (versus age-matched wildtype). Data collected by E. Tyler.
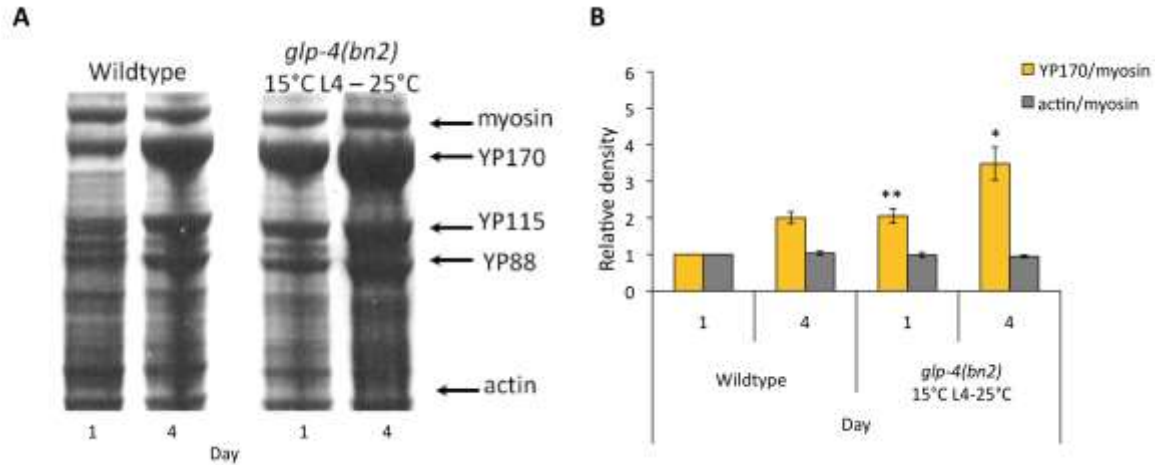
Figure 3.15 Increased levels of yolk protein on day 1 and 4 in *glp-4(bn2)* shifted at L4 from 15°C to 25°C. A) Coomassie stained SDS-PAGE gels showing yolk protein abundance. B) *glp-4(bn2)* shifted to 25°C posses an arrested germline and no oocytes, *glp-4* worms have higher levels of yolk protein on day 1 and day 4 compared to wildtype. Data is the mean of three biological replicates (100 worms per replicate); error bars, SEM; Student's t-test **p<0.01, *p<0.05 (versus age-matched wildtype). Data collected by E. Tyler.
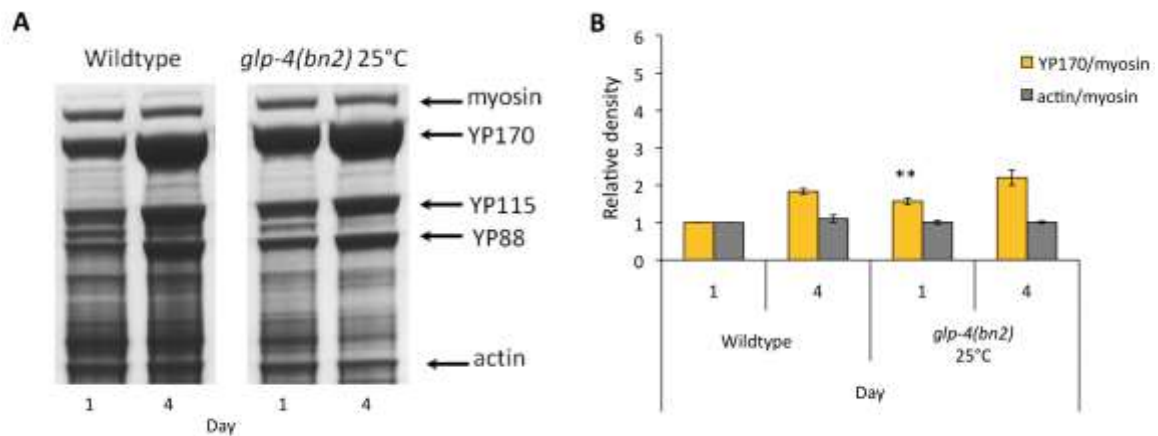
Figure 3.16 Increased levels of yolk protein on day 1 in *glp-4(bn2)* hatched at 25°C. A) Coomassie stained SDS-PAGE gels showing YP abundance. B) *glp-4(bn2)* at 25°C from egg posses no germline, have higher levels of yolk protein on day 1 compared to wildtype. Data is the mean of three biological replicates (100 worms per replicate); error bars, SEM; Student's t-test **p<0.01(versus age-matched wildtype). Data collected by E. Tyler.

3.2.9 Effect of germline signalling on yolk protein levels is DAF-16 dependent

Loss of the germline in hermaphrodite worms results in a 60% lifespan extension, which is DAF-16 dependent (Hsin and Kenyon, 1999). This suggests that under normal conditions signals from the germline accelerate ageing of the animal (Hsin and Kenyon, 1999). We wanted to know if the reduced yolk protein levels we observed in germline-less *glp-4(bn2)* worms at 25°C with respect to worms shifted to 25°C at L4 was DAF-16 dependent.

To do this we used *daf-16(mgDf50); glp-4(bn2)* worms and raised them at 25°C to block development of the germline. We found that in the absence of DAF-16 YP170 accumulates at higher levels in *daf-16(mgDf50); glp-4(bn2)* mutants with respect to wildtype (Figure 3.17). Levels of YP115 and YP88 remain similar to wildtype (Appendix 1, Figure A-1.9 C,D). Thus, as in *daf-2* mutants, the reduction in yolk levels in germlineless worms is DAF-16 dependant.
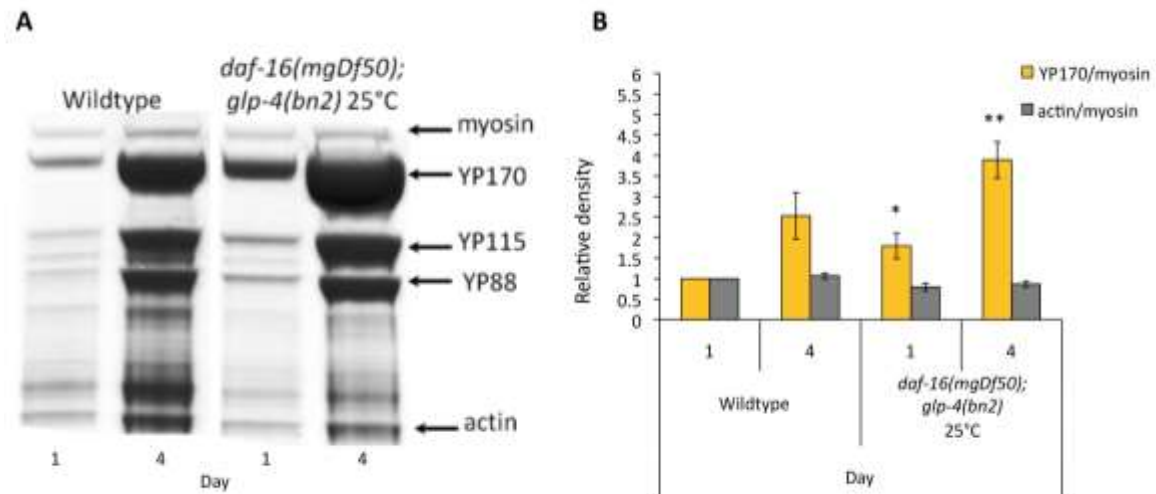
Figure 3.17 Yolk protein levels in *daf-16(mgDf50), glp-4(bn2)* worms. A) Coomassie stained SDS-PAGE gels showing yolk protein abundance. B) Levels of yolk protein in *daf-16(mgDf50), glp-4(bn2)* mutants were higher on day 1 and 4 with respect to wildtype. Data is the mean of three biological replicates (100 worms per replicate); error bars, SEM; Student's t-test **p<0.01, *p<0.05 (versus age-matched wildtype). Data collected by E. Tyler.

3.2.10 Tor, DR and Mit longevity mutants are not typically Yol-d

We examined whether a reduction in yolk protein synthesis is a hallmark of mutant strains with an increased longevity phenotype.

3.2.10.1 TOR pathway mutant

The target of rapamycin (TOR) pathway is a conserved, nutrient sensing pathway that modulates ageing. Inhibition of TOR causes a decrease in protein synthesis and inhibition of genes that regulate mRNA translation can increase lifespan (Hansen et al., 2007; Kapahi et al., 2010; Pan et al., 2007). RSKS-1 is the worm homologue of ribosomal S6 kinase (S6K), which is directly downstream of TOR. Mutation in this gene in worms causes slower development, reduced fecundity and increased lifespan (Pan et al., 2007; Hansen et al., 2007). Surprisingly, despite having lower levels of protein synthesis *rsks-1(ok1255)* mutants had higher levels of YP170 on day 1 and wildtype levels of yolk protein on day 4 (Figure 3.18). Levels of YP115 and YP88 remained similar to wildtype (Appendix 1, Figure A-1.10). Increased YP170 on day 1 may reflect reduced fecundity observed in *rsks-1* mutants. It may be that due to a lessening of the main yolk sink (oocytes) yolk levels accumulate to higher levels on day 1. It remains possible that in the absence of oocytes (e.g. *glp-4* background), *rsks-1(-)* would reduce YP levels.
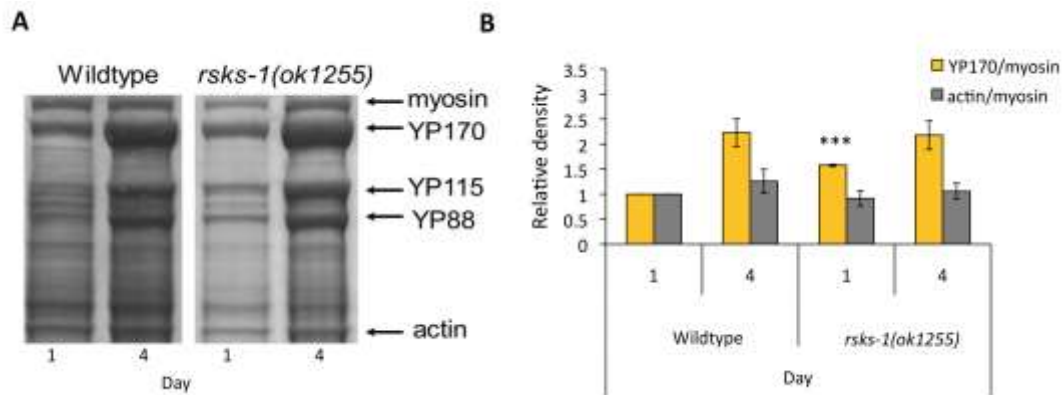
Figure 3.18   Effect of *rsks-1(ok1255)* on yolk protein levels. A) Coomassie stained SDS-PAGE gels showing yolk protein abundance. B) *rsks-1(ok1255)* worms have higher levels of YP on day 1 but not day 4 compared to wildtype. Data is the mean of three biological replicates (100 worms per replicate); error bars, SEM; Student's t-test ***p<0.001 (versus age-matched wildtype). Data collected by E.Tyler.

3.2.10.2 Dietary restriction mutant

Dietary restriction can extend lifespan in a wide range of organisms (Weindruch and Walford, 1988). In *C. elegans*, *eat-2* mutants that have a defect in pharyngeal pumping resulting in reduced food intake can be used as a genetic model for dietary restriction (Lakowski and Hekimi, 1998). Mutations in *eat-2* can increase lifespan by more than 50%, and the more severe the mutation, the bigger the extension (Lakowski and Hekimi, 1998). The lifespan extension in *eat-2* worms does not require DAF-16, suggesting the longevity in these strains are caused by a mechanism distinct from IIS (Lakowski and Hekimi, 1998). We examined whether *eat-2(ad1116)* had a reduction in YP levels and found that they had wildtype levels for day 1 and 4 (Figure 3.19; Appendix 1, Figure A-1.11). These results imply that longevity observed in *eat-2* mutants is not dependent on reduced levels of yolk. It is surprising, given the global protein reduction observed in *eat-2* mutants (Hansen *et al*, 2007) that YP levels remained similar to WT. This raises the possibility that YP production may be prioritized, despite lower fecundity (Crawford *et al*, 2007), given its importance in oocyte viability (Andux and Ellis, 2008).
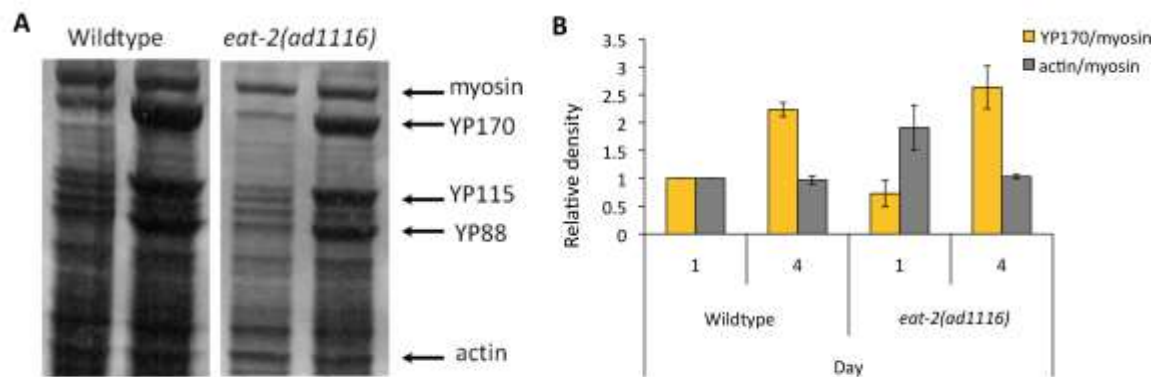
Figure 3.19 Effect of *eat-2(ad1116)* on yolk protein levels. A) Coomassie stained SDS-PAGE gels showing yolk protein abundance. B) *eat-2(ad1116)* has wildtype yolk protein levels on day 1 and 4. Data is the mean of three biological replicates (100 worms per replicate); error bars, SEM; Student's t-test (versus age-matched wildtype). Data collected by E. Tyler.

3.2.10.3 Mit mutants

C. elegans mitochondrial (*Mit*) mutants have disruptions in the electron transport chain but are long-lived. The longevity in these worms is thought to be a result of

differences in metabolism, supported by the fact that *clk-1(qm30)* and *isp-1(qm150)* have a common metabolic profile which is distinct to that of wildtype worms (Butler et al., 2010). We tested two *Mit* mutants: *nuo-6(qm200)* and *isp-1(qm150)* which are loss-of-function mutations of the mitochondrial complex subunit I and III, respectively (Feng et al., 2001; Yang and Hekimi, 2010b). Both of these mutations result in low oxygen consumption, slow development, low fecundity and increased lifespan (Feng et al., 2001; Yang and Hekimi, 2010b). Due to slow development our protocol had to be modified and for this experiment worms were synchronized to L4 at 20°C instead of 15°C.

We found that *nuo-6(qm200)* and *isp-1(qm150)* worms had wildtype YP levels on day 4 (Figure 3.20; Appendix 1, Figure A-1.12). However, *nuo-6(qm200)* had slightly lower levels of YP on day 1, which is surprising due to their low fecundity phenotype. One possibility is that lower YP levels day 1 may reflect an early deficit in ATP, resulting in lower energy levels, due to mitochondrial disruption (Figure 3.20).
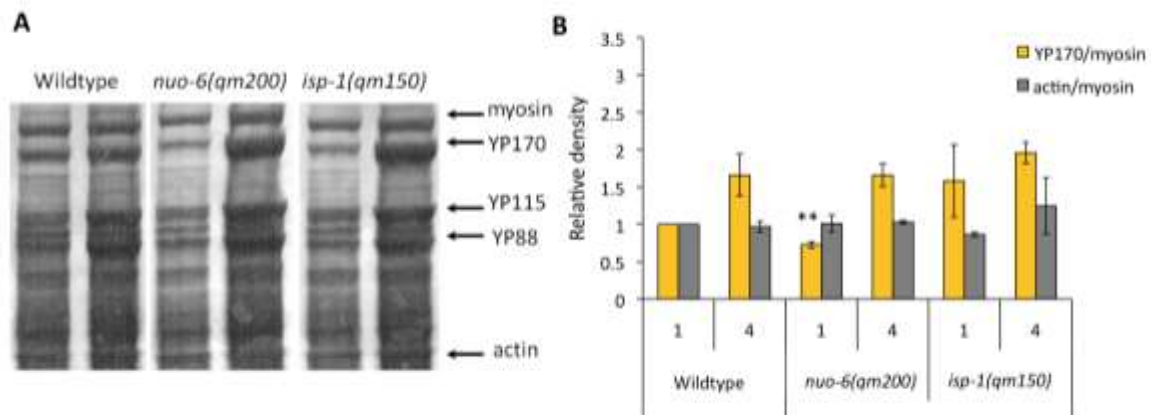
Figure 3.20 Effect of *nuo-6(qm200)* and *isp-1(qm150)* on yolk protein levels. A) Coomassie stained SDS-PAGE gels showing yolk protein abundance. B) *nuo-6(qm200)* and *isp-1(qm150)* have wildtype yolk protein levels on day 4, but yolk protein levels in *nuo-6(qm200)* are slightly lower on day 1. Data is the mean of three biological replicates (100 worms per replicate); error bars, SEM; Student's t-test **$p<0.01$(versus age-matched wildtype). Data collected by E. Tyler.

We saw no overall Yol-d pattern amongst other longevity mutant strains. However, reduced yolk production could be masked by reduced oocyte production in these strains.

3.2.11 Reduction in levels of yolk protein does not increase lifespan

After finding that yolk is continuously produced throughout adulthood we wanted to verify that yolk accumulation has an effect on lifespan as suggested by previous RNAi studies of *vit-2* and *vit-5* (Murphy *et al*., 2003). We used RNAi of *vit-5, vit-6* and double RNAi (1:1 mixture) of *vit-5/vit-6*. We obtained the *vit-5* feeding clone from the Ahringer library kindly shared with us by the Nurrish lab (UCL). The *vit-6* feeding clone was not available in this library but was sent to us by the Ahringer lab. Wildtype worms were placed on RNAi treatment from egg and raised at 15°C until L4. Worms were then transferred to plates containing 15µM FUdR.

3.2.11.1   Reduction in one yolk protein leads to an increase in others

We first checked the effect of *vit-5(RNAi)*, *vit-6(RNAi)* and *vit-5/vit-6(RNAi)* on yolk protein by collecting samples and running them on Coomassie stained SDS-PAGE gels. We found that *vit-5(RNAi)* greatly reduced yolk protein levels on day 1 and 4 of adulthood compared to wildtype (Figure 3.21 A,B). It also blocked the accumulation of YP170 which otherwise occurs on day 4 (Figure 3.21 A). Unexpectedly, we found that RNAi of *vit-5* caused a marked increase in YP115 and YP88 on day 4 (Figure 3.21 A,C). Similarly, RNAi of *vit-6* greatly reduced YP115 and YP88 on day 4 while causing a marked increase in YP170 (Figure 3.21 A,B). *vit-5/vit-6(RNAi)* decreased levels of YP170, YP115 and YP88, blocking their day 4 accumulation. Increased YP levels resulting from RNAi could reflect either a compensatory increase in *vit* gene transcription or competition between *vit* RNAs for access to ribosomes. The former is more likely as if it is mostly a matter of clogging up the translational machinery one would expect an increase in other proteins as well.
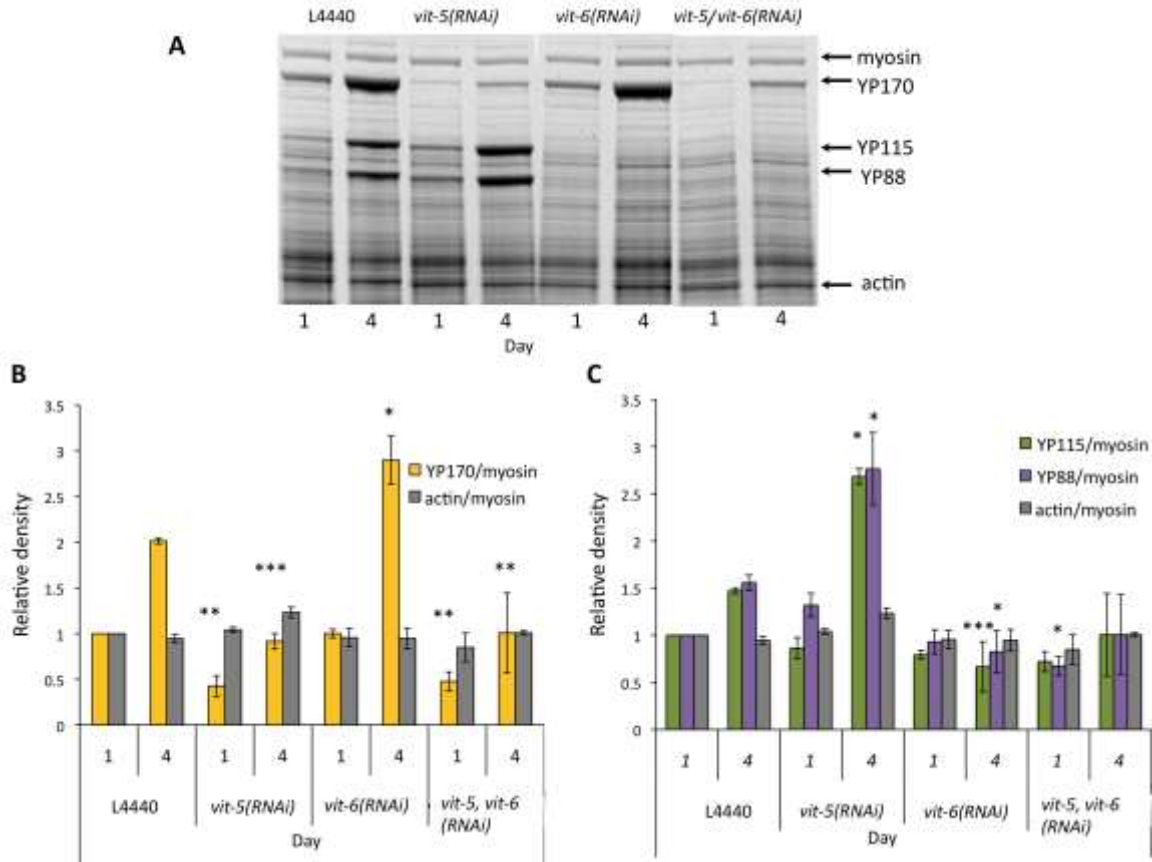
Figure 3.21 Effect of RNAi on YP abundance levels. A) Coomassie stained SDS-PAGE gels showing yolk protein abundance. B) Quantitation of YP170 bands show Yol-d phenotype on *vit-5(RNAi)* and *vit-5/vit-6(RNAi)* and a Yol-o phenotype on *vit-6(RNAi)* compared to age-matched L4440 control. C) Quantitation of YP115 and YP88 show Yol-d phenotype on *vit-6(RNAi)* and a Yol-o phenotype on *vit-5(RNAi)* compared L4440 control. Data is the mean of three biological replicates (25 worms per replicate); error bars, SEM; Student's t-test ***p<0.001, **p<0.01, *p<0.05 (versus age-matched wildtype).

3.2.11.2   *vit-2* is a minor contributor to YP170 levels

There is high sequence similarity between *vit-3*, *vit-4*, and *vit-5,* and our data suggests that *vit-5(RNAi)* knocksdown all three mRNA transcripts. There is less sequence similarity between *vit-2* and *vit-5* (**Figure 3.1**), so knockdown by *vit-5(RNAi)* seems unlikely. We examined the effect of *vit-5(RNAi)*, *vit-6(RNAi)* and *vit-5/vit-6(RNAi)* on the VIT-2::GFP translational reporter strain GA1500. We found that *vit-5(RNAi)* did reduce fluorescence levels on day 1 and 4, but only slightly (Figure 3.22). This implies that *vit-5(RNAi)* only slightly reduces VIT-2 protein levels, possibly due to a small degree of

sequence similarity. This in turn suggests that VIT-2 is not a major contributor of the YP170 yolk protein.

On day 4, VIT-2::GFP worms on *vit-6(RNAi)* and *vit-5/vit-6(RNAi)* treatments do not show increased fluorescence. Interestingly, *vit-5/vit-6(RNAi)* slightly increased fluorescence on day 1 (Figure 3.22). *vit-6(RNAi)* alone did not have this effect, nor did *vit-5/vit-6(RNAi)* on day 4. Thus, the combined absence of *vit-5* and *vit-6* mRNA is sufficient to increase VIT-2 protein levels on day1, perhaps by increasing *vit-2* mRNA access to ribosomes.
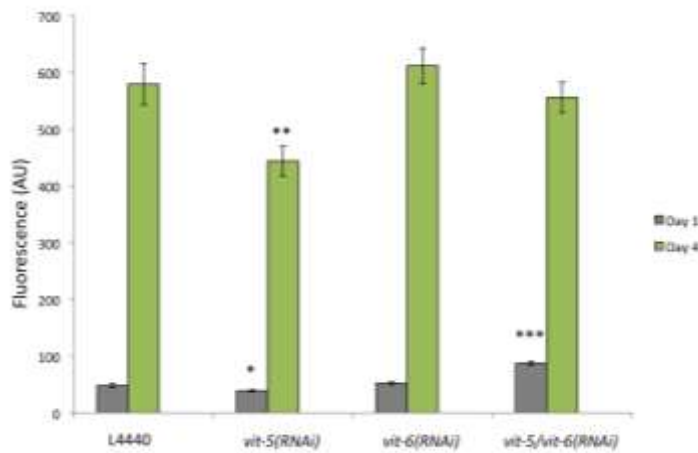
Figure 3.22 Effect of *vit-5*, *vit-6*, *vit-5/vit-6* RNAi on VIT-2::GFP expression. Worms on *vit-5(RNAi)* show a slight reduction of fluorescence on day 1 and 4 compared to worms on L4440 (control RNAi). *vit-6(RNAi)* and *vit-5/vit-6(RNAi)* did not affect VIT-2::GFP on day 4, but caused a slight increase on day 1. One replicate was performed. Data is the mean (15-25 worms); error bars, SEM; Student's t-test ***p<0.001, **p<0.01, *p<0.05 (versus age-matched wildtype).

3.2.11.3   Effects of *vit* RNAi on lifespan

A previous study found that *vit-2* and *vit-5* gene expression is down regulated in *daf-2(-)* worms and that RNAi of these genes modestly extends lifespan in *daf-2(+)* worms (Murphy *et al*., 2003). This result suggests that yolk accumulation has a harmful effect on worms. We set out to replicate this finding using *vit-5(RNAi),* which greatly reduces YP170 levels (Figure 3.5). We could not obtain the *vit-2* clone from the Ahringer library nor the lab that conducted the earlier study. To test the full extent of the effect of yolk accumulation on lifespan we used *vit-6(RNAi)*, which lowers YP115 and YP88, and *vit-5/vit-6(RNAi),* which lowers levels of all three yolk proteins (Figure 3.21).   We conducted 4 trials with varied results (Table 3-1). We observed increased variation in

lifespan in worms subjected to *vit-6(RNAi)*, which suggests that an increase in YP170 may result in lifespan fluctuations. Surprisingly we could not replicate previous findings in which *vit* RNAi extends lifespan. Instead our combined data implied that none of our RNAi treatments extend lifespan. This implies that yolk accumulation does not limit lifespan.
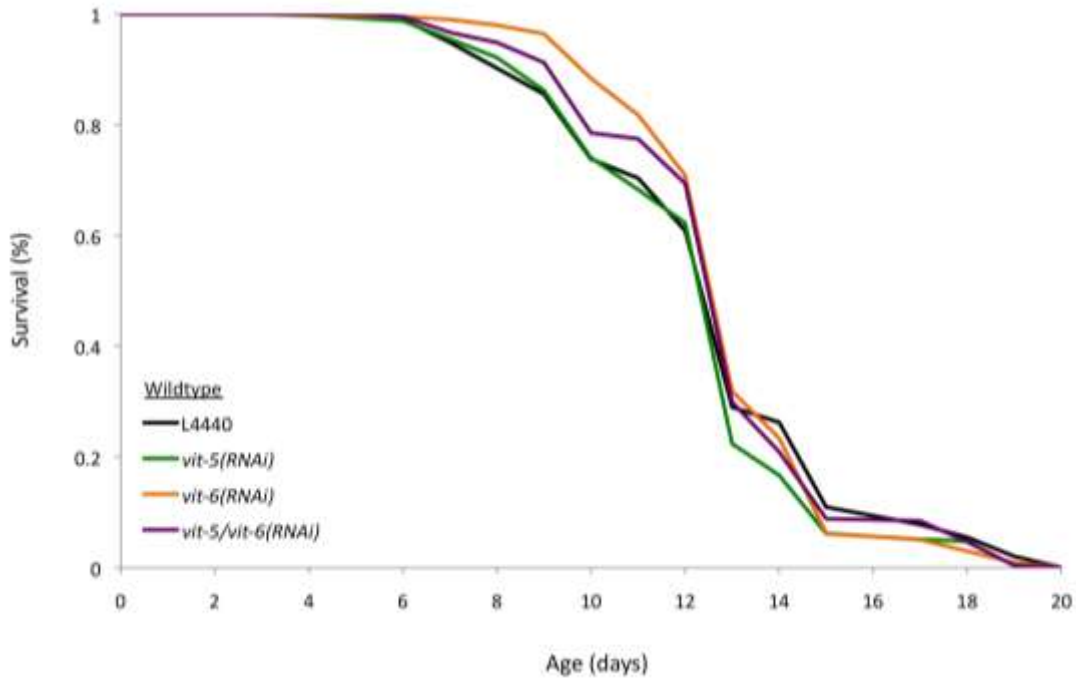
Figure 3.23 RNAi of *vit* genes does not extend lifespan. In all assays worms were hatched on to RNAi treatment and raised at 15˚C to L4. Worms were then transferred to plates with 15μM FUdR applied topically and maintained at 25˚C for duration of the experiment. Data mean of 4 biological replicates (100 worms per treatment).

RNAi treatment	Mean lifespan [median] (days)	% of control lifespan	Log Rank (p vs. control)	Deaths [censored]
L4440 (control) Combined	**12.7 [13]**			**371 [29]**
Trial 1	13.7 [13]			97 [3]
Trial 2	12.5 [13]			85 [15]
Trial 3	11.9 [12]			93 [7]
Trial 4	12.5 [13]			96 [4]
vit-5(RNAi) Combined	**12.3 [13]**	**-4**	**0.09**	**361 [39]**
Trial 1	12.9 [13]	-6	0.01	82 [18]
Trial 2	12.6 [13]	+0.7	0.49	93 [7]
Trial 3	12.3 [12]	+3	0.62	89 [11]
Trial 4	11.8 [13]	-6	0.06	97 [3]
vit-6(RNAi) Combined	**13.1 [13]**	**+3**	**0.30**	**364 [36]**
Trial 1	12.8 [13]	-8	0.0002	96 [4]
Trial 2	13.6 [13]	+9	0.002	90 [10]
Trial 3	13.6 [12]	+14	0.005	92 [8]
Trial 4	12.5 [13]	+0.7	0.98	86 [14]
vit-5/vit-6(RNAi) Combined	**12.9 [13]**	**+2**	**0.72**	**346 [54]**
Trial 1	14.6 [15]	+7	0.04	68 [32]
Trial 2	12.2 [13]	-2	0.21	87 [13]
Trial 3	12.5 [12]	+5	0.30	95 [5]
Trial 4	12.3 [13]	-1	0.31	96 [4]

Table 3-1 Effect of *vit* RNAi treatments on lifespan. This table contains data corresponding to Figure 3.23.

3.3   Discussion

3.3.1 Yolk protein accumulation in post-reproductive worms is consistent with hyperfunction

The accumulation of yolk protein throughout the body cavity in wildtype worms is consistent with the idea that biosynthesis is not regulated in ageing worms. By following changes in YP in wildtype worms we observed an increase in yolk protein levels in post reproductive worms until an apparent peak level is reached at around day 12, after which levels remain high. This YP accumulation was absent in *daf-2(-)* worms.

Though yolk production is part of an evolved reproductive program the accumulation of YP in post-reproductive worms suggests there is no evolutionary mechanism to switch off vitellogenesis (Herndon *et al*., 2002). Is the yolk accumulation we observe in older worms a quasi-programme? In order for it to be deemed so, accumulation of yolk should not bestow a benefit in post-reproductive worms. One study found that YP115, one of the two proteins encoded for by *vit-6* is the major carbonylated protein in older worms, suggesting a role as a ROS scavenger (Nakamura et al., 1999). However, observing our Coomassie stained gels of whole worm lysates, yolk protein bands seem to make up a large proportion of the total protein. So, it's not surprising that they would turn up in an experiment looking for carbonylated proteins in older worms.

A second study found that in insects vitellogenins can store free iron, potentially acting as a chelator (van Heusden et al., 1991). These studies suggest a beneficial effect of YP accumulation as it could store toxic compounds, protecting the worm. This could be tested by seeing if RNAi of *vit* genes makes worms more sensitive to drug toxicity.

Another possibility is that to maintain yolk production at such high levels to ensure reproductive output is costly to the worms and diverts resources from somatic maintenance (DePina *et al*., 2011). If this were true it could be probed by placing worms on *vit* RNAi and examining whether worms under this treatment have increased resistance to stress, on the assumption that increased stress resistance reflects increased somatic maintenance.

3.3.2 IIS/IGF-1 strongly represses yolk protein translation

Accumulation of yolk protein was strongly reduced in long lived *daf-2(e1370)* mutants. The *daf-2(e1370)* mutation is a class 2 allele; these are pleiotropic and have decreased fecundity and feeding rate in addition to the Age phenotype (Gems *et al*., 1998). To rule out the possibility that Yol-d in *daf-2(e1370)* worms is a result of pleiotropy we also tested the less pleiotropic allele *daf-2(m577)* and found that it was also Yol-d. Reduction in YP levels in *daf-2(-)* mutants was dependent on DAF-16, the lack of which restored wildtype YP levels. Other long-lived IIS mutants tested were *age-1(hx546)* and *age-1(mg109)*. The weak allele *age-1(hx546)* caused a reduction in YP levels on day 1 but not day 4. The stronger null allele *age-1(mg109)* was also tested and caused a reduction in YP levels on day 4 compared to wildtype, to a lesser extent than in *daf-2(-)* worms. This may be due to maternal rescue of *age-1* (Gottlieb and Ruvkun, 1994). Thus, there is a strong correlation between the effects of IIS on yolk production and lifespan, suggesting a close connection between these two traits.

Two possible scenarios of how IIS mutants reduce YP levels are that DAF-16 activity can decrease YP synthesis or increase its degradation. As a test whether YP was being degraded we used RNAi of *bec-1*, a gene required for *C. elegans* autophagy (Meléndez *et al*., 2003). Results of our RNAi screen found *bec-1*(RNAi) did not increase VIT-2::GFP levels in a *daf-2(e1370)* background. This suggests that *daf-2(-)* worms are not Yol-d due to increased autophagy, but does not rule out that other yolk degradation mechanisms may be activated in IIS mutants; e.g. proteosome-mediated protein degradation. Additionally, dietary restriction mutant *eat-2(ad1116)* activates autophagy (Hansen *et al*., 2008) but did not suppress YP accumulation.

The alternative possibility is that DAF-16 promotes longevity by decreasing protein synthesis. Arguing against this, one study found that *daf-2(-)* worms show no reduction in global translation, measured by ^{35}S-methionine incorporation (Hansen *et al*., 2007). However, a more recent study used ^{35}S-labelled bacteria and found that protein synthesis was greatly reduced in *daf-2(-)* worms (Depuydt *et al*., 2013). Vitellogenin protein abundance was also examined and all six *vit* genes were strongly reduced in *daf-2(-),* and *vit-1, vit-3* and *vit-4* were reduced in DR worms (Depuydt *et al*., 2013; Stout *et al*., 2013). A global reduction in protein synthesis could account for the Yol-d in *daf-2(-).*

3.3.3 Germline regulation of yolk protein

In this study we sought to identify the tissue in which DAF-16 activity regulates yolk protein synthesis. We used *daf-16(mu86); daf-2(e1370)* transgenic strains in which DAF-16 was rescued in the neurons, intestine and muscle (Libina *et al*., 2003). Of these strains DAF-16 expression in the intestine partially restores lifespan of *daf-2(-)*, neuronal DAF-16 does so marginally and muscular DAF-16 had no effect on lifespan (Libina *et al*., 2003). We found that none of these strains were able to strongly suppress day 4 YP accumulation. It is somewhat surprising that intestinal DAF-16 rescue only partially restored *daf-2(-)* Yol-d as this is the tissue where yolk is synthesized (Kimble and Sharrock, 1983). This implies that one or more tissues other than the intestine act to reduce yolk levels. One possibility is that the gonad plays a role in to signalling the intestine to regulate yolk protein synthesis. Our examination of germline effects on YP levels suggests the gonad to be a likely candidate for the tissue which signals to regulate YP synthesis. Another hint comes from the finding by DePina *et al* in which mating *daf-2(e1370)* mutants with wildtype worms increases *vit-2/5* mRNA but not YP levels (DePina *et al*., 2011). This suggests that presence of sperm in the spermatheca triggers a signal to increase YP gene transcription. This would be a good strategy as after the L4 stage hermaphrodite worms switch from sperm production to oocyte production (Hubbard and Greenstein, 2005). In this way a surplus of mRNA is transcribed to ensure there will be enough yolk availability to supply developing oocytes. It is possible DAF-16 activation in the spermatheca or other regions of the somatic gonad represses YP translation in the intestine in *daf-2(-)* worms.

DePina *et al* also found that feminized *fem-1(hc17)* mutants that produced no sperm had lower levels of *vit-2/5* mRNA yet higher YP levels on day 1 but not day 4, while masculinised *fem-3(q20gf)* mutants that only produce sperm had wildtype *vit-2/5* mRNA and higher levels of YP on day 1 and 4 (DePina *et al*., 2011). We found similar results with respect to YP levels in our experiments with *glp-4* worms. *glp-4* worms grown at 15˚C and switched to 25˚C make sperm but not oocytes (Arantes-Oliveira *et al*., 2002) and similar to masculinised *fem-3(q20gf)* mutants these worms had increased levels of YP on day 1 and 4. At 25˚C *glp-4* germline-less worms are Yol-o on day 1 but have wildtype YP levels on day 4. This is consistent with early observations in which

yolk protein was present at high levels in worms with laser ablated gonads in young adults (Kimble and Sharrock, 1983). Germline ablation causes a DAF-16 dependent increase in lifespan, it also causes nuclear localization of DAF-16 in the intestine (Hsin and Kenyon, 1999; Lin et al., 2001). We found that *daf-16(mgDf50);glp-4(bn2)* raised at 25°C had levels of YP higher than *glp-4(bn2)* controls. This increase in YP in the absence of DAF-16 suggests that *glp-4(bn2)* worms raised at 25°C may have reduced levels of YP synthesis, but this is masked by the lack of oocytes to take it up. Thus, absence of a germline may induce a DAF-16 dependent signal in the somatic gonad, which is relayed to the intestine to repress translation.
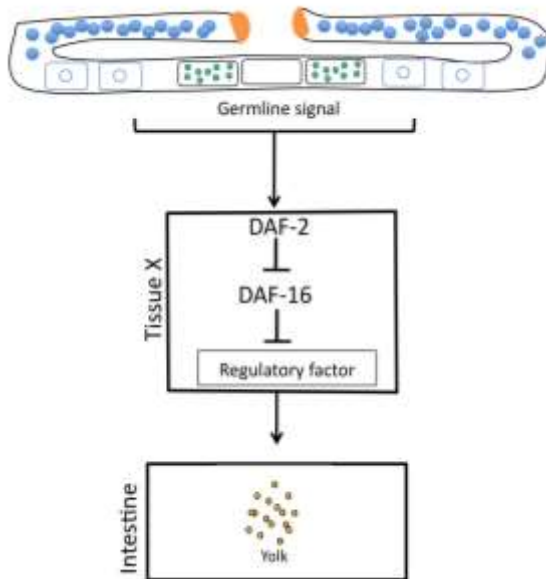
Figure 3.24 Model for YP translational regulation. IIS regulates YP synthesis in the intestine via signals from the germline or somatic gonad, which activate DAF-2 in an unidentified tissue (Tissue X). In the absence of a germline a DAF-16 dependent signal causes a decrease in a regulatory factor, which reduces YP translation in the intestine.

The finding that yolk accumulates in hermaphrodites without a gonad hints that a signal outside of the gonad stimulates yolk protein synthesis (Kimble and Sharrock, 1983). In *Drosophila*, vitellogenins synthesis is regulated in response to 20-hydroxyecdysone and juvenile hormone (JH) (Jowett and Postlethwait, 1980) which is in turn regulated by IIS (Tatar *et al*., 2001). It is possible that *C. elegans* also have a regulatory factor, which is produced in early adulthood in anticipation of reproductive needs, and hence worms without a gonad still produce yolk. One possible scenario is that the germline or somatic gonad generates a signal to increase DAF-2 activity in a currently unidentified tissue, which in turn stimulates a further increase in a regulatory hormone,

conveying a signal to increase yolk translation to the intestine (Figure 3.24). Presumably *daf-2(-)* worms are Yol-d because the production of regulatory factor is repressed from early adulthood.

3.3.4 Yolk accumulation is not a life limiting pathology

During the course of our studies we examined a range of longevity mutants and found that in most cases they did not repress YP accumulation on day 4 (Table 3-2). Some of these mutants such as *glp-4(bn2)* and *rsks-1(ok1255)* had higher levels of YP on day 1 which likely result from their reduced fecundity.

Strain	Lifespan (% Wildtype)	Fecundity (% Wildtype)	YP170 Yol	YP115 Yol	YP88 Yol	Source
daf-2(e1370)	+[b]30,+[a]110%	-[b]61%	Yol-d	Yol-d	Yol-d	1,2
daf-2(m577)	+[b]59%	+[b]14%	Yol-d	Yol-d	Yol-d	2
age-1(hx546)	+[a]40%,+[b]60%	-[a]75%	Yol-d (day 1)	WT	WT	3
age-1(mg109)	+[b]40%	N.A.	Yol-d	WT	WT	4
glp-4(bn2)	+[b]17%	sterile	Yol-o (day 1)	WT	WT	5
rsks-1(ok1255)	+[a]9%	-[a]46%	Yol-o (day 1)	WT	WT	6,7
eat-2(ad1116)	+[a]45%	-[a]51%	WT	WT	Yol-d (day 1)	8,9
nuo-6(qm200)	+[a]73	-[a]79%	Yol-d (day 1)	WT	WT	10
isp-1(qm150)	+[a]77%	-[a]75%	WT	WT	WT	11

Table 3-2 Lifespan, fecundity and Yol phenotype of longevity mutants. Data on mean lifespan and fecundity was compiled from various sources ([a]20˚C or [b]25˚C): [1](Kenyon et al., 1993), [2](Gems *et al*., 1998), [3](Friedman and Johnson, 1988), [4](Gami et al., 2006), [5](Arantes-Oliveira *et al*., 2002), [6](Pan et al., 2007), [7](Selman *et al*., 2009), [8](Lakowski and Hekimi, 1998), [9](Crawford et al., 2007), [10](Yang and Hekimi, 2010b), [11](Feng *et al*., 2001).

We also lowered YP levels in wildtype worms using RNAi of *vit-5*, *vit-6* and *vit-5/vit-6* to test whether reduction in yolk protein increased longevity. We measured YP levels using Coomassie stained SDS-PAGE gels and found that RNAi of *vit-5* greatly reduced levels of YP170, while causing a large increase in YP115 and YP88. RNAi of *vit-6* showed a similar effect, resulting in a reduction of YP115 and YP88 but an increase in YP170. Combined RNAi of both *vit-5/vit-6* lowered the levels of all three YP bands. Our results could imply that because *vit* genes are transcribed and translated at high levels, removal of one frees the translational machinery to allow increased translation of other *vit* transcripts. By performing lifespans we found that RNAi of *vit* genes did not increase lifespan. These results contradict earlier findings in which *vit-2* and *vit-5* RNAi increased lifespan (Murphy *et al*., 2003). It is possible that failure to replicate previous finding reflect differences in culture conditions between labs. In a third lab where tests of vit RNAi on lifespan were performed, no consistent increases in lifespan were seen (Cathy Wolkow, personal communication).

The accumulation of yolk protein, of which the only known function is the nourishment of oocytes, after reproduction is consistent with a biosynthetic open faucet model. Yolk accumulation appears pathological, but our data in this study strongly suggests that it does not in itself toxic to worms and is not a predictor of longevity. Thus, lifespan must be limited by a different pathology- perhaps the same that limits lifespan in male *C. elegans*, where yolk is not synthesized.

Chapter 4: Ageing in the *C. elegans* germline

4.1 Introduction to *C. elegans* reproductive system

In this chapter we will describe changes that occur in the hermaphrodite reproductive system with age. We will then examine age-related changes in the germline, particularly gonad degeneration, to determine if their origin is linked to quasi-programmes.

4.1.1 *C. elegans* hermaphrodite reproductive system

The hermaphrodite reproductive system is comprised of three main components: the somatic gonad, the germline and the egg-laying apparatus. Together they form two symmetrical U-shaped gonad arms with an egg-laying apparatus in the mid-body (Lints and Hall, 2009c). Each gonad arm consists of the distal tip cell (DTC), gonadal sheath and spermatheca; the egg-laying apparatus includes the uterus, vulva and its respective muscles; and the germline includes cell lineages that create sperm and oocytes (Lints and Hall, 2009c) (Figure 4.1). In *C. elegans* the germline is arranged in a distal to proximal orientation with germ cells near the DTC undergoing mitosis, while as the germ cells move proximally, away from the DTC, they enter meiosis (Kimble and Crittenden, 2005).

Figure 4.1 *C. elegans* hermaphrodite reproductive system. Depiction of the germline and somatic gonad with labelled structures: distal tip cell (DTC), distal gonad (DG), proximal gonad (PG) spermatheca (Sp). Image modified from Lints & Hall, 2009.

Hermaphrodite worms have a soma that is female, but a gonad that produces approximately 300 sperm cells during the L4 stage before switching to oocyte production in early adulthood (Hirsh et al., 1976; L'Hernault, 2006). Spermatids accumulate at the end of the proximal arm until they are pushed into the spermatheca by the first oocyte where they undergo spermiogenesis (Ward and Carrel, 1979). At 20°C a hermaphrodite worm lays approximately 300 fertilized eggs, which coincides with the amount of self-sperm available, thus sperm is the limiting factor for reproduction (Singson, 2001; Ward and Carrel, 1979). Introducing male sperm by mating increases the brood size and duration of progeny production, in addition to doubling total oocyte production (Ward and Carrel, 1979).

Germ cells in the distal gonad are not completely cellularized and share a common core (rachis) (Gilbert et al., 1984). As germ cells move toward the loop region apoptosis takes place, and surviving cells exit pachytene and move down the proximal arm in a linear manner (Greenstein, 2005). Oocytes in diakinesis contain a nuclear envelope, the most proximal oocyte (terminal oocyte) completes meiotic maturation and loses the nucleolus in response to stimulus from sperm (McCarter et al., 1999) (Figure 4.2). The mature oocyte passes through the spermatheca, becomes fertilized and is ovulated in a process that is repeated approximately every 23 minutes (Greenstein, 2005; McCarter *et al*., 1999).
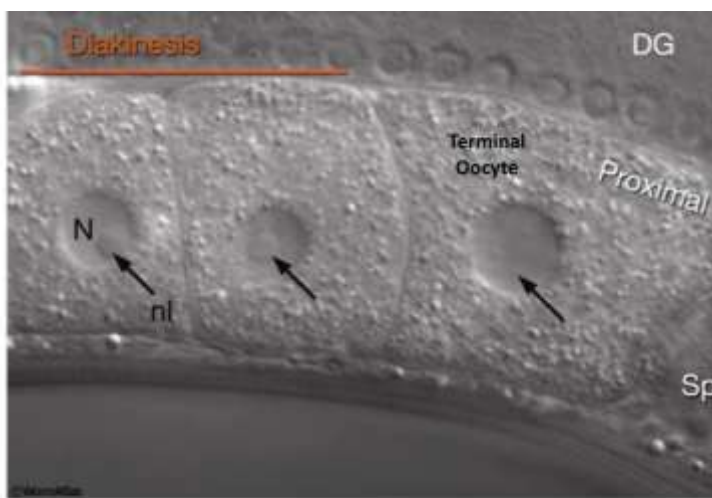
Figure 4.2 Position of terminal oocyte. DIC image depicting loss of the nucleolus (nl) from the nucleus (N) in the terminal oocyte, which is located prior to the spermatheca (Sp). DG, distal gonad. Image reproduced from Lints & Hall, 2009 and modified.

4.1.2 *C. elegans* male reproductive system

The male reproductive system of worms is a J-shaped arm, consisting of the somatic gonad, the germline and the proctodeum (Lints and Hall, 2009a). The male *C. elegans* germline only produces sperm, which progresses in a linear sequence of spermatogenesis from the distal arm continuously throughout adulthood (Klass et al., 1976). As in hermaphrodites, germ cells near the DTC undergo mitosis, and as they move away progress through the different stages of meiosis (Kimble and Hirsh, 1979). Germ cells are connected to the rachis until pachytene at which point spermatocytes (spermatid precursor cells) detach and complete meiosis to generate spermatids, which are stored in the seminal vesicle (Lints and Hall, 2009a). The cloaca and spicules are located in the proctodeum, and during copulation spicules are used to find and anchor the hermaphrodite vulva after which ejaculation occurs via the cloaca (Ward and Carrel, 1979). Spermiogenesis, the process through which sessile spermatids become motile spermatozoa, takes place in the hermaphrodite vulva after mating (L'Hernault, 2006; Ward and Carrel, 1979). Male derived sperm crawl into the hermaphrodite spermatheca were they outcompete the smaller hermaphrodite sperm (LaMunyon and Ward, 1998; Ward and Carrel, 1979).
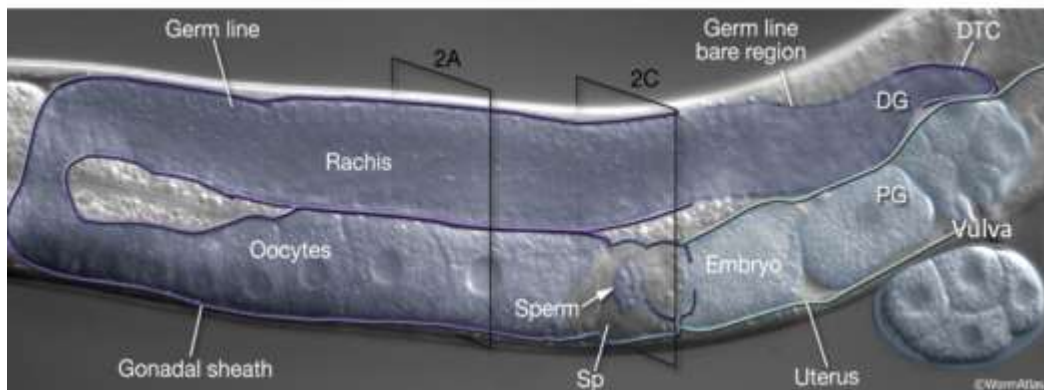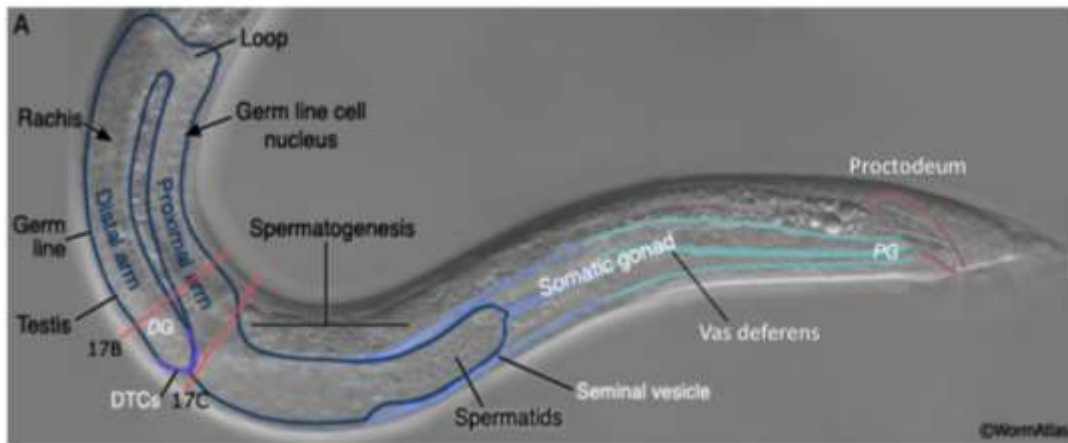

Figure 4.3 *C. elegans* male reproductive system. Depiction of male germline and somatic gonad with labelled structures: proximal gonad (PG), distal gonad (DG), distal tip cell (DTC). Image reproduced from Lints & Hall, 2009 and modified.

4.1.3 Loss of germline integrity in ageing hermaphrodites

Oocyte production is not tightly linked to sperm availability. When sperm count drops to ~40, hermaphrodites continue to produce oocytes which pass through the spermatheca and uterus, being laid unfertilized (Ward and Carrel, 1979). These unfertilized oocytes undergo several rounds of nuclear division becoming highly polyploid (Ward and Carrel, 1979). Shortly after reproduction halts there is a two-fold accumulation of unfertilized oocytes (compared to day 1 adults) in the proximal arm which become stacked in a columnar fashion (Jud *et al*., 2007). This continued oocyte production in the absence of sperm shows that oocyte production is relatively unregulated in post-reproductive adult hermaphrodite worms.

Germlines in older worms show significant signs of deterioration from around day 5 of adulthood and this deterioration increases with age (Garigan *et al*., 2002). In older animals, germline nuclei in the distal arms become more widely spaced and cavities begin to appear between them (Garigan *et al*., 2002). Germ cells, which in young worms are connected in a syncytium, become increasingly cellularized (Garigan *et al*., 2002). In later stages of deterioration the gonad shrivels (Garigan *et al*., 2002). The mechanism by which this striking deterioration occurs is not yet known. One possibility is that disintegration of the gonad is caused by molecular damage. In this chapter and the next we will explore an alternative possibility: that it is caused by hyperfunction.

Examination of the germline of adult hermaphrodites using Nomarski microscopy revealed condensed structures which were not observed at larval stages or in male worms (Gumienny *et al*., 1999). By using vital DNA-staining dyes such as Hoechst 33342, SYTO 12, and DAPI these condensed structures were recognised as apoptotic cells. The number of apoptotic cells increased during the reproductive life of worms (Gumienny *et al*., 1999). A central hypothesis explored in this thesis is that due to an age reduction in the force of natural selection, no mechanism exists to switch off germline apoptosis at the end of reproduction. We postulate that the resulting apoptotic tap left on contributes to age-related gonad disintegration.

4.2 Results

4.2.1 Measurement of gonad degeneration in post-reproductive hermaphrodites

In unmated wildtype hermaphrodites reproduction ceases after sperm depletion at around day 5 of adulthood (Lints and Hall, 2009c). After this the germline shows progressive decline with age (Garigan *et al*., 2002). To quantify gonad degeneration (GD) we developed a protocol modified from the study by Garigan *et al*. (2002). We captured images of wildtype worms maintained at 20˚C (unless otherwise stated) on days 1, 8, and 12 of adulthood using DIC microscopy. For each worm, only one gonad arm was clearly visible, the other arm being usually hidden beneath the intestine. One image was selected per worm and images were compiled into a Microsoft PowerPoint file, which was then examined and each image given a score of 1-5 representing different degree of gonad degeneration. Scoring of each image was performed blindly by three individuals.

We defined 5 stages of gonad degeneration as follows. Worms given a score of 1 had gonads that appeared youthful and healthy. If the gonad showed slight atrophy and subtle signs of deterioration, having lost some of its diameter, but the general structure remained intact it received a score of 2. Gonads showing signs of impending breakage, such as markedly reduced diameter, and reduction in size (shrivelling) were given a score of 3. Gonads that fragmented, forming islands of gonad tissue were given a score of 4 (Figure 4.4). Worms with no recognizable gonad received a score of 5.

For each image a mean score was calculated and the data assembled into a scatter diagram, as shown in Figure 4.5, in which each dot represents one worm. For statistical comparisons the non-parametric Wilcoxon-Mann Whitney test was performed.
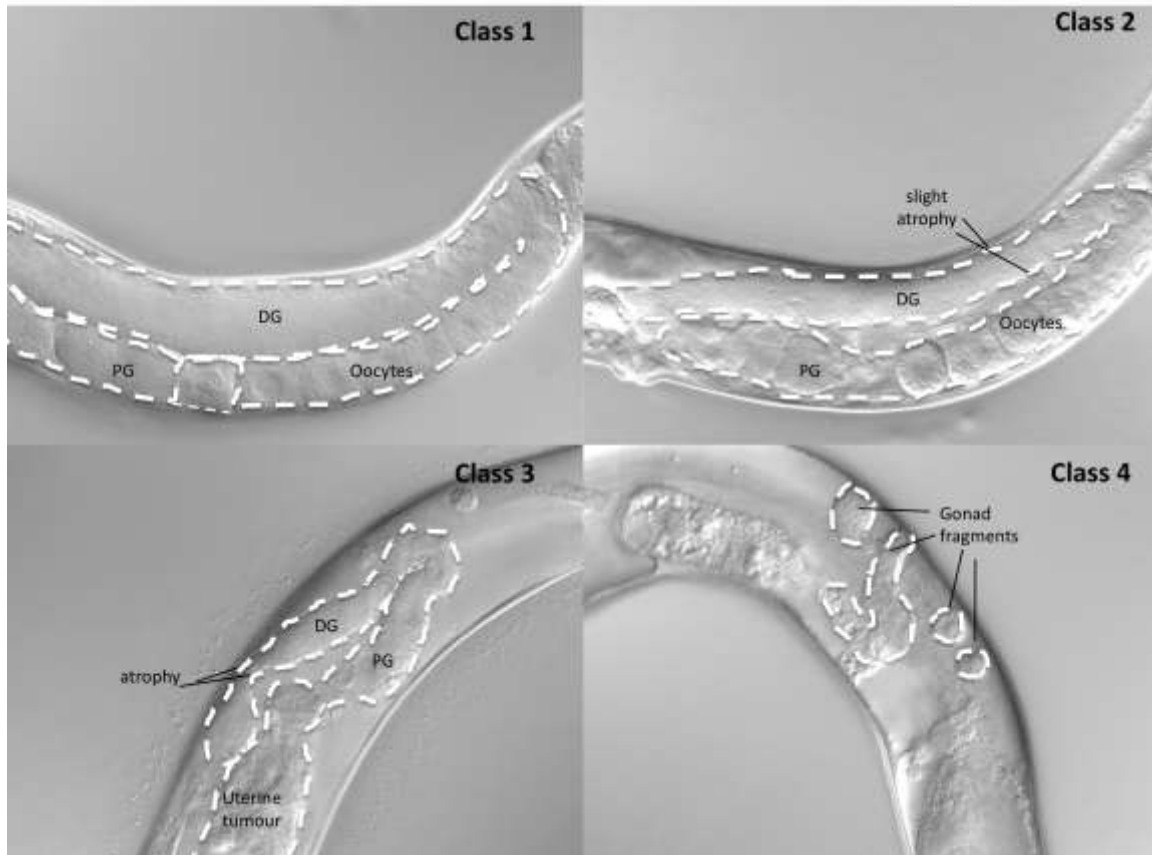
Figure 4.4 Scoring levels of gonad degeneration. Class 1 worms had intact, healthy gonads. Class 2 worms had gonads showing slight distal gonad (DG) atrophy. Class 3 worms showed a marked reduction in diameter of gonad arm (PG and/or DG), shrivelling, a ragged appearance and signs of impending fragmentation. Class 4 worms contained gonads that had broken into fragments.

To characterize this pathology, worms were examined on day 8 and 12 at 20˚C, at which time reproduction has long ceased. Worms showed a progressive increase in gonad deterioration. By day 8 all worms had undergone some degree of atrophy, exhibiting a spread in GD between classes 2-4 with the majority of worms scored at the higher levels of disintegration (classes 3-4). By day 12 most hermaphrodite worms showed severe gonad disintegration, some of which had no remnants of gonad tissue (Figure 4.5).
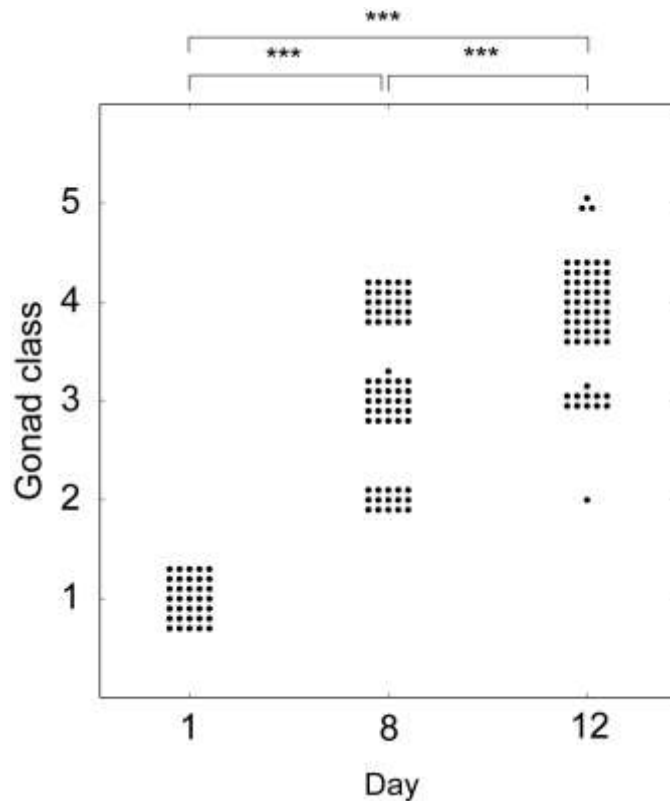
Figure 4.5 Hermaphrodite worms exhibit increasing levels of gonad degeneration with age. Each dot in this scatter diagram represents an individual worm. A progressive degeneration of the gonad was observed between day 1 and 12 in wildtype hermaphrodite worms. Statistical comparisons were performed using the Wilcoxon-Mann Whitney test ***$p<0.001$.

4.2.2 Uterine tumour formation in older worms

In our observations collecting data for gonad deterioration studies we noted the presence of uterine tumours in ageing worms. The appearance of DAPI-stained masses in the uterus of ageing worms has been previously noted apparently as the result of endoreduplication of unfertilized oocytes (Golden *et al*., 2007). This age increase in DNA content was not observed in male worms, hermaphrodite worms treated with FUdR or, to a lesser extent, in *daf-2(e1370)* hermaphrodites (Golden *et al*., 2007). The growth of uterine tumours can case squashing of the intestine (Golden *et al*., 2007; McGee *et al*., 2011). Such tumours likely represent a form of hyperfunction in the gonad, from non-adaptive run-on of a reproductive programme (specifically, embryonic development). Unfertilized oocytes undergo nuclear division without cytokinesis, which fertilization would otherwise allow (Ward and Carrel, 1979).

We developed a scoring system to quantify tumour development during ageing by placing worms into 4 uterine status categories (Figure 4.6). Worms receiving a score of 1 had mostly (not exclusively) young-looking gonads with no visible tumour. If a small tumour mass was visible, it received a score of 2. Large masses which took up more than

half the diameter of the worms were scored as 3. Large tumours filling the diameter of the worm received a score of 4.
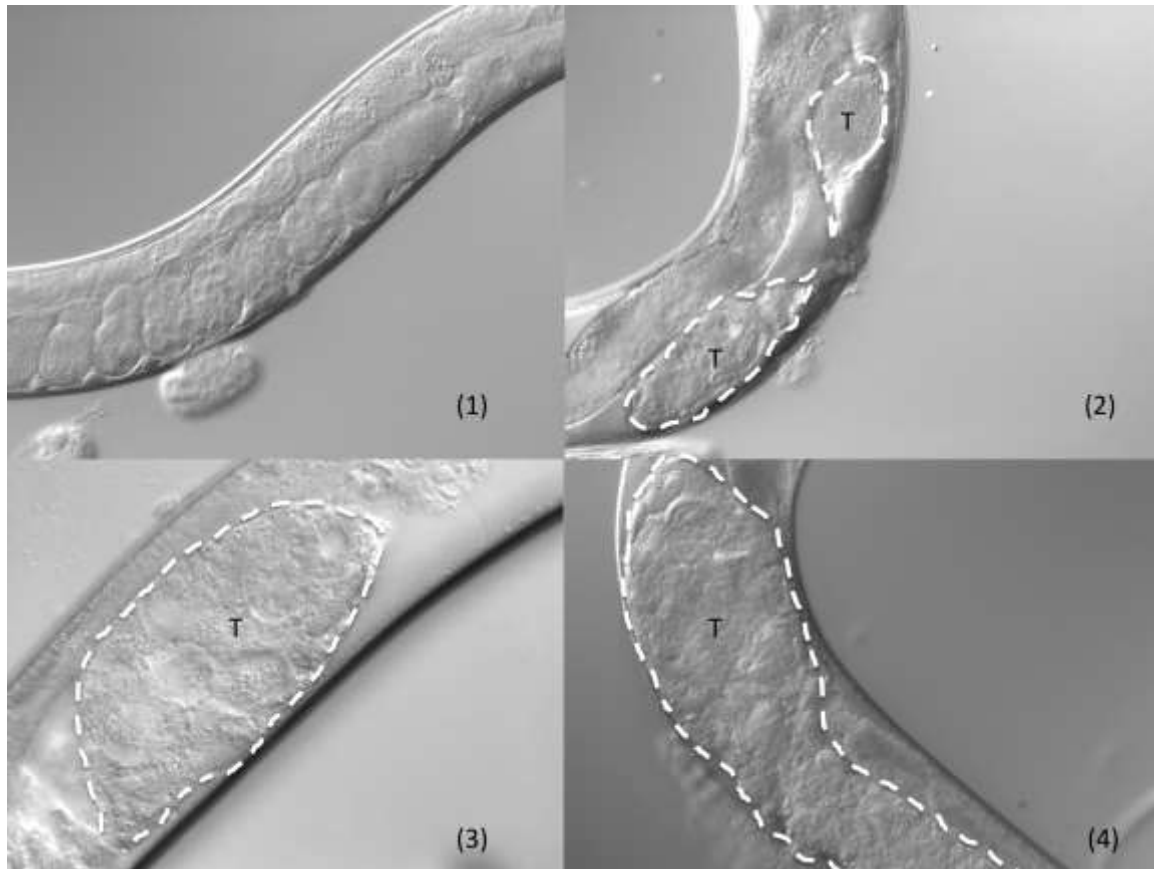
Figure 4.6 Scoring of uterine tumour formation in ageing hermaphrodites. (1) Worms that have no visible tumour (T). (2) Worms with small tumours. (3) Medium sized tumours. (4) Large tumours, filling the whole worm diameter.

We followed a similar protocol to analyse tumour formation as we did with our gonad degeneration experiments. One image of a tumour was collected per worm and scored blindly by three people. The average of these scores was compiled into a scatter diagram and statistical comparisons were obtained using the Wilcoxon Mann-Whitney test. We found a similar trend in tumour formation as seen with gonad degeneration, namely there was a progressive increase in tumour size between day 1 and 12 (Figure 4.7). By day 8 there was a range of tumour sizes, scoring between 1-3 with most worms exhibiting small tumours. By day 12 all worms examined had developed tumours (score 2-4) most of which had medium-sized tumours (score 3).
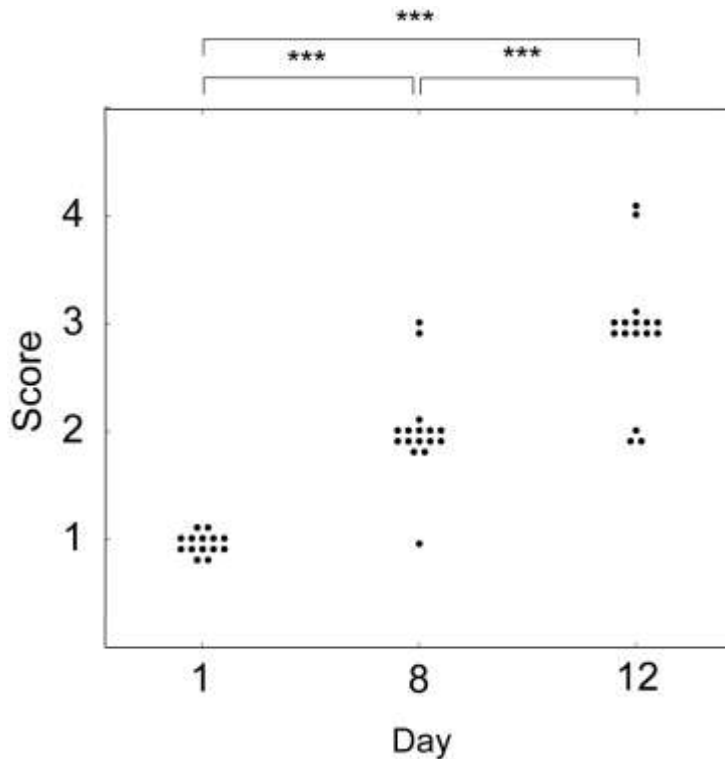
Figure 4.7 Uterine tumour size increases with age. Each dot in this scatter diagram represents an individual worm. A progressive increase in tumour size was observed between day 1 and 12 in wildtype hermaphrodite worms at 20˚C. Statistical comparisons were performed using the Wilcoxon-Mann Whitney test ***p<0.001.

4.2.3 Yolk protein accumulation does not promote tumour growth

During our experiments we noticed that large amounts of lipid-like substance, potentially yolk, accumulates in the body cavity in older worms (Figure 4.8). Other research groups have also noted the appearance of yolk-like shiny mobile droplets in older worms (Angelo and Van Gilst, 2009; Garigan et al., 2002; Herndon et al., 2002; McGee et al., 2011). Studies using the VIT-2::GFP translational reporter implied that this lipid-like often contains VIT-2, though not all lipid pools do (Marina Ezcurra, personal communication). In our yolk protein study we found that VIT-2 contributes relatively little to the YP170 band. Thus, it is possible that the lipid pools that do not contain VIT-2::GFP contain different yolk protein.

Figure 4.8 Yolk pools appear in ageing worms. DIC image showing accumulation of yolk in the body cavity of ageing hermaphrodite worms, indicated by red arrowheads.

DAPI staining confirmed an increase of DNA content with age, which correlates with the appearance of uterine tumours, and results from endoreduplication of unfertilized oocytes (Golden *et al.*, 2007). The yolk receptor RME-2 continues to be expressed in fertilized oocytes (Grant and Hirsh, 1999), implying that unfertilized oocytes retain the ability to take up yolk. This suggests the possibility that the availability of large quantities of yolk in the body cavity in old worms provides a nutrient source promoting tumour growth. Additionally, studies of the VIT-2::GFP reporter revealed large amounts of GFP in the mid-body of post-reproductive worms (Marina Ezcurra, personal communication).

To test this idea, we conducted a small trial using *vit-5*(RNAi), *vit-6*(RNAi) and *vit-5/vit-6*(RNAi) treatments, to probe for an effect of yolk accumulation on tumour

formation. We previously found that reduction on YP170 by *vit-5*(RNAi) caused an increase in YP115 and YP88 levels. Similarly, if YP115 and YP88 were lowered, causing an increase in YP170 (Figure 3.21). This allows us to see which one (if any) of the YP has an effect on tumour growth. We used the *vit-5/vit-6*(RNAi) treatment to lower all three YP and thereby test if in the absence of yolk you can 'starve' tumour growth. We performed this experiment at 25˚C and examined worms on day 1 and 4, which were the conditions previously used for the YP experiments. We found that none of these treatments block tumour formation; all day 4 worms examined had developed minor tumours (Figure 4.9). This argues against yolk accumulation as a driver of tumour growth. However, it remains possible that effects might be detected at later ages.

Tumour growth is likely promoted by increased DNA content in unfertilized oocytes. FUdR inhibits the increase in DNA content observed in ageing hermaphrodites (Golden *et al*., 2007) and also inhibits tumour growth in a dose dependent manner (Riesen *et al*., 2014).
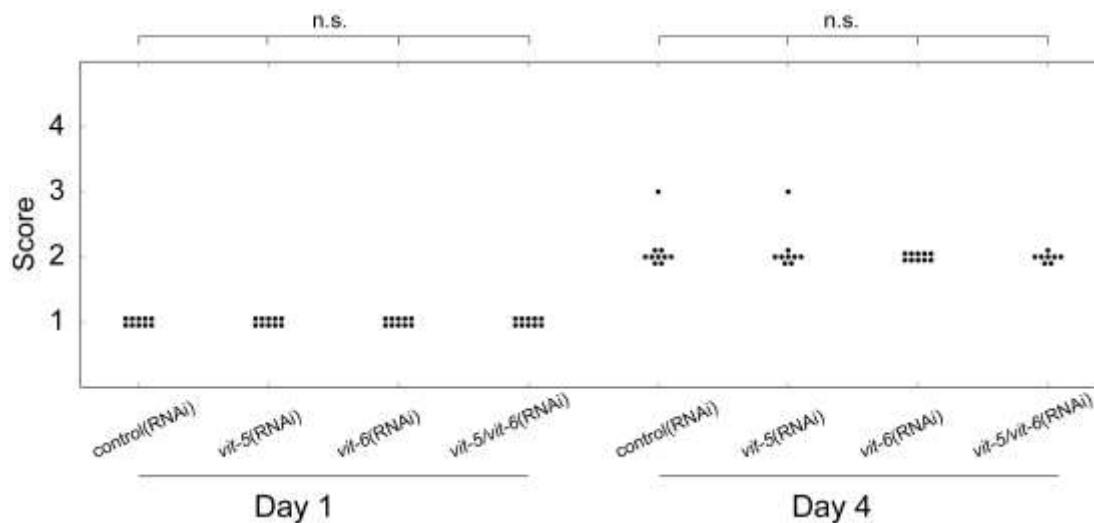
Figure 4.9 Lowering YP levels does not inhibit tumour formation. Reducing YP levels using *vit-5*(RNAi), *vit-6*(RNAi) and *vit-5/vit-6*(RNAi) treatment does not block tumour formation. There was a significant increase in all four treatments with respect to their day 1 control ($p<0.01$), but no difference between treatments. Statistical comparisons were obtained performed using the Wilcoxon-Mann Whitney test, n.s.=not significant.

4.2.4 Apoptosis carries on in post-reproductive hermaphrodites

Why does the distal gonad of ageing worms atrophy and disintegrate? The hyperfunction theory suggests that continuation of developmental and reproductive processes in late life contributes to age-related pathology. During reproduction, apoptosis in the germline results in loss of at least half of all germ cells, possibly acting as nurse cells (Gumienny *et al*., 1999). While another study estimates that up to 95% of germ cells are lost via apoptosis (Jaramillo-Lambert et al., 2007). Germline apoptosis begins during adulthood and levels increase during the first 60 hours (Gumienny *et al*., 1999). The period measured coincides with the peak of reproduction at 20˚C (Byerly *et al*., 1976); however, levels of germline apoptosis in post-reproductive worms have not been studied. To test whether apoptosis continues in later life, we used a CED-1::GFP strain (MD701), which allows visualization of sheath cells as they engulf apoptotic germ cells (Schumacher et al., 2005a). This strain provided a sensitive method for detection of early apoptotic corpses, which are not visible using DIC (Gartner et al., 2008). We found that apoptosis continues in hermaphrodite worms throughout adulthood. Numbers of apoptotic corpses increased between day 1 and 2, remained high on day 4 and there was a decline on day 8. However, day 8 levels were similar to those observed on day 1 in which worms are reproductively active and have an intact, healthy gonad (Figure 4.10 A,B). The numbers of apoptotic corpses on day 8 may reflect the reduction in germ cells previously observed to occur after day 6 of adulthood (Figure 4.13).
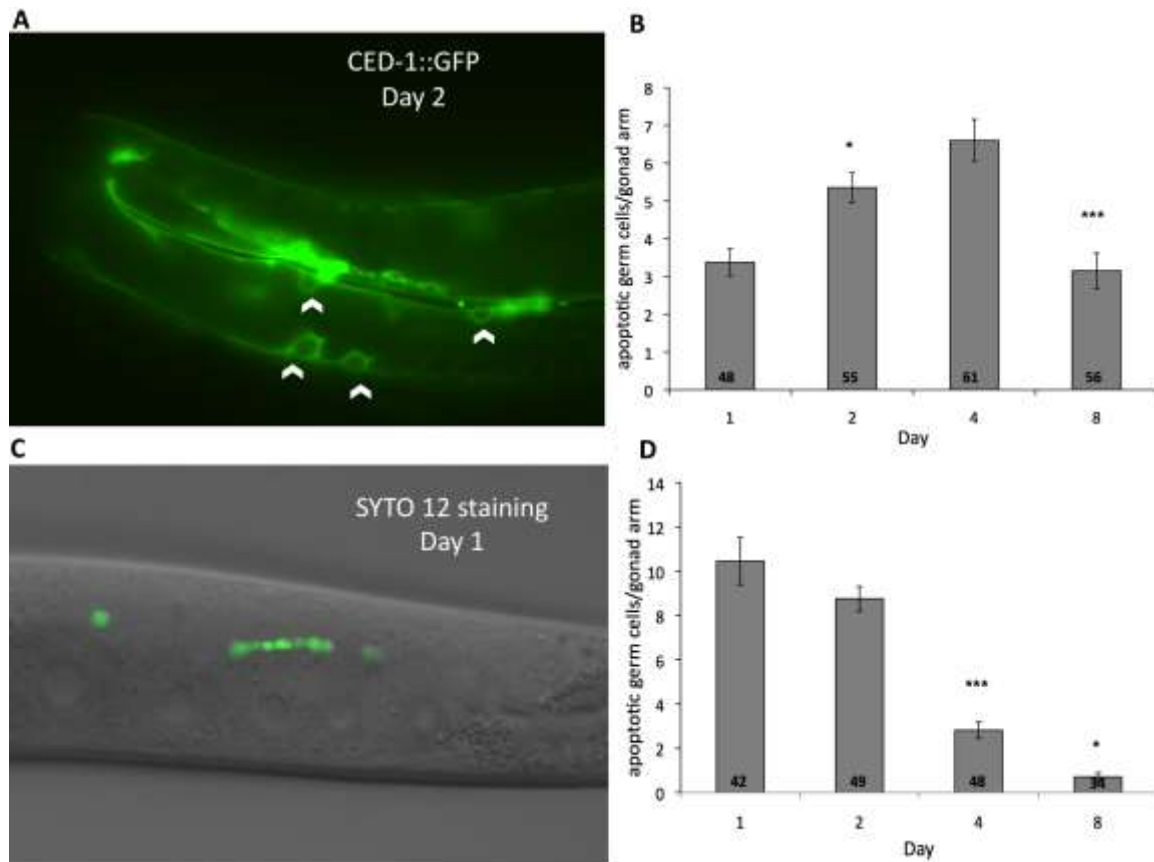
Figure 4.10 Apoptosis continues in post-reproductive hermaphrodites. Representative image of A) CED-1::GFP reporter strain showing engulfed germ cells (white arrowheads) and C) SYTO 12 stained apoptotic cells. B) Quantification of apoptotic germ cell corpse number increases during the reproductive period between day 1 and 2 and remain high until day 4, dropping back to day 1 levels on day 8. D) Bar graph showing reduction in levels of apoptosis with age. Data is the mean of mean of number of gonads examined indicated inside bar; error bars, SEM; ANOVA ($p<0.0001$), Tukey's (HSD) test ***$p<0.001$, *$p<0.05$ (consecutive days). C,D) Data obtained by J. Hellberg.

We verified that apoptosis continues in late life using SYTO 12, a vital dye used in previous studies (Gumienny et al., 1999; Pinkston et al., 2006). SYTO 12 staining is convenient as it facilitates observation of apoptotic cells in different strains. Age changes in the number of apoptotic corpses were observed using SYTO 12. Levels of apoptosis remained high during the first two days when the gonad is young and at height of reproductive capabilities. At day 4 there was a significant reduction in apoptotic corpses and a further reduction was observed on day 8 (Figure 4.10 C,D). Thus, estimates of apoptosis levels differed using SYTO 12 versus CED-1::GFP. One possibility is that

SYTO 12 stains both early and late apoptotic corpses, whereas CED-1::GFP is better for early apoptotic corpse detection (Gartner *et al*., 2008), this would explain the higher apoptotic germ cell numbers observed using SYTO 12. A second possibility is that because of the protocol we used in which live worms were placed on SYTO 12, the reduction in stained apoptotic corpses reflects reduction in pharyngeal pumping that occurs in ageing worms.
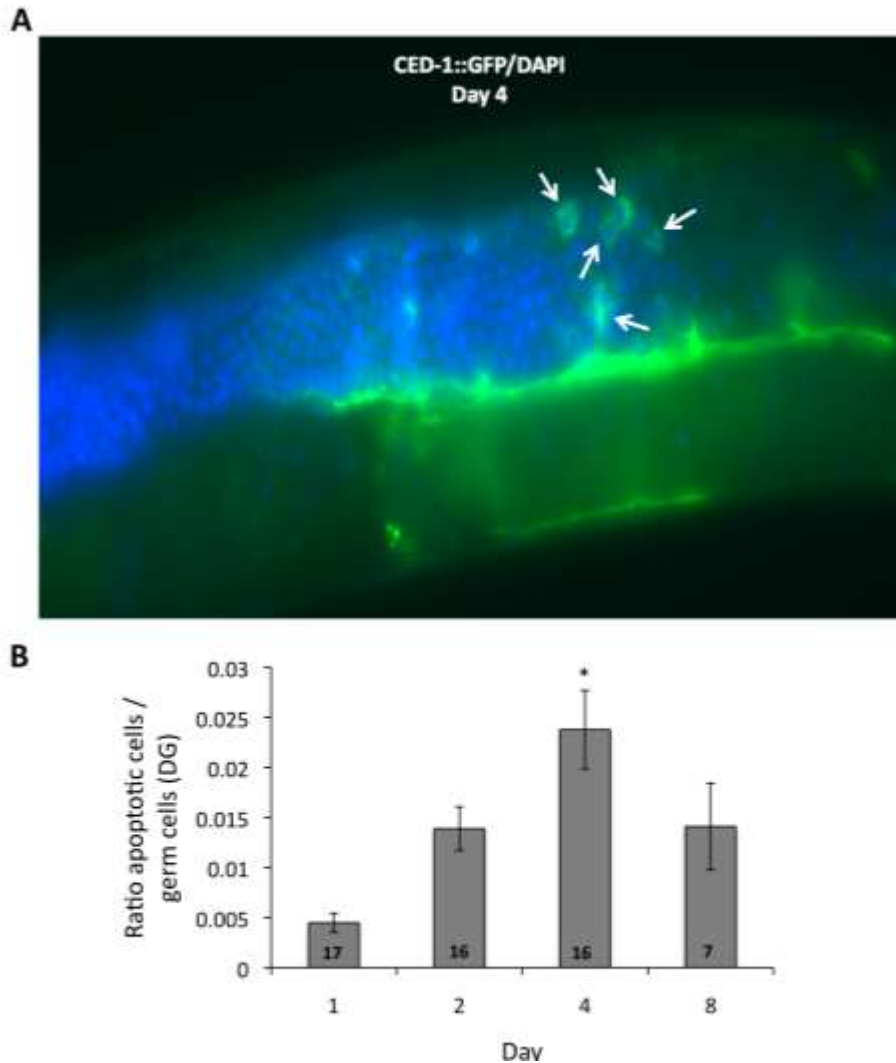
Figure 4.11 Apoptosis ratio in the distal gonad increases with age. A) Representative image of DAPI stained day 4 CED-1::GFP worms, white arrows indicate . B) Bar graph showing an age-increase in the ratio of germ cells to apoptotic cells between days 1 an 4, after which apoptotic ratio returns to levels similar to day 1. Data is the mean of (number of gonads examined indicated inside bar); error bars, SEM; ANOVA (p<0.0001), Tukey's (HSD) test *p<0.05 (consecutive days).

The age-related changes in apoptosis does not give a clear picture of the changes in rate of apoptosis, as total germ cell number decreases with age. Apoptosis levels decrease with age in conjunction with germ cells, suggesting that the overall rate of germ cell removal may remain the same. To test this we used DAPI staining to count germ cells in the CED-1::GFP strain to obtain a ratio of germ cells/apoptotic cells per worm (Figure 4.11 A). We found that the ratio of apoptosis increases slightly between day 1 and 2 (p=0.06) and a further increase was observed on day 4. We observed a reduction in the apoptosis ratio on day 8 to levels similar than those observed on day 1 (Figure 4.11 B). However, a smaller sample size was obtained for day 8 as the DAPI did not properly mark germ cells and was very faint and had to be discarded as it would make germ cell counts inaccurate. One reason could be that the appearance of uterine tumours takes up a lot of the dye and thus the staining protocol should be adjusted for longer incubation in older worms. It is also possible that the thickening of the cuticle in older worms (Herndon *et al.*, 2002) causes the dye to permeate less.

4.2.5 Gonad degeneration is apoptosis dependant

The gonad in *C. elegans* has been shown to atrophy in response to starvation during a process termed adult reproductive diapause (ARD) (Angelo and Van Gilst, 2009). ARD-associated gonad atrophy allows the germline to survive starvation and requires apoptosis, and was not observed in *ced-3(n1286)* mutants undergoing ARD (Angelo and Van Gilst, 2009). These results point to a link between germline apoptosis and gonad atrophy. Based on the hyperfunction theory, we postulated that gonad disintegration could be caused by quasi-programmed continuation of programmed cell death. To explore whether continuation of apoptosis caused gonad degeneration we first blocked apoptosis using the *ced-3(n717)* mutation, which abrogates both somatic and germline cell death (Gumienny *et al.*, 1999). We found that *ced-3(n717)* worms were protected from gonad disintegration (Figure 4.12). The gonad of these mutants developed a 'grainy' appearance, but failed to fragment (Figure 4.12 A). The 'graininess' observed may be caused by deterioration of germ cells which, in the absence of apoptosis, accumulate at higher levels and are pushed down the proximal gonad due to overcrowding (Gumienny *et al.*, 1999).

By day 8 the gonads of *ced-3(n717)* worms were mostly intact, although they had lost some of their integrity. By day 12 *ced-3(n717)* worms exhibited further loss of gonad integrity, and gonad fragmentation occurred in a few cases, but protective effect was still clearly evident.
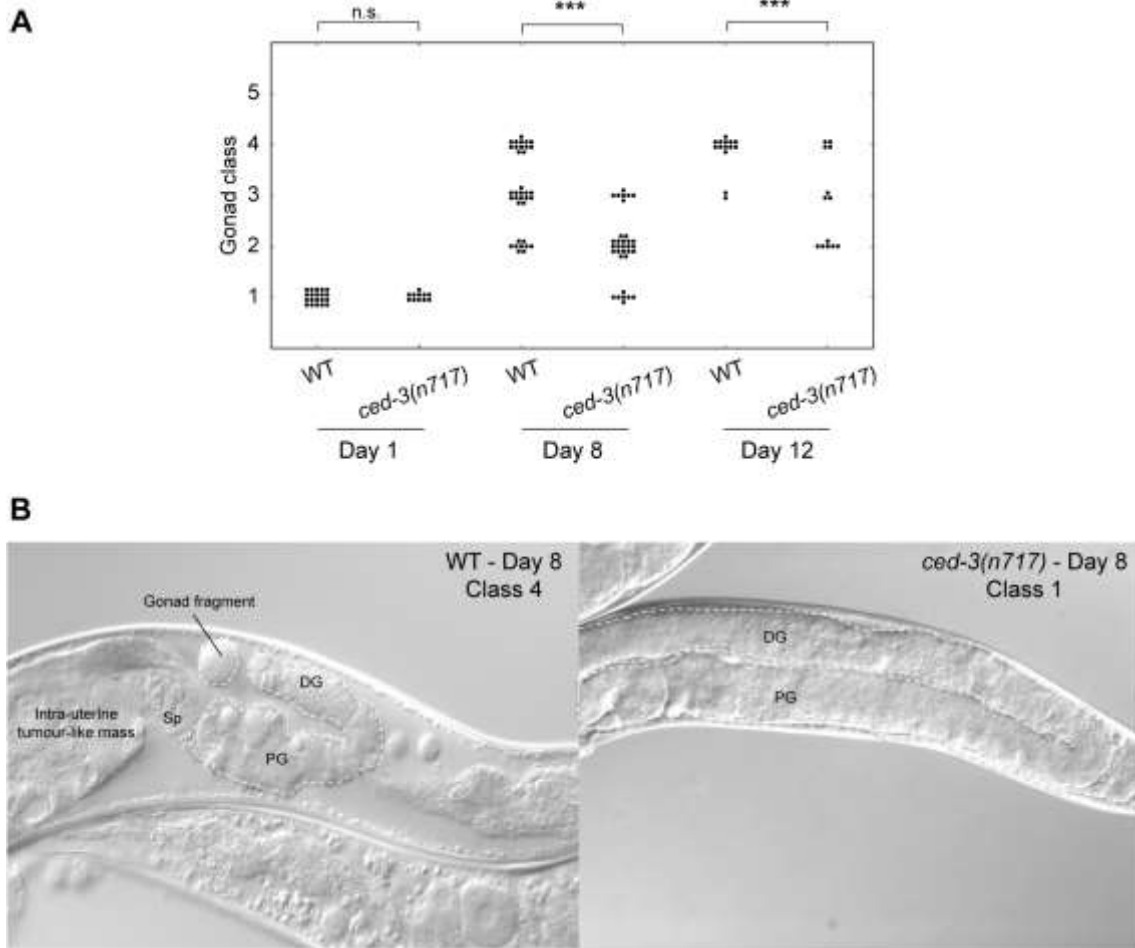
Figure 4.12 *ced-3(n1717)* hermaphrodites are protected from gonad degeneration. A) Diagram showing protective effect of *ced-3(n717)* worms on GD. There is a progressive increase in GD in wildtype and *ced-3(n717)* though it occurs at a slower rate in the absence of apoptosis. B) Representative images of day 8 wildtype and *ced-3(n717)* worms. Statistical comparisons were obtained performed the Wilcoxon-Mann Whitney test n.s.=not significant, ***p<0.001.

4.2.6 Reduced germ cell number in ageing worms

To further characterise age changes in the distal gonad, we visualized germ cell nuclei using DAPI staining to measure age changes in nuclear number (Figure 4.13 A).

Germ cell number remained at similar levels between day 1 and 6 in wildtype worms. There was a slight reduction in germ cell count on day 6, but it did not attain statistical significance (p=0.09). There was a reduction in germ cell number by day 8 (p=0.04), consistent with the gonad degeneration observed at this age.
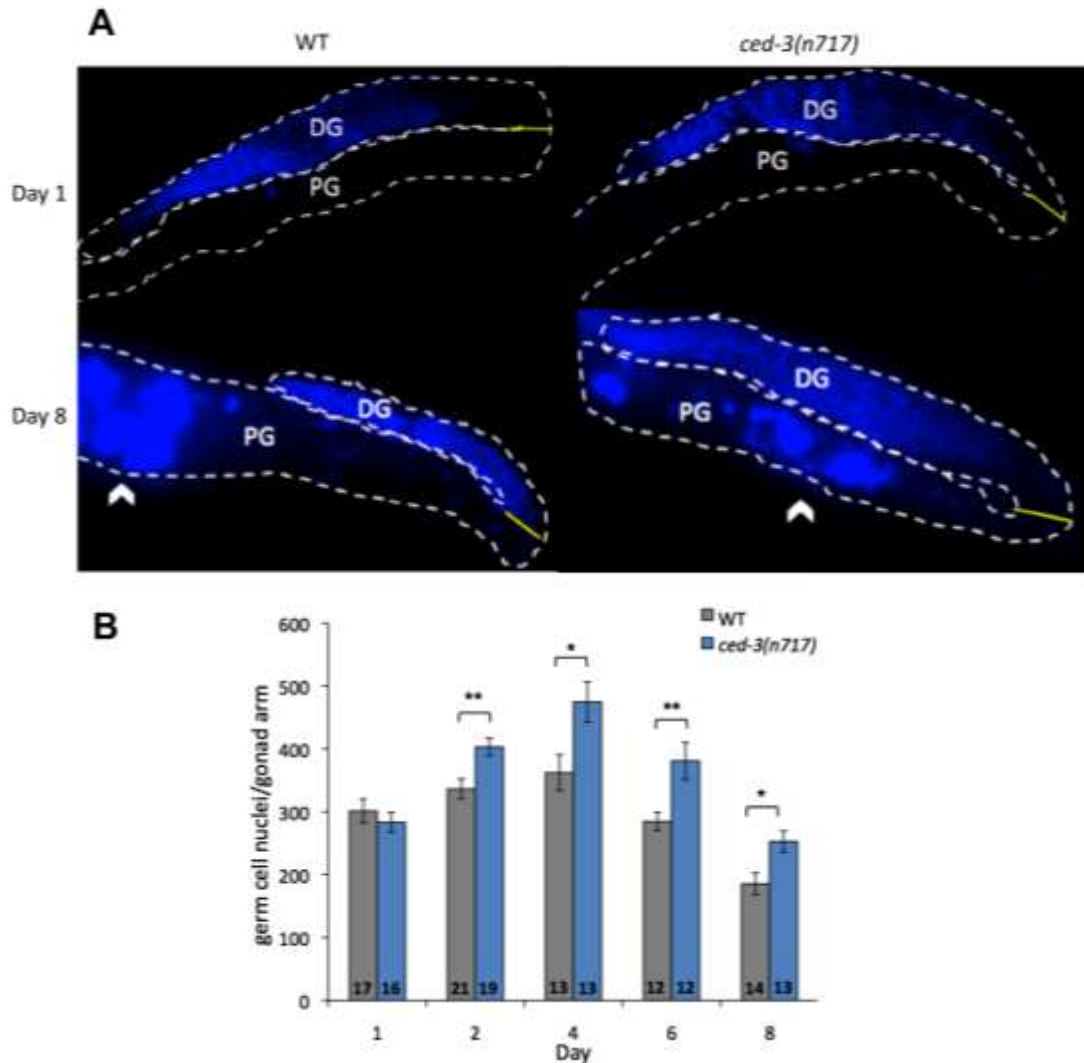
Figure 4.13 Germ cell number decreases with age. A) Representative images of DAPI stained wildtype and *ced-3(n717)* worms on days 1 and day 8. The gonad has been outlined in white. Arrowheads label DAPI stained masses (tumours) in the proximal gonad (PG) of day 8 worms. B) Bar graph showing increased levels of germ cells in the DG of *ced-3(n717)* with respect to wildtype on days 2 to 8. Data is the mean of (number of gonads examined indicated inside bar); error bars, SEM; Student's t-test (age-matched control); ANOVA (p<0.0001), Tukey's (HSD) (consecutive days) **p<0.01, p<0.05.

We also tested the effect of apoptosis on germ cell population during ageing by using *ced-3(n717)* mutants. There was an increase in germ cell number between *ced-3(n717)* and wildtype of 20-35% from day 2 onward (Student's t-test, $p<0.05$) (Figure 4.13 B). The total germ cell number for *ced-3(n717)* increased on day 2 (p=0.0004) and remained at similar levels on day 4. On day 6 there was a reduction in germ cell count (p=0.038), and a further decrease was observed on day 8 (p=0.0016). Our results suggest that during the reproductive period germ cells are produced at a constant rate in wildtype worms. The increase in germ cells in *ced-3(n717)* worms reflect the surplus of cells in the absence of apoptosis. After day 4 germ cell production slows down resulting in lower germ cell counts in the distal gonad. Statistical significance on consecutive days was detected using the Tukey Kramer honest significant difference (HSD) test

4.2.7 Male *C. elegans* do not exhibit gonad degeneration

Male worms do not show germline apoptosis (Gumienny *et al*., 1999). Our working hypothesis suggests that male worms should therefore not exhibit gonad disintegration. We compared changes in gonad integrity during ageing in hermaphrodites and males. As predicted, we found that in males, the gonad does not fragment. Between day 1 and 8 of adulthood the male gonad shows only slight deterioration (p=0.007) but retains overall structural integrity (Figure 4.14 A,B). From day 8 to 12 no significant change was observed. Fragmentation of the gonad was not observed in male worms, i.e. no class 4 worms were observed.
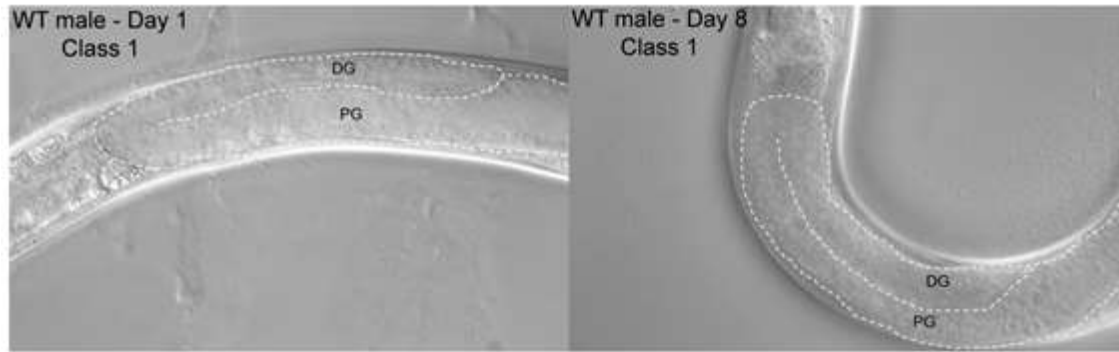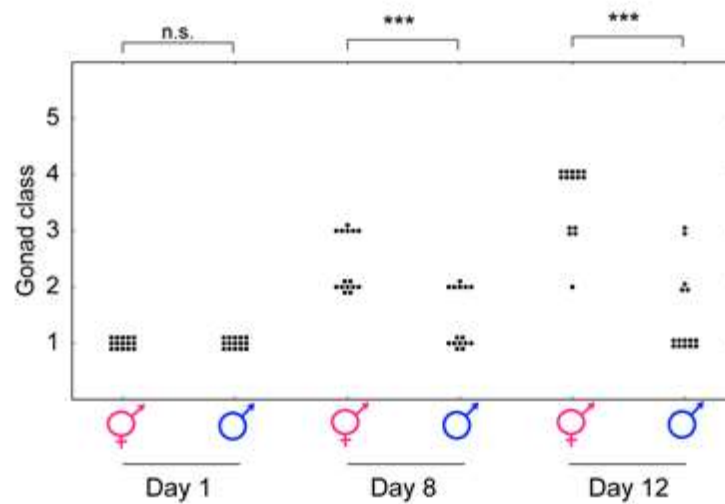
Figure 4.14 Male gonads do not disintegrate. A) Diagram comparing wildtype hermaphrodite and male worms. The male gonad deteriorates slightly between day 1 and 12, but does not fragment. B) Representative image of day 1 and day 8 worms showing little change in gonad integrity. Statistical comparisons were by performing the Wilcoxon-Mann Whitney test n.s.=not significant, ***p<0.001. Data for these experiments was collected in collaboration with A. Gilliat.

We also examined *ced-3(n717)* males on day 8 and found no difference from wildtype worms in terms of gonad disintegration (Figure 4.15). The minor signs of tissue ageing observed between day 1 and 8 in wildtype (p=0.004) were also observed in *ced-3(n717)* male worms (p=0.003). These results reveal a major sex difference in age-related pathology in *C. elegans*. Absence of germline apoptosis in males has been postulated to reflect the disparity between male and female gamete size (Gumienny *et al.*, 1999). Males produce sperm which are much smaller than oocytes and thus require less cytoplasm

(Gumienny *et al*., 1999). Our results revealed that gonad disintegration is restricted to hermaphrodite worms, perhaps due to the absence of germline apoptosis in males.
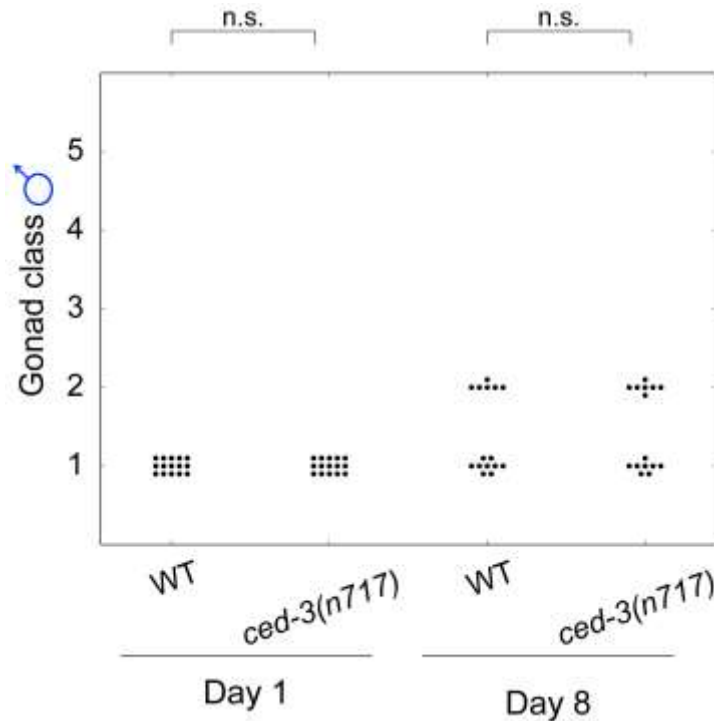
Figure 4.15 No difference in gonad degeneration in *ced-3(n717)* males. Diagram comparing wildtype and *ced-3(n717)* male worms. Statistical comparisons were performed using the Wilcoxon-Mann Whitney test, n.s.=not significant. Data for these experiments was collected in collaboration with A. Gilliat.

4.2.8 Oocyte size variation in ageing hermaphrodites

During observations of gonad atrophy we noticed that in ageing worms terminal oocytes appear to vary greatly in size (Figure 4.16 A). It has been previously shown that apoptosis plays an important role in maintaining oocyte size and *ced* mutants exhibit a faster decline in oocyte size than wildtype worms (Andux and Ellis, 2008). Curiously, during our studies we noted that in some worms oocytes would become enlarged relative to those in young adults. Such enlarged oocytes showed slight twitching movement and were often attached to the remains of the proximal gonad arm, within the gonad sheath. By contrast with surrounding tissues, these oocytes appear quite healthy and vigorous. We wondered whether changes in oocyte size in older worms were due to apoptotic run-on, specifically whether continuation of germline apoptosis leads to further release of nutrients, which provisions the remaining terminal oocyte, resulting in an enlarged oocyte.

To quantitate age-related changes in oocyte size, we measured the cross sectional area of the terminal oocyte in adult hermaphrodite worms on days 1, 8, and 12. We

recognized terminal oocytes based on the following criteria: 1) position, near the end of the proximal gonad, prior to the spermatheca; and 2) mature oocyte, only one visible nucleus, without a nucleolus. Terminal oocytes were visible in 100% of day 1 adult worms, however with increasing age the proportion of worms with visible oocytes declined. One reason for this decline in oocyte visibility is that tumours developed in older worms taking up much of the body cavity.
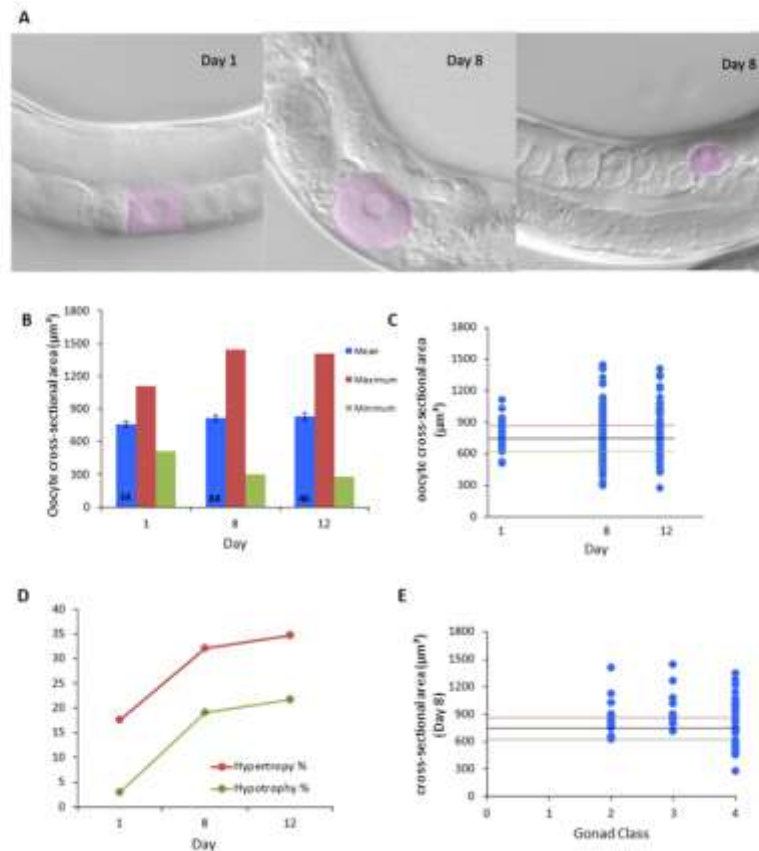
Figure 4.16 Variation in terminal oocyte size with age. A) Representative image of variation in day 8 terminal oocyte size compared to day 1 young adults (left). The middle panel shows a hypertrophic oocyte while the right panel shows a hypotrophic oocyte. B) No increase was observed in mean terminal oocyte size. An increase in maximum size of 30% and a decrease of 40% was observed between day 1 and day 8, with no further change on day 12. Data is the mean of number of worms examined indicated inside bar; error bars, SEM; ANOVA (p<0.0001), Tukey's (HSD) test (consecutive days). C) Scatter plot showing oocyte size on day 1, 8 and 12. Oocytes with means above 895μm^2 (red line) are considered hypertrophic and means below are considered hypotrophic (green line). The black line marks oocyte mean size. D) Graph showing that percentages of hypertrophic and hypotrophic oocytes increase with age. E) Scatter graph showing terminal oocyte size relative to gonad ageing in day 8 worms.

We measured the cross-sectional area of the terminal oocytes observed and found no increase in the mean size of terminal oocytes with age. This is likely due to large variation between terminal oocyte size among worms. An increase in maximum size of approximately 30% was observed between day 1 and 8, with no further increase on day 12 (Figure 4.16 B). Additionally, we observed a decrease of 40% in the minimum oocyte size between day 1 and 8, and only a small decrease thereafter (6%). We then estimated the age increase in proportion of hypertrophic and hypotrophic oocytes. We defined hypertrophic oocytes as those being 1 standard deviation above the mean in day 1 adults, which was approximately $895\mu m^2$ (Figure 4.16 C). In the same way, we defined hypotrophic oocytes as those being 1 standard deviation below the mean in day 1 adults, or $620\mu m^2$. By this measure the percentage of both hypertrophic and hypotrophic oocytes increased with age (Figure 4.16 D). Thus, terminal oocyte size varies greatly with increased age.

To determine if variation in oocyte size could be linked to the level of gonad degeneration we compared the two traits in worms of the same age. We examined terminal oocytes on day 8 where there is large variation in the level of deterioration. As expected, there was a high degree of variation in oocyte sizes within each gonad class (Figure 4.16 E). We then calculated percentages of both hypertrophic and hypotrophic terminal oocytes for each gonad class in day 8 worms. This revealed an increase in percentage of hypertrophic oocytes with degree of gonad fragmentation (Class 2:20%, Class 3: 25% and Class 4: 55%). On day 8 hypotrophic oocytes were observed only in worms with Class 4 gonads (Figure 4.16 E). Our results suggest that gonad disintegration may be associated with the fluctuations in oocyte size. One possibility is that apoptosis levels, which show a reduction on day 8, may cause differences in cytoplasmic streaming which can affect oocyte volume.

4.2.9 Extending reproductive period does not delay gonad degeneration.

We have verified previous results showing that the gonad progressively deteriorates in hermaphrodite worms (Garigan *et al*., 2002), and identified a link between gonad degeneration and germline apoptosis. We next sought to test the effect degeneration of the gonad of extending the reproductive period by mating. Arguably, a delay in the end of the reproductive period should cause a delay in the transition from the germline apoptosis program to a post-reproductive quasi-programme and thus result in a protective effect on gonad degeneration. By the same token, causing more rapid gonad quiescence should accelerate gonad degeneration. To test this prediction we used *fog-2(q71)* mutation that causes feminization in hermaphrodites, which only produce oocytes, but has no effect on male spermatogenesis (Schedl and Kimble, 1988). This strain was maintained by co-culturing with *fog-2* males. Unfertilized oocytes accumulate in unmated *fog-2* worms, which have a very low ovulation rate producing approximately 20 oocytes before entering quiescence (Miller et al., 2003). Thus, unmated *fog-2* worms can be used to test the effect of shortening the reproductive period on gonad ageing.

We first examined the effect of *fog-2* on germline apoptosis and found that unmated *fog-2* worms had lower levels of apoptosis compared to mated *fog-2* worms (Figure 4.17 A). This is somewhat expected as unmated *fog-2* worms have less active gonads and the low apoptosis rate could reflect germline quiescence. Mated *fog-2* worms had increased levels of apoptosis compared to unmated worms but significantly lower levels than unmated wildtype. On day 4 onwards there was no significant difference between wildtype and *fog-2* worms following a similar trend of reduced levels of apoptosis with age. The decrease in apoptosis from day 4 onwards in wildtype and mated *fog-2* may be caused by sperm depletion.

We also looked at the effect of *fog-2* and mating on gonad degeneration. Expectations here were unclear: in unmated *fog-2* hermaphrodites the transition to quasi-programme should occur sooner, resulting in faster gonad disintegration; but lower germline apoptosis should delay gonad disintegration. Gonads of unmated *fog-2* worms disintegrated at a similar rate that wildtype worms (Figure 4.17 B). In contrast, mated *fog-2* had an accelerated gonad degeneration phenotype.
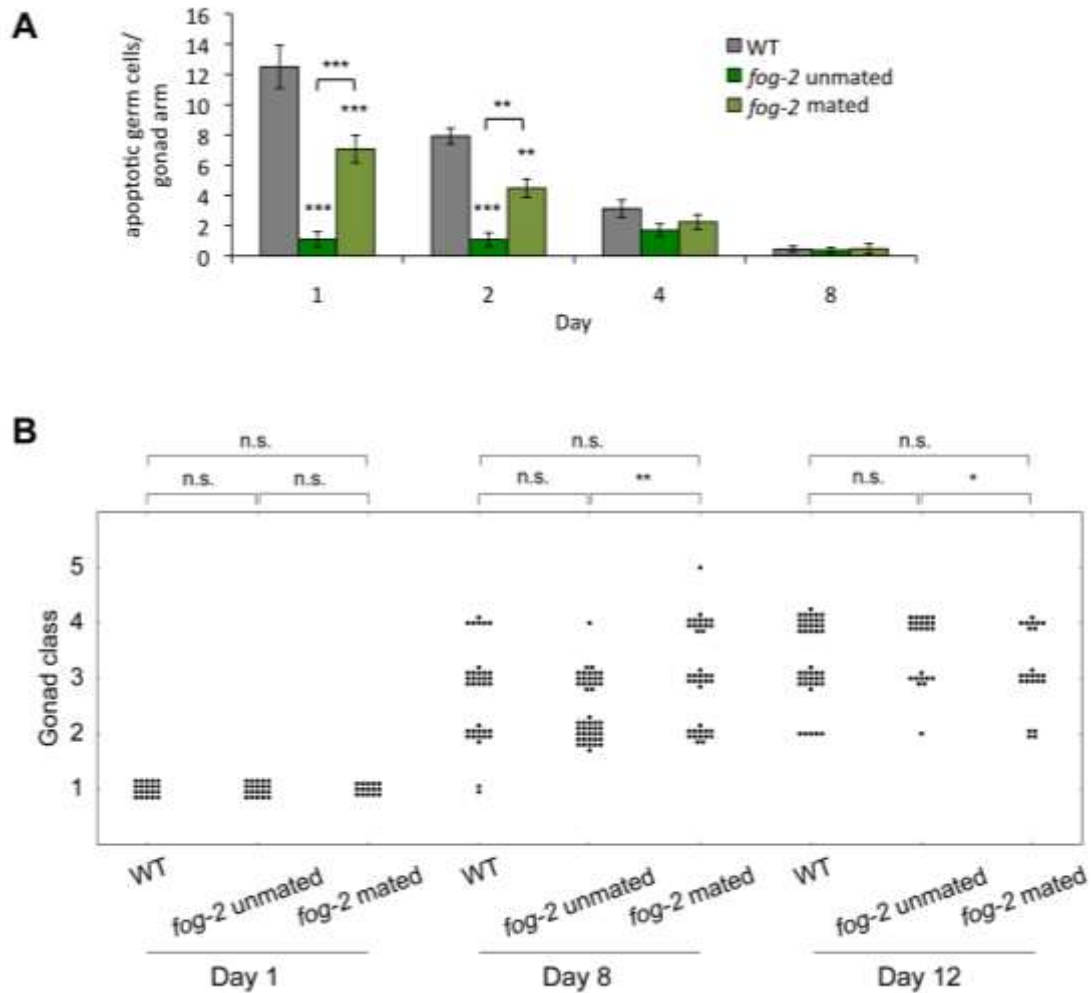
Figure 4.17 No clear effect of timing of reproduction cessation. A) SYTO 12 staining implies *fog-2(q71)* causes reduced levels of germline apoptosis. Data is the mean of 14-25 worms; error bars, SEM. B) Scatter diagram showing unmated *fog-2* mutants, in which quiescence is accelerated, has gonad degeneration levels similar to wildtype. Brief mating of *fog-2* hermaphrodites resulted in a faster rate of gonad degeneration compared to unmated worms. Statistical comparisons were obtained performing (A) ANOVA (p<0.0001), Tukey's (HSD) test, (B) Wilcoxon Mann-Whitney test ***p<0.001, ** p<0.01, *p<0.05. Data was obtained in collaboration with J. Hellberg.

To further test the effect of timing of the reproductive period on gonad ageing we mated wildtype hermaphrodite worms to extend the reproductive period. We also reduced germline proliferation by treating worms with 15 µM FUdR from the L4 stage. We found no difference in germline apoptosis between mated and unmated wildtype worms. In contrast, levels of apoptosis were significantly lower on day 1 and 2 in worms treated

with FUdR (Figure 4.18 A). Lower levels of apoptosis in worms with reduced germ cell proliferation imply that apoptotic rate is not fixed, and is instead linked to germ cell proliferative rate. Surprisingly, on day 8, both mated and FUdR-treated worms had apoptosis levels higher that the unmated control. This raises the possibility that FUdR may have been metabolized by bacteria after a few days leading to loss of the protective effect on germline apoptosis. To avoid this issue worms should be maintained on fresh OP50 seeded plates in which FUdR has been added one day prior to transferring the worms.
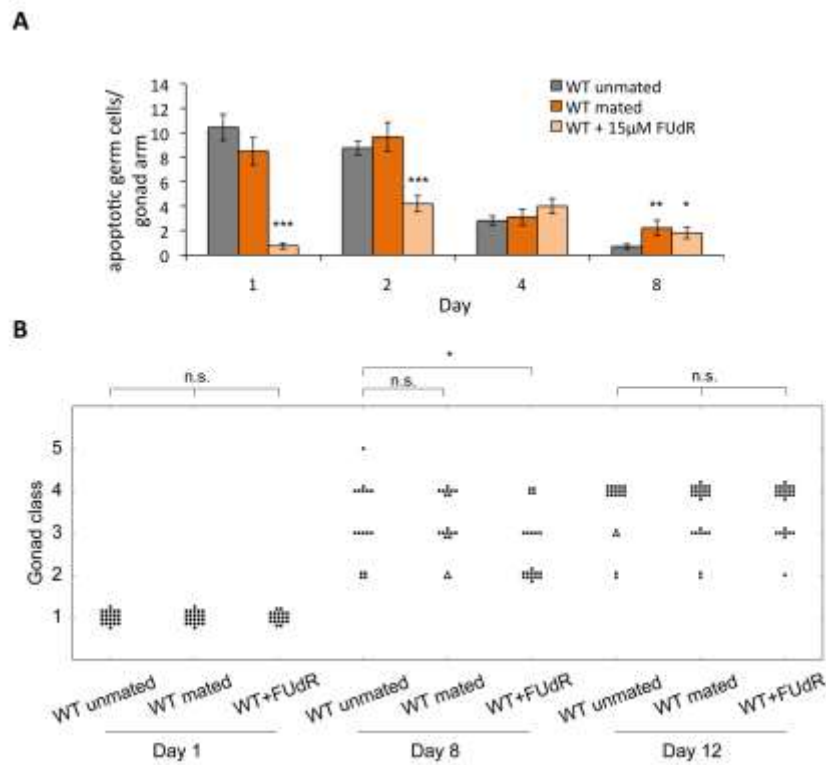
Figure 4.18 Extending the reproductive period does not delay gonad degeneration.
A) SYTO 12 staining revealed similar apoptosis levels between mated and unmated wildtype worms. Worms treated with 15μM FUdR have reduced levels of germline apoptosis. Data is the mean of 20-30 worms; error bars, SEM. B) No significant difference in GD was observed between mated and unmated wildtype worms. Worms treated with 15μM FUdR had a transient protective effect on GD on day 8. Statistical comparisons were obtained performing using (A), Student's t-test (compared age-matched unmated WT control), (B) Wilcoxon Mann-Whitney test n.s.=not significant ***$p<0.001$, **$p<0.01$, * = $p<0.05$. Data was obtained in collaboration with J. Hellberg.

Despite our initial theory that extending the reproductive period would delay gonad degeneration, we found no protective effect from mating. We did observe slower gonad degeneration in worms treated with FUdR on day 8, though this protection was lost by day 12, perhaps due to reduced apoptotic rate (Figure 4.18 B). Taken together, our mating experiments show that extending or delaying the timing of the end of reproduction does not have the postulated effect on gonad degeneration.

4.2.10 Blocking apoptosis in post-reproductive worms reduces lifespan.

Findings in this study suggest that quasi-programmed apoptosis contributes to an age-related decline in one of the major organs in *C. elegans*, the gonad. A previous study has found that inhibition of CED-3 by RNAi at the L4 larval stage causes an increase in lifespan (Curran and Ruvkun, 2007). Such a lifespan increase was not present in *ced-3(n1286)* mutants (Garigan *et al*., 2002). This suggests the possibility that *ced-3* mutation may mask a lifespan extension due to loss of essential somatic cells during early development. An interesting possibility is that selective inhibition of germline apoptosis extends lifespan by suppressing age-related pathology in the germline.

We first tested if *ced-3*(RNAi) from L4 larval stage had the same protective effect as *ced-3(n717)*. We examined the gonads of day 8 hermaphrodite worms and verified that apoptosis inhibition exclusively during adulthood is enough to protect against gonad degeneration (Figure 4.19 A). We sought to replicate the lifespan extension observed by Curran *et al* (2007) by placing wildtype worms on *ced-3*(RNAi) at L4. FUdR was not used to avoid the inhibitory effects it has on DNA replication in the germline. Notably, we saw an opposite effect to the previous studies. In neither of the two trials conducted was there an increase in lifespan. Analysis of pooled data from the two trials showed that *ced-3*(RNAi) from L4 slightly reduced lifespan (Figure 4.19 B).
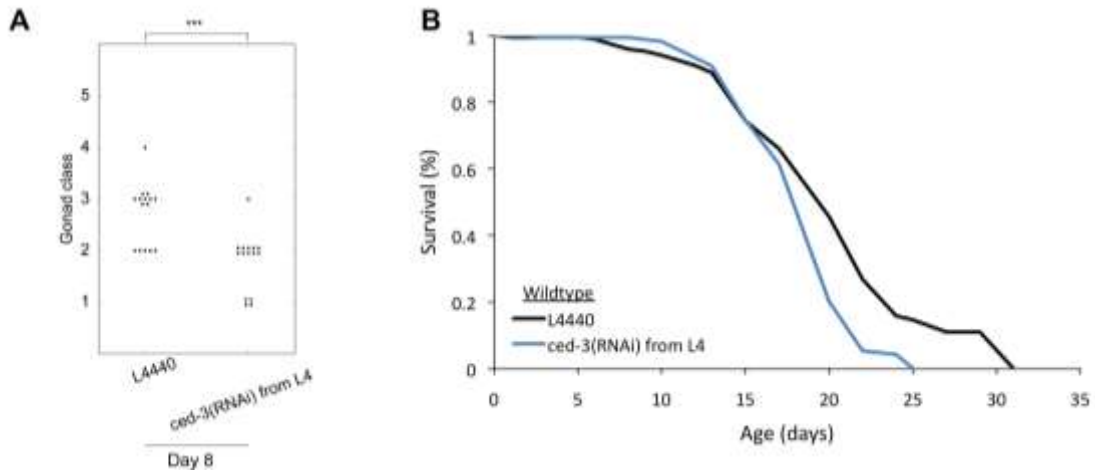
Figure 4.19 Treatment of *ced-3*(RNAi) from L4 larval stage reduces lifespan. A) Protective effect of *ced-3*(RNAi) from L4 on GD compared to control. Statistical comparisons were obtained using the Wilcoxon-Mann Whitney test ***p<0.001. B) *ced-3*(RNAi) from L4 causes a slight lifespan reduction. Assays were conducted at 20˚C, worms were raised on L4440 to L4 and transferred to *ced-3*(RNAi) treatment for the duration of the experiment. Data mean of 2 biological replicates.

Treatment	Mean lifespan [Median] (days)	% of control lifespan	Log rank (p vs. control)	Deaths [censored]
L4440 (control)	19.8 [20]			100 [100]
ced-3(RNAi)	18.6 [20]	-6%	0.0006	144 [56]

Table 4-1 Effect of *ced-3*(RNAi) treatments on lifespan. This table contains data corresponding to Figure 4.20 B.

Subsequent to the above trial, another study reported that *ced-3(n717)* mutants show extended lifespan (Judy *et al*., 2013), an effect that was not observed in the different allele *ced-3(n1286)* (Garigan *et al*., 2002). We therefore conducted another lifespan trial to compare the lifespan effect of *ced-3(n717),* and *ced-3*(RNAi) treatment from hatching and from L4. We wanted to test if timing of exposure of worms to *ced-3*(RNAi) had an effect on lifespan. We tested *ced-3*(RNAi) treatment from egg and from L4 larval stage. Consistent with our previous findings, *ced-3(n717)* and *ced-3*(RNAi) resulted in slight decreases in lifespan (Figure 4.20). Together these results suggest that

gonad disintegration, despite being a severe pathology of a major organ, does not contribute to age-related mortality. This indicates that pathology in other organs limits *C. elegans* lifespan. The reason for the discrepancy in the observed effects of *ced-3(n717)* is unclear. Possibly, genetic background differences shorten control lifespan in the Judy *et al* study (2013).
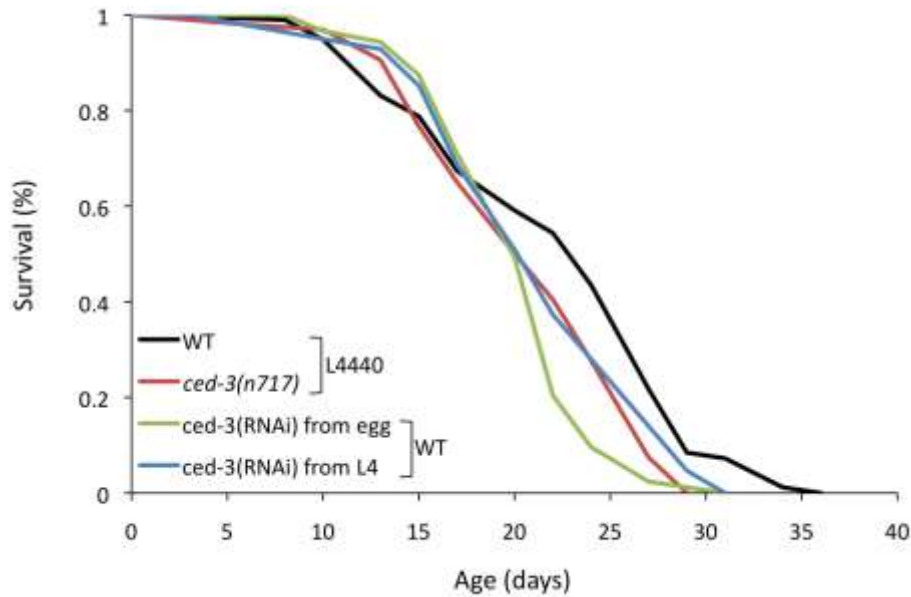
Figure 4.20 Inhibition of apoptosis shortens lifespan. Assays were conducted at 20˚C and worms were transferred to IPTG plates with the desired RNAi treatment (control or *ced-3*) containing 15μM FUdR at L4. Data mean of 1 biological replicate.

Treatment	Mean lifespan [Median] (days)	% of control lifespan	Log Rank (p vs. control)	Deaths [censored]
WT, L4440 (control)	22.5 [24]			86 [11]
ced-3(n717), L4440	20.9 [22]	-7% [-8%]	0.008	94 [5]
WT, *ced-3*(RNAi) from egg	21.4 [22]	-5% [-8%]	0.0001	84 [16]
WT, *ced-3*(RNAi) from L4	20.4 [20]	-9% [-17%]	0.06	89 [11]

Table 4-2 Effect of timing of *ced-3(n717) ced-3*(RNAi) treatments on lifespan. This table contains data corresponding to Figure 4.21.

4.3   Discussion

4.3.1 Germline atrophy and hypertrophy in hermaphrodite worms

During the course of our studies we found that the germline is prone to gross morphological change with age, and these changes are consistent with hyperfunction. As worms aged we commonly observed the appearance of uterine tumours, fluctuations in size of the terminal oocyte and gonad degeneration (Figure 4.21).
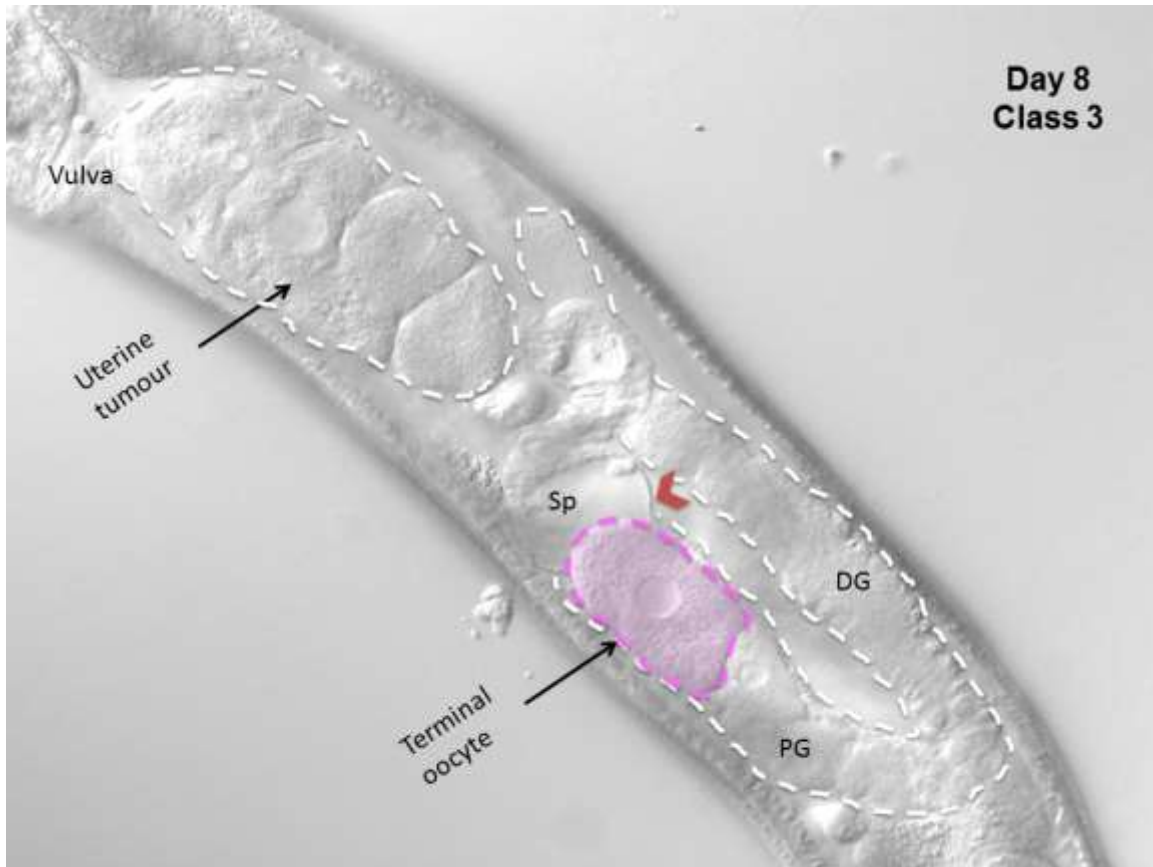
Figure 4.21 Age-related changes in the hermaphrodite reproductive system. Representative image of a day 8 worm showing changes that occur in the germline such as gonad atrophy, oocyte enlargement and tumour formation (distal gonad, DG; proximal gonad, PG). Red arrowhead indicating gonad sheath surrounding the spermatheca (Sp).

4.3.1.1   Gonad atrophy may result from quasi-programmed apoptosis

Gonad disintegration is interesting as a potential example of hyperfunction resulting in atrophy. In *C. elegans* apoptosis increases reproductive fitness by removing around half of germ cells to ensure that those that will develop into oocytes have

sufficient cytoplasm, increasing oocyte quality (Gumienny *et al*., 1999). We conducted a quantitative characterization of gonad degeneration by defining stages of increased atrophy between 1 and 5. Using this system we compared germline status on day 1, 8 and 12 at 20°C and found a progressive measurable increase in gonad disintegration. In this study we found that germline apoptosis does not halt after reproduction as apoptotic corpses were still detected in day 8 hermaphrodite worms. We propose that post-reproductive continuation of the apoptotic program causes the gonad to fragment and atrophy. This atrophy does not occur if apoptosis is absent, in the case of male worms, or if apoptosis is blocked by the *ced-3(n717)* mutation. Additionally, lowering germline proliferation by using DNA synthesis inhibitor FUdR resulted in lower apoptosis levels and slowing of gonad degeneration.

We also tested the effect of changes in the timing of the reproductive period. We speculated that increasing the length of reproduction might result in a protective effect on gonad disintegration and causing reproduction to halt sooner should accelerate it. We tested this using unmated *fog-2(q71)* worms that only produce oocytes and thus become quiescent sooner and mated wildtype worms to extend their reproductive period by removing sperm depletion as a limiting factor. We found that unmated *fog-2(q71)* exhibited slower gonad degeneration when compared to mated *fog-2(q71),* contradicting our initial hypothesis. We also observed that mating wildtype worms had no effect on gonad degeneration. Thus, changing the timing of the transition from programme to quasi-programme did not have the expected effect on germline ageing.

Gonad disintegration is a striking age-related pathology in ageing worms. However, it seems not to be life-limiting as removal of the entire gonad by laser ablation does not extend lifespan (Kenyon et al., 1993). An additional study found that apoptotic defective mutants *ced-3(n1286)* had wildtype lifespan (Garigan *et al*., 2002). A third study found that worms on *ced-3*(RNAi) after L4 has a slightly increased lifespan (Curran and Ruvkun, 2007). A more recent study found that *ced-3(n717)* mutants extend lifespan by increasing resistance to environmental stress (Judy *et al*., 2013). In our study we examined the effect of post-developmental treatment of *ced-3*(RNAi), *ced-3*(RNAi) from hatching and *ced-3(n717)* mutants and found a slight reduction in lifespan. Our results support the conclusion that apoptosis does not promote age-related mortality.

4.3.1.2   Gonad hypertrophy: tumour formation

The development of large DAPI stained masses correlate with the formation of uterine tumours (Golden *et al.*, 2007; McGee *et al.*, 2011). During our studies we found that these DAPI stained masses were visible as early as day 6 of adulthood. The appearance of uterine tumours is the result of endomitosis in unfertilized oocytes and the timing of their formation correlates with the end of the reproductive period (Golden *et al.*, 2007). Furthermore, tumour formation could be blocked with FUdR treatment (Golden *et al.*, 2007; Riesen *et al.*, 2014). In unmated *fog-2(q71)* worms, in the absence of sperm, unfertilized oocytes are produced faster forming tumours earlier from day 4 (Josephine Hellberg, unpublished). Thus, tumour formation is dependent on the timing of the formation of unfertilized oocytes, which corresponds with the end of the reproductive period. We therefore postulate that reproductive processes such as nuclear division carry on in the oocyte in the absence of fertilization resulting in quasi-programmed formation of uterine tumour-like masses (Gems and de la Guardia, 2013). Thus, the timing of the switch from programme to quasi-programme affects the timing of pathogenesis in tumour formation but not GD. However it should be noted that that uterine tumours are not life-limiting to the worm, since FUdR treatment, which reduces tumour formation, does not extend lifespan (Gandhi et al., 1980; Golden et al., 2007; Riesen et al., 2014). One possibility is that yolk overproduction feeds tumour formation. Preliminary experiments found that reducing total yolk protein levels using *vit-5/vit-6*(RNAi) did not block tumour formation as of day 4 at 25°C. Future experiments could be conducted using a combination of *rme-2*(RNAi) and FUdR to properly determine the role of yolk and DNA synthesis on tumour and hypertrophic oocyte formation.

The post-reproductive continuation of apoptosis, which may contribute to gonad fragmentation, could also result in the continuous release of cytoplasm giving rise to hypertrophic oocytes. In support of this, the percentage of hypertrophic oocytes steadily increased with the levels of gonad degeneration (Class 2-4). However, we also found a high percentage of hypotrophic oocytes in worms with fragmented gonads (Class 4). During reproduction oocyte enlargement is the result of streaming of cytoplasm from the germ cell rachis to the first three oocytes of the proximal gonad before complete cellularization takes place (Wolke et al., 2007) (Figure 4.22). This argues against

apoptosis as a cause of oocyte enlargement as oocytes undergoing hypertrophy have undergone maturation and should have severed the connection to the core. However, images of hypertrophic oocytes suggest that in 8 and 12 day old worms oocyte number in the proximal gonad drops to ~2-3 (Figure 4.21). It is possible that as tumours form, pushing back the spermatheca from the mid-body region, these few remaining oocytes stay connected to the rachis for longer periods of time resulting in their increased size. On the other hand, worms in which hypotrophic oocytes were observed had a higher oocyte density in the proximal arm (see Figure 4.16 A). Thus, these smaller oocytes were farther away from the gonad loop and have severed their connexion to the rachis. Their smaller size could result from lower apoptosis levels with age which decreases the pool of cytoplasm resulting in less of it being incorporated to these oocytes while they were connected to the rachis. Thus, changes in apoptosis levels with age in relation to gonad ageing could explain the variation in oocyte size observed in ageing worms.

Furthermore, hypertrophic oocytes were not observed in *ced-3(n717)* worms which are protected against gonad degeneration. These *ced-3* worms show an increased density of hypotrophic oocytes in the proximal arm (Gumienny *et al*, 1999). This supports our hypothesis that in the absence of apoptosis oocytes do not have a continuous release of cytoplasm from apoptotic hyperfunction and causing a decrease in size.

As is expected with quasi-programmes, gonad degeneration, tumour-like mass size and terminal oocyte size was highly variable between worms. This is due to the fact that being a non-intended continuation of developmental and reproductive programme it has not been fine-tuned by evolution.
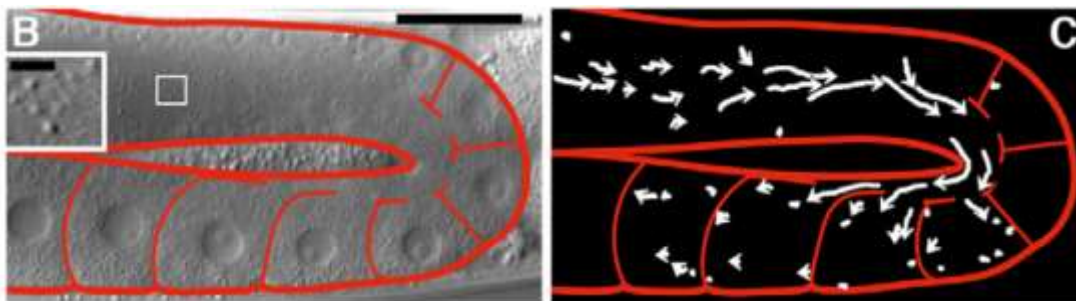
Figure 4.22 Cytoplasmic streaming in the hermaphrodite gonad. The image on the left shows particle movement (white box) through the rachis towards the loop of the gonad. The image on the right uses white arrows to indicate movement of cytoplasm into oocytes that remain attached to rachis. Image reproduced from Wolke *et al*., 2007.

4.3.2 Apoptosis levels reflect proliferative state of the germline

Apoptosis levels have previously shown to increase in hermaphrodites during the first 2.5 days of adulthood (Gumienny *et al*., 1999). In this study we confirmed the increase of apoptotic germ cells between day 1 and 2 and the continuation of apoptosis on day 4 and 8 using CED-1::GFP and SYTO 12 staining. The presence of apoptotic corpses implies that germline apoptosis continues in post-reproductive worms. Additionally, mating experiments revealed that unmated *fog-2(q71)* hermaphrodites which enter germline quiescence faster had reduced levels of apoptosis. Similarly, blocking DNA-synthesis in the germline by treating worms with FUdR at L4 also reduced levels of apoptosis. These results unveil a relationship between germline activity, reproductive timing and apoptosis.

The methods used to measure apoptosis in the germline allow us to estimate the number of apoptotic cell corpses, but this is not indicative of the frequency at which apoptosis takes place and DIC microscopy clearly suggests a reduction in germline nuclear number. Using DAPI staining we could estimate age changes in germ cell number in the distal arm. We found a trend of increasing germ cell number between day 1 and 4, which coincides with the reproductive period and a decrease thereafter. To test the actual ratio of germ cells to apoptotic cells remains constant we DAPI stained CED-1::GFP expressing worms to obtain the apoptotic ratio of each worm. These results show that the ratio of apoptosis increases in the first 4 days of adulthood and goes back down to day 1 levels by day 8. However, this result does not take into account the rate at which new cells are being produced. The ideal scenario would be to measure the proliferative state of the gonad and compare that to the rate of apoptosis.

A further caveat is that our experiments do not measure the rate of apoptotic corpse removal. In young adults apoptotic cells were observed to disappear within an hour of formation (Gumienny *et al*., 1999). It is possible that in older worms apoptotic corpses form at an earlier stage but are not engulfed. To rule out the possibility that apoptotic corpses detected on day 8 are not remnants of earlier apoptotic events time course assays should be performed to look for changes in the rate of engulfment.

In this chapter we have described changes that occur in the germline in ageing hermaphrodites such as gonad degeneration, uterine tumour formation and oocyte enlargement. We also proposed a possible mechanism for gonad disintegration, quasi-programmed germline apoptosis. In the next chapter we will seek further evidence to support our hypothesis that germline apoptosis run-on is the main driver of gonad disintegration.

Chapter 5: Gonad disintegration is driven by germ cell apoptosis in *C. elegans*

5.1 Introduction to apoptosis in *C. elegans*

In the previous chapter we explored changes in the ageing hermaphrodite gonad and found a connection between germline apoptosis and gonad atrophy. In this chapter we will test a model in which run-on of germline apoptosis in post-reproductive worms results in gonad fragmentation.

The model organism *C. elegans* has been a very useful tool to elucidate the genetics of conserved biological processes. It was in *C. elegans* that the evolutionary conserved genes involved in programmed cell death were first identified by John Sulston, Sydney Brenner and Robert Horvitz (Conradt and Xue, 2005). *C. elegans* provides a valuable tool for the study of this process due to the ability to view apoptotic cells in live *C. elegans* using Differential Interference Contrast (DIC) microscopy, also known as Nomarski microscopy (Robertson and Thomson, 1982). Changes in the morphology of apoptotic cells in *C. elegans* resemble those described in mammals such as condensation of the cytoplasm and chromatin, followed by cell fragmentation (Kerr et al., 1972; Robertson and Thomson, 1982). Similar to mammals, programmed cell death is *C. elegans* is essential during development, and of the 1090 somatic cells in the hermaphrodite, 131 undergo programmed cell death (Sulston et al., 1983).

The regulation of somatic programmed cell death involves the interaction of key components EGL-1, CED-9, CED-4 and CED-3 (Conradt and Xue, 2005) (Figure 5.1). The small protein EGL-1 is an activator of apoptosis that shares common motifs with mammalian BH3 (<u>B</u>cl-2 <u>H</u>omology region <u>3</u>) which is present in pro-apoptotic Bcl-2 proteins (Conradt and Horvitz, 1998; Conradt and Xue, 2005). Inhibition of EGL-1 results in the survival of nearly all somatic cells that would normally undergo apoptosis (Conradt and Horvitz, 1998). The genes *ced-3* and *ced-4* (<u>cel</u>l <u>d</u>eath abnormal) are the essential for programmed cell death to occur and blocking either of these results in the survival of the 131 cells that die during development (Ellis and Horvitz, 1986; Hengartner, 1997). The *ced-4* gene encodes a product similar to human Apaf-1 (<u>apoptotic</u>

protease <u>a</u>ctivating <u>f</u>actors) which activates caspases (Zou et al., 1997). The CED-3 protein resembles mammalian interleukin-1β converting enzyme, also known as caspase-1 (Yuan and Horvitz, 2004; Yuan et al., 1993). Surprisingly, although *ced-3* and *ced-4* mutants have more somatic cells than wildtype there seems to be no major behavioural anomaly in these worms (Ellis and Horvitz, 1986). They exhibit normal locomotion, feeding and egg-laying rate, but brood sizes are slightly lower (Ellis and Horvitz, 1986). CED-9 is a negative regulator of apoptosis which is structurally similar to mammalian Bcl-2, the loss of this gene causes cells that normally survive to undergo apoptosis and is lethal (Hengartner and Horvitz, 1994; Hengartner et al., 1992). Over-expression of CED-9 results in survival of somatic cells that would normally die and these worms have a similar phenotype than *ced-3* and *ced-4* mutants (Hengartner and Horvitz, 1994). The similarity in structure and function between *C. elegans* and mammalian genes mediating programmed cell death reflect evolutionary conservation of the cell death pathway (Hengartner, 1997).

Figure 5.1 Core apoptotic pathway in *C. elegans*. Representation of the interaction among proteins in the core apoptotic pathway, which are required for embryonic and developmental apoptosis. Genes *ced-3* and *ced-4* encode the cell death effector proteins required for all known *C. elegans* apoptosis pathways (red box).

Programmed cell death occurs in *C. elegans* during embryogenesis and larval development in somatic cells and exclusively in the germline of adult hermaphrodites (Conradt and Xue, 2005; Gumienny et al., 1999; Sulston and Horvitz, 1977). Though the death inducing proteins CED-4 and CED-3 are crucial requirements for both somatic and germline apoptosis, there are differences in their regulation (Gartner *et al*., 2008).

5.1.1 Germ cell apoptosis in *C. elegans* hermaphrodites

Multicellular organisms rely on apoptosis to rid the body of unwanted and damaged cells. Apoptosis is also a hallmark in oogenesis and gastrulation across various species

where the germline uses distinct mechanisms to induce the cell death machinery (Greenwood and Gautier, 2005). In adult *C. elegans* all somatic cells are post-mitotic and do not undergo apoptosis; the only tissue with replenishing cells is the germline which is thus more similar to mammalian tissue (Gartner *et al.*, 2008). One type of germ cell apoptosis occurs as part of the oogenesis program whereas a second type of cell death occurs in response to DNA damage or environmental insults (Gartner *et al.*, 2008). We will refer to the two main categories of apoptosis present in the germline as physiological apoptosis (PA) and stress-induced apoptosis (SIA).

5.1.1.1 Germline physiological apoptosis

Apoptosis in the germline occurs only in adult hermaphrodites under no perceivable external stress and seems to be part of the oogenic program (Gartner *et al.*, 2008). Activation of CED-4 and CED-3 during physiological apoptosis is different in the germline in that inhibition of the pro-apoptotic factor EGL-1 and *ced-9(n1950)* gain of function mutations, both of which block apoptosis in the soma, are not required for germ cell apoptosis (Gumienny *et al.*, 1999). The signal that causes the induction of CED-4 and CED-3 in physiological germline apoptosis is currently not known (Gartner *et al.*, 2008).

Physiological germline apoptosis is a reproductive mechanism responsible for the removal of at least 50% (Gumienny *et al.*, 1999) or as much as 97% (Jaramillo-Lambert *et al.*, 2007) of all oogenic germ cells. In *C. elegans* germ cells at different stages of mitosis and meiosis are connected to each other through a syncytium allowing them to share a common cytoplasm (Lints and Hall, 2009c). During programmed cell death (PCD) apoptotic cells are quickly engulfed to reduce the spread of apoptotic trigger factors to neighbouring cells, whilst the majority of the cytoplasm is exuded to provision growing oocytes (Gumienny *et al.*, 1999) (Figure 5.2). It has been proposed that germ cells are produced in excess to act as nurse cells, supplying nourishment for developing oocytes (Gartner *et al.*, 2008; Gumienny *et al.*, 1999). Germ cell apoptosis takes place in the gonad loop just before germ cells differentiate thus allowing germ cells to act as cytoplasm "factories" for as long as possible (Gumienny *et al.*, 1999; Wolke *et al.*, 2007). In further support, one study found that there is cytoplasmic streaming from the rachis to first three oocytes still connected to it, accounting for most of the oocyte enlargement

(Wolke *et al*., 2007). Physiological apoptosis does not occur in male *C. elegans,* probably because sperm, being so small, do not require large amounts of cytoplasm, allowing all germ cells to become gametes (Gumienny *et al*., 1999). Additionally although *ced-4* and *ced-3* mutants are fertile, they produce smaller oocytes and lay more dead eggs, indicating that germ cell apoptosis improves oocyte quality (Andux and Ellis, 2008).
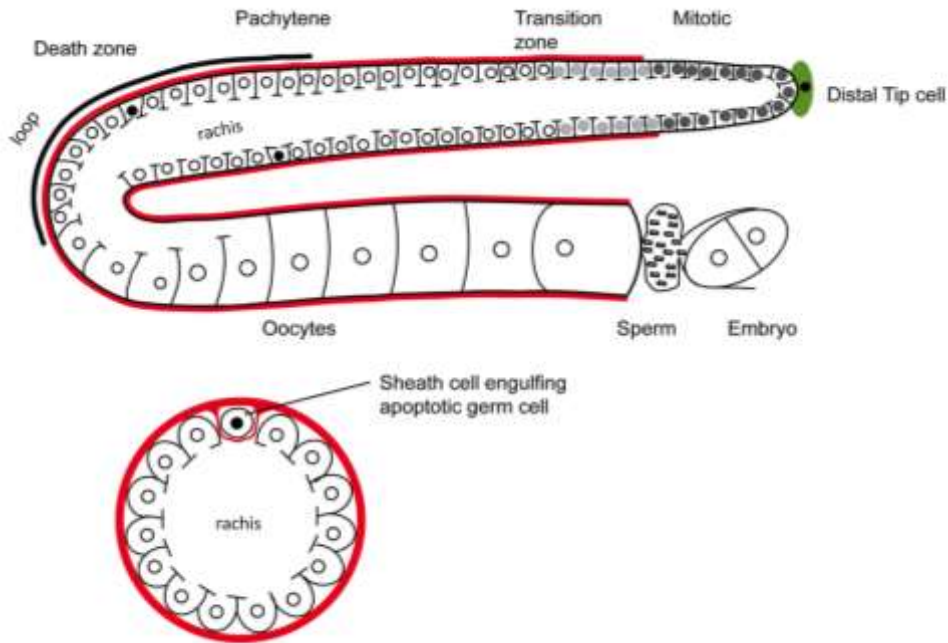
Figure 5.2 Representation of the nurse cell theory. Physiological apoptosis in worms occurs in the "death zone" in the loop region of the distal gonad where germ cells are in the pachytene stage. Germ cells are not completely cellularized, instead they are connected through the shared rachis. Image modified from Gartner *et al* 2008.

5.1.1.2 Stress-induced apoptosis

The finding that apoptosis takes place in the gonad led researchers to test whether germ cell apoptosis could be induced by stress. Consequently, separate mechanisms were discovered in which apoptosis can be triggered in the germline by genotoxic and environmental stressors, starvation and infection probably to prevent the passing on of genetic abnormalities to the next generation to preserve resources (Gartner *et al.*, 2008) (Figure 5.3).
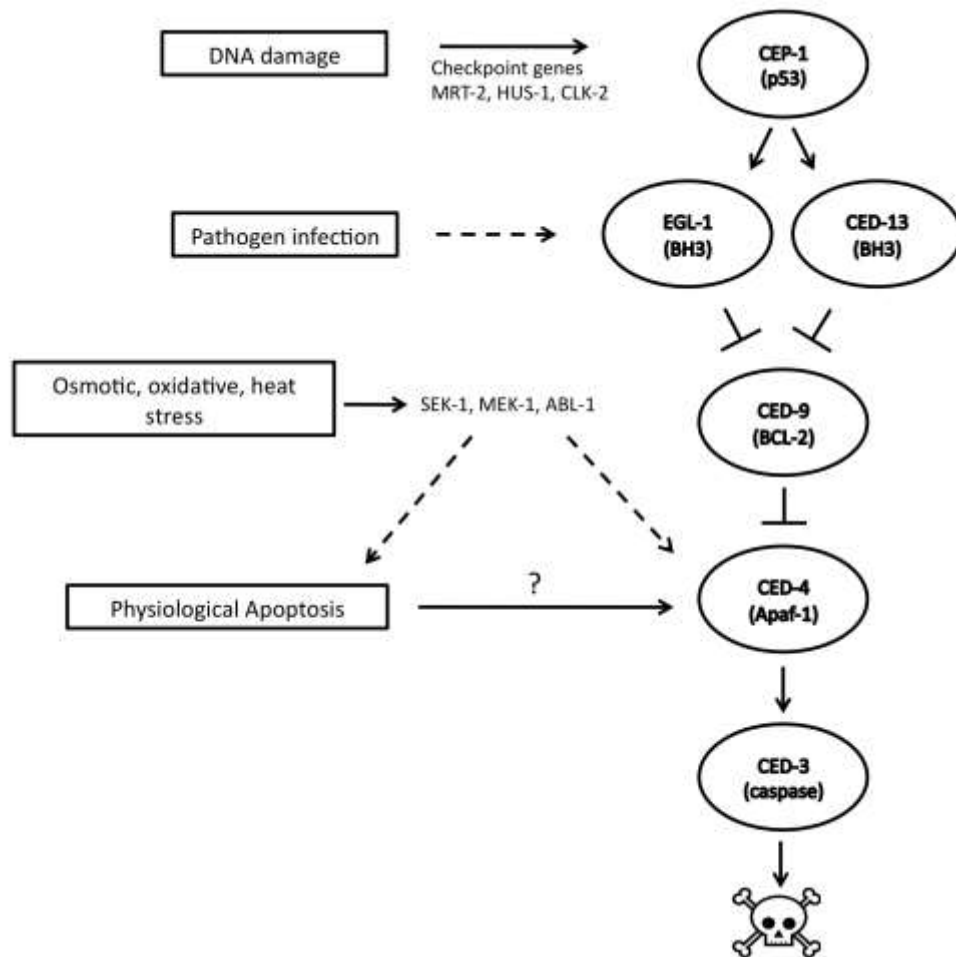
Figure 5.3 Germline apoptosis genetic pathways in *C. elegans.* Representation of the different mechanisms for germline apoptosis in *C. elegans.* DNA damage promotes germline apoptosis via CEP-1 activity. DNA damage-induced apoptosis and pathogen induced apoptosis require EGL-1; it is not known whether pathogen induced apoptosis acts via CEP-1. Physiological apoptosis does not require EGL-1 and can activate CED-4 and CED-3 through an unknown mechanism. Stress-induced apoptosis (osmotic, oxidative and heat stress) is EGL-1 independent and acts via MEK-1, SEK-1 and ABL-1 which may activate physiological apoptosis or act via an alternative mechanism. This figure has been modified from Gartner *et al*, 2008.

5.1.1.2.1 DNA damage-induced apoptosis

Studies examining the effect of inducing DNA damage in *C. elegans* using ionizing radiation found an alternate genetic pathway for apoptosis distinct from physiological apoptosis (Gartner *et al*., 2000). Stress induced apoptotic cells have the same morphological characteristics and occur in the same region of the gonad (pachytene) as physiological apoptosis (Gartner *et al*., 2008). Similar to physiological apoptosis, DNA damage induced apoptosis has not been observed in the male *C. elegans* germline (Gartner *et al*., 2000). Germline apoptosis in response to genotoxic stress requires EGL-1 and CED-9, which are not necessary for physiological apoptosis, implying that the signal to activate DNA damage-induced apoptosis is further upstream (Gartner *et al*., 2000). CEP-1, a homologue of the mammalian tumour suppressor p53, is required for DNA damage-induced apoptosis but not apoptosis in the soma nor physiological apoptosis (Schumacher et al., 2001). CEP-1 acts as a transcriptional activator of pro-apoptotic factors that can induce apoptosis via EGL-1 or CED-13 (Schumacher et al., 2005a).

5.1.1.2.2 Other stressors that induce germline apoptosis

Programmed cell death also occurs in the germline in response to pathogen infection (Aballay et al., 2000). The pathogenic bacteria *Salmonella typhimurium* and *Salmonella enterica* cause an increase in germline apoptosis which does not occur in *ced-3* and *ced-4* mutants (Aballay and Ausubel, 2001; Aballay et al., 2003). Pathogen-induced germline apoptosis requires EGL-1, MAPK kinase SEK-1 and the p38 homologue PMK-1 (Aballay and Ausubel, 2001). Colonization of the worms by *S. typhimurium* causes an increase in intact bacteria within the worm which is restricted to the lumen of the intestine (Aballay et al., 2000). This implies that a signal from intestinal somatic tissue in response to the infection triggers apoptosis in the gonad. Inhibition of apoptosis in the worms using *ced-3* and *ced-4* mutations results in increased sensitivity to death by *S. typhimurium* infection, which suggests germline apoptosis is somehow involved in defence against infection (Aballay and Ausubel, 2001).

Apoptosis can be induced in the germline by oxidative, heat shock, osmotic and starvation stressors through a pathway which does not require CEP-1 and EGL-1 (Salinas

et al., 2006). MAPK kinases MEK-1 and SEK-1 in addition to the p53 antagonist tyrosine kinase ABL-1 are necessary for germline apoptosis in response to oxidative, osmotic and thermal stressors but not starvation which seems to work through an unknown alternate mechanism (Salinas *et al*., 2006). Curiously, ABL-1 represses CEP-1 dependent apoptosis, so it is involved in repressing DNA-damage induced apoptosis whilst promoting environmental stress induced apoptosis (Deng *et al*., 2004; Gartner *et al*., 2008). Pathogen and DNA damage induced germline apoptosis require EGL-1 while physiological and environmental stress induced apoptosis do not. Additionally MAPK kinase is also involved in physiological apoptosis. This suggests the possibility that environmental stress-induced apoptosis may act via the physiological apoptosis pathway or a novel, separate mechanism (Gartner *et al*., 2008).

Bacterial infection, osmotic stress, starvation, heat shock and oxidative stress do not challenge the genomic integrity of the germline yet cause an increase in apoptosis. It is possible that signals from the somatic tissue cause increased germline apoptosis to divert resources to battle the adverse conditions (Gartner *et al*., 2008). Furthermore, one study found that starvation in early adulthood results in removal of all germ cells except for a small mitotic germ cell population which is then entirely replenished when placed back on food (Angelo and Van Gilst, 2009).

Based on the hyperfunction theory we hypothesize that germline apoptosis continues in the germline after reproduction has stopped, and that it is this quasi-programmed apoptotic hyperfunction that causes disintegration of the gonad. Results described in the previous chapter provide support for this hypothesis. In this chapter, we will test this idea further, and examine which type of germline apoptosis is more likely to contribute to gonad ageing.

5.2   Results

5.2.1 Gonad disintegration is apoptosis dependent

We previously found that blocking apoptosis using mutation of *ced-3(n717)* protects the gonad from disintegration suggesting a link between apoptosis in the gonad and GD. To test whether this is typically the case for *ced-3* alleles we examined germline disintegration in *ced-3(n1286)*, *ced-3(n2454)* and *ced-3(n288)* mutants. We first used SYTO 12 staining to verify effects of these alleles on germline apoptosis measuring apoptosis levels on day 1 of adulthood. Previously, only effects of *ced-3(n717)* on germline apoptosis have been tested (Gumienny *et al*., 1999). All *ced-3* alleles examined prevented germline apoptosis (Figure 5.4 A).
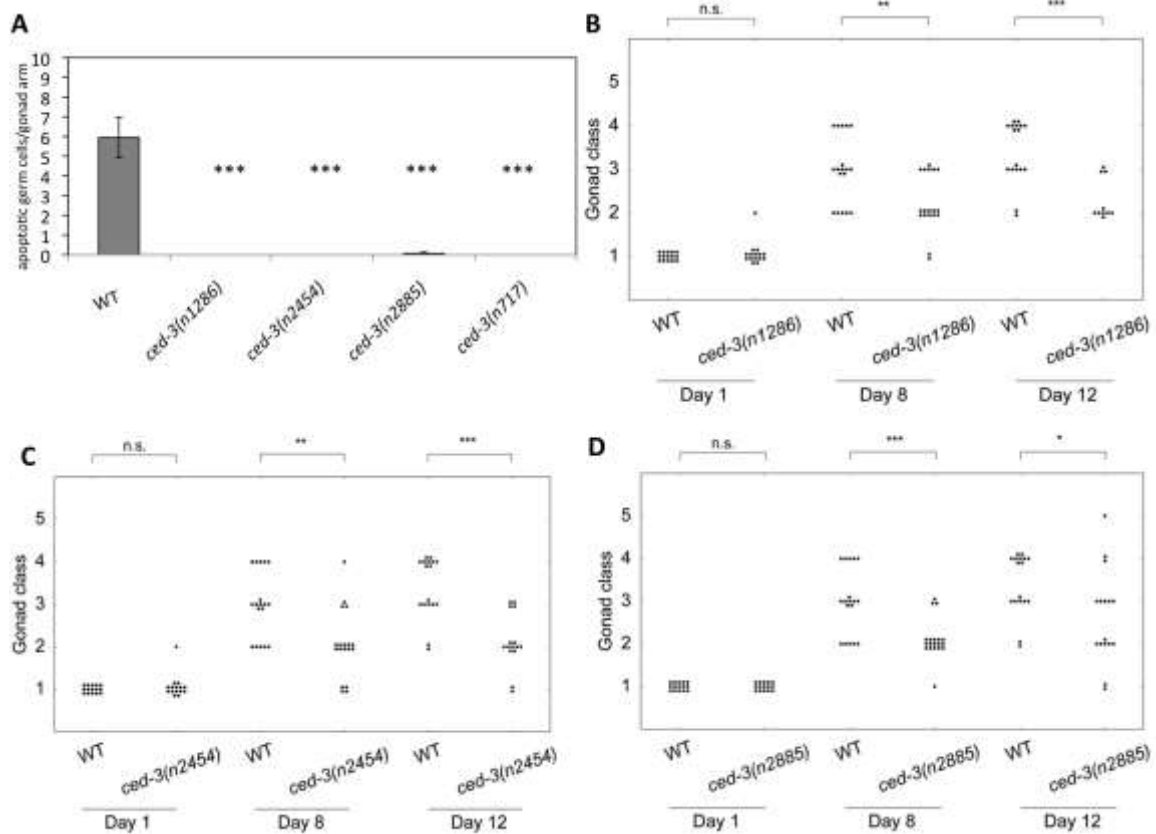
Figure 5.4 Gonad disintegration is delayed in *ced-3(-)* mutants. A) SYTO 12 staining revealed germline apoptosis is nearly absent in *ced-3(n1286)*, *ced-3(n2454)*, *ced-3(n288)* and *ced-3(n717)* worms. Data is the mean of 11-20 worms; error bars, SEM, Students t-test (compared to WT control). Data obtained by J. Hellberg. Scatter diagrams showing protective effect of B) *ced-3(n1286)*, C) *ced-3(n2454)*, D) *ced-3(n288)* on gonad disintegration compared to wildtype worms. Statistics were obtained by performing the Wilcoxon-Mann Whitney test, n.s.=not significant ***p<0.001, **p<0.01, *p<0.05.

Then we examined the gonad in *ced-3(n1286)*, *ced-3(n2454)*, and *ced-3(n288)* mutants and found that gonad disintegration is delayed compared to wildtype in all cases (Figure 5.4 B-D). Thus, suppression of gonad degeneration by mutation of *ced-3* is a robust and reproducible phenomenon.

The anti-apoptosic factor CED-9 acts by forming a complex with the pro-apoptotic protein CED-4, sequestering it in the mitochondria (Chen et al., 2000; del Peso et al., 2000). In cells undergoing programmed cell death CED-4 is localized in the nucleus, thus once CED-4 translocates to the nucleus it activates CED-3 to initiate apoptosis (Chen *et al*., 2000; del Peso *et al*., 2000). Mutations in *ced-3* and *ced-4* successfully block all somatic programmed cell death (Ellis and Horvitz, 1986). Additionally, in *ced-4(n1162)* mutants germ cell death is inhibited (Gumienny *et al*., 1999). We examined the effect of apoptosis defective *ced-4(n1162)* mutants to determine if gonad disintegration is inhibited as in *ced-3* mutants and found that it was (Figure 5.5). Together these results further suggests that apoptosis is a contributor of gonad ageing in hermaphrodite worms.
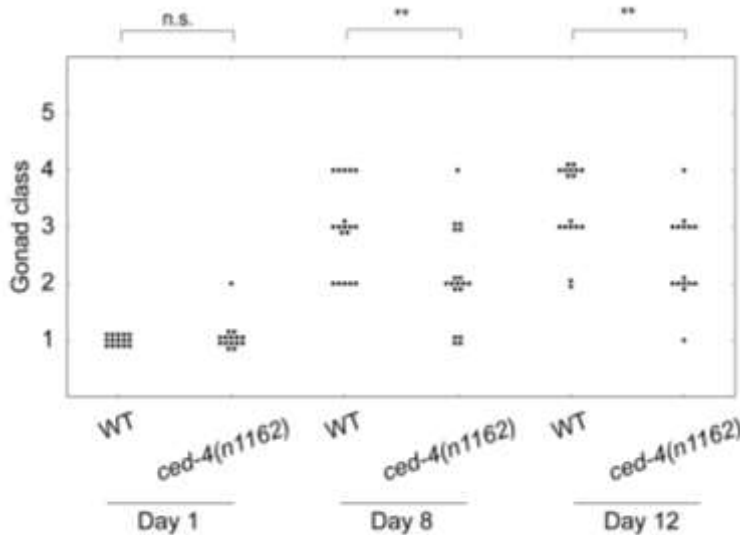
Figure 5.5 Gonad deterioration is slowed down in *ced-4(n116)* worms. Scatter diagram showing protective effect of *ced-4(n1116)* on gonad disintegration compared to wildtype. Statistics were obtained by performing the Wilcoxon-Mann Whitney test, **p<0.01, *p<0.05.

5.2.2 Somatic apoptosis does not influence gonad disintegration

Apoptosis that occurs in the *C. elegans* hermaphrodite gonad in the absence of any environmental stressors is known as physiological apoptosis (Gumienny *et al*., 1999). This type of germline apoptosis requires the core apoptotic machinery CED-3 and CED-4, but not death-inhibitor protein CED-9 (Gartner *et al*., 2008; Gumienny *et al*., 1999). Loss of function (lf) mutations in CED-9 cause cells that would normally survive to undergo apoptosis and is embryonic lethal; gain of function (gf) mutation *ced-9(n1950)* blocks apoptosis, resulting in a phenotype similar to *ced-3* and *ced-4* mutants (Hengartner et al., 1992). The *ced-9(n1950gf)* mutation completely represses somatic apoptosis (Hengartner et al., 1992) but not germline apoptosis in hermaphrodite worms (Gumienny *et al*., 1999). To exclude the possibility that somatic apoptosis causes gonad degeneration we tested whether *ced-9(n1950)*, which has wildtype levels of gonad apoptosis, but no somatic apoptosis, has any effect on gonad ageing. We predicted that due to the presence of germline apoptosis the gonad would not be protected from degeneration. As expected, there was no difference in the rate of gonad degeneration in *ced-9(n1950)* compared to wildtype, possibly due to similar germline apoptosis levels (Figure 5.6). Furthermore, our results suggest that somatic apoptosis does not influence gonad degeneration.
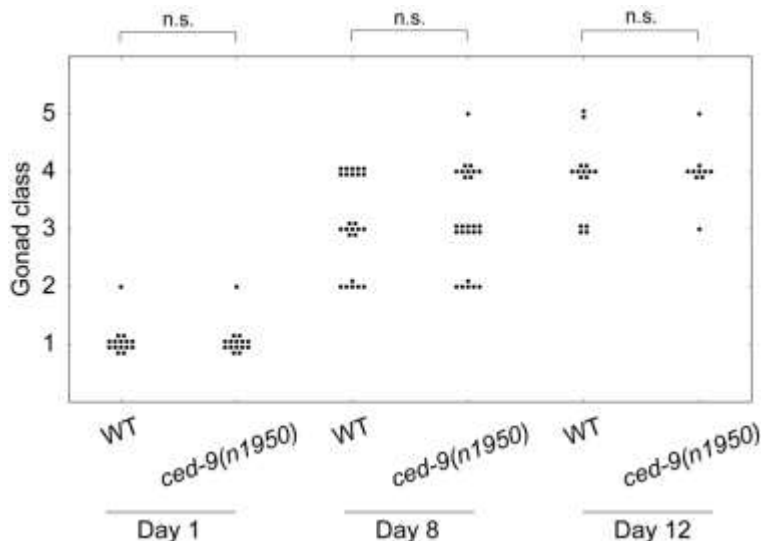
Figure 5.6 Effect of the gain of function mutation *ced-9(n1950)* on gonad degeneration. Diagram showing no difference in gonad degeneration rate between *ced-9(n1950)* and wildtype. Statistics were obtained by performing the Wilcoxon-Mann Whitney test, n.s.=not significant.

5.2.3 Increasing apoptosis levels causes faster gonad disintegration

We have shown that blocking apoptosis using *ced-3* and *ced-4* mutations slows gonad degeneration. We were therefore interested in testing if increasing apoptosis levels would result in a faster rate of gonad degeneration. To do so we used the *gld-1(op236)* mutation which causes the upregulation of CEP-1 dependent translation of apoptotic factors (Schumacher et al., 2005b). GLD-1 is a translational repressor of CEP-1 related to mammalian Quaking proteins (Schumacher et al., 2005b). At 20˚C the *gld-1(op236)* mutation causes a small increase in germline apoptosis levels and this effect is dramatically increased in response to radiation (Schumacher et al., 2005b). The *gld-1(op236)* mutation is temperature sensitive causing a massive increase in germ cell apoptosis at 25˚C by induction of EGL-1 pro-apoptotic factors via CEP-1 activity, independently of DNA damage (Schumacher et al., 2005b).

We sought to replicate this finding using SYTO 12 staining and found that at 20˚C apoptotic levels in the germline were similar between wildtype and *gld-(op236)* on day 1 of adulthood, however there was a large increase in apoptosis in *gld-1(op236)* at 25˚C (Figure 5.7 A,C). It is worth noting that in the study conducted by Schumacher *et al* the enhancement in germline apoptosis in *gld-1(op236)* worms was higher (~13X) than those obtained in this study (~4X). Due to high levels of germline apoptosis in *gld-1(op236)* mutants at 25˚C, it is possible that our absolute values are underestimated as stained apoptotic germ cells appear in large clumps making it difficult to count individual cells.

We tested the effect of *gld-1(op236)* mutation on gonad disintegration at 20˚C. We chose this temperature to look at worms with mildly enhanced apoptosis (Schumacher et al., 2005b). If apoptosis causes gonad atrophy, the higher apoptosis rates could lead to gonad atrophy that occurs too rapidly. We found that GD was accelerated in *gld-1(op236)* worms at this temperature compared to wildtype on day 8 but not day 12 (Figure 5.7 B). We also examined worms with a greater enhancement of apoptosis at 25˚C and found that GD was greatly accelerated. At this temperature, a significant increase in gonad degeneration was seen in even young day 1 adults and this trend continued on day 6 by which time all *gld-1(op236)* worms examined had gonads with a high degree of degeneration (class 3-5) (Figure 5.7 D). Our results indicate a positive correlation between germline apoptosis levels and rate of gonad disintegration.

Figure 5.7 Increasing germline apoptosis results in faster gonad disintegration. A) SYTO 12 staining revealed similar apoptosis levels between *gld-1(op236)* and wildtype worms at 20˚C in day 1 adults. B) At 20˚C gonad disintegration is slightly accelerated in day 8 *gld-1(op236)* worms. C) At 25˚C germline apoptosis levels in *gld-1(op236)* worms were three times higher than those observed in wildtype. D) At 25˚C gonad deterioration is greatly accelerated, showing greater decline in *gld-1(op236)* on day 1 and day 6. A,C) Data is the mean of (n, indicated inside bar); error bars, SEM; Students t-test (compared to temperature-matched WT control). B,D) Statistics were obtained by performing the Wilcoxon-Mann Whitney test, n.s.=not significant *** = p<0.001, ** = p<0.01, * = p<0.05

5.2.4 No evidence that molecular damage is a major contributor to gonad ageing

It has been suggested that molecular damage causes ageing and age-related pathology. If gonad degeneration is the direct result of oxidative damage we would expect that treatments that increase protein oxidation should result in faster gonad disintegration. We probed whether molecular damage is involved in gonad degeneration by using the *sod-2(gk257)* mutation, which abrogates the main *C. elegans* mitochondrial superoxide dismutase, and 9mM iron supplementation. Both these treatments have been

shown to increase protein carbonylation without affecting lifespan (Doonan et al., 2008; Van Raamsdonk and Hekimi, 2009; Valentini et al., 2012). We chose treatments that do not reduce lifespan to avoid life-shortening broad pathological effects unrelated to ageing that could complicate the interpretation of results. We performed oxyblots to verify that our treatments increased protein carbonyls and found an increase in protein carbonylation on 9mM ferric ammonium citrate (FAC) supplementation. Mutation of *sod-2(gk257)* also increased protein carbonylation though this did not attain significance, possibly due to high variability between replicates (Figure 5.8).
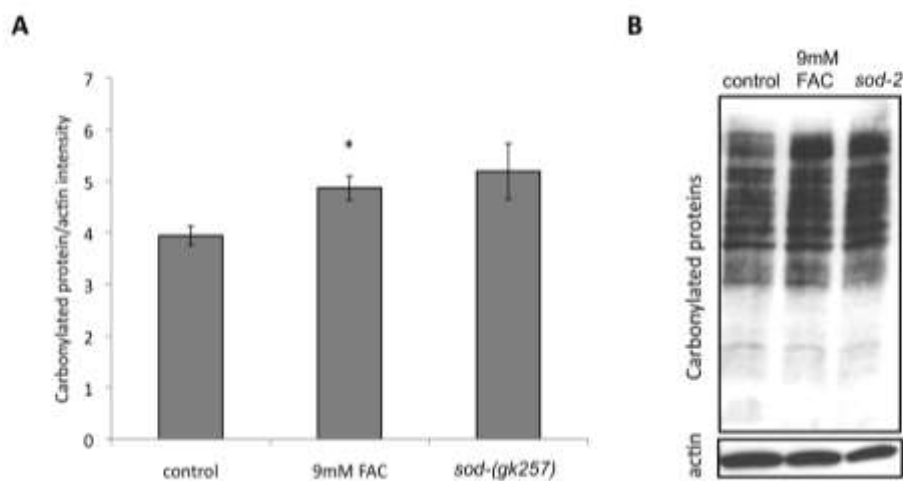
Figure 5.8 Increased protein carbonylation in *sod-2(gk257)* and 9mM FAC treated *C. elegans*. A) Protein oxidation is significantly increased in worms with moderate iron supplementation (9mM FAC) and appears increased in *sod-2(gk257)* worms. B) Representative oxyblot showing increase in protein carbonylation for 9mM FAC and *sod-2(gk257)* compared to control. Data is the mean of three biological replicates; error bars, SEM; Student's t-test, *p<0.05. Data obtained in collaboration with F. Cabreiro.

We then examined effects of treatments that increase protein oxidation on gonad degeneration and found no difference to wildtype control for either *sod-2(gk257)* mutants or 9mM FAC treatment (Figure 5.9 A,B). These results suggest that under standard culture conditions gonad degeneration is not caused by increased levels of protein oxidation.
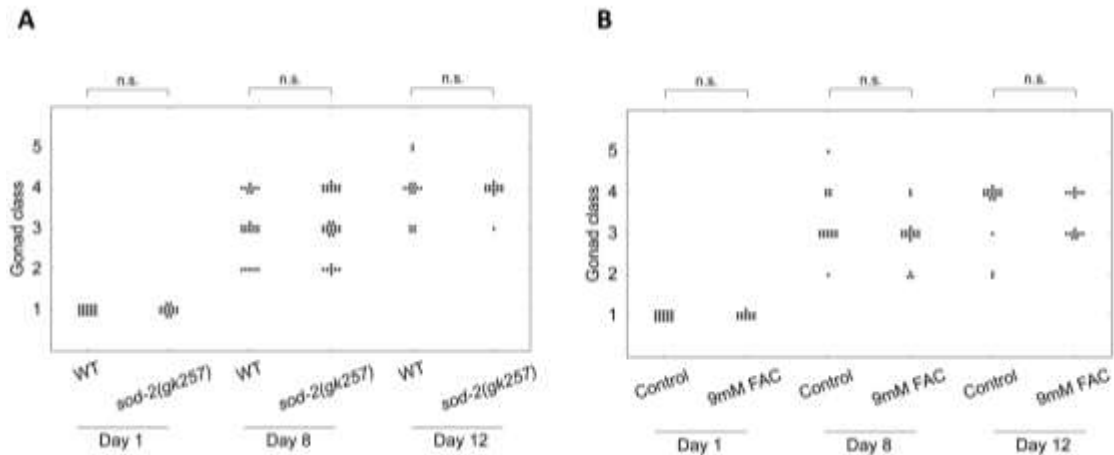
Figure 5.9 Protein oxidation does not affect gonad deterioration. A,B) Scatter diagrams showing no effect of increased protein carbonylation on gonad degeneration for *sod-2(gk257)* mutants nor 9mM FAC treatment. Statistics obtained by performing the Wilcoxon-Mann Whitney test, n.s.=not significant.

5.2.5 DNA damage is not a major contributor to gonad degeneration

One scenario is that gonad degeneration is the result of DNA damage-induced apoptosis. This apoptosis pathway in the germline helps to avoid passing on genetic aberrations to the offspring. Studies examining the effect of ionizing radiation (IR) on germline apoptosis revealed a distinct genotoxic response to checkpoint genes *rad-5*, *mrt-2* and *him-7* (Gartner *et al*., 2000). Apoptosis in response to DNA damage has only been observed in pachytene stage cells in the germline and has not been observed in somatic cells nor in male *C. elegans* (Gartner *et al*., 2008). In this way, DNA-damage induced apoptosis may remove any damage caused by SPO-11 induced double strand breaks during meiotic crossover, which occurs during pachytene (Dernburg et al., 1998; Schumacher et al., 2001). Thus, it is conceivable that an apoptotic programme that exists to safeguard the germline from accumulating DNA damage could potentially become a quasi-programme in later life.

The SPO-11 protein is a meiotic recombination protein which is the homologue of yeast Spo11 and is related to Topoisomerases (Dernburg *et al*., 1998). To test if DNA damage-induced apoptosis is the main cause of gonad degeneration we used *spo-11(ok79)* mutants that are unable to form double strand breaks, which is a major source of

DNA damage during meiosis (Dernburg *et al*., 1998). Thus, *spo-11* mutants should have negligible amounts of DNA damage in the germline and should not trigger the DNA-damage induced apoptotic pathway. Crossing over is not observed in the *spo-11(ok79)* deletion mutants and although homozygote hermaphrodites are behaviourally normal and have normal fecundity, 99% of eggs do not hatch and survivors are mostly male (Dernburg *et al*., 1998). The unusual large amount of males arising from self-fertilization is indicative of errors in chromosomal segregation, and indeed all chromosomes in *spo-11(ok79)* mutants lack chiasmata which link homologous chromosomes during crossover (Dernburg et al., 1998; Hodgkin et al., 1979). We found that the *spo-11(ok79)* mutation did not affect the rate of gonad degeneration which argues against a role of DNA damage-induced apoptosis in GD (Figure 5.10).
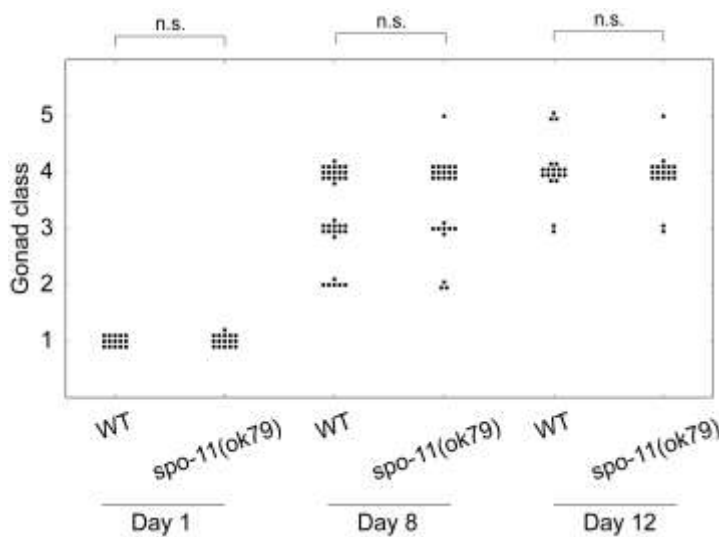
Figure 5.10 Little effect of DNA damage on gonad degeneration. Scatter diagram showing no effect of reducing DNA damage levels using *spo-11(ok79)* on gonad atrophy. Statistics were obtained performing Wilcoxon-Mann Whitney test, n.s.=not significant.

The p53 transcription factor is a mammalian tumour suppressor necessary to activate apoptosis in abnormal cells (Levine et al., 2004). Moreover mutations in p53 have been implicated in more than 50% of human cancers (Levine, 1997). The *C. elegans* transcription factor CEP-1 is a homologue of mammalian p53 and is required for the DNA damage induced apoptosis response (Derry et al., 2001; Schumacher et al., 2001). RNAi of *cep-1* has been shown to abrogate DNA damage induced apoptosis in response to ionizing radiation (Schumacher et al., 2001). Un-irradiated worms subjected to *cep-1* RNAi and *cep-1(gk138)* mutants have apoptosis levels similar to wildtype (Pinkston-

Gosse and Kenyon, 2007; Pinkston et al., 2006; Schumacher et al., 2001), as presumably in the absence of genotoxic stress physiological apoptosis still takes place. We used *cep-1(gk138)* mutants to test whether in the absence of the mediator for DNA damage induced apoptosis gonad degeneration still occurred.

We found that there was no difference in gonad disintegration on day 1 and 8 between wildtype and *cep-1(gk138)* worms. However, a slight protective effect was observed on day 12 in *cep-1(gk138)* worms (Figure 5.11). Thus, the possibility of a slight effect of DNA damage on GD cannot be excluded.
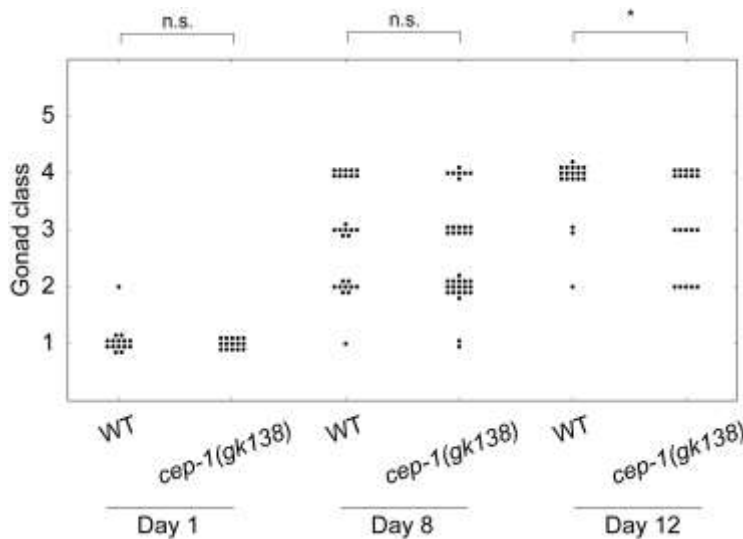
Figure 5.11 Little effect of CEP-1 dependent DNA-damage induced apoptosis on GD. Diagram showing effects on gonad degeneration of *cep-1(gk138)* worms. No effect was seen, but a slight protective effect was observed for *cep-1(gk138)* on day 12. Statistics were obtained by performing the Wilcoxon-Mann Whitney test, n.s.=not significant, *p<0.05.

5.2.5.1 Stress-induced apoptosis is a minor contributor to gonad degeneration

A separate mechanism for germline apoptosis in response to stressors such as osmotic, thermal and oxidative stress has been discovered which is independent of CEP-1 and EGL-1 and involves the MAPK kinases MEK-1 and SEK-1, and the tyrosine kinase ABL-1 (Salinas *et al.*, 2006). ABL-1 has been previously found to be an anti-apoptotic factor which negatively regulates CEP-1 (Deng *et al.*, 2004). However, it seems ABL-1 can also act as a pro-apoptotic factor in response to non-genotoxic stressors which may activate the physiological apoptosis pathway (Salinas *et al.*, 2006) or an alternative unknown factor that induces the core apoptotic machinery.

Worms with deletion allele *abl-1(ok171)* have higher levels of basal germline apoptosis and are hypersensitive to radiation, and this is lost in the absence of CEP-1 (Deng *et al*., 2004). We checked effects of *abl-1* and *cep-1* on germline apoptosis levels and obtained similar results. On control RNAi germline apoptosis was slightly higher in *abl-1(ok171)* mutants than wildtype. When worms were treated with *cep-1*(RNAi) there was no effect on wildtype but the apoptotic enhancement of *abl-1(ok171)* was lost (Figure 5.12 A).
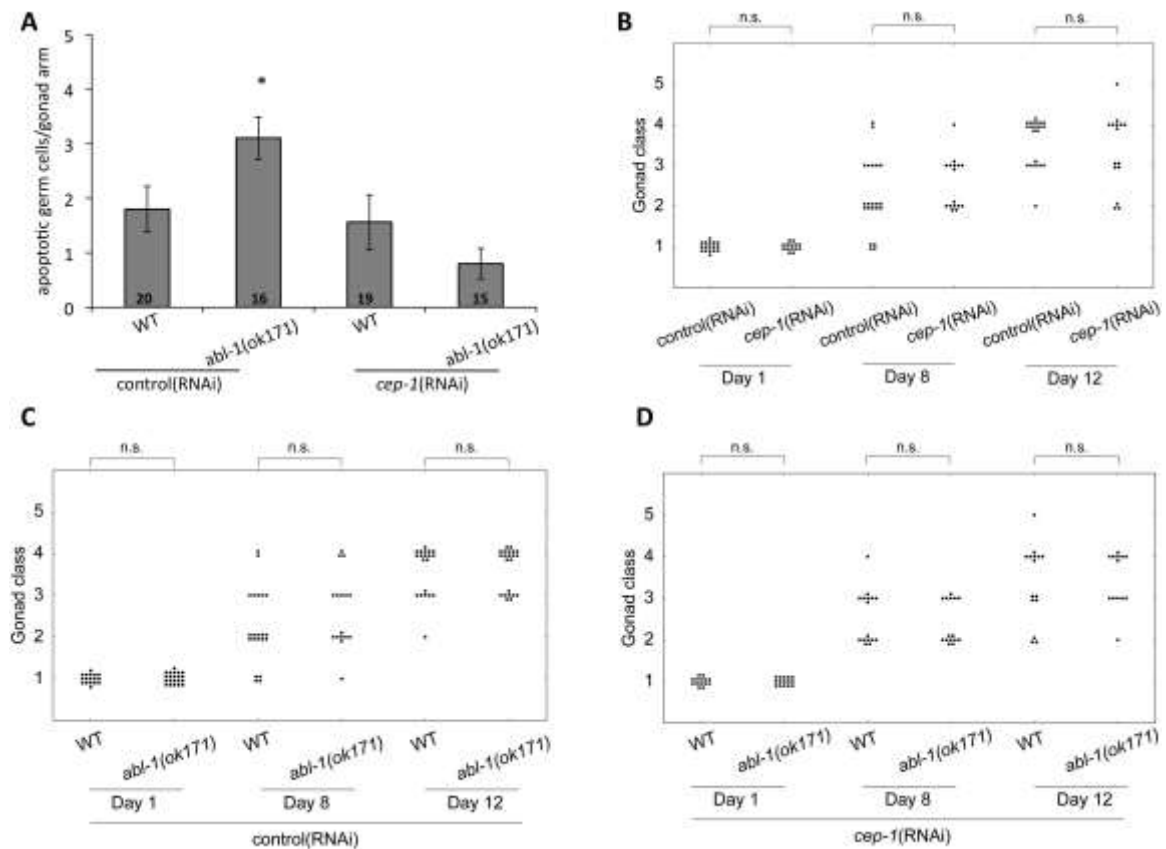
Figure 5.12 Blocking stress-induced germline apoptosis does not reduce germline atrophy. A) SYTO 12 staining revealed germline apoptosis levels are higher in day 1 adult *abl-1(ok171)* than wildtype. This enhancement is lost if *abl-1(ok171)* worms are subjected to *cep-1*(RNAi), resulting in levels slightly lower (p=0.07) than wildtype control. Data is the mean of (n, indicated inside bar); error bars, SEM; Students t-test (compared to WT control),* p<0.05. B) There was no difference in gonad degeneration between wildtype on control(RNAi) and *cep-1*(RNAi) C) Similar rate of gonad degeneration was observed between wildtype and *abl-1(ok171)* worms. D) Inhibition of CEP-1 by RNAi in wildtype and *abl-1(ok171)* has little effect on gonad degeneration. Statistics were obtained by performing the Wilcoxon-Mann Whitney test, n.s.=not significan

145

If physiological apoptosis causes gonad degeneration then neither inhibition of *cep-1* or *abl-1* should suppress gonad atrophy. We first looked at the effect of inhibiting the non-genotoxic SIA response using *abl-1(ok171)* and saw no effect on gonad degeneration (Figure 5.12 C). We also disabled two mechanisms of SIA (DNA damage and stress-induced) by subjecting *abl-1(ok171)* worms to *cep-1*(RNAi) and again saw no effect (Figure 5.12 D). We also confirmed, using *cep-1*(RNAi) the previous finding with *cep-1(gk138)* in which there is no major effect of DNA damage-induced suppression on gonad disintegration (Figure 5.12 B). We saw no protective effect on day 12 in worms on *cep-1*(RNAi) suggesting that the slightly lower levels of GD observed in the single *cep-1(gk138)* trial may not reflect a robust effect. Taken together these results suggest that age-related gonad disintegration is the result of continued physiological apoptosis, not stress-induced apoptosis.

5.2.6 Mutations in *daf-2* delay gonad ageing

The insulin/IGf-1 signalling pathway greatly influences ageing in *C. elegans* through processes that remain poorly understood. Gonad ageing has been previously shown to occur at a slower rate in *daf-2(-)* worms which have reduced IIS (Garigan *et al*., 2002). Our working model suggests that *daf-2(-)* worms might delay gonad degeneration by decreasing germline apoptosis.

A previous study examined germline apoptosis in *daf-2(e1370)* worms at 25°C and found they have an increased rate of apoptosis (Pinkston *et al*., 2006). However, another study quantified germline apoptosis at 20°C in *daf-2(e1370)* and found the opposite: lower levels of apoptosis in *daf-2(-)* worms (Perrin *et al*., 2013). The class 2 allele *daf-2(e1370)* used in both of these studies causes pleiotropic effects such as reduced fertility and reduced pharyngeal pumping. We used SYTO 12 staining to measure germline apoptosis in the class 2 allele *daf-2(e1370)* and also the less pleiotropic class 1 allele *daf-2(m577)* at 20°C and 25°C. *daf-2(m577)* increases lifespan weakly at 20°C and robustly at 25°C.

At 20°C we observed lower levels of apoptosis for *daf-2(e1370)* on day 1 and 2 of adulthood, consistent with the results of Perrin *et al* (2013). A similar trend was observed for *daf-2(e1370)* at 20°C where apoptosis levels were lower on day 1, and this pattern continued on day 2 but did not reach statistical significance. Germline apoptosis levels in

146

daf-2(m577) were similar to wildtype at both temperatures (Figure 5.13 A,B). These results suggest that the lower germline apoptosis levels in *daf-2(e1370)* mutants are the result of its pleiotropic effects.

The study by Garrigan *et al* (2002) examined gonad ageing in class 2 allele *daf-2(e1370)* and class 1 allele *daf-2(mu86)* and found that both delay gonad deterioration. We sought to replicate this result using *daf-2(m577)* worms (25˚C) and we were able to verify that this allele has a protective effect on GD (Figure 5.13 C). Thus, *daf-2(m577)* animals exhibit less gonad deterioration despite having unaltered levels of germline apoptosis. Our results imply that *daf-2(m577)* inhibits gonad disintegration by a mechanism other than reduced apoptosis, which also drives gonad ageing.
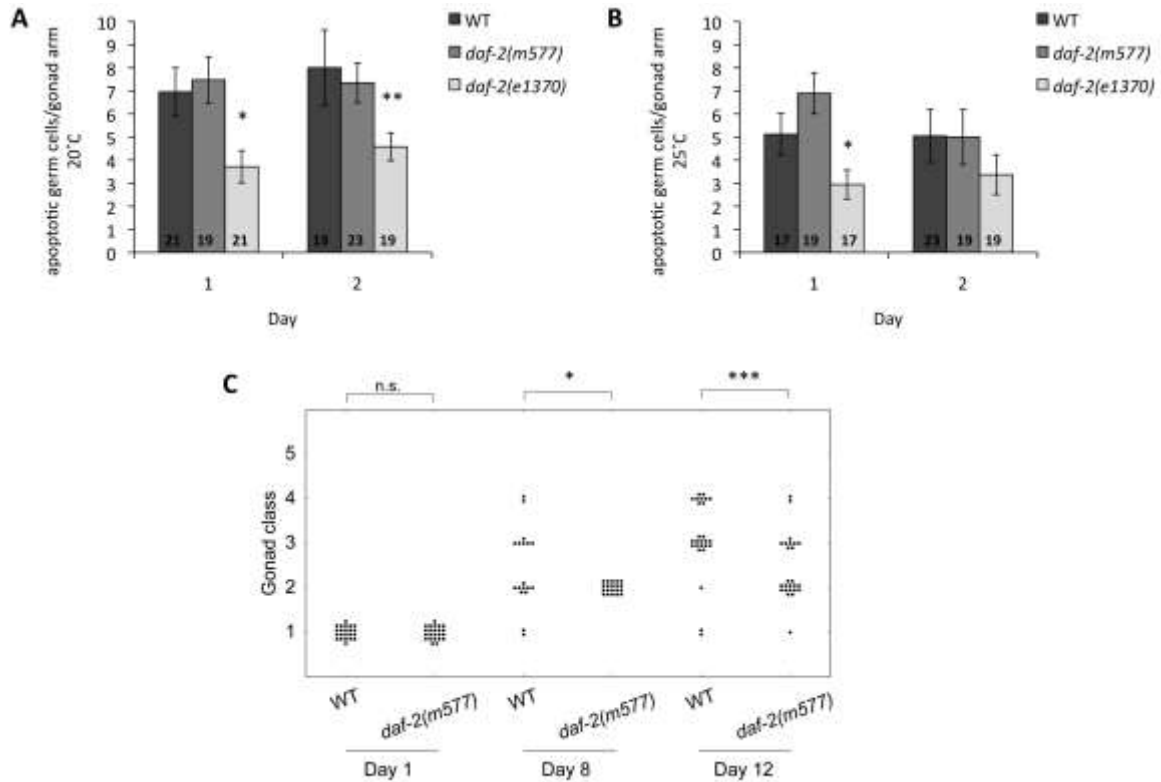
Figure 5.13 Gonad ageing is delayed in *daf-2(m577)* worms. A,B) Germ cell measurements using SYTO 12 staining show reduced levels of germline apoptosis in *daf-2(e1370)*, but not *daf-2(m5577)* which had levels similar to wildtype. Data is the mean of number of worms indicated inside bars; error bars, SEM; Student's t-test test (compared to same day wildtype control) **p<0.01, *p<0.05. C) Gonad disintegration is delayed in *daf-2(m577)* worms compared to wildtype. Statistics were obtained by performing the Wilcoxon-Mann Whitney test, n.s.=not significant ***p<0.001, **p<0.01, *p<0.05. Data obtained in collaboration with Josephine Hellberg.

5.2.7 TOR pathway mutant *rsks-1(ok1255)* does not affect gonad disintegration

In addition to the IIS pathway, TOR signalling is also involved in sensing nutrients and promoting growth and is a modulator of the ageing process. Inhibition of RSKS-1, a homologue of S6 kinase downstream of TOR, modestly increases lifespan in worms (Hansen et al., 2007; Kapahi et al., 2010; Pan et al., 2007). The hyperfunction theory proposes that inhibition of IIS and TOR pathways extend lifespan by inhibiting quasi-programmes (Blagosklonny, 2007, 2008). We therefore tested whether *rsks-1(ok1255)* mutants have a similar pattern of delay in gonad ageing as do *daf-2(-)* worms.

We measured germ cell apoptosis using SYTO 12 staining on day 1 of adulthood and found that *rsks-1(ok1255)* mutants had reduced levels of apoptosis compared to wildtype (Figure 5.14 A). This is consistent with reduced and delayed fertility in this mutant (Selman *et al*., 2009). However, despite lower levels of germline apoptosis in *rsks-1(ok1255)* mutants gonad disintegration rate in these worms is not different to wildtype (Figure 5.14 B).
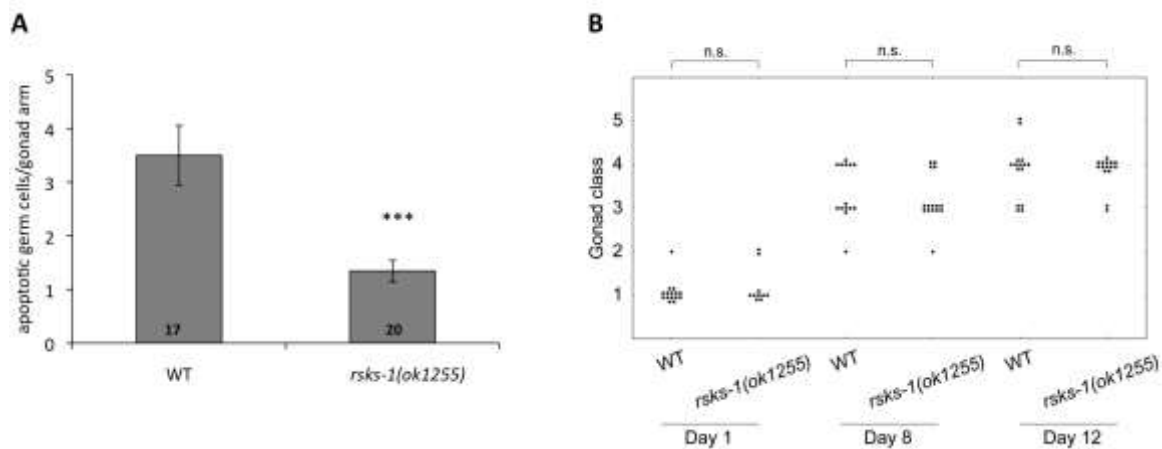
Figure 5.14 Reduced TOR signalling does not have a protective effect on GD. A) Measurement of SYTO 12 stained apoptotic cells show a reduction in germ cell apoptosis levels in *rsks-1(ok1255)* mutants on day 1 of adulthood compared to wildtype. Data is the mean of number of worms indicated inside bars; error bars, SEM; Students t-test (compared to same day wildtype control) *** p<0.001. B) Scatter diagram showing no difference in GD between *rsks-1(ok1255)* and wildtype worms. Statistics obtained using the Wilcoxon-Mann Whitney test, n.s.=not significant.

5.2.8 Effect of bacteria on gonad degeneration

Under standard laboratory conditions *C. elegans* are cultured on agar plates seeded with *Escherichia coli* strain OP50 as their main food source (Brenner, 1974b). Alternatively, when performing RNAi by feeding worms are maintained on *E. coli* containing the L4440 plasmid (Timmons and Fire, 1998). The *E. coli* strain most used for RNAi is HT115 because it lacks RNAse III, improving the efficacy of RNAi (Timmons et al., 2001). During experiments conducted on RNAi we noticed a protective effect on gonad degeneration. Thus we compared worms on standard agar plates seeded with OP50 and worms on IPTG agar plates seeded with HT115 containing empty vector L4440. For the latter, an antibiotic (carbenicillin) was added to maintain the L4440 plasmid, which confers carbenicillin resistance. Worms were examined on day 8 and day 12 and we found that maintenance on HT115+L4440+carbenicillin had a protective effect on gonad degeneration (Figure 5.15). This could reflect an effect of HT115, or L4440, or carbenicillin.
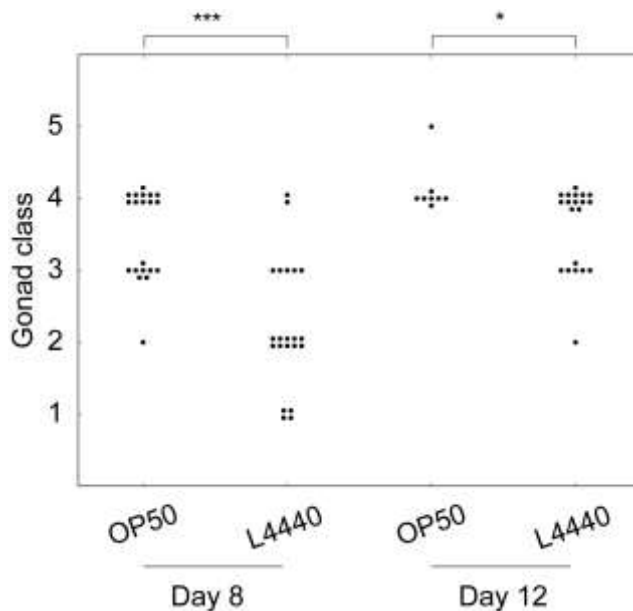
Figure 5.15 Worms on control(RNAi) have reduced gonad degeneration. Diagram comparing gonad degeneration in wildtype worms cultured on standard agar plates seeded with OP50 versus IPTG plates seeded with L4440 control(RNAi). Statistics were obtained bt performing the Wilcoxon-Mann Whitney test, ***$p<0.001$, *$p<0.05$.

Different *E. coli* strains can modulate *C. elegans* lifespan in a process that involves sensory perception of food (Maier et al., 2010). Worms maintained on HT115 or HB101 show a 15% and 19% increase in lifespan, respectively, compared to those on OP50 (Maier *et al*., 2010). We were curious to test if HT115, HB101 and OP50 have different effects on gonad degeneration. In addition, we tested the effect of a non-*E. coli* bacteria, *Bacillus subtilis.* Culture of worms on *B. subtilis,* which is commonly found in

soil and thought to be a food source of *C. elegans* in its natural environment, extends lifespan by up to 100% compared to OP50 (Garsin *et al.*, 2003). The lifespan increase caused by *B. subtilis* implies that it may be less pathogenic to *C. elegans* than *E. coli.*
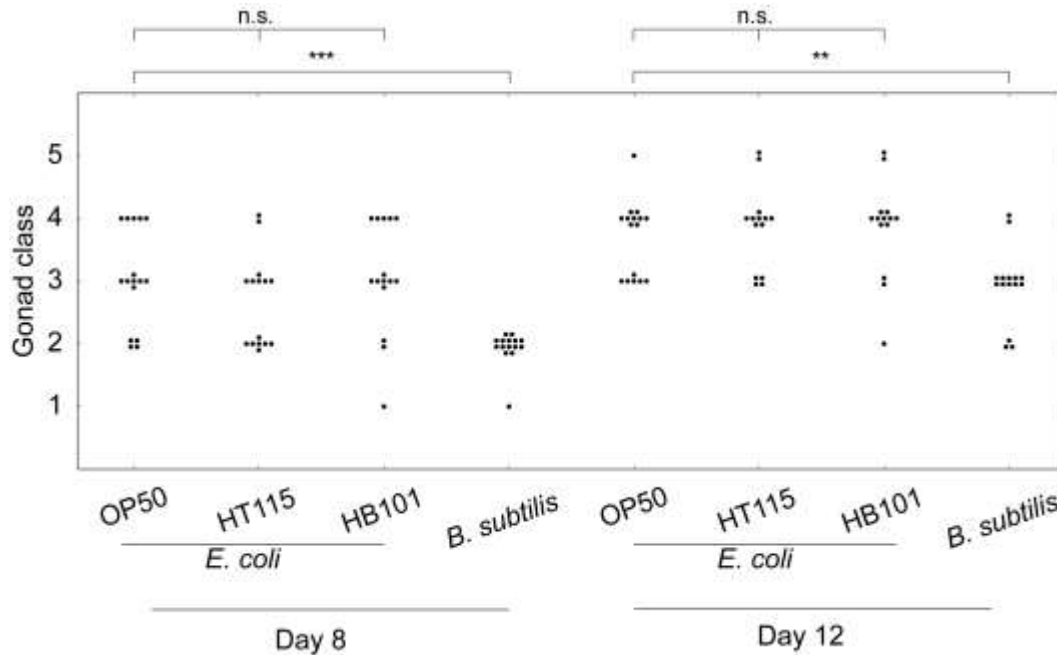
Figure 5.16 Bacterial food source has an effect on gonad degeneration. Diagram comparing gonad degeneration in wildtype worms cultured on standard agar plates seeded with *E. coli* (OP50, HT115 and HB101) and *B. subtilis* (no antibiotics). No differences in gonad disintegration were observed among *E. coli* strains. However, culture on *B. subtilis* had a protective effect on gonad ageing compared to OP50 control on day 8 and 12. Statistics were obtained by performing the Wilcoxon-Mann Whitney test, n.s.=not significant, *** $p<0.001$, **$p<0.01$.

We cultured wildtype worms on standard NGM plates seeded with OP50, HT115, HB101 or *B. subtilis* and found no differences in gonad degeneration between *E. coli* strains (Figure 5.16). This suggests that the differences previously observed between OP50 and HT115/L4440 was due to the presence of antibiotics in the latter. However, we did observe a strong protective effect of *B. subtilis* on day 8 and 12, consistent with the l increase in worm lifespan observed on this strain. These results are consistent with the view that *E. coli* is more pathogenic that *B. subtilis* (Garsin et al., 2003; Sánchez-Blanco and Kim, 2011), and suggests that it could be triggering SIA by pathogen-induced apoptosis.

5.3   Discussion

5.3.1   Gonad disintegration is mainly driven by physiological germline apoptosis

Findings during the course of these studies on hermaphrodite gonad disintegration strongly support the hypothesis that quasi-programmed germline apoptosis is a contributor of gonad ageing in *C. elegans*. All known mechanisms for both somatic and germline apoptosis require genes CED-3 and CED-4. We examined *ced-3(n717), ced-3(n1286), ced-3(n2454), ced-3(n288)* mutants and found that all the alleles examined successfully blocked germline apoptosis, which is consistent with previous results (Gumienny *et al*., 1999). We also looked at gonad disintegration in four *ced-3* alleles and in *ced-4(n1162)* and found that blocking germline apoptosis markedly slows gonad disintegration in all cases. However, all *ced-3* and *ced-4* mutants examined still showed a gradual loss of gonad integrity occurring between day 1 and 12 but at a slower rate than wildtype. This implies that while apoptosis is a contributor to gonad ageing other unknown factors also play a role. To exclude the possibility that somatic apoptosis influences gonad disintegration we tested *ced-9(n1950gf)*, which blocks apoptosis in the soma but not physiological germline apoptosis (Gumienny et al., 1999; Hengartner et al., 1992) and found that their gonads disintegrate at a similar rate as wildtype. This result further suggests that germline apoptosis plays a role in gonad degeneration. If blocking apoptosis can slow gonad disintegration down, the opposite should also be true and increasing apoptosis in the gonad should accelerate gonad ageing. This turned out to be true. We examined *gld-1(op236)* which increase germ cell death via CEP-1 activation (Schumacher et al., 2005b) and found that gonad disintegration occurs at a faster rate in these worms.

A plausible scenario is that DNA-damage induced germ cell death is essential to patrol the germline to rid the worm of damaged gametes to prevent passing on genetic defects to subsequent generations. The presence of a separate mechanism that activates the apoptotic machinery via CEP-1 could suggest another candidate for a quasi-programme. In our studies we found that inhibition of CEP-1 by RNAi had no distinguishable effect on germline apoptotic levels which is consistent with previous results (Pinkston-Gosse and Kenyon, 2007; Pinkston et al., 2006; Schumacher et al., 2001). We also examined gonad disintegration using *cep-1(gk138)* and *cep-1*(RNAi) and

151

found little difference in gonad disintegration compared to wildtype. These results imply that DNA damage induced apoptosis is not a likely candidate for the main cause of gonad degeneration. Because it acts in response to genotoxic stress and is not seen under normal conditions it is not likely to become a quasi-programme. That *spo-11(ok79)* does not suppress gonad disintegration supports this interpretation.

We also examined the effect of oxidative stress on gonad degeneration to determine if it has some contribution to this age-related pathology. We used two treatments that have been shown to increase protein oxidation without affecting lifespan: *sod-2(gk257)* and 9mM iron supplementation (Van Raamsdonk and Hekimi *et al*., 2009; Valentini *et al*., 2012). We found that neither intervention affected gonad disintegration. This implies that if in fact gonad disintegration is driven by germline apoptosis it is not via environmental stress-induced germline apoptosis. Furthermore, environmental stressors (oxidative, thermal, and osmotic) require ABL-1 to promote germline apoptosis (Salinas *et al*., 2006). We subjected worms to *abl-1(ok171)* and found that gonad disintegration was not slowed down in these worms, as would be expected if environmental stress induced apoptosis was a significant contributor to gonad ageing. Additionally we also disabled DNA damage induced germline apoptosis by feeding *cep-1*(RNAi) to *abl-1(ok171)* mutants and found they had wildtype pattern of gonad disintegration. Thus gonad disintegration occurs despite blocking two apoptotic stress response mechanisms to DNA damage and environmental stressors. Under these circumstances germline apoptosis was slightly reduced, yet the apoptotic corpses observed must have been generated by physiological apoptosis.

It is unclear how starvation induces germ cell apoptosis. However, under all conditions we examined worms were maintained well-fed. Additionally, they were transferred daily throughout the reproductive period so it is highly unlikely that gonad disintegration would be the direct result of starvation-induced apoptosis. Gonad disintegration is also not likely to be caused by pathogen induced apoptosis because this pathway requires EGl-1, which is not necessary for germline apoptosis (Gumienny *et al*., 1999). However, it would be interesting to see if infection could affect gonad disintegration. The higher levels of GD seen on *E. coli* than *B. subtilis* suggest that it might.

5.3.1.1 Other possible mechanisms for gonad disintegration

Mutations that reduce IIS can delay the advent of gonad disintegration in *C. elegans* (Garigan *et al*., 2002). Previous studies have found *daf-2(e1370)* mutants to have higher (Pinkston *et al*., 2006) or slightly lower (Perrin *et al*., 2013) levels of germline apoptosis. In this study we measured germline apoptosis levels in *daf-2(e1370)* and *daf-2(m577)* and found that *daf-2(e1370)* had lower germline apoptosis while *daf-2(m577)* had wildtype levels. Thus protection against GD in *daf-2* mutants is not necessarily accompanied by reduced germline apoptosis. This suggests that the reduced apoptosis in *daf-2(e1370)* worms does not cause their reduced GD rate, and may be due to its pleiotropic effects. That both *daf-2(-)* alleles successfully slow down gonad ageing implies the presence of a mechanism other than apoptosis that slows gonad ageing in *daf-2(-)* mutants. In support of this *ced-3* and *ced-4* mutations, which also delay gonad ageing, still exhibit an increased loss of gonad integrity with age. Overall, these results imply that germ cell death is a contributor of gonad disintegration but that one or more other mechanisms also play a role.

Alternatively, it may be that counting germ cells in the gonad only allows us to view part of the puzzle. It could be that it is actually the balance between rate of germ cell removal by apoptosis and germ cell production in the distal gonad, that determines how fast the gonad will disintegrate. It is possible that *daf-2(-)* mutants maintain a youthful gonad by having germ cells in a higher proliferative state in later life. In support of this one study used DAPI to count proliferating germline stem cells (GSC) and found that while GSCs are lost as worms age, the percentage decrease is much lower in *daf-2* compared to wildtype worms indicating that proliferative germ cell capabilities may be conserved in ageing IIS mutants (Luo et al., 2010). Thus, despite having germ cell apoptosis levels similar to wildtype there might be a greater supply of new germ cells moving towards the gonad loop, which sustains the gonad and reduces the rate of cell loss. One possibility would be to study this further by measuring the mitotic index (i.e. the rate of cell division), e.g. by using EdU labelling, where thymidine analogue ethynyl deoxyuridine (EdU) is incorporated into dividing cells allowing the mitotic index to be measured (Chehrehasa et al., 2009; Michaelson et al., 2010). It would be of great interest to see how germ cell proliferation correlates with apoptosis in *daf-2(m577)* mutants and

see how it compares to wildtype worms. However, a previous study found EdU-labelled germ cell nuclei to be significantly reduced in of *daf-2(e1370)* mutants during L4 stage (Michaelson *et al*., 2010). It would be useful to measure the mitotic index in ageing adult worms to see if this same trend is the same in older worms.

We also examined the TOR pathway mutant *rsks-1(ok1255)* and found that despite lower levels of apoptosis observed on day 1 compared to wildtype, gonad disintegration was not delayed. One possibility is that the reduced germ cell death observed on day 1 of adulthood is due to a slight delay in development in *rsks-1(ok1255)* mutants relative to wildtype worms (Selman *et al*., 2009). It would be useful to examine day 2 adults to see if germline apoptosis is similar to wildtype. An additional possibility is that *rsks-1(ok1255)* has fewer germ cells so that lower levels of apoptosis observed in this mutant actually reflect a balance between germ cell removal and proliferation similar to wildtype. One study used DAPI staining to count proliferating germline stem cells and found a reduction of 50% in *rsks-1(sv31)* and *rsks-1(ok1255)* during L4 and early adulthood (Korta et al., 2012). EdU-labelling of *rsks-1(sv31)* mutants during L4 also found reduced mitotic index compared to wildtype (Korta *et al*., 2012). Thus reduced germline proliferation in *rsks-1(ok1255)* is balanced by having reduced germline apoptosis, which could explain the gonad disintegration rate being similar to wildtype. However, germline proliferation should be measured in older *rsks-1(ok1255)* worms to rule out the possibility that during ageing proliferative ability is maintained for longer. It is also important to note that lifespan increase in *rsks-1(ok1255)* mutants is modest, about 10% (Kapahi et al., 2010; Pan et al., 2007) whereas the increase in *daf-2(-)* is much more robust (e.g. 150%) (Kenyon et al., 1993).

5.3.2 Quasi-programmed physiological apoptosis causes gonad degeneration

Taken together our results imply that under normal conditions gonad disintegration is caused, at least in part, by continuation of physiological apoptosis, but not stress-induced apoptosis. This is consistent with the hyperfunction theory, which postulates that ageing is caused by run-on of developmental and reproductive programmes in later life, becoming quasi-programmes that cause ageing. Thus, physiological germ cell death is a reproductive program in hermaphrodite worms to improve oocyte quality that becomes a quasi-programme that causes gonad disintegration.

We previously found that apoptotic corpses persist in later life in post-reproductive worms. Our results in this chapter would suggest that physiological germline apoptosis is a contributor of gonad deterioration. In contrast stress-induced apoptosis occurs in response to a condition that is interpreted as noxious to the organism (pathogens, environmental stressors) or future generations (genotoxic stress) and as such in the absence of the trigger posses no threat of becoming a quasi-programme to promote gonad ageing.

Chapter 6:   Concluding remarks

"It is a capital mistake to theorize before one has data. Insensibly one begins to twist facts to suit theories, instead of theories to suit facts" – Sir Arthur Conan Doyle

The discovery of single gene mutations resulting in large extensions of lifespan in model organisms has greatly increased interest in the biology of ageing. What has been considered an unavoidable natural process akin to the wear and tear observed in complex inanimate objects (e.g. accumulation of rust in an old car), is thought to be controlled by genetic pathways. However, despite advances in finding genes that affect ageing rate the nature of the ageing process that such genes influence remains a mystery.

Mikhail Blagosklonny conceived the hyperfunction theory by incorporating findings produced in the last decades from model organisms and reflecting on human age-related pathology with which he was familiar given his medical background. The TOR pathway promotes growth by increasing protein translation, while decreasing autophagy. Mutations that reduce the activity of the TOR pathway or the linked IIS pathway, increase lifespan in model organisms (Kapahi et al., 2010; Kenyon, 2010). TOR over-activity is also associated with mammalian diseases of ageing such as arteriosclerosis, cardiac hypertrophy and type II diabetes (Blagosklonny, 2008). Thus, he proposes that activity of these growth-promoting pathways generate age-related pathology and death. By combining this information he was able to discern a bigger picture, and create a cohesive, plausible theory to explain many aspects of the biology of ageing. The theory encompasses evolutionary concepts arguing that developmental and reproductive programmes under strong selection to bestow early life fitness are, due to waning selective pressure, not switched-off or fine-tuned post-reproduction and become quasi-programmes in older animals that generate pathology and death (Blagosklonny, 2006, 2008). Our main goal for the experimental work described in this thesis was to use *C. elegans* to test this novel theory and establish its validity in explaining pathologies observed in ageing *C. elegans*. We examined age-related changes in the reproductive system and sought explanations for their origins.

In chapter 3 we examined yolk protein accumulation which had previously been shown to be present in high quantities in the body cavities of post-reproductive adult hermaphrodites (Herndon *et al*., 2002). We confirmed that the three *C. elegans* yolk proteins YP170, YP115 and YP88 increased progressively in hermaphrodite worms from day 1 to 8 and were maintained at high levels on day 12. This accumulation was not observed in long-lived *daf-2(-)* mutants. We examined other longevity mutants and found that this characteristic is only present in IIS pathway mutants. Moreover, our *vit-5/vit-6* RNAi results imply that high yolk levels do not affect mortality. Yolk protein accumulation represent a simple quasi-programme: yolk production has no known function aside from provisioning oocytes, and its accumulation post-reproduction implies the absence of an evolved mechanism to turn off its synthesis.

In chapters 4 and 5 we studied changes that occur in the hermaphrodite gonad and found examples of atrophy (gonad deterioration) and hypertrophy (uterine tumours), which are consistent with quasi-programmed ageing. A striking age-related pathology in *C. elegans* is the disintegration of the hermaphrodite reproductive organ – the gonad (Garigan *et al*., 2002). This provides an interesting example as old age in mammals is often accompanied by atrophy affecting multiple organs. This phenomenon has previously been described but a mechanism of action, to our knowledge, has not been proposed. In our studies we found a positive correlation between germline apoptosis and gonad disintegration. If apoptosis in the germline is increased the gonad fragments earlier and if apoptosis is blocked by *ced-3* or *ced-4* mutations gonad disintegration is slowed down. Furthermore, we could find no evidence of a role of DNA damage or oxidative damage on gonad ageing.

The results in this thesis support the hyperfunction theory as a plausible explanation for the emergence of pathologies of the reproductive system in *C. elegans*. However, the age-related phenomena examined in this study did not increase mortality. This could imply that other ageing pathologies kill the worm before gonad disintegration or yolk accumulation can exert its harmful effect. A possibility is that pathologies that do increase mortality are also caused by quasi-programmes.

The addition of hyperfunction as an alternative to the damage/maintenance paradigm provides a new perspective to examine the processes that cause organisms to

age (Gems and Partridge, 2013). Mutations in IIS and TOR which extend lifespan, while increasing stress response and slowing development and reducing fertility, were thought to do so by reducing damage (Partridge and Gems, 2002). However, in light of the hyperfunction theories a future course of action would be to look at its effects on growth and development and the quasi-programmes that run on from these processes. Further examination of possible hyperfunction-driven pathologies in *C. elegans* and other model organisms are crucial to establish the validity of hyperfunction as an ageing theory.

Appendix 1
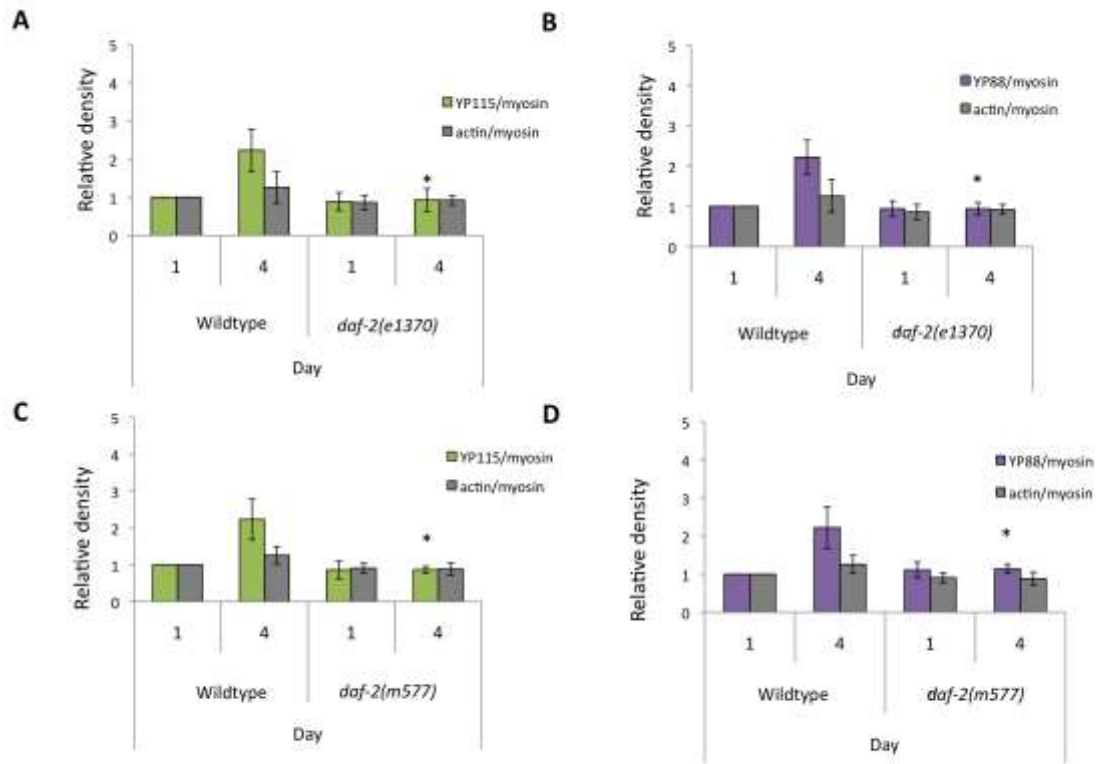
Figure A-1. 1 Levels of YP115 and YP88 in *daf-2(-)* worms. Analysis of YP abundance revealed that *daf-2(e1370)* worms are Yol-d on day 4 for (A) YP115 and (B) YP88. *daf-2(m577)* worms are Yol-d on day 4 for (C) YP115 and (D) YP88. Data is the mean of three biological replicates (100 worms per replicate); standard error, SEM; Student's t-test *p<0.05 (versus age-matched control).

Figure A-1. 2 Levels of YP115 and YP88 in *age-1* mutants. Analysis of YP abundance revealed that *age-1(hx546)* worms have wildtype levels of (A) YP115 and (B) YP88. *age-1(mg109)* worms did not follow a similar trend as observed in YP170, there was no reduction in (C) YP115 and (D) YP88 on day 4. Data is the mean of three biological replicates (100 worms per replicate); standard error, SEM; Student's t-test *** p<0.001 (versus age-matched control).

Figure A-1. 3 Levels of YP115 and YP88 in *daf-16(mgDf50); daf-2(m577)* worms. Analysis of YP abundance revealed that *daf-16(mgDf50); daf-2(m577)* have wildtype levels of (A) YP115 and (B) YP88. This trend is similar to the results of YP170. Data is the mean of three biological replicates (100 worms per replicate); standard error, SEM; Student's t-test *p<0.05 (versus age-matched control).
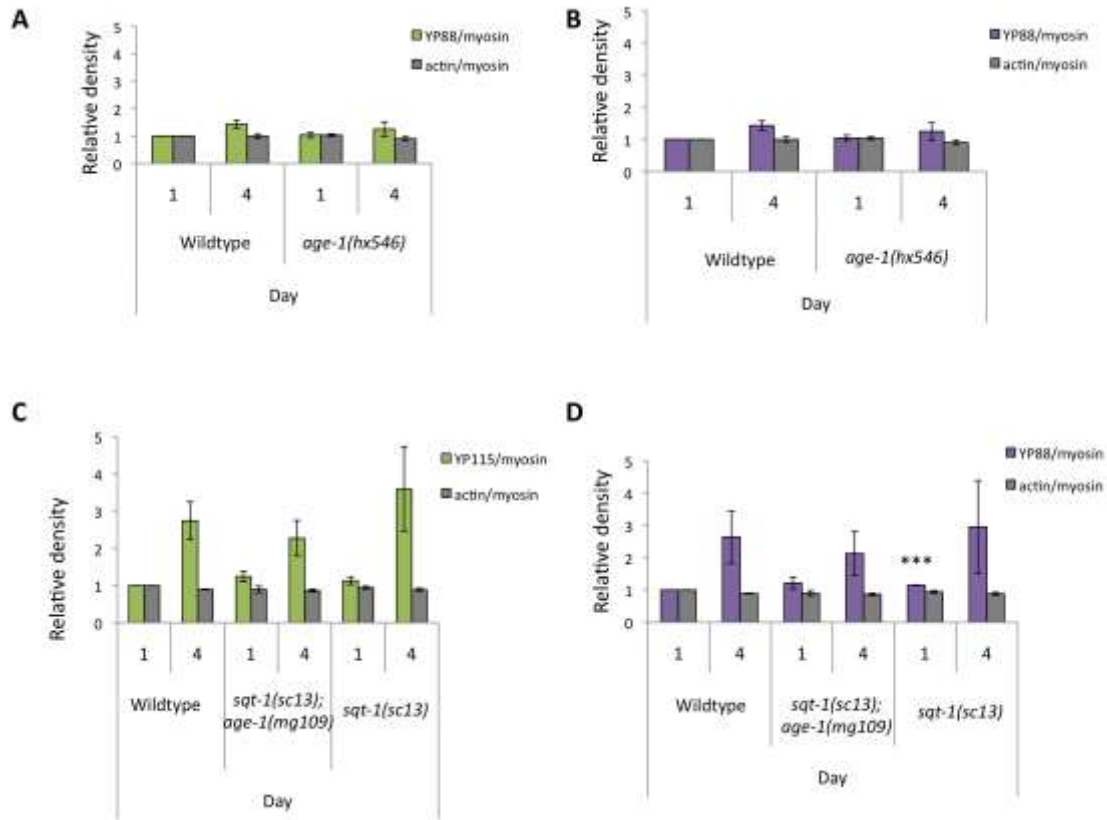

Figure A-1. 4 Levels of YP115 and YP88 in *daf-16(mu88); daf-2(e1370)* in which DAF-16 is driven by its own promoter. Analysis of YP abundance revealed that DAF-16 is driven by its own promoter results in Yol-d on day 4 for (A) YP115 and (B) YP88. Data is the mean of three biological replicates (100 worms per replicate); standard error, SEM; Student's t-test *p<0.05, ***p<0.001 (versus age-matched control).
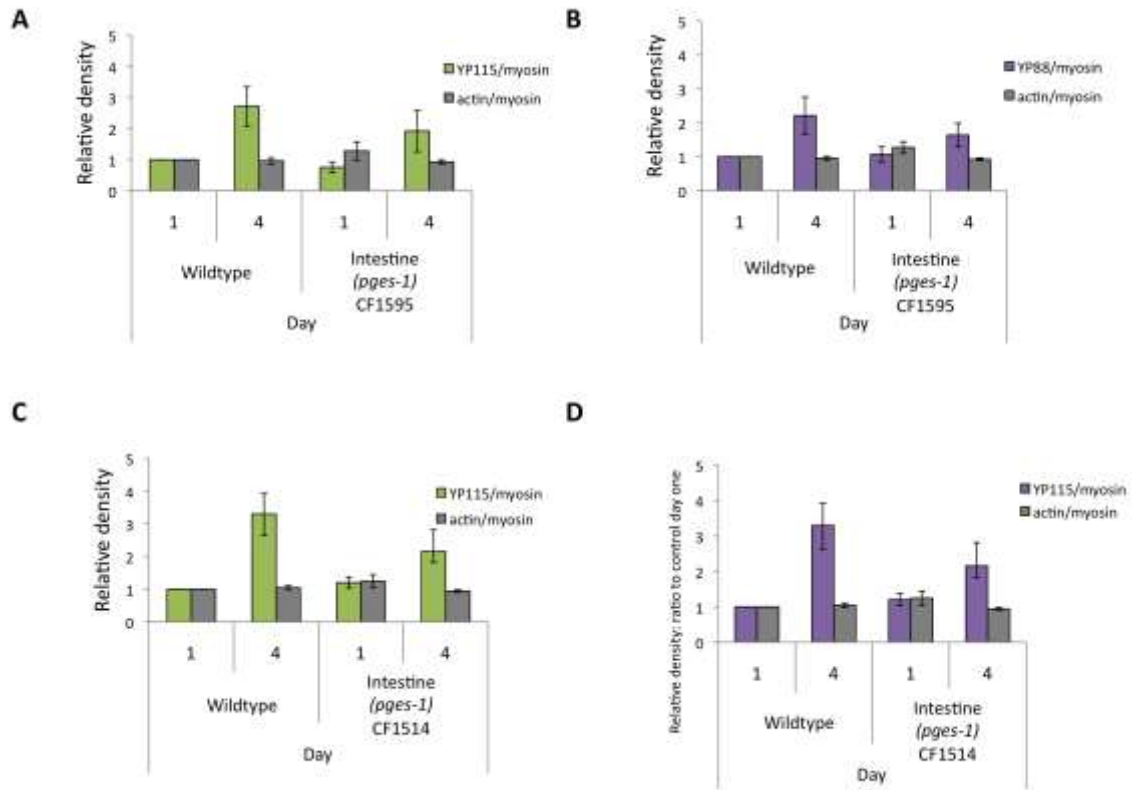
Figure A-1. 5 Levels of YP115 and YP88 in *daf-16(mu88); daf-2(e1370)* in which DAF-16 is expressed in the intestine. Analysis of YP abundance revealed that intestinal expression of DAF-16 in *daf-16(mgDf50); daf-2(m577)* does not reduce YP to statistically significant levels in (A,C) YP115 and (B,D) YP88. Data is the mean of three biological replicates (100 worms per replicate); standard error, SEM; Student's t-test (versus age-matched control).

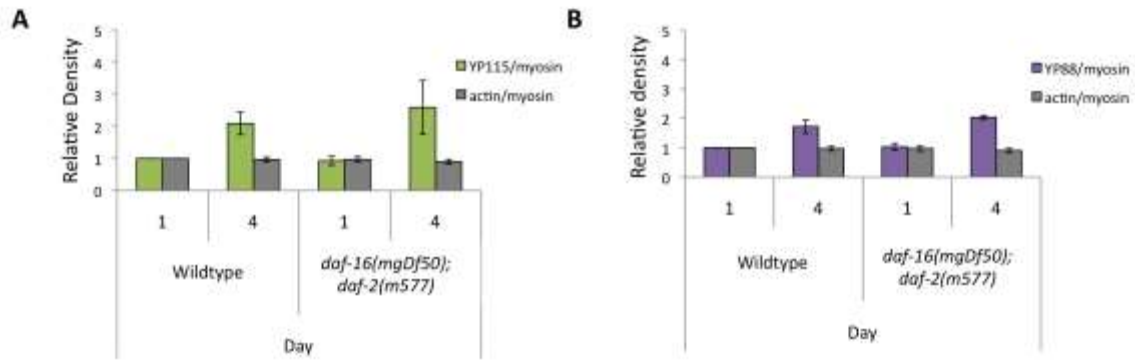**Figure A-1. 6 Levels of YP115 and YP88 in *daf-16(mu88); daf-2(e1370)* with DAF-16 expression in the muscle and neurons.** Analysis of YP abundance revealed that intestinal expression of DAF-16 in the muscle and neurons in *daf-16(mgDf50); daf-2(m577)* does not rescue *daf-2(-)* Yol-d for (A,C) YP115 and (B,D) YP88. Data is the mean of three biological replicates (100 worms per replicate); standard error, SEM; Student's t-test *p<0.05 (versus age-matched control).
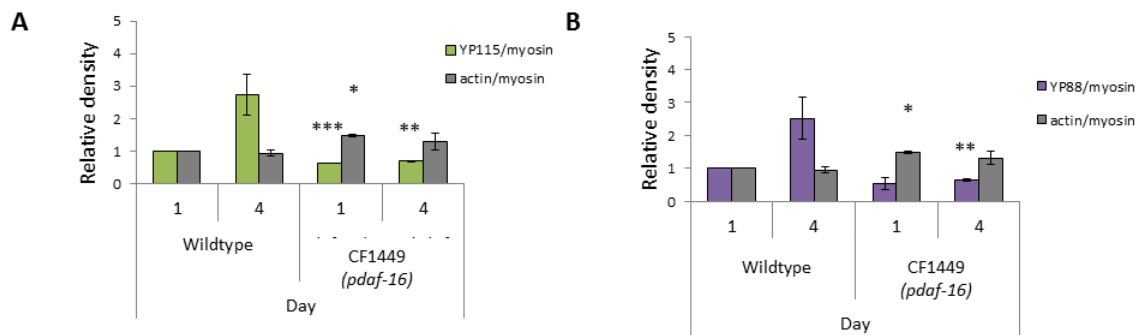
Figure A-1. 7 Levels of YP115 and YP88 in worms treated with 10μM FUdR.
Analysis of YP abundance revealed that worms transferred to plates with 10μM applied topically at L4 have wildtype levels of for (A) YP115 and (B) YP88. Data is the mean of three biological replicates (100 worms per replicate); standard error, SEM; Student's t-test (versus age-matched control).
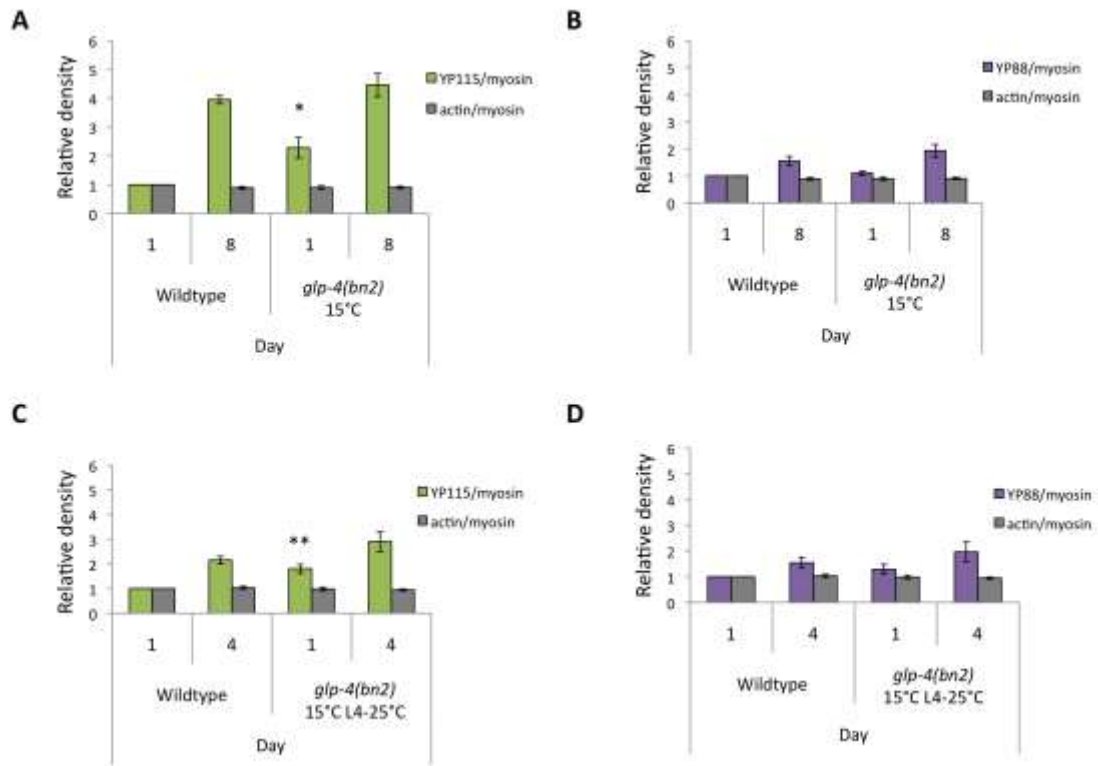
Figure A-1. 8 Levels of YP115 and YP88 in *glp-4(bn2)* maintained at 15˚C or shifted to 25˚C at L4. Analysis of YP abundance revealed that both fertile *glp-4(bn2)* maintained at 15˚C and worms shifted to 25˚C at L4 are Yol-o on day 1 for (A,C) YP115 but have wildtype YP levels for (B,C) YP88. Data is the mean of three biological replicates (100 worms per replicate); standard error, SEM; Student's t-test *p<0.05 (versus age-matched control).
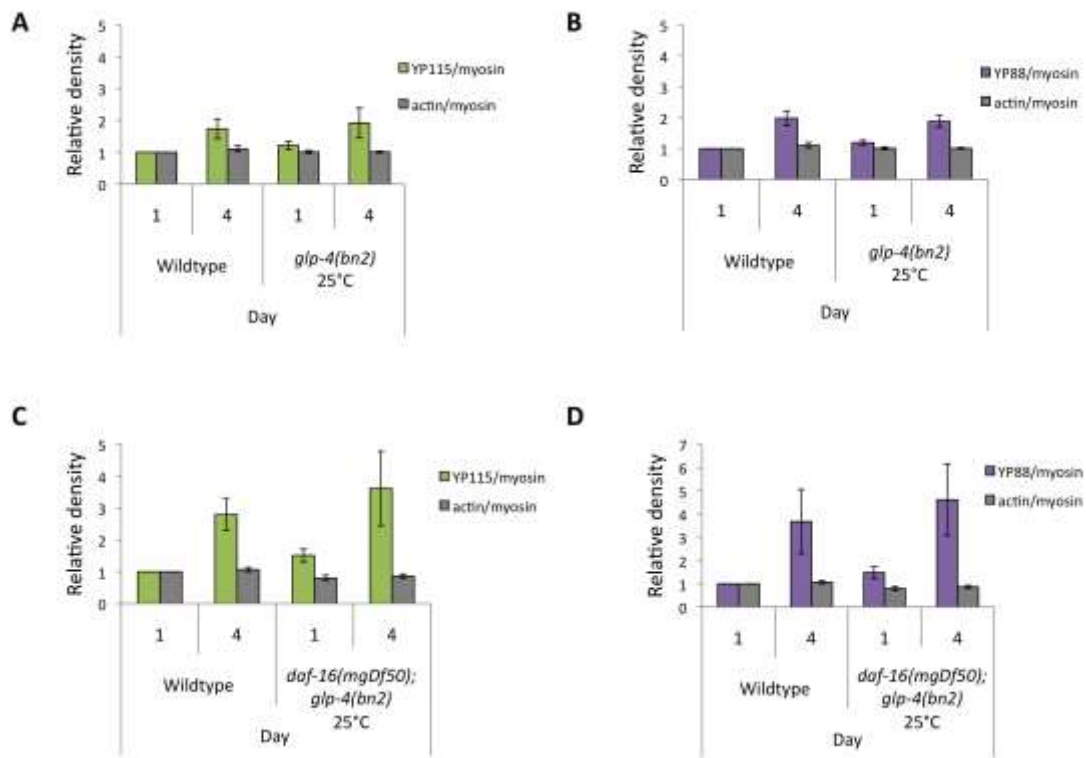
Figure A-1. 9 Effect of DAF-16 on levels of YP115 and YP88 in *glp-4(bn2)* hatched at 25˚C. Analysis of YP abundance revealed that germline-less *glp-4(bn2)* and d*af-16(mgDf50); glp-4(bn2)* maintained at 25˚C from hatching have wildtype YP levels for (A,C) YP115 and (B,D) YP88. Data is the mean of three biological replicates (100 worms per replicate); standard error, SEM; Student's t-test (versus age-matched control).
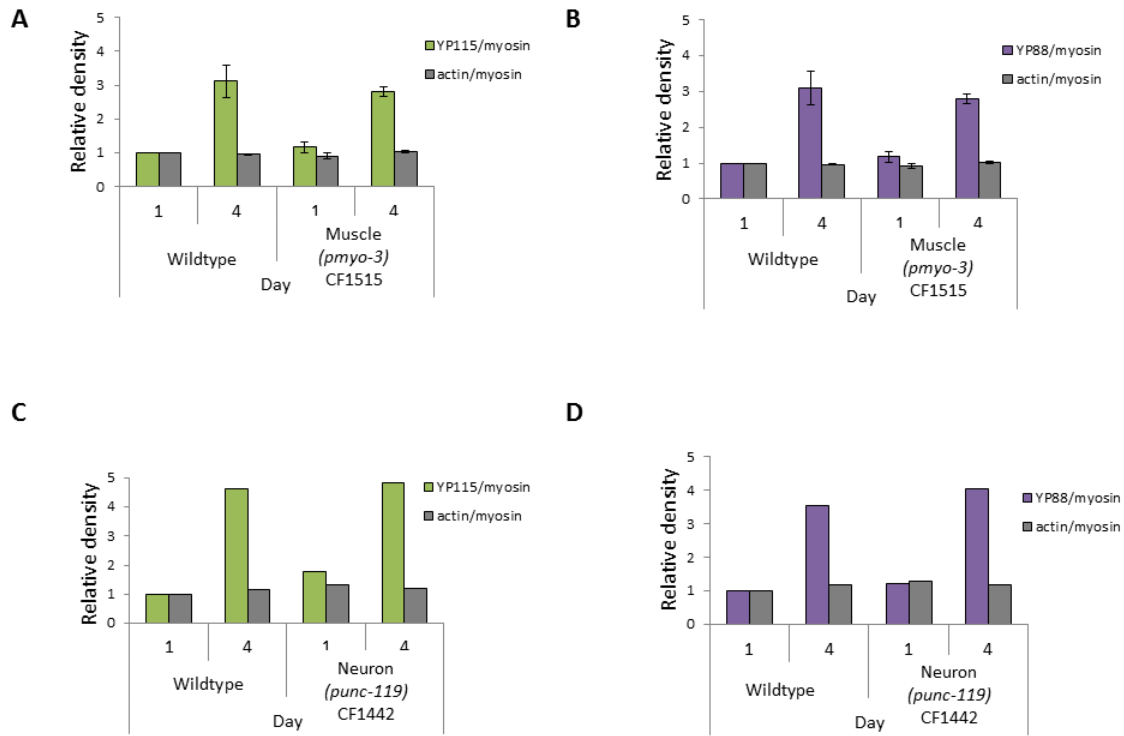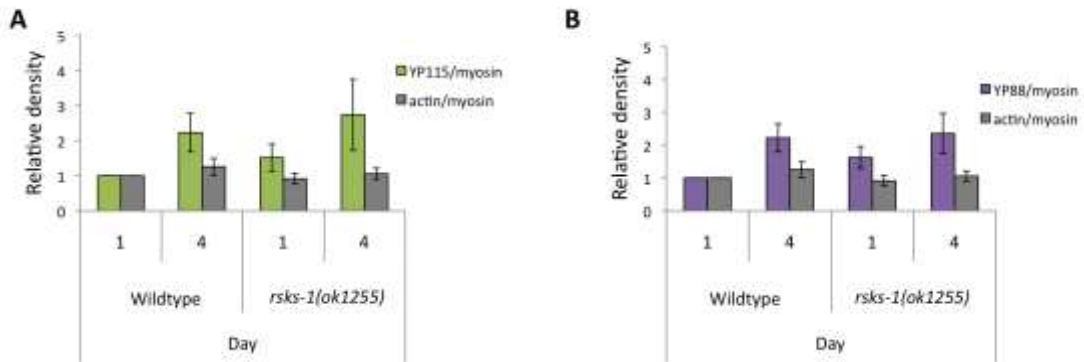
Figure A-1. 10 Levels of YP115 and YP88 in *rsks-1(ok1255)* worms. Analysis of YP abundance revealed that *rsks-1(ok1255)* have wildtype YP levels for (A) YP115 and (B) YP88. Data is the mean of three biological replicates (100 worms per replicate); standard error, SEM; Student's t-test (versus age-matched control).
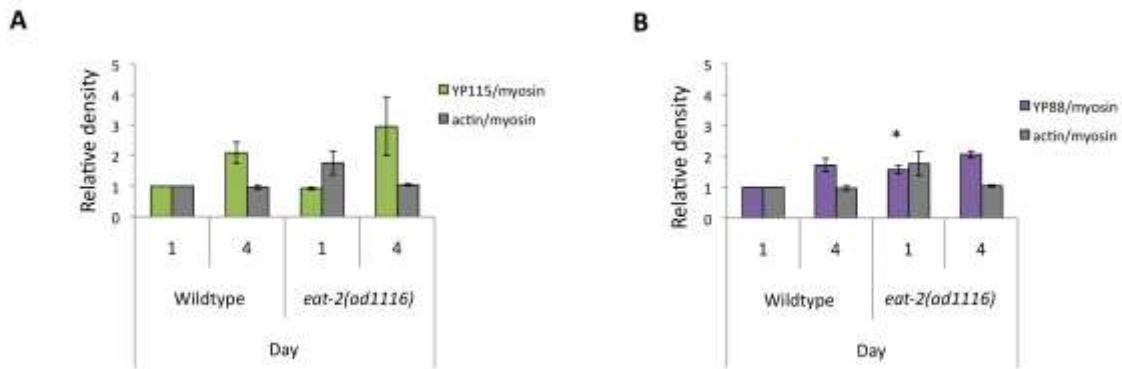
Figure A-1. 11 Levels of YP115 and YP88 in *eat-2(ad1116)* worms. Analysis of YP abundance revealed that *rsks-1(ok1255)* have wildtype YP levels for (A) YP115. *eat-2(ad1116)* worms were Yol-d on day 1 for (B) YP88. Data is the mean of three biological replicates (100 worms per replicate); standard error, SEM; Student's t-test *p<0.05 (versus age-matched control).
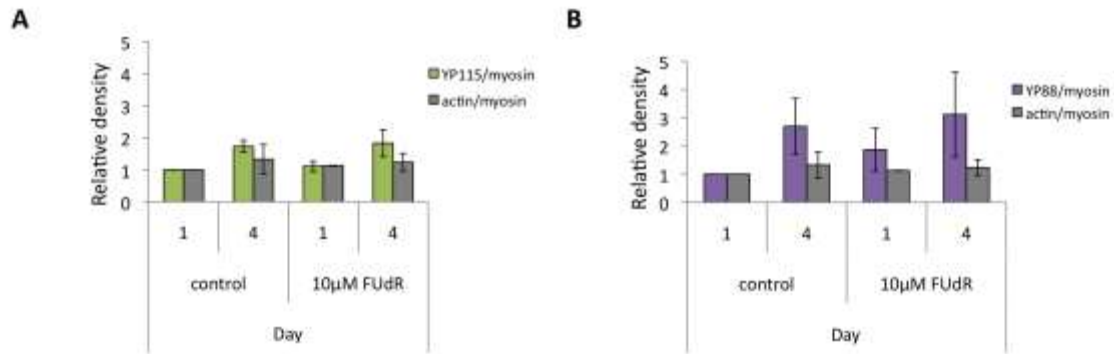
Figure A-1. 12 Levels of YP115 and YP88 in *nuo-6(qm200)* and *isp-1(qm150)* worms. Analysis of YP abundance revealed that *nuo-6(qm200)* and *isp-1(qm150)* have wildtype YP levels for (A) YP115 and (B) YP88. Data is the mean of three biological replicates (100 worms per replicate); standard error, SEM; Student's t-test (versus age-matched control).

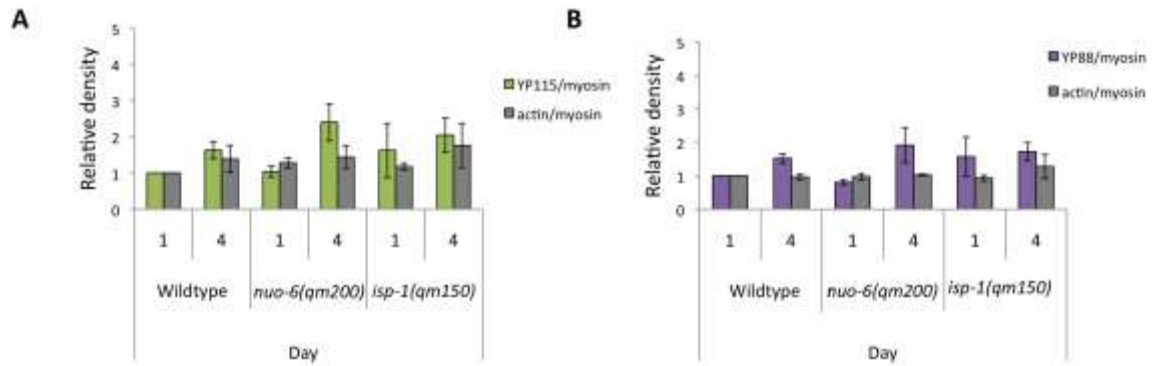# Appendix 2: Gems and de la Guardia, 2013

Bibliography

Aballay, A., and Ausubel, F.M. (2001). Programmed cell death mediated by *ced-3* and *ced-4* protects *Caenorhabditis elegans* from *Salmonella typhimurium*-mediated killing. Proc. Natl. Acad. Sci. U. S. A. *98*, 2735–2739.

Aballay, A., Yorgey, P., and Ausubel, F.M. (2000). *Salmonella typhimurium* proliferates and establishes a persistent infection in the intestine of *Caenorhabditis elegans*. Curr. Biol. *10*, 1539–1542.

Aballay, A., Drenkard, E., Hilbun, L.R., and Ausubel, F.M. (2003). *Caenorhabditis elegans* innate immune response triggered *by Salmonella enterica* requires intact LPS and is mediated by a MAPK signaling pathway. Curr. Biol. *13*, 47–52.

Ackerman, D., and Gems, D. (2012). The mystery of *C. elegans* aging: an emerging role for fat. Bioessays *34*, 466–471.

Adachi, H., Fujiwara, Y., and Ishii, N. (1998). Effects of oxygen on protein carbonyl and aging in *Caenorhabditis elegans* mutants with long (*age-1*) and short (*mev-1*) life spans. Journals Gerontol. Biol. Sci. Med. Sci. *53A*, 240–244.

Ahringer, J. (2006). Reverse genetics. WormBook 1–43.

Altun, Z.F., and Hall, D.H. (2009). Handbook of *C. elegans* anatomy. WormAtlas.

Andux, S., and Ellis, R.E. (2008). Apoptosis maintains oocyte quality in aging *Caenorhabditis elegans* females. PLoS Genet. *4*, e1000295.

Angelo, G., and Van Gilst, M.R. (2009). Starvation protects germline stem cells and extends reproductive longevity in *C. elegans*. Science. *326*, 954–958.

Antebi, A., Culotti, J.G., and Hedgecock, E.M. (1998). *daf-12* regulates developmental age and the dauer alternative in *Caenorhabditis elegans*. Development *125*, 1191–1205.

Apfeld, J., O'Connor, G., McDonagh, T., DiStefano, P.S., and Curtis, R. (2004). The AMP-activated protein kinase AAK-2 links energy levels and insulin-like signals to lifespan in *C. elegans*. Genes Dev. *18*, 3004–3009.

Arantes-Oliveira, N., Apfeld, J., Dillin, A., and Kenyon, C. (2002). Regulation of life-span by germ-line stem cells in *Caenorhabditis elegans*. Science. *295*, 502–505.

Ayyadevara, S., Alla, R., Thaden, J.J., and Shmookler Reis, R.J. (2008). Remarkable longevity and stress resistance of nematode PI3K-null mutants. Aging Cell *7*, 13–22.

Azorsa, D.O., Mousses, S., and Caplen, N.J. (2006). Gene silencing through RNA interference: potential for therapeutics and functional genomics. In Peptide Nucleic Acids, Morpholinos, and Related Antisense Biomolecules, C. Janson, and M. During, eds. (New York, NY: Springer New York), pp. 252–264.

Baker, M.E. (1988a). Is vitellogenin an ancestor of apolipoprotein B-100 of human low-density lipoprotein and human lipoprotein lipase? Biochem. J. *255*, 1057–1060.

Baker, M.E. (1988b). Invertebrate vitellogenin is homologous to human von Willebrand factor. Biochem. J. *256*, 1059–1061.

Beanan, M.J., and Strome, S. (1992). Characterization of a germ-line proliferation mutation in *C. elegans*. Development *116*, 755–766.

Beckman, K.B., and Ames, B.N. (1998). The free radical theory of aging matures. Physiol. Rev. *78*, 547–581.

Bishop, N. a, and Guarente, L. (2007). Genetic links between diet and lifespan: shared mechanisms from yeast to humans. Nat. Rev. Genet. *8*, 835–844.

Blagosklonny, M. V (2006). Aging and immortality: quasi-programmed senescence and its pharmacologic inhibition. Cell Cycle *5*, 2087–2102.

Blagosklonny, M. V (2007). Paradoxes of aging. Cell Cycle *6*, 2997–3003.

Blagosklonny, M. V (2008). ROS or TOR. Cell Cycle *7*, 3344–3354.

Bownes, M., Dempster, M., and Blair, M. (1983). The regulation of yolk protein gene expression in *Drosophila melanogaster*. Ciba Found. Symp. *98*, 63–79.

Brandt, B.W., Zwaan, B.J., Beekman, M., Westendorp, R.G.J., and Slagboom, P.E. (2005). Shuttling between species for pathways of lifespan regulation: a central role for the vitellogenin gene family? BioEssays *27*, 339–346.

Brenner, S. (1974a). The genetics of *Caenorhabditis elegans*. Genetics *77*, 71–94.

Brenner, S. (1974b). *Caenorhabditis elegans*. Methods 71–94.

Butler, J.A., Ventura, N., Johnson, T.E., and Rea, S.L. (2010). Long-lived mitochondrial (Mit) mutants of *Caenorhabditis elegans* utilize a novel metabolism. FASEB J. *24*, 4977–4988.

Byerly, L., Cassada, R.C., and Russell, R.L. (1976). The life cycle of the nematode *Caenorhabditis elegans.* Dev. Biol. *51*, 23–33.

Byrne, B.M., Gruber, M., and Ab, G. (1989). The evolution of egg yolk proteins. Prog. Biophys. Mol. Biol. *53*, 33–69.

Carter, C.S., Ramsey, M.M., and Sonntag, W.E. (2002). A critical analysis of the role of growth hormone and IGF-1 in aging and lifespan. Trends Genet. *18*, 295–301.

Cassada, R.C., and Russell, R.L. (1975). The Dauerlarva, a post-embryonic developmental variant of the nematode *Caenorhabditis elegans*. Dev. Biol. *46*, 326–342.

Chehrehasa, F., Meedeniya, A.C.B., Dwyer, P., Abrahamsen, G., and Mackay-Sim, A. (2009). EdU, a new thymidine analogue for labelling proliferating cells in the nervous system. J. Neurosci. Methods *177*, 122–130.

Chen, F., Hersh, B.M., Conradt, B., Zhou, Z., Riemer, D., Horvitz, R.H., and Gruenbaum, Y. (2000). Translocation of *C. elegans* CED-4 to nuclear membranes during programmed cell death. Science (80-.). *287*, 1485–1489.

Conradt, B., and Horvitz, H.R. (1998). The *C. elegans* protein EGL-1 is required for programmed cell death and interacts with the Bcl-2-like protein CED-9. Cell *93*, 519–529.

Conradt, B., and Xue, D. (2005). Programmed cell death. WormBook 1–13.

Contois, J.H., Warnick, G.R., and Sniderman, A.D. (2011). Reliability of low-density lipoprotein cholesterol, non-high-density lipoprotein cholesterol, and apolipoprotein B measurement. J. Clin. Lipidol. *5*, 264–272.

Crawford, D., Libina, N., and Kenyon, C. (2007). *Caenorhabditis elegans* integrates food and reproductive signals in lifespan determination. Aging Cell *6*, 715–721.

Curran, S.P., and Ruvkun, G. (2007). Lifespan regulation by evolutionarily conserved genes essential for viability. PLoS Genet. *3*, e56.

Darwin, C.R. (1859). On the origin of species (New York, NY: Son, Collier &).

Deng, X., Hofmann, E.R., Villanueva, A., Hobert, O., Capodieci, P., Veach, D.R., Yin, X., Campodonico, L., Glekas, A., Cordon-Cardo, C., et al. (2004). *Caenorhabditis elegans* ABL-1 antagonizes p53-mediated germline apoptosis after ionizing irradiation. Nat. Genet. *36*, 906–912.

DePina, A.S., Iser, W.B., Park, S.-S., Maudsley, S., Wilson, M. a, and Wolkow, C. A (2011). Regulation of *Caenorhabditis elegans* vitellogenesis by DAF-2/IIS through separable transcriptional and posttranscriptional mechanisms. BMC Physiol. *11*.

Depuydt, G., Xie, F., Petyuk, V.A., Shanmugam, N., Smolders, A., Dhondt, I., Brewer, H.M., Camp II, D.G., Smith, R.D., and Braeckman, B.P. (2013). Reduced insulin/IGF-1 signaling and dietary restriction inhibit translation but preserve muscle mass in *Caenorhabditis elegans*. Mol. Cell. Proteomics. 12, 3624-3639.

Dernburg, A.F., McDonald, K., Moulder, G., Barstead, R., Dresser, M., and Villeneuve, a M. (1998). Meiotic recombination in *C. elegans* initiates by a conserved mechanism and is dispensable for homologous chromosome synapsis. Cell *94*, 387–398.

Derry, W.B., Putzke, A.P., and Rothman, J.H. (2001). *Caenorhabditis elegans* p53: role in apoptosis, meiosis, and stress resistance. Science (80-.). *294*, 591–595.

Doonan, R., McElwee, J.J., Matthijssens, F., Walker, G., Hothhoofdt, K., Back, P., Matscheski, A., Vanfleteren, J.R., and Gems, D. (2008). Against the oxidative damage theory of aging: superoxide dismutases protect against oxidative stress but have little or no effect on life span in *Caenorhabditis elegans*. Genes Dev. *22*, 3236–3241.

Dorman, J.B., Albinder, B., Shroyer, T., and Kenyon, C. (1995). The *age-1* and *daf-2* genes function in a common pathway to control lifespan of *Caenorhabditis elegans*. Genetics *141*, 1399–1406.

Ellis, H.M., and Horvitz, H.R. (1986). Genetic control of programmed cell death in the nematode *C. elegans*. Cell *44*, 817–829.

Evans, D.S., Kapahi, P., Hsueh, W.-C., and Kockel, L. (2011). TOR signaling never gets old: aging, longevity and TORC1 activity. Ageing Res. Rev. *10*, 225–237.

Fabian, D., and Flatt, T. (2011). The Evolution of Aging. Nat. Educ. Knowl. *2*, 1–10.

Fabian, T.J., and Johnson, T.E. (1995). Identification genes that are differentially expressed during aging in *Caenorhabditis elegans*. J. Gerontol. A. Biol. Sci. Med. Sci. *50*, B245–53.

Feng, J., Bussière, F., and Hekimi, S. (2001). Mitochondrial electron transport is a key determinant of life span in *Caenorhabditis elegans*. Dev. Cell *1*, 633–644.

Fire, A., Xu, S., Montgomery, M.K., Kostas, S.A., Driver, S.E., and Mello, C.C. (1998). Potent and specific genetic interference by double-stranded RNA in *Caenorhabditis elegans*. Nature *391*, 806–811.

Flatt, T., and Schmidt, P.S. (2009). Integrating evolutionary and molecular genetics of aging. Biochim. Biophys. Acta *1790*, 951–962.

Flatt, T., Min, K.-J., D'Alterio, C., Villa-Cuesta, E., Cumbers, J., Lehmann, R., Jones, D.L., and Tatar, M. (2008). *Drosophila* germ-line modulation of insulin signaling and lifespan. Proc. Natl. Acad. Sci. U. S. A. *105*, 6368–6373.

Friedman, D.B., and Johnson, T.E. (1988). A mutation in the age-1 gene in *Caenorhabditis elegans* lengthens life and reduces hermaphrodite fertility. Genetics *118*, 75–86.

Gami, M.S., Iser, W.B., Hanselman, K.B., and Wolkow, C.A. (2006). Activated AKT/PKB signaling in *C. elegans* uncouples temporally distinct outputs of DAF-2/insulin-like signaling. BMC Dev. Biol. *6*, 45.

Gandhi, S., Santelli, J., Mitchell, D., Stiles, J., and Sanadi, D. (1980). A simple method for maintaining large, aging populations of *Caenorhabditis elegans*. Mech. Ageing Dev. *12*, 137–150.

Garigan, D., Hsu, A.-L., Fraser, A.G., Kamath, R.S., Ahringer, J., and Kenyon, C. (2002). Genetic analysis of tissue aging in *Caenorhabditis elegans*: a role for heat-shock factor and bacterial proliferation. Genetics *161*, 1101–1112.

Garsin, D.A., Villanueva, J.M., Begun, J., Kim, D.H., Sifri, C.D., Calderwood, S.B., Ruvkun, G., and Ausubel, F.M. (2003). Long-lived *C. elegans daf-2* mutants are resistant to bacterial pathogens. Science. *300*, 1921.

Gartner, A., Milstein, S., Ahmed, S., Hodgkin, J., Hengartner, M.O., Brook, S., and York, N. (2000). A conserved checkpoint pathway mediates DNA damage – induced apoptosis and cell cycle arrest in *C . elegans*. Mol. Cell *5*, 435–443.

Gartner, A., Boag, P.R., and Blackwell, T.K. (2008). Germline survival and apoptosis. WormBook 1–20.

Gems, D., and Doonan, R. (2009). Antioxidant defense and aging in *C. elegans*: is the oxidative damage theory of aging wrong? Cell Cycle *8*, 1681–1687.

Gems, D., and de la Guardia, Y. (2013). Alternative perspectives on aging in *Caenorhabditis elegans*: reactive oxygen species or hyperfunction? Antioxid. Redox Signal. *19*, 321–329.

Gems, D., and Partridge, L. (2013). Genetics of longevity in model organisms: debates and paradigm shifts. Annu. Rev. Physiol. *75*, 621–644.

Gems, D., and Riddle, D.L. (1996). Longevity in *Caenorhabditis elegans* reduced by mating but not gamete production. Nature *379*, 735–725.

Gems, D., and Riddle, D.L. (2000). Genetic, behavioral and environmental determinants of male longevity in *Caenorhabditis elegans*. Genetics *154*, 1597–1610.

Gems, D., Sutton, A.J., Sundermeyer, M.L., Albert, P.S., King, K. V, Edgley, M.L., Larsen, P.L., and Riddle, D.L. (1998). Two pleiotropic classes of *daf-2* mutation affect larval arrest, adult behavior, reproduction and longevity in *Caenorhabditis elegans*. Genetics *150*, 129–155.

Gilbert, M., Beguet, B., and Starck, J. (1984). Role of the gonad cytoplasmic core during oogenesis of the nematode *Caenorhabditis elegans*. Biol. Cell *50*, 77–85.

Golden, T.R., Beckman, K.B., Lee, A.H.J., Dudek, N., Hubbard, A., Samper, E., and Melov, S. (2007). Dramatic age-related changes in nuclear and genome copy number in the nematode *Caenorhabditis elegans*. Aging Cell *6*, 179–188.

Gottlieb, S., and Ruvkun, G. (1994). *daf-2*, *daf-16* and *daf-23*: genetically interacting genes controlling dauer formation in *Caenorhabditis elegans*. Genetics *137*, 107–120.

Grandison, R.C., Piper, M.D.W., and Partridge, L. (2009). Amino-acid imbalance explains extension of lifespan by dietary restriction in *Drosophila*. Nature *462*, 1061–1064.

Grant, B., and Hirsh, D. (1999). Receptor-mediated endocytosis in the *Caenorhabditis elegans* oocyte. Mol. Biol. Cell *10*, 4311–4326.

Greenstein, D. (2005). Control of oocyte meiotic maturation and fertilization. WormBook 1–12.

Greenwood, J., and Gautier, J. (2005). From oogenesis through gastrulation: developmental regulation of apoptosis. Semin. Cell Dev. Biol. *16*, 215–224.

Gumienny, T.L., Lambie, E., Hartwieg, E., Horvitz, H.R., and Hengartner, M.O. (1999). Genetic control of programmed cell death in the *Caenorhabditis elegans* hermaphrodite germline. Development *126*, 1011–1022.

Haldane, J.B.S. (1941). New paths in genetics (London, UK: Allen & Unwin).

Hall, D.H., Winfrey, V.P., Blaeuer, G., Hoffman, L.H., Furuta, T., Rose, K.L., Hobert, O., and Greenstein, D. (1999). Ultrastructural features of the adult hermaphrodite gonad of *Caenorhabditis elegans*: relations between the germ line and soma. Dev. Biol. *212*, 101–123.

Hansen, M., Taubert, S., Crawford, D., Libina, N., Lee, S.-J., and Kenyon, C. (2007). Lifespan extension by conditions that inhibit translation in *Caenorhabditis elegans*. Aging Cell *6*, 95–110.

Hansen, M., Chandra, A., Mitic, L.L., Onken, B., Driscoll, M., and Kenyon, C. (2008). A role for autophagy in the extension of lifespan by dietary restriction in *C. elegans.* PLoS Genet. *4*, e24.

Harman, D. (1956). Aging: a theory based on free radical and radiation chemistry. J. Gerontol. *11*, 298–300.

Harrington, L.A., and Harley, C.B. (1987). Effect of vitamin E on lifespan and reproduction in *Caenorhabditis elegans*. Mech. Ageing Dev. *43*, 71–78.

Hay, N., and Sonenberg, N. (2004). Upstream and downstream of mTOR. Genes Dev. *18*, 1926–1945.

Heidler, T., Hartwig, K., Daniel, H., and Wenzel, U. (2010). *Caenorhabditis elegans* lifespan extension caused by treatment with an orally active ROS-generator is dependent on DAF-16 and SIR-2.1. Biogerontology *11*, 183–195.

Heitman, J., Movva, N.R., and Hall, M.N. (1991). Targets for cell cycle arrest by the immunosuppressant rapamycin in yeast. Science. *253*, 905–909.

Hengartner, M. (1997). Genetic control of programmed cell death and aging in the nematode *Caenorhabditis elegans*. Exp. Gerontol. *32*, 363–374.

Hengartner, M., and Horvitz, H.R. (1994). *C. elegans* cell survival gene ced-9 encodes a functional homolog of the mammalian proto-oncogene bcl-2. Cell *76*, 666–676.

Hengartner, M.O., Ellis, R.E., and Horvitz, H.R. (1992). *Caenorhabditis elegans* gene ced-9 protects cells from programmed cell death. Nature *356*, 494–499.

Herndon, L. a, Schmeissner, P.J., Dudaronek, J.M., Brown, P. a, Listner, K.M., Sakano, Y., Paupard, M.C., Hall, D.H., and Driscoll, M. (2002). Stochastic and genetic factors influence tissue-specific decline in ageing *C. elegans*. Nature *419*, 808–814.

Hertweck, M., Göbel, C., and Baumeister, R. (2004). *C. elegans* SGK-1 is the critical component in the Akt/PKB kinase complex to control stress response and life span. Dev. Cell *6*, 577–588.

Van Heusden, M.C., Fogarty, S., Porath, J., and Law, J.H. (1991). Purification of insect vitellogenin and vitellin by gel-immobilized ferric chelate. Protein Expr. Purif. *2*, 24–28.

Heydari, A.R., Wu, B., Takahashi, R., Strong, R., and Richardson, A. (1993). Expression of heat shock protein 70 is altered by age and diet at the level of transcription. Mol. Cell. Biol. *13*, 2909–2918.

Hirsh, D., Oppenheim, D., and Klass, M. (1976). Development of the reproductive system of *Caenorhabditis elegans*. Dev. Biol. *49*, 200–219.

Hodgkin, J., Horvitz, R.H., and Brenner, S. (1979). Nondisjunction mutants of the nematode *Caenorhabditis elegans*. Genetics *91*, 67–94.

Holliday, R. (1989). Food, reproduction and longevity: is the extended lifespan of calorie restricted animals an evolutionary adaptation? BioEssays *4*, 125–127.

Honda, Y., and Honda, S. (1999). The *daf-2* gene network for longevity regulates oxidative stress resistance and Mn-superoxide dismutase gene expression in *Caenorhabditis elegans*. FASEB J. *13*, 1385–1393.

Honda, S., Ishii, N., Suzuki, K., and Matsuo, M. (1993). Oxygen-dependent perturbation of life span and aging rate in the nematode. J. Gerontol. *48*, B57–61.

Horvitz, H.R., Brenner, S., Hodgkin, J., and Herman, R.K. (1979). A uniform genetic nomenclature for the nematode *Caenorhabditis elegans*. Mol. Gen. Genet. *133*, 129–133.

Houthoofd, K., Johnson, T.E., and Vanfleteren, J.R. (2007). Dietary restriction in the nematode *Caenorhabditis elegans*. Interdiscip. Top. Gerontol. *35*, 98–114.

Hsin, H., and Kenyon, C. (1999). Signals from the reproductive system regulate the lifespan of *C. elegans.* Nature *399*.

Hubbard, E.J.A., and Greenstein, D. (2005). Introduction to the germ line. WormBook 1–4.

Ishii, N., Senoo-Matsuda, N., Miyake, K., Yasuda, K., Ishii, T., Hartman, P.S., and Furukawa, S. (2004). Coenzyme Q10 can prolong *C. elegans* lifespan by lowering oxidative stress. Mech. Ageing Dev. *125*, 41–46.

Jaramillo-Lambert, A., Ellefson, M., Villeneuve, A.M., and Engebrecht, J. (2007). Differential timing of S phases, X chromosome replication, and meiotic prophase in the *C. elegans* germ line. Dev. Biol. *308*, 206–221.

Jia, K., Chen, D., and Riddle, D.L. (2004). The TOR pathway interacts with the insulin signaling pathway to regulate *C. elegans* larval development, metabolism and life span. Development *131*, 3897–3906.

Johnson, T.E. (1986). Molecular and genetic analyses of a multivariate system specifying behavior and life span. Behav. Genet. *16*, 221–235.

Johnson, T.E., and Hartman, P.S. (1988). Radiation effects on life span in *Caenorhabditis elegans*. J. Gerontol. *43*, B137–41.

Jost, J., Onhno, T., Panyim, S., and Scherch, A. (1978). Appearance of vitellogenin mRNA sequences and rate of vitellogenin synthesis in chicken liver following primary and secondary stimulation by 17 beta-estradiol. Eur. J. Biochem. *84*, 355–361.

Jowett, T., and Postlethwait, H. (1980). The regulation of yolk polypeptide synthesis in Drosophila ovaries fat body by 20-Hydroxyecdysone and a juvenile hormone analog. Dev. Biol. *80*, 225–234.

Jud, M., Razelun, J., Bickel, J., Czerwinski, M., and Schisa, J.A. (2007). Conservation of large foci formation in arrested oocytes of Caenorhabditis nematodes. Dev. Genes Evol. *217*, 221–226.

Judy, M.E., Nakamura, A., Huang, A., Grant, H., McCurdy, H., Weiberth, K.F., Gao, F., Coppola, G., Kenyon, C., and Kao, A.W. (2013). A shift to organismal stress resistance in programmed cell death mutants. PLoS Genet. *9*, e1003714.

Kamath, R., and Ahringer, J. (2003). Genome-wide RNAi screening in *Caenorhabditis elegans*. Methods *30*, 313–321.

Kapahi, P., Chen, D., Rogers, A., Katewa, S., Wai-Lun Li, P., Thomas, E.L., and Kockel, L. (2010). With TOR, less is more: a key role for the conserved nutrient-sensing TOR pathway in aging. Cell Metab. *11*, 453–465.

Keaney, M., and Gems, D. (2003). No increase in lifespan in *Caenorhabditis elegans* upon treatment with the superoxide dismutase mimetic EUK-8. Free Radic. Biol. Med. *34*, 277–282.

Keaney, M., Matthijssens, F., Sharpe, M., Vanfleteren, J., and Gems, D. (2004). Superoxide dismutase mimetics elevate superoxide dismutase activity in vivo but do not retard aging in the nematode *Caenorhabditis elegans*. Free Radic. Biol. Med. *37*, 239–250.

Kenyon, C. (2005). The plasticity of aging: insights from long-lived mutants. Cell *120*, 449–460.

Kenyon, C. (2011). The first long-lived mutants: discovery of the insulin/IGF-1 pathway for ageing. Philos. Trans. R. Soc. Lond. B. Biol. Sci. *366*, 9–16.

Kenyon, C.J. (2010). The genetics of ageing. Nature *464*, 504–512.

Kenyon, C., Jean, C., Gensch, E., Rudner, A., and Tabtiang, R. (1993). A *C. elegans* mutant that lives twice as long as wild type. Nature *366*, 461–464.

Kerr, J.F.R., Wyllie, A.H., and Currie, A.R. (1972). Apoptosis: A basic biological phenomenon with wide-ranging implications in tissue kinetics. Br. J. Cancer *26*, 239–257.

Kim, J., Takahashi, M., Shimizu, T., Shirasawa, T., Kajita, M., Kanayama, A., and Miyamoto, Y. (2008). Effects of a potent antioxidant, platinum nanoparticle, on the lifespan of *Caenorhabditis elegans*. Mech. Ageing Dev. *129*, 322–331.

Kimble, J., and Crittenden, S.L. (2005). Germline proliferation and its control. WormBook 1–14.

Kimble, J., and Hirsh, D. (1979). The postembryonic cell lineages of the hermaphrodite and male gonads in *Caenorhabditis elegans*. Dev. Biol. *70*, 396–417.

Kimble, J., and Sharrock, W.J. (1983). Tissue-specific synthesis of yolk proteins in *Caenorhabditis elegans*. Dev. Biol. *96*, 189–196.

Kimura, K.D. (1997). daf-2, an insulin receptor-like gene that regulates longevity and diapause in *Caenorhabditis elegans*. Science. *277*, 942–946.

Kirkwood, T. (1977). Evolution of ageing. Nature *270*, 301–304.

Kirkwood, T.B.L., and Holliday, R. (1979). The evolution of ageing and longevity. Proc. R. Soc. B Biol. Sci. *205*, 531–546.

Klass, M.R. (1977). Aging in the nematode *Caenorhabditis elegans*: major biological and environmental factors influencing life span. Mech. Ageing Dev. *6*, 413–429.

Klass, M.R. (1983). A method for the isolation of longevity mutants in the nematode *Caenorhabditis elegans* and initial results. Mech. Ageing Dev. *22*, 279–286.

Klass, M., and Hirsh, D. (1976). Non-ageing developmental variant of *Caenorhabditis elegans*. Nature *260*, 523–525.

Klass, M., Wolf, N., and Hirsh, D. (1976). Development of the male reproductive system and sexual transformation in the nematode *Caenorhabditis elegans*. Dev. Biol. *52*, 1–18.

Korta, D.Z., Tuck, S., and Hubbard, E.J.A. (2012). S6K links cell fate, cell cycle and nutrient response in *C. elegans* germline stem/progenitor cells. Development *139*, 859–870.

L'Hernault, S.W. (2006). Spermatogenesis. WormBook 1–14.

Lakowski, B., and Hekimi, S. (1998). The genetics of caloric restriction in *Caenorhabditis elegans*. Proc. Natl. Acad. Sci. U. S. A. *95*, 13091–13096.

LaMunyon, C.W., and Ward, S. (1998). Larger sperm outcompete smaller sperm in the nematode *Caenorhabditis elegans*. Proc. Biol. Sci. *265*, 1997–2002.

Levine, A.J. (1997). P53, the cellular gatekeeper for growth and division. Cell *88*, 323–331.

Levine, A.J., Finlay, C.A., Hinds, P.W., Drive, M., and Carolina, N. (2004). P53 is a tumor suppressor gene. Cell *S116*, 67–70.

Libina, N., Berman, J.R., and Kenyon, C. (2003). Tissue-specific activities of *C. elegans* DAF-16 in the regulation of lifespan. Cell *115*, 489–502.

Lin, K., Dorman, J.B., Rodan, A., and Kenyon, C. (1997). daf-16: an HNF-3/forkhead family member that can function to double the life-span of *Caenorhabditis elegans*. Science. *278*, 1319–1322.

Lin, K., Hsin, H., Libina, N., and Kenyon, C.J. (2001). Regulation of the *Caenorhabditis elegans* longevity protein DAF-16 by insulin/IGF-1 and germline signaling. Nat. Genet. *28*, 139–145.

Lints, R., and Hall, D.H. (2009a). Male reproductive system, general description. WormAtlas.

Lints, R., and Hall, D.H. (2009b). Male introduction. WormAtlas.

Lints, R., and Hall, D.H. (2009c). Reproductive system, germ line. WormAtlas.

Ljubuncic, P., and Reznick, A.Z. (2009). The evolutionary theories of aging revisited--a mini-review. Gerontology *55*, 205–216.

Luo, S., Kleemann, G. a, Ashraf, J.M., Shaw, W.M., and Murphy, C.T. (2010). TGF-β and insulin signaling regulate reproductive aging via oocyte and germline quality maintenance. Cell *143*, 299–312.

Maier, W., Adilov, B., Regenass, M., and Alcedo, J. (2010). A neuromedin U receptor acts with the sensory system to modulate food type-dependent effects on *C. elegans* lifespan. PLoS Biol. *8*, e1000376.

Mair, W., and Dillin, A. (2008). Aging and survival: the genetics of life span extension by dietary restriction. Annu. Rev. Biochem. *77*, 727–754.

Martínez, D.E. (1998). Mortality patterns suggest lack of senescence in hydra. Exp. Gerontol. *33*, 217–225.

Matyash, V., Geier, C., Henske, A., Mukherjee, S., Hirsh, D., Thiele, C., Grant, B., Maxfield, F.R., and Kurzchalia, T. V (2001). Distribution and transport of cholesterol in *Caenorhabditis elegans*. Mol. Biol. Cell *12*, 1725–1736.

McCarter, J., Bartlett, B., Dang, T., and Schedl, T. (1999). On the control of oocyte meiotic maturation and ovulation in *Caenorhabditis elegans*. Dev. Biol. *205*, 111–128.

McCay, C.M., Crowell, M.F., and Maynard, L.A. (1935). The effect of retarded growth upon the length of life span upon the ultimate body size. J. Nutr. *10*, 63–79.

McElwee, J.J., Schuster, E., Blanc, E., Thomas, J.H., and Gems, D. (2004). Shared transcriptional signature in *Caenorhabditis elegans* Dauer larvae and long-lived daf-2 mutants implicates detoxification system in longevity assurance. J. Biol. Chem. *279*, 44533–44543.

McGee, M.D., Weber, D., Day, N., Vitelli, C., Crippen, D., Herndon, L.A., Hall, D.H., and Melov, S. (2011). Loss of intestinal nuclei and intestinal integrity in aging *C. elegans*. Aging Cell *10*, 699–710.

Medawar (1952). An unsolved problem of biology (London, UK: H. K. Lewis).

Meléndez, A., Tallóczy, Z., Seaman, M., Eskelinen, E.-L., Hall, D.H., and Levine, B. (2003). Autophagy genes are essential for dauer development and life-span extension in *C. elegans*. Science. *301*, 1387–1391.

Melov, S., Ravenscroft, J., Malik, S., Gill, M.S., Walker, D.W., Clayton, P.E., Wallace, D.C., Malfroy, B., Doctrow, S.R., and Lithgow, G.J. (2000). Extension of life-span with superoxide dismutase/catalase mimetics. Science. *289*, 1567–1569.

Michaelson, D., Korta, D.Z., Capua, Y., and Hubbard, E.J.A. (2010). Insulin signaling promotes germline proliferation in *C. elegans*. Development *137*, 671–680.

Miller, M. a, Ruest, P.J., Kosinski, M., Hanks, S.K., and Greenstein, D. (2003). An Eph receptor sperm-sensing control mechanism for oocyte meiotic maturation in *Caenorhabditis elegans*. Genes Dev. *17*, 187–200.

Mitchell, D.H., Stiles, J.W., Santelli, J., and Sanadi, D.R. (1979). Synchronous growth and aging of *Caenorhabditis elegans* in the presence of fluorodeoxyuridine. J. Gerontol. *34*, 28–36.

Morris, J.Z., Tissenbaum, H.A., and Ruvkun, G. (1996). A phosphatidylinositol-3-OH kinase family member regulating longevity and diapause in *Caenorhabditis elegans*. Nature *382*, 536–539.

Murphy, C.T., McCarroll, S.A., Bargmann, C.I., Fraser, A., Kamath, R.S., Ahringer, J., Li, H., and Kenyon, C. (2003). Genes that act downstream of DAF-16 to influence the lifespan of *Caenorhabditis elegans*. Nature *424*, 277–283.

Nakamura, A., Yasuda, K., and Adachi, H. (1999). Vitellogenin-6 is a major carbonylated protein in aged nematode, *Caenorhabditis elegans*. Biochem. Biophys. Res. Commun. *264*, 580–583.

Nardelli, D., Gerber-Huber, S., van het Schip, F.D., Gruber, M., Ab, G., and Wahli, W. (1987). Vertebrate and nematode genes coding for yolk proteins are derived from a common ancestor. Biochemistry *26*, 6397–6402.

Ogg, S., and Ruvkun, G. (1998). The *C. elegans* PTEN homolog, DAF-18, acts in the insulin receptor-like metabolic signaling pathway. Mol. Cell *2*, 887–893.

Ogg, S., Paradis, S., Gottlieb, S., Patterson, G.I., Lee, L., Tissenbaum, H. A, and Ruvkun, G. (1997). The Fork head transcription factor DAF-16 transduces insulin-like metabolic and longevity signals in *C. elegans*. Nature *389*, 994–999.

Pan, C.-L., Peng, C.-Y., Chen, C.-H., and McIntire, S. (2011). Genetic analysis of age-dependent defects of the *Caenorhabditis elegans* touch receptor neurons. Proc. Natl. Acad. Sci. U. S. A. *108*, 9274–9279.

Pan, K., Palter, J., and Rogers, A. (2007). Inhibition of mRNA translation extends lifespan in *Caenorhabditis elegans*. Aging Cell *6*, 111–119.

Pan, M.L., Bell, W.J., and Telfer, W.H. (1969). Vitellogenic blood protein synthesis by insect fat body. Science. *165*, 393–394.

Paradis, S., and Ruvkun, G. (1998). *Caenorhabditis elegans* Akt/PKB transduces insulin receptor-like signals from AGE-1 PI3 kinase to the DAF-16 transcription factor. Genes Dev. *12*, 2488–2498.

Partridge, L., and Gems, D. (2002). Mechanisms of ageing: public or private? Nat. Rev. Genet. *3*, 165–175.

Partridge, L., and Gems, D. (2006). Beyond the evolutionary theory of ageing, from functional genomics to evo-gero. Trends Ecol. Evol. *21*.

Perrin, A.J., Gunda, M., Yu, B., Yen, K., Ito, S., Forster, S., Tissenbaum, H. a, and Derry, W.B. (2013). Noncanonical control of *C. elegans* germline apoptosis by the insulin/IGF-1 and Ras/MAPK signaling pathways. Cell Death Differ. *20*, 97–107.

Del Peso, L., Gonzalez, V.M., Inohara, N., Ellis, R.E., and Núñez, G. (2000). Disruption of the CED-9.CED-4 complex by EGL-1 is a critical step for programmed cell death in *Caenorhabditis elegans*. J. Biol. Chem. *275*, 27205–27211.

Pinkston, J.M., Garigan, D., Hansen, M., and Kenyon, C. (2006). Mutations that increase the life span of *C. elegans* inhibit tumor growth. Science. *313*, 971–975.

Pinkston-Gosse, J., and Kenyon, C. (2007). DAF-16/FOXO targets genes that regulate tumor growth in *Caenorhabditis elegans*. Nat. Genet. *39*, 1403–1409.

Piper, M.D.W., Partridge, L., Raubenheimer, D., and Simpson, S.J. (2011). Dietary restriction and aging: a unifying perspective. Cell Metab. *14*, 154–160.

Qiao, L., Lissemore, J.L., Pei, S., Smardon, A., Gelber, M.B., and Maine, E.M. (1995). Enhancers of glp-1, a gene required for cell-signaling in *Caenorhabditis elegans*, define a set of genes required for germline development. Genetics *141*, 551–569.

Van Raamsdonk, J.M., and Hekimi, S. (2009). Deletion of the mitochondrial superoxide dismutase sod-2 extends lifespan in *Caenorhabditis elegans*. PLoS Genet. *5*, e1000361.

Van Raamsdonk, J.M., and Hekimi, S. (2010). Reactive oxygen species and aging in *Caenorhabditis elegans*: causal or casual relationship? Antioxid. Redox Signal. *13*, 1911–1953.

Reznick, D.N., Bryant, M.J., Roff, D., Ghalambor, C.K., and Ghalambor, D.E. (2004). Effect of extrinsic mortality on the evolution of senescence in guppies. Nature *431*, 1095–1099.

Riddle, D.L., Swanson, M.M., and Albert, P.S. (1981). Interacting genes in nematode dauer larva formation. Nature *290*, 668–671.

Riddle, D.L., Blumenthal, T., Meyer, B.J., and Priess, J.R. (1997). *C. elegans* II (Cold Spring Harbor (NY): Cold Spring Harbor Laboratory Press).

Riesen, M., Feyst, I., Rattanavirotkul, N., Ezcurra, M., Jennifer, M.A., Papatheodorou, I., Ziehm, M., Au, C., Gilliat, A.F., Thornton, J.M., et al. (2014). MDL-1 , a growth- and tumor-suppressor, slows aging and prevents germline hyperplasia and hypertrophy in C . elegans. Aging (Albany. NY). *6*, 1–20.

Robertson, A.M.G., and Thomson, J.N. (1982). Morphology of programmed cell death in the ventral nerve cord of *Caenorhabditis elegans* larvae. J. Embryol. Exp. Morphol. *67*, 89–100.

Rual, J.-F., Ceron, J., Koreth, J., Hao, T., Nicot, A.-S., Hirozane-Kishikawa, T., Vandenhaute, J., Orkin, S.H., Hill, D.E., van den Heuvel, S., et al. (2004). Toward improving *Caenorhabditis elegans* phenome mapping with an ORFeome-based RNAi library. Genome Res. *14*, 2162–2168.

Salinas, L.S., Maldonado, E., and Navarro, R.E. (2006). Stress-induced germ cell apoptosis by a p53 independent pathway in *Caenorhabditis elegans*. Cell Death Differ. *13*, 2129–2139.

Sampayo, J.N., Olsen, A., and Lithgow, G.J. (2003). Oxidative stress in *Caenorhabditis elegans*: protective effects of superoxide dismutase/catalase mimetics. Aging Cell *2*, 319–326.

Sánchez-Blanco, A., and Kim, S.K. (2011). Variable pathogenicity determines individual lifespan in *Caenorhabditis elegans*. PLoS Genet. *7*, e1002047.

Schedl, T., and Kimble, J. (1988). a germ-line-specific Sex determination gene required for hermaphrodite spermatogenesis in *Caenorhabditis elegans*. Genetics *119*, 43–61.

Schulz, T.J., Zarse, K., Voigt, A., Urban, N., Birringer, M., and Ristow, M. (2007). Glucose restriction extends *Caenorhabditis elegans* life span by inducing mitochondrial respiration and increasing oxidative stress. Cell Metab. *6*, 280–293.

Schumacher, B., Hofmann, K., Boulton, S., and Gartner, A. (2001). The *C. elegans* homolog of the p53 tumor suppressor is required for DNA damage-induced apoptosis. Curr. Biol. *11*, 1722–1727.

Schumacher, B., Schertel, C., Wittenburg, N., Tuck, S., Mitani, S., Gartner, A., Conradt, B., and Shaham, S. (2005a). *C. elegans* ced-13 can promote apoptosis and is induced in response to DNA damage. Cell Death Differ. *12*, 153–161.

Schumacher, B., Hanazawa, M., Lee, M.-H., Nayak, S., Volkmann, K., Hofmann, E.R., Hofmann, R., Hengartner, M., Schedl, T., and Gartner, A. (2005b). Translational repression of *C. elegans* p53 by GLD-1 regulates DNA damage-induced apoptosis. Cell *120*, 357–368.

Selman, C., Tullet, J.M., Wieser, D., Irvine, E., Lingard, S.J., Choudhury, A.I., Claret, M., Al-Qassab, H., Carmignac, D., Ramadani, F., et al. (2009). Ribosomal protein S6 kinase 1 signaling regulates mammalian life span. Science (80-.). *326*, 140–144.

Shanley, D.P., and Kirkwood, T.B. (2000). Calorie restriction and aging: a life-history analysis. Evolution *54*, 740–750.

Sharrock, W., Sutherlin, M., Leske, K., Cheng, T., and Kim, T. (1990). Two distinct yolk lipoprotein complexes from *Caenorhabditis elegans*. J. Biol. *265*, 14422–14431.

Shyu, a B., Raff, R. a, and Blumenthal, T. (1986). Expression of the vitellogenin gene in female and male sea urchin. Proc. Natl. Acad. Sci. U. S. A. *83*, 3865–3869.

Singson, a (2001). Every sperm is sacred: fertilization in *Caenorhabditis elegans*. Dev. Biol. *230*, 101–109.

Sohal, R.S., and Sohal, B.H. (1991). Hydrogen peroxide release by mitochondria increases during ageing. Mech. Ageing Dev. *57*, 187–202.

Sohal, R.S., and Weindruch, R. (1996). Oxidative Stress, caloric restriction, and aging. Science. *273*, 59–63.

Sonenberg, N., and Gingras, A.C. (1998). The mRNA 5' cap-binding protein eIF4E and control of cell growth. Curr. Opin. Cell Biol. *10*, 268–275.

Spieth, J., and Blumenthal, T. (1985). *Caenorhabditis elegans* Vitellogenin. Microbiology *5*, 2495–2501.

Spieth, J., Denison, K., Kirtland, S., Cane, J., and Blumenthal, T. (1985). The *C. elegans* vitellogenin genes: short sequence repeats in the promoter regions and homology to the vertebrate genes. Nucleic Acids Res. *13*, 5283–5295.

Stout, G.J., Stigter, E.C.A., Essers, P.B., Mulder, K.W., Kolkman, A., Snijders, D.S., van den Broek, N.J.F., Betist, M.C., Korswagen, H.C., Macinnes, A.W., et al. (2013). Insulin/IGF-1-mediated longevity is marked by reduced protein metabolism. Mol. Syst. Biol. *9*, 679.

Sulston, J.E., and Horvitz, H.R. (1977). Post-embryonic cell lineages of the nematode, *Caenorhabditis elegans*. Dev. Biol. *56*, 110–156.

Sulston, J.E., Schierenberg, E., White, J.G., and Thomson, J.N. (1983). The embryonic cell lineage of the nematode *Caenorhabditis elegans*. Dev. Biol. *100*, 64–119.

Syntichaki, P., Troulinaki, K., and Tavernarakis, N. (2007). eIF4E function in somatic cells modulates ageing in *Caenorhabditis elegans*. Nature *445*, 922–926.

Tabara, H., Grishok, A., and Mello, C.C. (1998). RNAi in *C. elegans*: soaking in the genome sequence. Science. *282*, 430–431.

Tank, E.M.H., Rodgers, K.E., and Kenyon, C. (2011). Spontaneous age-related neurite branching in *Caenorhabditis elegans*. J. Neurosci. *31*, 9279–9288.

Tatar, M., Kopelman, A., Epstein, D., Tu, M.P., Yin, C.M., and Garofalo, R.S. (2001). A mutant Drosophila insulin receptor homolog that extends life-span and impairs neuroendocrine function. Science. *292*, 107–110.

Terpstra, P., and Ab, G. (1988). Homology of Drosophila yolk proteins and the triacylglycerol lipase family. J. Mol. Biol. *202*, 663–665.

Timmons, L., and Fire, A. (1998). Specific interference by ingested dsRNA. Nature *395*, 854.

Timmons, L., Court, D.L., and Fire, A (2001). Ingestion of bacterially expressed dsRNAs can produce specific and potent genetic interference in *Caenorhabditis elegans*. Gene *263*, 103–112.

Tullet, J., Hertweck, M., An, J., and Baker, J. (2008). Direct inhibition of the longevity promoting factor SKN-1 by Insulin-like signaling in *C. elegans*. Cell *132*, 1025–1038.

Uchiyama, S., Koike, H., Shimizu, T., and Shirasawa, T. (2005). A superoxide dismutase/catalase mimetic extends the lifespan of short-lived mev-1 mutant but not the wild type strain in *Caenorhabditis elegans*. Anti-Ageing Med. Res. *2*, 39–47.

Unger, R.H., and Scherer, P.E. (2010). Gluttony, sloth and the metabolic syndrome: a roadmap to lipotoxicity. Trends Endocrinol. Metab. *21*, 345–352.

Valentini, S., Cabreiro, F., Ackerman, D., Alam, M.M., Kunze, M.B.A., Kay, C.W.M., and Gems, D. (2012). Manipulation of in vivo iron levels can alter resistance to oxidative stress without affecting ageing in the nematode *C. elegans*. Mech. Ageing Dev. *133*, 282–290.

Vanfleteren, J.R. (1993). Oxidative stress and ageing in *Caenorhabditis elegans*. Biochem. J. *292*, 605–608.

Viña, J., Borrás, C., and Miquel, J. (2007). Theories of ageing. IUBMB Life *59*, 249–254.

Virtue, S., and Vidal-Puig, A. (2008). It's not how fat you are, it's what you do with it that counts. PLoS Biol. *6*, e237.

Ward, S., and Carrel, J.S. (1979). Fertilization and sperm competition in the nematode *Caenorhabditis elegans*. Dev. Biol. *73*, 304–321.

Weindruch, R., and Walford, R.L. (1988). The retardation of aging and disease by dietary restriction (Springfield, IL).

Weindruch, R., Walford, R.L., Fligiel, S., and Guthrie, D. (1986). The retardation of aging in mice by dietary restriction: longevity, cancer, immunity and lifetime energy intake. J. Nutr. *116*, 641–654.

Weismann, A. (1889). Essays upon heredity (Oxford: Clarendon Press).

Wiley, H.S., and Wallace, R.A. (1981). The structure of vitellogenin. Multiple vitellogenins in *Xenopus laevis* give rise to multiple forms of the yolk proteins. J. Biol. Chem. *256*, 8626–8634.

Williams, G.C. (1957). Pleiotropy, natural Selection, and the Evolution of senescence. Evolution (N. Y). *11*, 398–411.

Wolke, U., Jezuit, E.A., and Priess, J.R. (2007). Actin-dependent cytoplasmic streaming in *C. elegans* oogenesis. Development *134*, 2227–2236.

Wullschleger, S., Loewith, R., and Hall, M.N. (2006). TOR signaling in growth and metabolism. Cell *124*, 471–484.

Yamawaki, T.M., Arantes-Oliveira, N., Berman, J.R., Zhang, P., and Kenyon, C. (2008). Distinct activities of the germline and somatic reproductive tissues in the regulation of *Caenorhabditis elegans*' longevity. Genetics *178*, 513–526.

Yang, W., and Hekimi, S. (2010a). A mitochondrial superoxide signal triggers increased longevity in *Caenorhabditis elegans*. PLoS Biol. *8*, e1000556.

Yang, W., and Hekimi, S. (2010b). Two modes of mitochondrial dysfunction lead independently to lifespan extension in *Caenorhabditis elegans*. Aging Cell *9*, 433–447.

Yuan, J., and Horvitz, H.R. (2004). A first insight into the molecular mechanisms of apoptosis. Cell *S116*, S53–6.

Yuan, J., Shaham, S., Ledoux, S., Ellis, H.M., and Horvitz, H.R. (1993). The *C. elegans* cell death gene ced-3 encodes a protein similar to mammalian interleukin-1 beta-converting enzyme. Cell *75*, 641–652.

Zarkower, D. (2006). Somatic sex determination. WormBook 1–12.

Zou, H., Henzel, W.J., Liu, X., Lutschg, a, and Wang, X. (1997). Apaf-1, a human protein homologous to *C. elegans* CED-4, participates in cytochrome c-dependent activation of caspase-3. Cell *90*, 405–413.